Ultrasonic Inspection of Gas Porosity Defects in Aluminium Die Castings

by

Suresh Palanisamy

B. Eng. (Mechanical Engineering)

M. Eng. (Computer Integrated Manufacturing)

A thesis submitted to the Industrial Research Institute Swinburne, Swinburne University of Technology in fulfilment of the requirements to the degree of Doctor of Philosophy

Hawthorn, Melbourne, Australia

July 2006

DECLARATION

This thesis contains no material that has been accepted for the award of any degree or diploma in any university or college of advanced education, and to the best of my knowledge and belief, contains no material previously published or written by another person, except where due reference has been made.

Suresh Palanisamy
Date: 17/7/2006

ACKNOWLEDGEMENTS

The author wishes to express his gratitude to the Co-operative Research Centre for Cast Metals Manufacturing (CRC CAST) and the participating companies Nissan Casting Australia Pty. Ltd., (Mr. Ken Porter and Mr. Leng Lim) and the Ford Motor Company Australia Pty. Ltd., (Mr. Darren Mathews) for their support, and access to testing equipments and castings throughout the research program.

The author is grateful for the support obtained from both his supervisors, Prof. Romesh Nagarajah and Dr. Pio Iovenitti at the Industrial Research Institute Swinburne (IRIS), all the way through this project. In particular, Prof. Romesh Nagarajah bestowed constant guidance and encouragement with this thesis. Valuable support was also obtained from NDT researchers, Mr. Howard Morton and Mr. Peter Virtue at Defence Science and Technology Organisation, Melbourne.

The author wishes to acknowledge the support received from the Metallurgical, Laser, Micro-tech and Non-contact inspection research groups and technicians (Mr. Brian Dempster) at IRIS. He also wishes to thank his research colleagues, especially Dr. Kynan Graves at IRIS, and Dr. Chinnu Subramaniam for their constant encouragement especially in difficult times.

The author has benefited greatly from discussions with other research groups (CSIRO, Monash University) and its members within the CRC CAST. He thanks Mr. Paul Spurling for proof reading the thesis.

Finally, the author would like to express his gratefulness to his mother Mrs. P. Bagyalakshmi and late father Mr. P.M. Palanisamy, and constant encouragement from his wife Mrs. Kothainayaki and also other family members for their support, patience and endurance, which have enabled him to achieve his goal.

Abstract

This thesis documents a PhD research program undertaken at Swinburne University of Technology between the years 2000 and 2004. The research was funded by the Cooperative Research Centre for Cast Metals Manufacturing and was undertaken in collaboration with Nissan Casting Plant Australia Pty Ltd and the Ford Motor Company Australia Limited. This thesis reports on the investigation of the possibility of using an ultrasonic sensing-based, non-destructive testing system to detect gas porosity defects in aluminium die casting parts with rough surfaces. The initial intention was to develop a procedure to obtain ultrasonic signals with the maximum possible amplitude from defects within the rough surface areas of the castings. A further intention was to identify defects with the application of a suitable signal processing technique to the raw ultrasonic signal. The literature review has indicated that ultrasonic techniques have the potential to be used to detect sub-surface defects in castings. The possibility of classifying very weak ultrasonic signals obtained from rough surface sections of castings through a neural network approach was also mentioned in the literature. An extensive search of the literature has indicated that ultrasonic sensing techniques have not been successfully used to detect sub-surface defects in aluminium die castings with rough surfaces.

Ultrasonic inspection of castings is difficult due to the influence of microstructural variations, surface roughness and the complex shape of castings. The design of the experimental set-up used is also critical in developing a proper inspection procedure. The experimental set-up of an A-scan ultrasonic inspection rig used in the research is described in this thesis. Calibration of the apparatus used in the inspection rig was carried out to ensure the reliability and repeatability of the results. This thesis describes the procedure used to determine a suitable frequency range for the inspection of CA313 aluminium alloy castings and detecting porosity defects while accommodating material variations within the part. The results obtained from ultrasonic immersion testing indicated that focused probes operating at frequencies between 5 MHz and 10 MHz are best suited for the inspection of castings with surface roughness R_a values varying between 50 μm and 100 μm. For

the purpose of validating the proposed inspection methodology, gas porosity defects were simulated through side-drilled holes in the in-gate section of selected sample castings. Castings with actual porosity defects were also used in this research.

One of the conclusions of this research was that it was extremely difficult to detect defects in castings with surface roughness above 125 μm. Once the ultrasonic signal data was obtained from the sample aluminium die castings with different surface roughness values ranging from 5 μm to 150 μm, signal analysis was carried out. Signal feature extraction was achieved using Fast Fourier Transforms (FFT), Principal Component Analysis (PCA) and Wavelet Transforms (WT) prior to passing the ultrasonic signals into a neural network for defect classification. MATLAB tools were used for neural network and signal pre-processing analysis. The results indicated that poor classification (less than 75%) was achieved with the WT, PCA and combination of FFT/PCA and WT/PCA pre-processing techniques for rough surface signals. However, the classification of the signals pre-processed with the combination of WT/FFT, FFT/WT and FFT/WT/PCA classifiers provided much better classification of more than 90% for smooth surface signals and 78% to 84% for rough surface signals. The results obtained from ultrasonic testing of castings with both real and simulated defects were validated with X-ray analysis of the sample castings. The results obtained from this research encourage deeper investigation of the detection and characterisation of sub-surface defects in castings at the as-cast stage. Implications for the industrial application of these findings are discussed and directions for further research presented in this thesis.

Table of Contents

List of Figures

List of Tables

List of Acronyms

Symbol	Description
AI	Artificial Intelligence
ANN	Artificial Neural Networks
BP	Back Propagation
BWE	Back Wall Echo
CRC CAST	Cooperative Research Centre for Cast Metals Manufacturing
CRT	Cathode Ray Tube
CWT	Continuous Wavelet Transform
DFT	Discrete Fourier Transform
DWT	Discrete Wavelet Transform
ECT	Eddy Current Testing
FFT	Fast Fourier Transform
FSH	Full Screen Height
HPDC	High Pressure Die Casting
ISO	International Standard Organisation
KBIS	Knowledge Based Inspection System
LPT	Liquid Penetrant Testing
LSF	Line Spread Function
MPT	Magnetic Particle Testing
MSE	Mean Square Error
MTC	Manual Transmission Case
NDE	Non Destructive Evaluation
NDT	Non Destructive Testing
NDT&E	Non Destructive Testing & Evaluation
PCA	Principal Component Analysis
QS	Quality Standards
ROI	Region Of Interest
RT	Radiographic Testing

SCG	Scaled Conjugate Gradient
SD	Standard Deviation
SOSP	Structural Oil Sump Pan
SUT	Swinburne University of Technology
TOFD	Time of Flight Diffraction
TQM	Total Quality Management
UT	Ultrasonic Testing
WP	Water Path
WT	Wavelet Transform

List of Variables

Symbol	Description	Unit
α	Ultrasonic Angle Beam Spread	^{o}
λ	Wavelength of the Signal	mm
ϕ_L	Incident Angle of the Longitudinal Beam	^{o}
ϕ_S	Reflected Shear Beam Angle	
b	Neural Network Bias	
D	Diameter of Transducer	mm
F	Frequency of Ultrasound Signal	MHz
F	Focal Length of the Transducer	mm
L	Total Attenuation of Ultrasonic Signal	dB/mm
L_{Diff}	Ultrasonic Beam Spread Loss	dB/mm
L_{Grain}	Grain Scattering Loss	dB/mm
L_{Imp}	Double Transmission Loss of Ultrasonic Signal	dB/mm
L_p	Attenuation Loss Due to Porosity	dB/mm
L_{Surf}	Surface Roughness Loss	dB/mm
MP	Material Path	mm
N	Near Field Length	mm
P_R	Neural Network Input	
h_{RMS}	Root Mean Square of Surface Roughness Heights	μm
R_1	Acoustic Impedance in Water	kg/m^2s
R_2	Acoustic Impedance in Aluminium Material	kg/m^2s
R_a	Arithmetic Mean Surface Roughness	μm
T	Time Period	s
T	Target Output in Neural Network	
V	Velocity of Ultrasound in the Material	m/s
V_L	Velocity of Longitudinal Beam	m/s
V_m	Velocity of Ultrasound in Aluminium Material	m/s

V_S	Velocity of Shear Beam	m/s
V_w	Velocity of Ultrasound in Water	m/s
w	Neural Network Weights	
z	Acoustic Impedance	kg/m^2s

CHAPTER 1.

INTRODUCTION

1.1 OVERVIEW

This thesis documents a Doctoral research program undertaken at Swinburne University of Technology (SUT), during the period from 2000 to 2004. The research work presented herein was part of a larger research program involving a number of researchers from SUT and Deakin University. The research was funded by the Cooperative Research Centre for Cast Metals Manufacturing (CRC CAST) at the Industrial Research Institute Swinburne, a research centre attached to SUT. It was undertaken with the co-operation of Nissan Casting Plant Australia Pty Ltd, and the Ford Motor Company Australia Limited. This research was a subset of an overall research program titled "Automated Fault Detection Systems" in the high pressure die casting industry.

The specific objective of this research project was the investigation and development of an ultrasonic inspection technique to detect gas porosity defects in aluminium die casting parts with rough surfaces. The motivation for this research was the casting industry's requirement for an advanced inspection system to identify sub-surface defects in aluminium die castings in the as-cast state.

The aim of this chapter is to provide a background to the research project and an overview of problems encountered in die casting quality inspection. This chapter also describes the objectives of the project and provides an outline of the whole thesis.

1.2 BACKGROUND

Casting is one of the most ancient metal-shaping techniques, and is the process of forming metal objects by melting metal and pouring it into moulds [1]. Discontinuities are a common problem in castings. Discontinuities are irregularities, breaks, or gaps in the material structure. Most types of casting discontinuities are visible to the naked eye and are caused by variation in the casting process. However, some of them are not detectable by visual inspection because they occur below the surface of the material. The sub-surface is the most highly loaded region of the material. Therefore, sub-surface discontinuities such as cracks, inclusions, or pores greatly influence the ability of a component to withstand load. Sub-surface discontinuities must be detected and identified before remedies can be developed to eliminate them [2].

The aluminium die casting industry is one of the foremost suppliers of castings to the automotive industry. The role of the die casting manufacturer is to deliver high quality castings to this industry. The manufacturer is usually required to replace the castings if found defective during the customer's machining process. This places a financial burden on the manufacturer. Hence, the die casting manufacturer prefers to detect discontinuities during the production process. The detection of faults prior to the transfer of products to the clients not only saves money and time, but also enhances the manufacturer's reputation in relation to quality. Therefore, it is essential to develop a technology that will assist the casting industry to achieve quality assurance and to remain competitive in the international market.

With the emergence of modern design techniques and aluminium alloys, the mechanical strength of castings is usually not a problem. However, automotive castings are often in contact with fluids under pressure, including transmission fluid, engine oil and coolant. Hence, a more likely problem is that, the castings with defects are subjected to leakage under pressure. Therefore, die casting manufacturers inspect their castings for defects that may cause leakage under pressure prior to supplying them to their customers. These defects primarily relate to porosity and cracks.

In the 21st century, casting manufacturers need to maintain standards and keep abreast of the latest technologies to be competitive in the international market. George Johnson[1] expressed a similar view in his keynote address on "The people/technology partnership".

"To survive and prosper in the coming years, successful foundries will have to be leaders in quality, cost, technology and response to customer needs"

Even though this statement was made in the early 1990's, it remains valid for the casting industries. Hence, maintaining an ISO 9000 series certification is not sufficient to maintain a market share of produced goods. Quality assurance programs will often pass or reject the entire production lot based on randomly inspected samples. If a quality system detects a fault in a single sample at customer's site, the whole consignment will be scrapped. Therefore, it is essential that the manufacturer detect every fault, in order to avoid costly delays, ever increasing scrapping cost and customer dissatisfaction. As the cost of scrapping goes up, there is an increasing need for a cost effective advanced inspection system. The new system should emulate the skills, decision making capacity and the supervisory control of the operator. A thorough knowledge of the casting process is an essential requirement for the development of a new quality inspection system [2].

As mentioned above, a casting organisation's relationship with a customer is enormously influenced by the quality of castings delivered and the satisfactory quality requirement varies from industry to industry. Thus, the inspection process is an important step in the quality assurance program for most die casting manufacturers [3]. While there are a number of elements that go into the implementation of a Total Quality Management (TQM) system, in this research the focus is on Non-Destructive Testing (NDT), specifically ultrasonic based inspection for detecting sub-surface defects in the aluminium die casting industry.

[1] The people/technology partnership, George. G. Johnson, General Manager Central Foundry Division, GM Corporation in Die Casting Engineer 1992, 36 (2) pp. 3

NDT techniques include ultrasonic, X-ray, liquid penetrant, eddy current, leak and magnetic particle testing. They have been previously used in different areas of the casting industry, mostly on machined casting products [4]. At present, in the automotive industry an operator detects defective castings off-line, using X-ray or leak NDT methods. However, none of these systems provides feedback to the die casting machines in real time. Due to the amount of time required, it is not possible to carry out a 100% inspection of all castings produced using these methods. Hence, there is a compelling need for a reliable high speed inspection system to identify defects.

Rickards and Wickens [3] identified the most important problem areas in the casting inspection process and brought courses of action to the attention of casting industries in their investigation. These were based upon the wider understanding of NDT techniques used, making the best use of the equipment available and ensuring that the correct procedures were employed.

In this investigation, importance of NDT inspection methods has been emphasised for overall casting inspection. However, the ability to test castings using NDT methods is dependent on the type of metal, surface roughness, grain structure and type of defect to be detected. These factors increase the overall complexity involved in identifying quality castings using ultrasonic inspection.

1.3 RESEARCH PROBLEM AND OBJECTIVES

Most ultrasonic techniques were developed in the die casting industry to inspect castings with simple geometries and machined surfaces. A technique could not be described as non-destructive if it requires alteration of a surface prior to inspection. Another problem with this method is that it may expose the porosity defects just beneath the rough surface. Defects at greater depth (more than 3 or 4 mm) are not of much consequence in casting inspection [5]. The machining process

would also change the substrate structure of the casting and therefore, change the overall properties of the part to be inspected.

In the past, ultrasonic inspection of castings was restricted by their metallurgical and physical characteristics. Typically, the grain size and surface roughness vary between castings manufactured within the same production cycle. This variation is acceptable in the die casting industry as long as it does not affect the integral strength and intended function of the castings. However, in the ultrasonic inspection of castings, the signal amplitude is significantly affected by the material variations such as rough surfaces and non-uniform grain size.

The noise contained in the ultrasonic signal caused by rough surfaces and grain size variations of castings is difficult to eliminate totally. Castings are less commonly tested by ultrasonic methods because these structural variations usually create high ultrasonic signal noise. Two research questions arise from these problems: (a) What are the limitations to obtaining useful signals from castings with rough surfaces using ultrasonic NDT techniques?; and (b) Once a ultrasonic signal is obtained, is it possible to identify porosity type defects in castings with the use of sophisticated signal processing techniques? These two questions were investigated and addressed in this research to the benefit of both the casting and NDT industries.

The research project was undertaken in accordance with the following problem statement:

To investigate the possibility of using an ultrasonic inspection technique to detect small sub-surface defects (gas porosity) near the front rough surface of castings with varying grain size, by classifying weak and noisy ultrasonic signals using suitable signal processing techniques.

According to Krautkrämer and Krautkrämer [5], the success of casting inspection generally depends on the selection of a suitable probe frequency. The resolution of the ultrasonic probe, or the smallest defect size that can be detected, is half the wavelength. Therefore, smaller defects can be detected with higher

frequencies of ultrasound. Unfortunately, the higher the frequency also means the higher the rate of signal damping in a material, and more scattering at the rough surface. In terms of this project the measurement capability of the probe is compromised if the frequency of the ultrasound is too low (1 MHz or 2 MHz) making it hard to detect defects less than one millimetre in size. Hence, there is a need to obtain a balance between the possibility of ultrasonic inspection and the requirement to detect small gas porosity defects in rough surface castings.

The overall aim of this project is to develop an ultrasonic based inspection system, with the potential for future automated on-line application to detect sub-surface defects in aluminium die castings. Specifically, the objectives as described in the research problem statement are:

- To investigate the use of an ultrasonic inspection system for detecting the smallest possible gas porosity defect near to the inspection surface (up to 4 mm in depth) of complex shaped aluminium die castings with varying grain size and surface roughness.
- To identify the presence of defects by classifying ultrasonic signals obtained from castings using suitable signal processing techniques.

It is anticipated that the outcomes of this investigation on the ultrasonic inspection of die castings will lead to the development of an ultrasonic based sub-surface defect detection system.

1.4 NEED FOR FAULT DETECTION

An inspection system based on use of an ultrasonic signal subject to suitable signal processing offers many advantages to casting manufacturers. Among them are consistent inspection to ensure that customer requirements are met, increased inspection throughput, reduced labour costs and statistical reporting to assist in in-process monitoring. Automation of a system based on this methodology enables

ultrasonic inspection to become an integral part of the manufacturing process. The integration of a modern inspection system into the production process will be one of the major challenges in the field of automated ultrasonic inspection.

The development of an effective ultrasonic signal processing method is necessary to achieve effective inspection. It eliminates the requirement for a manual operator as the decision maker in the ultrasonic inspection of castings. Automated ultrasonic inspection would make possible the checking of each casting, and immediately alert the operator about the presence of defects. Therefore, it would eliminate the sampling rate limitations, delays and much of the cost associated with X-ray and industrial computer tomography systems. High porosity castings would not be passed on to the customer, resulting in savings of transport; machining and re-inspection costs. This would enhance the reputation of the casting plant as a reliable supplier of high quality castings. The ability to detect a porosity problem immediately would also save valuable machine time, reduce scrap and re-melting and increase effective casting plant capacity. Furthermore, post-cast processes, such as machining, are carried out weeks or months later in another plant. Hence, early detection of porosity defects will result in greater cost savings for casting manufacturers.

1.5 OVERVIEW OF METHODOLOGY

To achieve the research objectives, a methodology was developed to determine the limitations of ultrasonic inspection of castings with rough surfaces and varying grain size. This methodology includes:

- Obtaining ultrasonic signals from selected sample castings with optimised inspection parameters such as frequency of operation and distance between probe and part
- Determining ultrasonic velocity in selected casting material

- Obtaining a signal with the maximum signal-to-noise ratio from the rough surface of the castings with the correct experimental set up, and
- Applying the appropriate signal pre-processing and artificial neural network techniques for data extraction. Then, classifying ultrasonic signals obtained from sample castings for the purpose of determining the presence of porosity type defects.

The starting point for any ultrasonic NDT testing is to select and study several sample castings and their defect types. For this research, production sample castings were selected due to the poor correlation between tests conducted on laboratory produced samples and shop floor produced die castings. An investigation was carried out to select an appropriate ultrasonic inspection technique (contact and immersion type) for the selected sample castings. An ultrasonic inspection rig was designed and constructed to inspect the samples with an ultrasonic immersion testing system. Procedures were developed such that the problems of surface roughness and grain size variation were properly addressed. Several experiments were carried out to determine the actual velocity of ultrasound energy in the selected material, optimum distance between probe and part and suitable frequency. Then, the signals were obtained from ultrasonic immersion testing of castings to determine the presence of both the simulated and real gas porosity defects.

The next step in the process of ultrasonic defect identification is pre-processing and analysis of the ultrasonic signals obtained from the rough surface of the castings. Signal processing and classification was carried out using the neural network toolbox in MATLAB software. Furthermore, a series of trials were done to obtain satisfactory ultrasonic signals from selected castings sections containing gas porosity type defects. Thereafter, a substantial number of inspection trials were done on both defective and non-defective castings to provide sufficient ultrasonic signals for training and testing the neural network component of the inspection system. Finally, a radiographic examination of castings subjected to ultrasonic inspection was carried out to validate the results obtained from ultrasonic inspection.

1.6 PERCEIVED CONTRIBUTIONS OF THIS RESEARCH

This research has made a number of specific contributions to the field of ultrasonic non-destructive testing in die casting applications. These contributions are summarized as follows:

- Calibration of experimental devices

  Different calibration methods have been used in ultrasonic inspection. In this research, emphasis was given to the apparatus used in the ultrasonic immersion testing, namely the PUMA robot and ultrasonic testing unit. A specific methodology was developed and implemented for repeatedly obtaining accurate ultrasonic signals from the components under inspection. Inspection trials were then carried out to determine the reproducibility of the measurement. This calibration process was carried out continually throughout the experimental phase of the project. The calibration results are described in Chapter 4. The implementation of a calibration methodology for the experimental devices reduced the amount of uncertainty and increased the inspection accuracy associated with the experimental results significantly.

  The results of this analysis were reported in a paper published in the Australian Non-destructive Testing Journal (listed in *Appendix A.1*).

- Ultrasonic testing of castings with material variation

  The effects of material variation on ultrasound signals were demonstrated with a comprehensive experimental program. These experiments addressed the problem of selecting a suitable frequency for inspecting inhomogeneous aluminium alloy castings. The grain size in the selected high pressure automotive die castings was mostly in the fine-to-medium range which is less than 0.5 mm in diameter. It has been determined in this research that the loss of ultrasonic signal echo due to grain size variation was small when, compared with the variation caused by changes in

the surface roughness of the casting. Hence, a technique was developed through isolation of the different factors affecting the signal echo in order to select a suitable frequency for inspecting the sample castings. The experiments relating to material variation demonstrated that the difficulty of testing castings arises from scattering of ultrasound at the rough front surface of the casting. The experimental results were used in developing a framework for a generic ultrasonic inspection procedure for aluminium alloy die castings. The experimental results also provided guidelines for selecting suitable transducer frequencies which would accommodate both the variation in material properties and the critical defect size to be detected.

The results of the analysis on the effects of grain size and surface roughness variation with respect to ultrasonic inspection of aluminium alloy die castings were published in Materials Evaluation, August 2005 (*Appendix A.1*).

- Classification of weak ultrasonic signals

The difficulty in identifying defects through visual analysis of the ultrasonic signals from rough surface aluminium die castings is emphasised in this research. Little research work had been carried out with castings having surface roughness values greater than 50 μm. It is important to inspect the castings in the as-cast state (surface roughness above 50 μm to 100 μm) because inspection after further processing will diminish the value of non-destructive testing. Hence, the proposed methodology for detecting gas porosity defects using actual and simulated defects of 0.5, 0.7 and 1 mm side-drilled holes in the as-cast castings using ultrasonic inspection was performed. The neural network approach successfully accommodated the noise in the ultrasonic signals obtained from castings with surface roughness ranging from 50 μm to 100 μm. Nevertheless, defects associated with castings of surface roughness beyond 50 μm could not be classified using this approach unless sophisticated signal pre-processing techniques are used. One of the contributions of this research was in obtaining and classifying weak

and noisy ultrasonic signals from as-cast rough surface die castings with defects (R_a value above 50 μm). It has been achieved through the selection and application of both appropriate ultrasonic inspection and signal processing techniques and parameters for this particular research problem. This achievement enables subsequent analysis leading to identification of defects in castings.

The results of this investigation were presented at the North American Die Casting Congress 2003 in Indianapolis, U.S.A. (*Appendix A.1*).

- Hybrid signal pre-processing technique

A contribution of this research was the investigation of combining existing signal pre-processing techniques for the purpose of maximising ultrasonic signal classification performance. The signal pre-processing techniques investigated included Fast Fourier Transform, Wavelet Transform and Principal Component Analysis. Signal pre-processing techniques usually use either time-variant or frequency-variant signals. However, in this research both the time-variant and frequency-variant signals were used in combination. The signal pre-processing was carried out prior to passing the ultrasonic signals into the neural network for defect classification. An approach to signal pre-processing not attempted previously has been investigated in this research. This approach was the application of FFT and WT pre-processing methods in sequence to investigate the possibility of achieving an improved classification percentage. The results indicated that this approach increased the defect classification percentage significantly – up to 84% for rough surface signals compared to 68% classification without signal pre-processing.

The outcomes of this research provide a basis for the development of an ultrasound based sub-surface defect detection system for aluminium die castings. The research exploits the advancements in Artificial Neural Networks, signal processing techniques and NDT technology in developing a non-contact inspection system to detect gas porosity defects in rough surface castings. Moreover, the inspection

system has the attributes required for on-line installation in the manufacturing environment.

1.7 OUTLINE OF THE THESIS

This thesis is divided into nine chapters as described below:

Chapter 1 presented a brief introduction to the background of the project and the problems to be investigated. The issue of inspection of castings for sub-surface defects is an old one and various inspection methods have been investigated over time. This project confines itself to the use of ultrasonic inspection techniques for the detection of sub-surface defects in rough surface aluminium die castings. Hence, the objectives emphasised the need to obtain an understanding of the casting process and the use of ultrasonic inspection techniques.

Chapter 2 contains an extensive literature review detailing the casting process and associated defects. It also deals with the external and internal factors affecting the ultrasonic inspection of castings and the work previously carried out in the area of NDT with respect to casting inspection. Also detailed is the application of artificial intelligence techniques in ultrasonic NDT, in particular, the application of neural network and signal pre-processing techniques for defect classification.

Chapter 3 describes the background theory and different methods of ultrasonic inspection, and provide details on ultrasonic transducers and different couplant types used in the ultrasonic inspection of castings. The background information on neural networks and their parameters is also provided in this chapter.

Chapter 4 presents the experimental program that was designed and implemented to inspect castings obtained from the Ford Motor Company and Nissan Casting Plant, Australia. The calibration of the test equipment is also described.

Chapter 5 outlines the ultrasonic inspection of castings, and explains the results obtained while varying the factors affecting ultrasonic inspection. This is one of the major building blocks of this thesis in that it provides an understanding of the practical difficulties in applying the ultrasonic inspection process to the casting application.

Chapter 6 details potential neural network topologies to be used in this research to detect defects once the best possible signal, in terms of amplitude, is obtained from the castings. This chapter also addresses the selection of each parameter of the neural network used in classifying ultrasonic signals from castings with and without defects.

Chapter 7 presents the results of the inspection carried out on aluminium castings with rough surfaces, including the results obtained from neural network classification of the ultrasonic signals from castings with defect and without defects. The classification performance obtained using neural networks and different signal pre-processing approaches are also presented.

Chapter 8 compares the results obtained using different signal pre-processing approaches with neural networks for defect classification. In addition, it evaluates the effectiveness of the developed methodology in relation to approaches described by other researchers.

Finally, Chapter 9 summarises the findings of the research program, and identifies areas for further research.

CHAPTER 2.
LITERATURE REVIEW

2.1 OVERVIEW

The literature review covers the following major areas:

- High Pressure Die Casting (referred to as die casting in this thesis)
- Sub-surface casting defects
- Non-Destructive Testing & Evaluation (NDT&E)
- Ultrasonic inspection
- Automated fault detection systems
- Artificial Neural Network (ANN), and
- Signal pre-processing techniques.

The objective of this review was to acquire an understanding of the context of the research and provide an impetus and background to the project methodology in the field of ultrasonic NDT of castings. Sources used included books, journal articles, trade journals, conference publications, International and Australian Standards on NDT, patent applications and NDT&E related websites.

As emphasised in the previous chapter, a deeper understanding in the area of NDT and casting quality was essential for this research. Hence, the literature review highlights the understanding of NDT and casting quality, their relationship and different signal processing techniques that can be used for defect classification. This chapter is divided into three major sections, namely:

- Die Casting
- Ultrasonic Inspection of Castings, and
- Signal Processing and Neural Networks.

An overview of the casting industry, its process and the defect types is presented in Section 2.2. The subsequent sections describe a review of ultrasonic testing and its limitations with respect to the inspection of castings. Finally, a review of automated inspection systems is presented. The emerging trends in this research area are also discussed.

2.2 CASTING INDUSTRY

2.2.1 Overview

A metal casting may be defined as a metal object produced by pouring molten metal into a mould containing a cavity which has the desired shape of the end product, and allowing the molten metal to solidify in the cavity [1]. Historical data indicates that casting began around 4000 B.C. According to Taylor *et al.* [6], copper was the first metal to be cast – it was used to produce bells for large cathedrals at the beginning of the 13^{th} century. In the 14^{th} through 16^{th} centuries, metal casting evolved from what was an art form to the casting of engineering shaped components [7]. However, the first authenticated casting in aluminium was produced in 1876 [8].

In the present context, die casting involves all processes that are based on use of metallic moulds [9]. The selection of the mould materials depends on the alloy being cast, the number of parts to be produced and the size of the parts. The process is a highly mechanised one, in which dies may be interchanged without making changes to the machine. Metal for die casting is melted in holding pots and transferred to the die casting machine pot as required. Dies are water-cooled so as to maintain them at constant operating temperatures. This prolongs the life of the die

and provides the fastest allowable cooling rate for castings so that they develop optimum properties [9].

High Pressure Die Casting (HPDC) differs from permanent mould castings wherein the metal is forced into the mould cavity under high pressure. In HPDC, molten metal is injected into a metal mould (die) at a high velocity. The solidification of the metal results in the end product [10].

As shown in Figure 2.1a, two die sections are mounted securely in a machine so that one is stationary, the other movable. The HPDC cycle starts when the two die halves are clamped together by the die casting machine. The metal is then injected into the die at very high velocity where it solidifies (Figure 2.1b). The die halves are separated and the casting is ejected from the die using ejector pins.

Advantages of the HPDC process include the ability to produce thin sections and the short cycle time involved. In comparison with other metal working methods, die casting is carried out with a minimum expansion of metal [11]. Die castings are so accurate in size that very little or no subsequent machining is necessary after removal of the gate[2].

[2] According to Taylor *et al.* [6], gates are channels through which molten metal flows to fill a mould cavity.

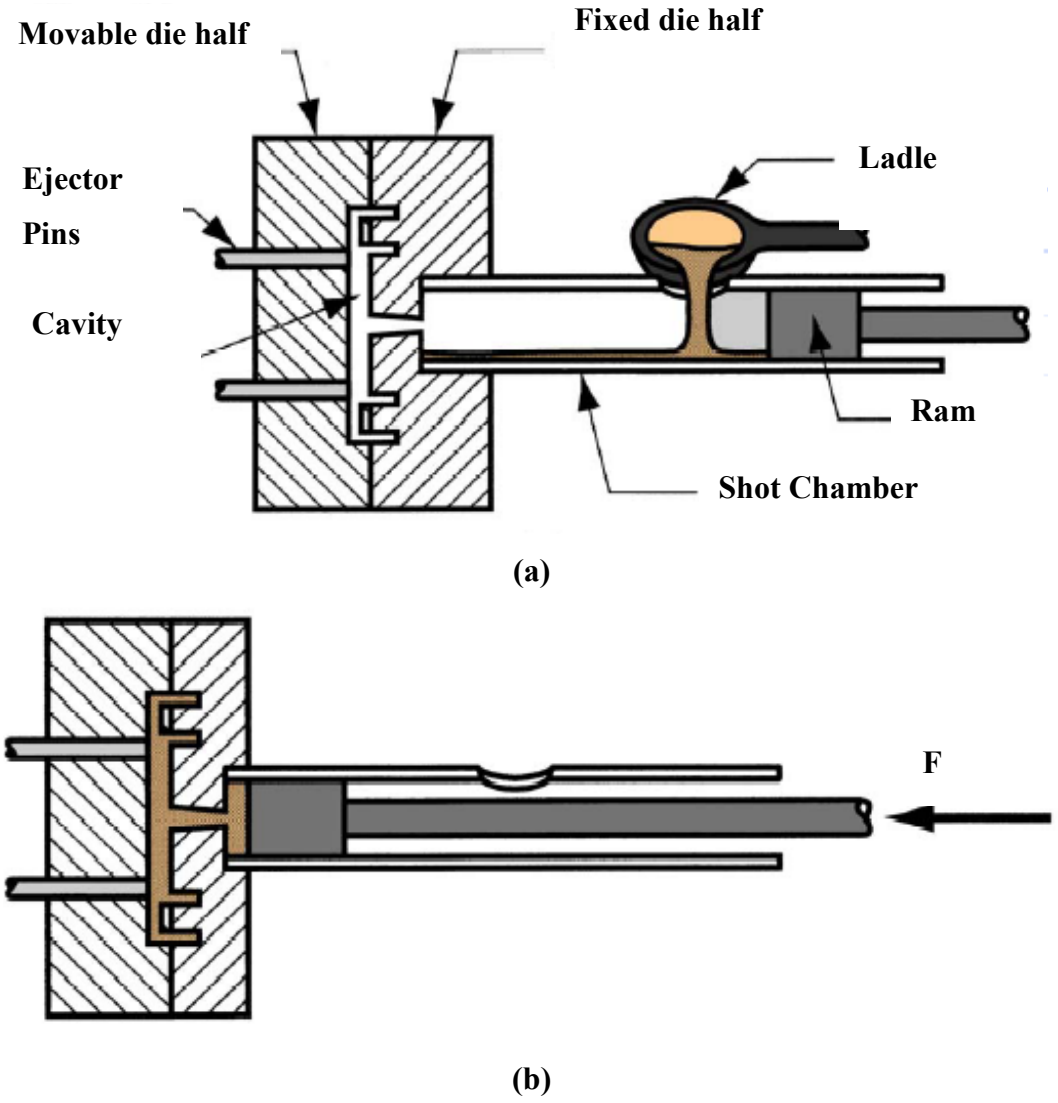

Figure 2.1 Cold chamber high pressure die casting set up (a) Molten metal poured into short sleeve chamber (b) Molten metal filled in the die cavity [12]

2.2.2 Casting Defects

In the high pressure die casting industry, the major problem is the inability of the die casting process to produce parts without discontinuity [13]. There are a number of factors that cause discontinuities in the castings. Sinha [14] investigated the types of failures in castings arising from manufacturing discontinuities. The discontinuities are regarded as true defects or flaws when the satisfactory function or appearance of the product is affected. Castings with such discontinuities are rejected and scrapped.

The logical classification of casting defects presents great difficulties due to a wide range of contributing causes, but grouping the defects in certain broad categories based on origin of defects is an accepted practice. Davies [15] stated that casting design and technique of manufacturing have an influence on the production of sound castings. According to Davies, depending on the location of the casting defects, they can be divided into two major categories, namely surface and sub-surface defects.

a. Surface Defects

Surface defects are discontinuities occurring on the surface or near to the surface (exposed to surface) of the castings. Surface defects in aluminium die castings can result from deficiencies at any stage of the manufacturing process [16]. The prevention of surface defects is a key requirement when producing most aluminium die castings. The prevention of defects related to the casting process can best be achieved through proper design of the die and feed system and control of the variables associated with the die casting process [16].

Rowley [17] has described in detail the major surface defects of castings – gas run, cope defect, seams, flow marks and slag inclusions. Most of these defects are related to the surface of the die and temperature of the mould, and result from pouring metal that is too cold into the mould. Usually these imperfections occur in castings with relatively light sections where two surfaces of flowing metal meet and do not fuse properly. In cold shuts, small shot-like spheres of metal are almost completely distinct from the casting. This can usually be prevented by using higher pouring temperatures. Surface defects may also be related to the finishing process at the surface. Crack-like defects that emerge on the surface of a material through propagation are possible sources of failure under conditions of either stress or corrosion, or both [6]. The types of inspection systems used to detect these defects are discussed in Section 2.3.3.

b. Sub-surface Defects

Sub-surface defects are not visible to the naked eye due to their occurrence below the surface of the castings. Typical casting sub-surface defects are [17]:

- Shrinkage cavities generated by contraction during solidification and insufficient feed of metal
- Blowholes and porosity occurring when gas bubbles are released during pouring and cooling
- Non-metallic inclusions generated by interaction between the molten metal and the mould material, a piece of the mould material itself, or by oxide films swept along with the metal pouring, and
- Hot tears caused by shrinkage during solidification, in combination with restrictive stresses.

Unlike the crack-like defects, all other casting defects are more or less voluminous and globular. For instance, the gas porosity defect is the most common voluminous and globular defect in high pressure die castings [16].

Among the different sub-surface defects presented in this section, porosity type defects may lead to hazardous flaws with regard to the loading capability of a material. These defects can be defined as voids in the material where the cast metal alloy is absent [18]. Much of the porosity is simply air entrapped as the metals move through the shot sleeve and runner as shown in Figure 2.2. Air will enter the die cavity unless it is removed using a vacuum technique. When such air or gas entrapment is sufficiently large and is located just under the skin of the casting, blistering may result. The air or gas in the void is subjected to the metal injection pressure. In the case of HPDC, the solidification of metals takes place in seconds, hence, air or gas entrapped cannot escape out of the vent in the die in that time [16].

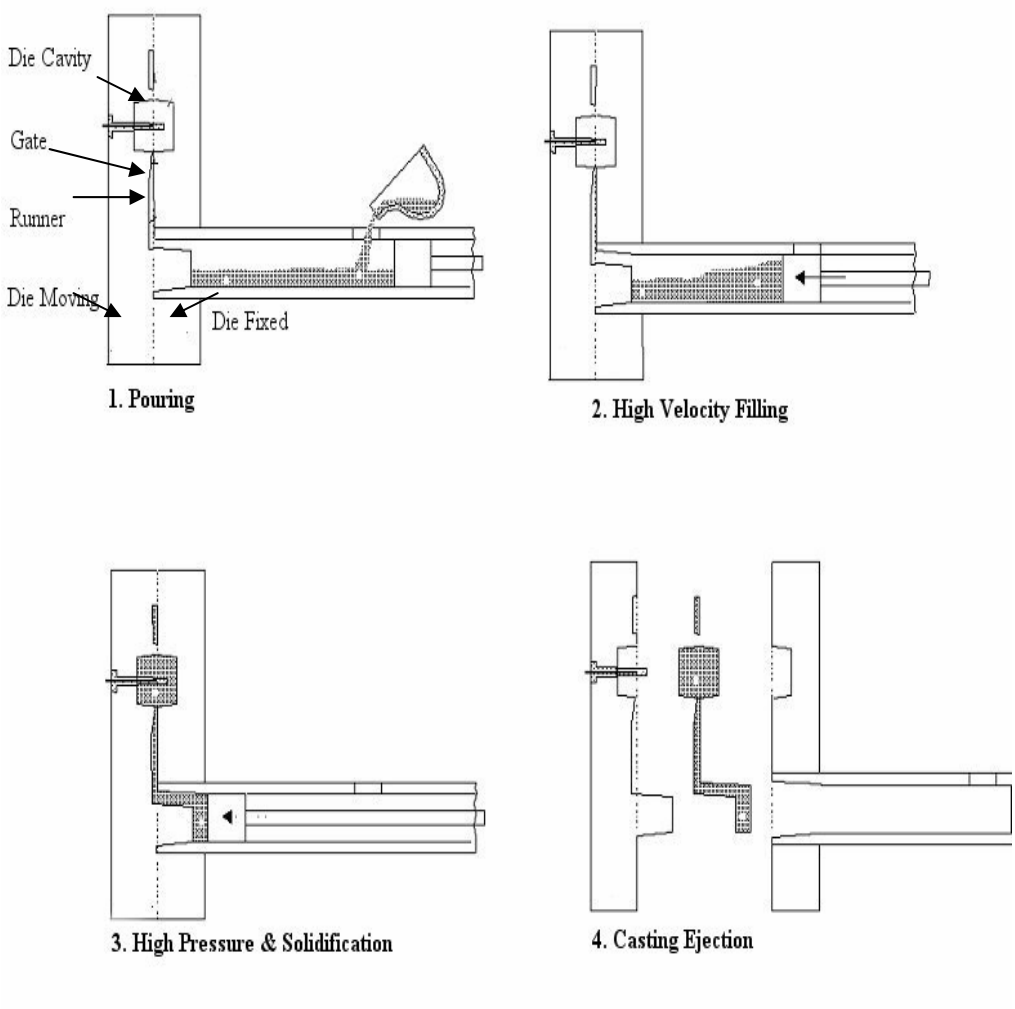

Figure 2.2 Stages of High Pressure Die Casting Process [19]

Surface reactions sometimes cause sub-surface porosity or pin holes. In aluminium alloys containing more than 1% magnesium, a reaction tends to occur between the magnesium of the alloy and the water vapour of the mould [6]:

$$Mg + H_20 = MgO + H_2 \text{ (gas)} \quad (2.1)$$

Gas porosity defects in aluminium alloy castings generally appear as rounded pores associated with gas, or as elongated inter-dendritic pores referred to as shrinkage porosity [13]. Common causes of excessive air porosity are turbulence in the shot sleeve and in the runner, poor flow patterns in the gating system, low metal temperature, blocked vents and overflows and excessive lubricants.

Figure 2.3 illustrates the shape of a typical gas porosity defect. They are formed by gas entrapped in the metal during solidification. The gas may be H_2 gas coming out of the solution within Aluminium, at the time of solidification or nitrogen, steam and air. Previous research work has shown that the location and area of porosity defects in relation to the free surface are important factors that determine the impact of defects on fatigue life of castings [20]. A large level of porosity, which is located in the centre of the casting may not effect mechanical properties or fatigue performance. A smaller, isolated pore near a surface may have a significant impact on the performance of the castings. However, according to Gupta *et al.*[21], the level of casting imperfections such as gas porosity is not always pre-determinable and they are generally unwanted in the end product.

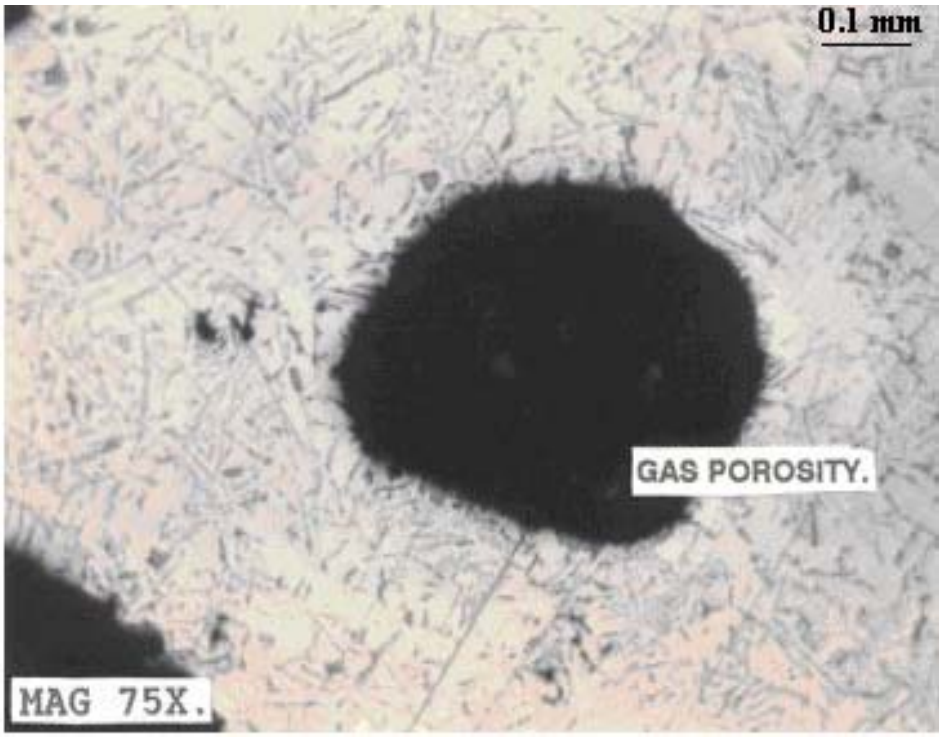

Figure 2.3 Gas Porosity in high pressure die casting part[3]

The solid metal that prevents gas from escaping to the vents can also prevent molten metal from feeding the area during the solidification process leading to gas porosity. However, the shrinkage due to gas porosity defects is minimal.

[3] Courtesy of Nissan Casting Plant Australia Pty Ltd

Before the problem of porosity can be addressed, it must be identified using an inspection system. Early detection of porosity defects can ensure that timely action is taken to rectify the situation [2]. Hence, casting inspection plays a vital role in delivering high quality castings to customers, and non-destructive testing is one of the tools used in casting quality inspection.

2.2.3 Summary

Richard *et al.* [1] and Taylor [6] undertook some of the earliest investigations in the field of metal castings. Even though their books were written nearly a half-century ago, they remain the main sources of reference on casting. Since then, the problem of porosity has remained a major concern. However, no method has been found to eliminate sub-surface defects completely from the die casting process. The importance of identifying sub-surface defects has been emphasised in this section. Especially, the exposure of new surfaces after machining operations must not reveal any defects. If any sub-surface defects are exposed after machining, then castings are considered as rejects. Deriving from this point, it is important to understand the different techniques available for die castings inspection to detect sub-surface defects.

2.3 NON-DESTRUCTIVE TESTING

2.3.1 Overview

Non-destructive testing (NDT) is the branch of engineering concerned with detecting flaws in materials. Flaws can affect the serviceability of the material or structure. Therefore, NDT is important to guarantee safe operation of the components and as well as quality control. NDT is also used for in-service inspection and condition monitoring of an operating plant and measurement of physical properties such as hardness and internal stress. The essential feature of NDT is that the test

process itself produces no deleterious effects on the material or structure under test [22].

Raj [23] highlighted the fact that the subject of NDT has no clearly defined boundaries. NDT ranges from simple techniques such as visual examination of surfaces to well-established methods such as radiography, eddy current testing, ultrasonic testing and magnetic particle crack detection. NDT methods can be adapted to integrate with automated production processes. Sattler [24] shared a parallel view that the term NDT is used to describe all methods which make the testing possible, or inspection of a material without impairing its future usefulness. Further, Sattler stated that from the industrial viewpoint, the purpose of NDT is to determine whether a material or part would satisfactorily perform its intended function.

2.3.2 Non Destructive Evaluation

Non-destructive evaluation (NDE) is a term used often interchangeably with NDT. However, technically, NDE is used to describe measurements that are more quantitative in nature. For example, an NDE method would not only locate a defect, but it would also be used to determine characteristics of that defect such as its size, shape, and orientation. NDE may also be used to determine material properties, such as fracture toughness, formability, and other physical characteristics [25].

2.3.3 NDT&E Technologies

At present, five major methods are available for inspecting metal casting. These methods are, Magnetic Particle Testing, Liquid Penetrant Testing, Ultrasonic Testing, Radiographic Testing, and Eddy Current Testing. Other less commonly used methods include Acoustic Emission and Thermal Radiation methods [4]. No single method can provide a complete solution for casting quality inspection. In some cases, a combination of NDT methods is usually used to determine the desired inspection

parameters [4]. Presented below is a brief literature review on the five major NDT methods.

a. Magnetic Particle Testing

Magnetic Particle Testing (MPT) is a NDT method that detects surface and near surface discontinuity in ferromagnetic materials using the principle of magnetisation [26]. Typically, a high current is passed through the casting, which in turn, establishes a magnetic field. If a discontinuity is present, it will disrupt the magnetic flux field from the current flow, resulting in a flux leakage. The inspection medium (iron particles) that is applied simultaneously with the current will be attracted to the areas of flux leakage and provide a visible indication of the discontinuity (i.e., particles will pile up over the area of the discontinuity). The external magnetic field indicates the internal defects. The surface condition of the component plays a vital role in MPT since it affects the flow of the magnetic field on the surface of the component.

The major advantage of this test method is that it is quick and simple in principle and application. It is very sensitive to the detection of very minute (less than 1 mm) shallow surface cracks. On the other hand, it has the disadvantage of being applicable only to ferrous materials. Furthermore, care is required to avoid burning of the casting surface at the points of electrical contact [27].

b. Liquid Penetrant Testing

Liquid Penetrant Testing (LPT) can detect surface discontinuity in both ferrous and non-ferrous castings [4]. This method uses the principle of capillary action which is the ability of a liquid to travel to or be drawn into a surface opening. The most critical step in this penetrant process is the pre-cleaning of the casting. Because the penetrant physically enters the discontinuity, the opening of the discontinuity must be free of any material that could inhibit the movement of penetrant.

This method is highly sensitive to fine, tight surface discontinuities such as cracks and cold shut. It is also effective in the detection of rounded indications, such as porosity. The discontinuity indications are viewed on the casting surface. The limitation of LPT is that the discontinuity must be open to the inspection surface. Based on the investigations carried out by Glatz [28], LPT is not always effective in locating small surface flaws in certain complex shaped parts. Further, the LPT method cannot be used detect sub-surface discontinuities.

c. Ultrasonic Testing

Ultrasonic testing (UT) methods use high frequency sound waves to detect surface and sub-surface discontinuities in both ferrous and non-ferrous castings [5]. UT can also be used to gauge the thickness of a casting. Because UT enables the investigation of the cross-sectional area of a casting, it is considered a volumetric inspection method.

UT has several advantages in both product quality control and in-service inspection for locating and characterising sub-surface defects and evaluating the mechanical properties [29]. These advantages include high probability of defect detection, less cost for automation and less hazardous to environment. However, there are problems in identifying defects such as porosity, inclusions and cracks in castings [30]. The major limitations are due to the sensitivity of ultrasonic inspection with respect to the grain size and surface roughness of the castings [31]. Detailed background information on ultrasonic inspection is presented in Chapter 3.

d. Radiographic Testing

Radiographic Testing (RT) is a method that uses X-ray or gamma energy to pass ionising radiation through a casting to reveal internal discontinuities on a film medium [32]. Gamma rays are ionising radiations which are the product of nuclear disintegration from a radioactive isotope. The RT method can be used with both ferrous and non-ferrous castings. This inspection technique utilises the ionising radiation to penetrate the cross-sectional area of a casting and expose a piece of radiographic film. When discontinuities such as cracks, gas and shrinkage porosity

are present in a casting, less radiation is absorbed and more radiation reaches the film. This increased film exposure to the radiation ultimately produces an image of the discontinuity on film.

Advances in computer technology have lead to a CRT screen replacing the film. With this technology internal discontinuities are revealed on the screen in real time. An advantage of radiography is that it can provide a permanent record of the casting quality after inspection. The orientation of the radiation source, the object and the film may cause distortion in the projected discontinuity image. The inspection requires access to both sides and surfaces of the casting. The discontinuity in the casting must be parallel to the radiation beam for the best possible detection. The disadvantage of this technique is that the casting thickness and density limit the possible range of inspection [31,32].

e. Eddy Current Testing

Eddy Current Testing (ECT) utilises an induced low-energy electrical current in conductive ferrous or non-ferrous materials. The alternating current creates an expanding and collapsing magnetic field in a longitudinal direction across coil windings. The magnetic flux is created, extending into the casting which in turn induces the flow of the eddy current. When a discontinuity is present, it affects the characteristics of the magnetic field associated with the eddy current, which then alters the interaction between the two magnetic fields detected at the surface. This altered interaction is displayed on the eddy current instrument display.

This inspection method is suitable for the detection of surface flaws or material changes that may not be detected by other NDT inspection methods [24]. A major limitation of the ECT inspection method is that it requires considerable knowledge and experience to properly establish inspection techniques and interpret the results. A further disadvantage is that it is only suitable for electrically conductive materials.

2.3.4 Flaw Detection in Castings

In the case of castings, flaw detection is almost exclusively concerned with manufacturing defects rather than with in-service inspection. The requirement for the quality inspection of castings is dictated by the end use of the casting. Each industry has specifications and acceptance criteria developed around each type of product manufactured. The testing of castings is complicated due to several variables such as the surface condition of the metal which are discussed later in this chapter.

In an investigative study, Barberis [33] found that NDT had been used in casting industries for more than 50 years. This was mainly due to the customers of die casting manufacturers, who expected castings to be supplied to a defined quality standard. Conformity to this standard usually depends on the quality of the inspection system. NDT of castings provides quality assurance for end products delivered to customers, and involves a combination of physical inspection methods that can be used to determine the integrity of a casting without causing physical damage to it.

Bowland [34] provided an extensive analysis of NDT inspection methods for castings in his research work. The importance of quality assurance and training was emphasised for each of the inspection methods used in the casting industry. Liquid penetrant, magnetic particle and visual test techniques have been used extensively for surface defect detection [4]. Radiography and ultrasonic techniques have been used for sub-surface defect detection [33,35]. In this section, emphasis has been given to inspection techniques that are relevant for sub-surface defect detection.

Leak testing of castings usually involves some form of wet bubble testing, often carried out in hostile environments [36]. Such testing usually has the relatively simple goal of determining whether a part leaks or not. The problem with using a leak test method to find a leak in a casting is the inability to identify the type and location of a defect. Heine [37] noted that evaluation of leak rates is qualitative, and subjective, and is always compared to standardised test procedures. Hence, tests should be conducted, beginning with leak tests and then progressing to more sensitive methods to obtain quantitative results.

Radiography has been the preferred method for testing castings. But radiography has inherent dangers because the radiation produced can have a detrimental effect on operators if they are exposed to it. The other problem with the X-ray image or radiography approach is related to the reliance on human operators to interpret the images produced. Human error in identifying defects in die castings may occur due to operator fatigue, distraction and lack of sufficient experience. There may be circumstances where orienting a casting properly for radiography is impossible due to shape and thickness constraints. In such cases, radiography is not useful in the inspection of castings. However, digital radioscopy has experienced a significant upturn in the past few years as noted by Hanke [38] due to better digital images plus the development of increasingly powerful and complex algorithms for image processing.

Even though radiography is the generally accepted test method for castings, ultrasonic inspection can also be used due to its low environmental impact and its effectiveness with respect to near-surface defect detection and location [35]. However, castings do present a problem in relation to ultrasonic inspection, the parameters affecting propagation of ultrasound in the die castings (test specimens) are discussed in Section 2.5. The surface roughness of die castings and their dimensional variations scatter the sound pulse and make discontinuities difficult to detect. Some of the problematic areas of ultrasonic NDT such as surface roughness and grain size variation need to be addressed as suggested by Rickards and Wickens [3]. Lavender [39] has discussed the effects of surface conditions on performance of different methods of NDT. Apart from these problems, the ultrasonic inspection method also requires a vast amount of knowledge and experience to fully establish an inspection methodology and interpret results[4].

Lavender and Wright [40] discussed some of the advantages of ultrasonic inspection over radiography, including the cost factor. According to their findings, ultrasonic inspection has a large cost benefit ratio compared to radiography due to

[4] A review of the influence of surface roughness and grain size on ultrasonic inspection is presented in Sections 2.5.3 and 2.5.4 respectively.

the ease of automation. Recently, Kleven and Blair [41] presented a comparison of ultrasonic and radiography inspection techniques for the testing of castings (Table 2.1). They concluded that a reasonable balance has to be maintained in the inspection of castings. When the defects are oriented parallel to the scan surface, ultrasonic inspection is suitable, and if oriented perpendicular to the inspection surface then X-ray inspection is suitable. In some cases, a combination of both ultrasonic and radiography has to be used. This also confirms the views of Long [4], who concluded that a single inspection technique does not provide a complete solution for casting inspection. Another factor indicated in Table 2.1 is that near-surface detection and surface roughness are not easily accommodated with ultrasonic inspection.

Characteristic	Ultrasonic	Radiography
Equipment cost	+	-
Operating training	-	+
Near surface detection	-	+
Portability	+	-
Large part size	=	-
Rough surface	-	=
Need for calibration	-	+
Part attenuation/grains	-	=
Intricacy of part geometry	-	=
Limited plant space	+	-
Discontinuity orientation	=*	=**
Permanent record	-	+

-	not advantageous
+	Advantageous
=	moderate advantageous
*	if oriented parallel to scan surface (planar or crack like)
**	if oriented perpendicular to part surface/radiation beam (planar or crack like)

Table 2.1 Comparison of ultrasonic and radiography inspection of castings [41]

2.3.5 Summary

The future of the casting industry depends on castings meeting the requirements of customers in terms of quality and performance. The ability to offer these guarantees will increasingly rest on casting manufacturers, who can provide NDT&E facilities to assess the quality of the castings. Additionally, the time spent on, and investment in, NDT&E by casting manufacturers is wasted if the test procedures are not reliable. The two common NDT technologies available for sub-surface defect detection are X-ray and ultrasonic inspection systems. It is important to recognise the advantages, and eliminate the problems associated with NDT methods. In ultrasonic inspection, major problems are associated with surface roughness, grain size, geometries of products being inspected, and lack of experienced operators. Flaw detection in castings with ultrasonic inspection is also difficult when there is a requirement to identify near-surface defects (Table 2.1). Hence, the importance of this research work is in understanding the limitations of ultrasonic testing particularly in its use in the inspection of castings to locate defects in the vicinity of rough surfaces.

2.4 ULTRASONIC INSPECTION OF CASTINGS

Ultrasonic NDT is useful in the inspection of castings of simple design where the echo pattern can be reliably interpreted [31]. The highest degree of reliability in ultrasonic testing of castings is obtained when the influence of test specimen variables and their effects are properly understood. The literature review documented in this section mainly focuses on the ultrasonic inspection of castings and the different factors influencing inspection of castings.

The application of ultrasound has a long history with respect to casting inspection in the foundry industries. During the period from 1940 to 1950, the use of ultrasound technology in examining castings was influenced by several difficulties [42]. This was mainly due to the many variables associated with the inspected

materials such as iron and steel. These variables include the microstructure characteristics, surface roughness, and exterior shape that affect the reliability of ultrasound testing. As a result, the use of ultrasound technology on as-cast products was not widely accepted at this time.

The use of aluminium castings in recent years has increased dramatically, emerging in applications such as the nuclear, aerospace and automotive industries. As a consequence, there has been much research to increase the reliability of ultrasonic technology in the testing of aluminium die castings. A recent literature review indicated that ultrasonic techniques are among the most popular NDT methods used for product quality evaluation [43].

Between 1985 and 1987, Kuppermar *et al.* [44,45] investigated the effect of structure orientation on ultrasound propagation. They also examined changes in ultrasound propagation speed and beam skewing, with respect to changes in material properties. Similarly, Boveyron *et al.* [46] examined the different structure types of material (columnar, fine and coarse) as well as changes in columnar angles and their effect on ultrasound propagation and attenuation in stainless steel casting ingot. It was found that material properties had an impact on ultrasonic inspection.

Kapranos *et al.* [47] presented results of X-rays and ultrasonic examination of porosity and depth of major voids in thixocasting products. They stated that NDE results correlated well with destructive microscopic analysis. Similarly, Yao and Liu [48] detected the porosity distribution in tensile test samples using the ultrasonic method to reveal the fracture zones.

Nelligan [49] demonstrated that ultrasonic flaw detectors can be used to detect internal flaws in castings. However, it was found that for shop floor applications, the operator should be experienced and have reference standards for reliable interpretation of the ultrasound echoes. Nelligan's research focused mainly on the thickness measurement of castings and material analysis. However, this research also investigated flaw detection of castings and concluded that defect

detection could be automated when the inspected parts had simple casting geometries and smooth surface finish.

This section of the literature on the ultrasonic inspection of castings has identified the challenges in carrying out inspection on castings with rough surface and non-uniform grain size [50]. The following section addresses the factors that affect the ultrasonic inspection of castings.

2.5 FACTORS AFFECTING ULTRASONIC INSPECTION

2.5.1 Overview

The variations in a typical aluminium alloy die casting relevant to ultrasonic inspection are associated with factors such as entry surface, part geometry and internal structure [51]. In addition, reflective surfaces (i.e. back surface of the casting) also contribute significantly to the effectiveness of the ultrasonic technique. Effectiveness of ultrasonic testing depends on a number of parameters, which may be divided into four groups: ultrasonic instrument performance; transducer performance; material variation; and defect variation [52]. A large number of studies have been undertaken in an attempt to understand the effect of roughness, grain structure and geometry on ultrasonic signals [53-56]. The aim of this section is to provide an overview of the various findings and developments in ultrasonic inspection systems in relation to detecting porosity defects in aluminium die castings.

2.5.2 Factors Affecting Velocity

Temperature has a direct effect on the velocity of sound in materials [25]. An increase in temperature results in an increase in velocity of ultrasound. However, this would not be the same with all metals and alloys [25]. If the material being examined is at a considerably higher temperature than the surrounding air, accurate

determination of the pulse-echo beam path can become more complicated. Brunk [57] stated that the effects of room temperature and immersion water temperature need further investigation while studying the influence of ambient temperature changes on ultrasonic immersion testing of steel parts.

Ambardar *et al.* [58] investigated the effects of grain size and porosity levels on the velocity of ultrasound. Their work highlighted the importance of achieving high accuracy in velocity measurement in order to gauge variations in material properties. Ambardar *et al.* [58] used the time delay between two back wall echo signals to measure the velocity of ultrasound and their approach yielded reliable and reproducible results even with coarse grained materials. One important finding in their work was that the velocity of ultrasound was independent of porosity size. Their work also highlighted the importance of tracking the changes in velocity of ultrasound with grain size variations in aluminium alloy castings.

2.5.3 Surface Roughness

The condition of the surface through which a sound beam enters a material is an important factor in ultrasonic NDT. Detectability of discontinuities such as cracks, voids and porosities is greatly affected by the extent of roughness. Increased roughness reduces the transmitted energy of the sound beam and this, in turn, reduces the amplitude of the received signal [59], leading to difficultly in measuring the size of the discontinuity. The measurement of back wall echo amplitude provides a better understanding of the attenuation due to the material characteristics [59]. Appreciation of the problem has led to a large number of studies investigating various aspects of the material characteristics on ultrasonic test signals [60]. From the literature, it is evident that the results obtained were based on theoretical or model based studies [61].

Blessing *et al.* [54] carried out ultrasonic inspection on the steel samples at a frequency range of 1 to 20 MHz to study the effects of surface roughness on the ultrasonic signal echo amplitude. They observed multiple back wall echoes (a total of

four) due to multiple reflections within the steel samples with surface roughness up to 23 μm R_{RMS} value. The effect of surface roughness was minimal up to 23 μm R_{RMS} value as observed by Blessing *et al.* [54] in their research work at the low frequency range compared to the high frequency range such as 15 and 20 MHz as shown in Figure 2.4.

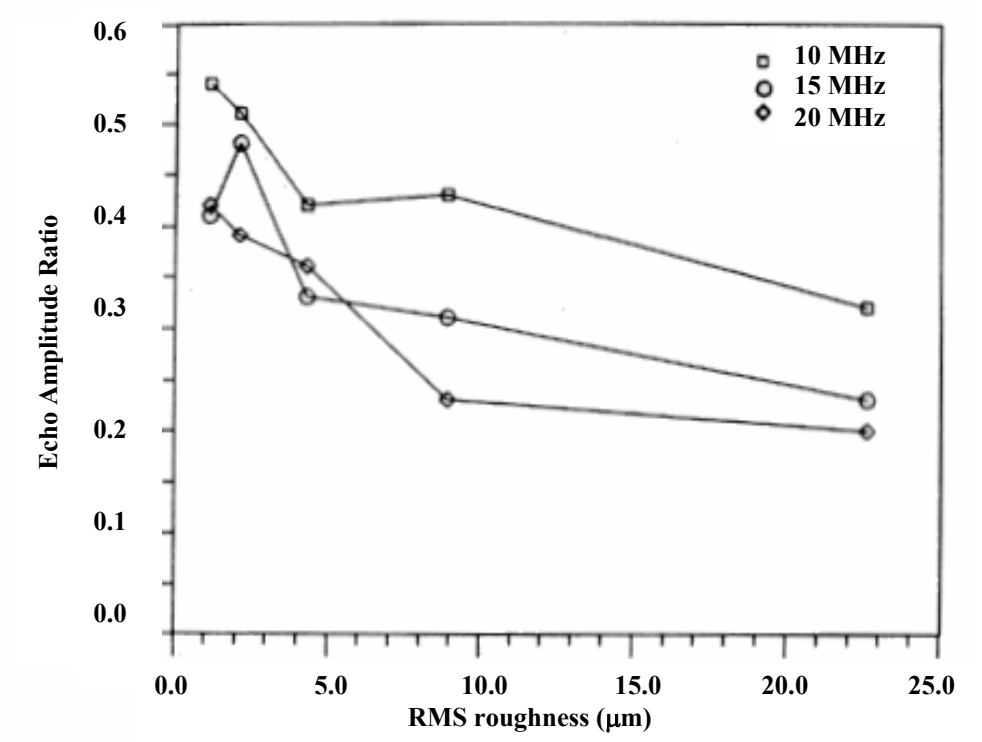

Figure 2.4 Fourth to first back wall echo amplitude ratio versus sample roughness at three discrete frequencies [54]

Thavasimuthu *et al.* [60] investigated the effect of front surface roughness on the ultrasonic signal amplitude in samples with various discontinuities. The effect of rough surface interaction with contact testing and effects of backscattering within the samples have been investigated using specimens with simulated surface roughness. The scattered signals that are directed back to the transducer are known as backscattered signals [60].

Bridge and Tahir [61,62] studied the scattering of ultrasound from periodically and randomly rough surfaces with the centre line average surface roughness ranging from 0.1 to 14 μm using 4-30 MHz frequency probes. Their

results indicated that a periodically rough surface acts like a diffraction grating and a random rough surface can be accommodated by a Rayleigh scattering model. They also stated that the distortion effect was more pronounced with random surfaces at the liquid-solid interface in ultrasonic immersion testing. Bridge and Tahir [61] concluded that there is a need to study the effect of surface roughness on ultrasonic immersion testing in detail.

Rose *et al.* [63] used an ultrasonic NDT method to identify gas porosity defects in aluminium alloy castings. They also investigated the effects of surface roughness on ultrasonic signals from the castings. Their study concentrated on quantitative assessment of gas porosity defects in die casting aluminium materials of plate-like geometries. Similarly, Adler *et al.* [64] investigated porosity defects in aluminium cast materials, and used volumetric analysis to identify gas porosity defects. They studied the effect of backscatter in their work on the ultrasonic inspection of aluminium cast materials. Their theoretical analysis of the attenuation ratio indicated that it was independent of frequency or surface roughness up to 40 μm root mean square value (i.e., equal to 36 μm R_a). They also found that the transmitted wave was attenuated in a similar way to the reflected wave at the water-aluminium interface during ultrasonic immersion testing.

Ambardar *et al.* [65] also investigated the effects of surface roughness and grain structure variations on ultrasonic signals obtained from sample aluminium die casting blocks using the backscattering of ultrasonic sound method. In these investigations, the arithmetic mean surface roughness (R_a) values were in the region of 50 μm. The results of their investigation lead to the conclusion that an increase in surface roughness decreased the back wall echo component of the ultrasonic signal.

In the late 1980s Onozawa *et al.* [66] constructed a multi-transducer (probe) head to detect near-surface flaws in castings with rough surfaces. Even though they stated that material with surface roughness of more than 50 μm (R_a) was inspected with the new probe, no detailed descriptions were provided on the effect of surface roughness on the performance of ultrasonic contact inspection. The work mostly

concentrated on the application of the multi-transducer head on cast iron castings to determine the capability of detecting flaws lying close to the surface.

Bilgen [67] in his doctoral research work investigated the effect of surface roughness on ultrasonic immersion testing in detail using a theoretical model. Bilgen [67] used a brass part for inspection with a surface roughness variation value between 1 and 500 μm root mean square (RMS) values, while the surface correlation length varied from 100 μm to several millimetres. Figure 2.5 compares the normalised variance Q(z) of the signal for four different surface roughness in RMS heights (h_{RMS}) from 12.5 μm to 50 μm for a varying focus distance (Z) of the ultrasonic signal within the brass castings. The normalised variance Q(z) was used to determine the variance in the backscattered signal as a function of depth in the material under inspection. The variance in the backscattered signal indicates the backscattered power received from the defects located at a particular depth (z). This variance value was then used to determine the signal variation due to change in surface roughness compared to the smooth surface. Figure 2.5 shows the dependence of Q(z) on the surface roughness, correlation length, frequency and focal length. It was found that the signal peak was larger for high surface roughness values and decayed faster than for the smaller surface roughness parts.

As illustrated in Figure 2.5, there was a pronounced dip in Q(z) value near the focal depth (4 cm). This dip in Q(z) was observed only with the focused probes and not with the unfocused probes when similar experiments were carried out [67]. According to Bilgen [67], only the coherent part of the ultrasonic wave field participates in focusing and it dominates the backscattered signal. Hence, in the focal region, the signal-to-noise ratio is relatively unaffected by surface roughness, as the signal and noise are altered in the same manner. However, for a surface roughness above 25 μm, the coherent part of the ultrasonic beam becomes negligible even in the focal area and a high loss in the signal-to-noise ratio results [67]. The large variation of Q(z) was observed for surface roughness greater than 25 μm illustrated in Figure 2.5. Focusing changes the backscattered signal and consequently attention must be given to select a suitable ultrasonic focus probe in order to accommodate the surface roughness variation.

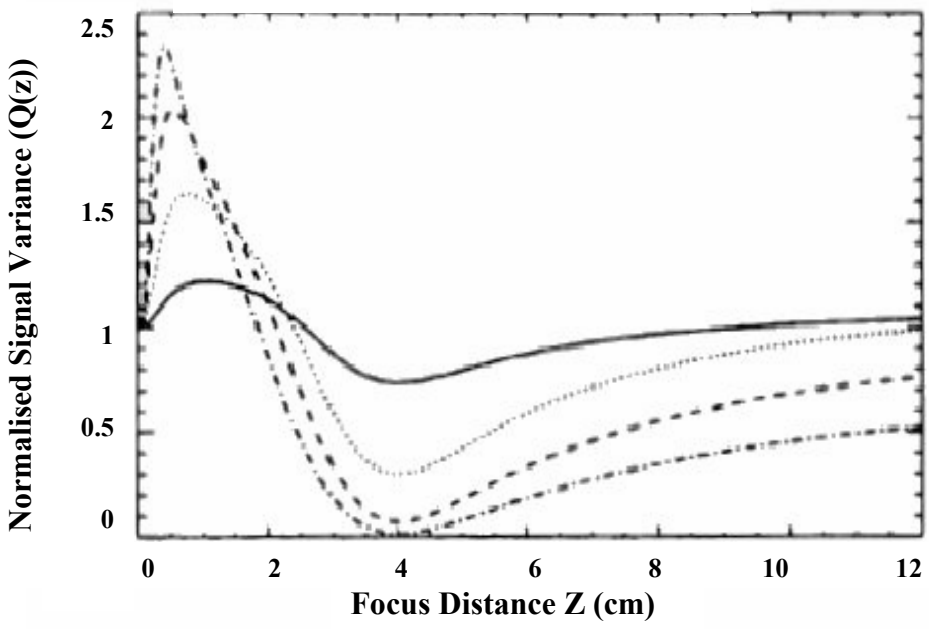

Figure 2.5 Comparison of the normalised variance Q(z) of the signal for four different RMS heights: solid line 12.5 μm , dotted lines 25 μm, dashed line 37.5 μm and dash-dotted line 50 μm with f = 10 MHz [67]

The casting surface roughness depends on the die casting process parameters (die temperature, cooling rate, etc.,) and the nature of the die surface. The surface roughness of the casting increased, as the die surface wear increased. It had random textures and there was no sequence to the peaks and valleys or to its height or depth [68]. It was found that, there was no uniform surface roughness value for castings manufactured from the same die casting machine with the same die or in the same batch [2].

A further review of the literature on the effects of surface roughness on ultrasonic signals revealed that no detailed investigation of castings with a roughness greater than 50 μm (R_a) has been carried out. The review of literature also indicated that ultrasonic immersion testing of aluminium die castings with varying surface roughness has not been adequately investigated. However, a limited number of studies [69,70] have been made to relate ultrasonic parameters to the micro structural characteristics and engineering properties of materials. Some investigations have also focused on surface roughness induced changes in ultrasound signals. Most of the

work with respect to surface roughness was carried out on surfaces with roughness (R_a) values around 50 μm.

In this particular research, it was important to inspect the casting in the as-cast state (with surface roughness between 50 μm and 150 μm) because further processing (i.e., machining) weakens the justification for a non-destructive testing application (Section 1.3). Hence, there is a need to determine the limitations of ultrasonic inspection of castings with surface roughness values greater than 50 μm.

2.5.4 Grain Size Variations

Metallurgical characteristics of castings have a strong influence on the performance of ultrasonic inspection. A large grain size relative to the wavelength of ultrasound gives rise to high background noise and high attenuation [29]. Scattering of ultrasound also occurs due to presence of large grain size leading to a low signal to noise ratio. Ambardar *et al.* [71] investigated the effect of porosity defects, defect size and grain size on ultrasonic signal attenuation. In their investigation, an Al-4.5% Cu alloy casting was used to determine an attenuation coefficient, which was influenced by porosity defects, defect size, grain size and probe frequency. Attenuation is inferred from a rate of decay of multiple echoes and attenuation coefficient is defined as the rate of reduction of average ultrasonic signal intensity with respect to distance along a transmission path [22]. The attenuation coefficient increases with increase in grain size, and decreases with decrease in porosity diameter and frequency. Since the attenuation is frequency dependent, a single attenuation coefficient only applies to a single frequency. It should be emphasised that Ambardar *et al.* [71] work was specifically on Al-Cu alloy and it would not be necessarily valid for other alloys. They concluded that a major factor in ultrasonic inspection was establishing a relationship between material grain structure and a suitable probe frequency. Howard and Enzukewich [72] carried out a similar research study on the effects of grain size variation on alloy steel inspection. The results of this investigation revealed that heat treatment of the materials under inspection lead to less attenuation of ultrasonic signals. However, they also stated

that this procedure would not suit all alloy metals due to the variations in the effect of the heat treatment process.

Adverse signal-to-noise ratio is one of the problems associated with ultrasonic inspection of aluminium castings. Inhomogeneous casting materials lead to a varying level of background noise arising from scattering at grain boundaries. Hence, a varying level of grain size in the material would result in varying level of scattering. One way to alleviate this problem involves the use of focused transducers – a high intensity, narrow beam will interact with a defect and provide a better signal to noise ratio when compared to a less intense and unfocused beam. Ogilvy [73] applied a theoretical model in the study of focused beam behavior in austenitic weld materials, and observed that focused transducers contribute to increasing the signal-to-noise ratio in ultrasonic inspection of austenitic weld materials. Stepinski and Wu [74] carried out a similar investigation on copper components. They evaluated attenuation coefficients for a number of copper specimens covering a certain range of grain sizes. There was a clear correlation between grain size variation in specimens and the attenuation due to scattering [74]. It may be argued, that a solution to this problem would be to simply reduce the grain size of castings such that higher frequency ultrasound may be used. Stepinski and Wu [74] stated, however, that the grain structure has a strong bearing on a casting's mechanical properties and performance and should be not be altered in the casting process. Hence, a thorough investigation of castings with varying grain structure is necessary in determining the effectiveness of ultrasonic inspection.

2.5.5 Mode Conversion within Test Specimen

Ultrasonic beams are reflected when they encounter a medium of a different acoustic impedance[5]. The surface at which this reflection occurs is called an interface. The amount of reflection depends on the acoustic impedance ratio between

[5] Acoustic impedance $Z = \rho v$ where ρ is the material density and v is the ultrasound velocity in the material [22]

the two media involved [22]. Mode conversion (the splitting of incident ultrasonic wave into longitudinal and shear components) takes place when an ultrasonic beam contacts the interface between two different media at an angle other than 90° to the surface. The transmitted ultrasonic waves can produce two refracted beams i.e., longitudinal and shear waves. Snell's law (Equation 2.2) can be used to determine the angular relationships between the incident and refracted beams when two different mediums are involved.

$$Sin\ \phi_1 / Sin\ \phi_2 = V_1 / V_2 \tag{2.2}$$

where ϕ_1 = Incident angle of the ultrasonic beam in medium 1,

ϕ_2 = Refracted angle of the ultrasonic beam in medium 2,

V_1 = Velocity of ultrasound in medium 1 and

V_2 = Velocity of ultrasound in medium 2 (either longitudinal or shear wave)

The refracted shear beam angle will be half the longitudinal beam angle, as the velocity of the shear wave is about half the velocity of the longitudinal wave [5]. The mode conversion has important implications for this research due to the requirement for ultrasonic immersion testing and presence of significant surface roughness in the castings.

2.5.6 Orientation and Depth of Discontinuity

Ultrasonic inspection of castings has limitations with regard to detection of discontinuities based on orientation, size and depth. Cracks and planar discontinuities must be oriented approximately perpendicular to the ultrasound waves. The return signal from the defect is influenced to a large extent by size and orientation of the defect. Few studies have dealt with the estimation of the combined effects of porosity and grain size on the attenuation coefficient [71]. The variation in the size of the defect can be detected by measuring the change in attenuation coefficient [71].

Thavasimuthu *et al.* [75] investigated the problems of mis-oriented defects (defects which are not exactly perpendicular to ultrasonic wave propagation) using angle beam inspection. The results of this research indicated that it was difficult to detect mis-oriented defects and the effectiveness of detection depended on the actual defect type. In the phenomenon of shrinkage, molten metal shrinks while cooling, leading to the formation of cavities within the solidified material. Crack formation then takes place due to the thermal stress introduced into the molten metal. Thavasimuthu *et al.* [75] have concluded that the selection of equipment and probe are dependent on the type of metal and defects to be inspected.

An international round robin test carried out by Engl *et al.* [76], indicated 100% detectability of defects ranging in size from 4 to 5 mm, only when a proper choice of inspection parameters was guaranteed. The effect of variation in the inspection parameters such as frequency, transducer size and incidence angles were considered for defect detection. Their work did not focus on rough surface castings or ultrasonic immersion testing. However, the investigation emphasised the importance of proper selection of inspection parameters and also the need for further work to determine the influence of the inspection parameters on ultrasonic based inspection of aluminium die castings.

2.5.7 Summary

In this Section 2.5, a review of previous literature investigating the problems encountered during ultrasonic inspection of die casting parts was presented. The importance of determining appropriate inspection parameters such as ultrasonic frequency and actual velocity of ultrasound within the material for the inspection of selected aluminium parts was emphasised. The literature review also identified the significance of the back wall echo in ultrasonic casting inspection, as it provides a measure of ultrasonic signal attenuation within the parts. However, it was found that there was uncertainty with respect to determining whether the ultrasonic signal loss was due to scattering from a discontinuity, non-uniform grain boundaries or a rough surface.

2.6 NEED FOR RELIABLE CASTING DEFECT DETECTION

A variety of defects can arise in die cast products during the manufacturing process. The impact of the defects on performance depends on their location, size and operational conditions. Hence, their classification holds much significance in determining the overall casting quality. The term 'imperfection' or 'defect' refers to any flaw, fault or irregularity in the structure of the material that may cause weakness or failure in the functioning of the product or system with which it is associated [77].

Defects are usually related to the method by which a component is produced. Manufacturing defects of castings are classified as rough or smooth cracks, porosity, inclusions or laminations. They may also be classified as planar wherein they have length and breadth but negligible depth, and non-planar or volumetric when they have length, breadth and depth [78]. Gas porosity type defects are considered to be volumetric, as shown in Figure 2.3.

According to Rajagopalan *et al.* [79], the main tasks of ultrasonic inspection of castings are:

- Reliable detection of all defects
- Location and classification
- Sizing and characterisation of defects, and
- Ease of interpretation of results.

Thavasimuthu *et al.* [80] observed that flaw detection was more difficult to address with human operators when associated with complicated geometries of the part and noisy or incomplete data. Recent advances in computing power enable NDT&E to be used for such practical applications as detecting and evaluating defects in casting structures. The use of computers to perform part of the analysis and classification process should result in improvement of overall testing performance [81]. According to Gayer *et al.* [82], the separation of relevant from non-relevant information and defect characterisation in manual testing are highly dependent on the examiner for the radiography testing application. These conclusions concur with those of Thavasimuthu *et al.* [80] in relation to manual ultrasonic inspection.

In order to remove the operator from the decision making area, Carter [83] used artificial intelligence tools for the purpose of automating the interpretation of signals received from the ultrasonic equipment. Among these tools, artificial neural networks have been recognised as being very efficient in the area of pattern recognition.

One of the problems associated with ultrasonic inspection is that the defect echo may not appear as an isolated response but may instead be surrounded by geometric echoes, and the defect may be a small addition to a large geometric echo. Also, movement of the transducer during scanning can change the timing of the echoes for both defect and geometric image patterns, which may lead to further inspection difficulties. To resolve some of these issues Sykes [84] used motorised probe heads for rapid and repeatable inspection of complex components with minimum human intervention. This system could also eliminate the human error in handling the ultrasonic probes. Atkinson *et al.* [85] also used a similar type of semi-automated inspection system for an austenitic casting and weld inspection application. Their approach brought together sophisticated data collection and display methods, signal processing and special scanning techniques in order to improve the inspection capability for coarse grained materials. Atkinson *et al.* [85] demonstrated useful improvements in inspection capability with their approach. They used the time-of-flight-diffraction[6] (TOFD) method and signal-to-noise ratio methods to identify defects.

Automation of the ultrasonic inspection process is highly desirable as overhead cost represents a significant proportion of inspection costs. Manual inspection with single-element probes is widely used because it can be adapted to the great range of materials and geometries encountered. The probes are used to inspect a point on the surface and are not well suited to area coverage, which is time-consuming and costly. Automated mechanical scanning can increase the inspection speed, but this is complex, costly and inflexible [84]. Hence, attention has to be

[6] According to Silk [147], TOFD method relies on the diffraction of ultrasonic energies from 'corners' and 'ends' of internal structures (primarily defects) in a component being tested

given to the development of low cost, flexible inspection methodologies and techniques that can be easily automated.

2.7 SIGNAL INTERPRETATION

2.7.1 Overview

The complexity of the inspection task and the common occurrence of large production runs increase the demand for signal processing analysis of ultrasonic signals. This section aims to highlight the need for signal analysis, and describes the different methods used in the automation of defect detection and signal classification in various applications. Furthermore, a review of the overall application of Artificial Intelligence (AI) and signal processing techniques is presented in relation to ultrasonic inspection.

2.7.2 Processing NDT data

Most NDT data has to be stored and displayed for assessment purposes. The basic requirements of this process are to:

- Extract the necessary information and store it in a suitable permanent form, and
- Display the information in a manner in which it can be easily accessed.

The techniques used for this purpose have typically been based on AI, Expert Systems and Neural Networks [83,86].

On the signal processing side, it appears that artificial intelligence technology is now sufficiently mature to be used on the shop floor. In this respect, sensor fusion, signal knowledge representation, expert systems, neural networks, fuzzy logic and computer vision are seen more frequently in NDT&E applications [86-89].

2.7.3 Signal Pre-Processing

2.7.3.1 Overview

Signal pre-processing is the first step in ultrasonic signal interpretation. Neural network training can be made more efficient if certain pre-processing steps are performed on the network input signals. Suppose that a non-stationary time series signal consisting of a transient component (e.g., target signal) superimposed on a signal-dependent interference (e.g., cluster) are to be classified. An neural network can be applied to the received signal directly, thereby forcing the neural network to discover the inherent features characterising the signals and then performing the desired detection. A practical drawback of this simplistic approach, particularly in the context of large-scale complex problems such as one presented in this thesis is that it can be clearly time-consuming and difficult. There is a need for signal pre-processing to be applied on the input signals to achieve better classification. Three commonly used types of signal pre-processing methods are discussed briefly in this section.

2.7.3.2 Fast Fourier Transform

The Fast Fourier Transform (FFT) algorithm is used for the conversion of time domain signals into frequency domain representations of signals [90]. According to Brigham [90], the FFT is a standard pre-processing technique used in digital image processing. The idea is to expand the signals in a Fourier series and use a limited number of Fourier coefficients to reduce the signal noise. The filtering or reducing of signal noise is carried out by highlighting particular frequency components that are associated with defect signals. To take the Fourier transform of a waveform is to decompose or separate the waveform into a sum of sinusoids of different frequencies [90]. The formula of the Fourier Transform of a continuous waveform $y(t)$ is [91]:

$$Y(f) = \int_{-\infty}^{\infty} y(t) e^{-2j\pi ft} dt \tag{2.3}$$

Where *f* is the frequency of the signal and *Y (f)* is the Fourier representation of the original time domain signal $y(t)$. In this application, however, the acquired signals are not continuous because they are computer real-world data (they are sampled), and belong to the discrete group. Therefore, it is necessary to use the Discrete Fourier Transform (DFT) [91], where:

$$Y(k) = \frac{1}{N}\sum_{n=1}^{N} y(n) e^{-j2\pi(k-1)\left(\frac{n-1}{N}\right)} \qquad 1 \le k \le N \tag{2.4}$$

Y (k) is the DFT of the signal as a function of the frequency *k.* The drawback of the FFT is that when transforming the signals into the frequency domain, the time information of the signals are lost [90].

2.7.3.3 Principal Component Analysis

Feature extraction is a process where the characteristics of the input signals are extracted from a dataset, serving to reduce the length of the data vector by eliminating redundancy in the signal, and compressing the relevant information into a feature vector of lower dimension [91]. In some signal processing problems, the dimension of the input signal vector is large but the components of the vectors are highly correlated. It is therefore, sometimes useful to reduce the dimension of the input vector. An effective procedure for performing this operation is called Principal Component Analysis (PCA). It involves a mathematical procedure that transforms a number of (possibly) correlated variables into a (smaller) number of uncorrelated variables called principal components. The first principal component accounts for the maximum variability, and each succeeding component accounts for the remaining maximum variability. This technique has three effects [91]:

- It orthogonalises the components of the input vector
- It orders the resulting orthogonal components so that the larger variations come first, and
- It eliminates the least significant components in the dataset.

Bae *et al.* [92] used PCA to calculate the statistical properties of a set of neighbouring ultrasonic A-scan data from a weld inspection. The rationale for this approach was that the irregular nature of surface roughness caused the greater variation of signals in the rough surface region as against the smaller variation of reflections obtained from a smooth surface region. The PCA exploited this information to discriminate between defect and no-defect type signals by the process of eliminating the redundant echoes from the front rough surface region. The results of their investigation revealed that the amount of discrimination depended on the type of part under inspection and surface roughness level [92].

2.7.3.4 Wavelet Transform and Wavelet Filters

The Wavelet Transform (WT) provides a time-frequency representation of the input data. Wavelet analysis represents a windowing technique with variable sized regions [93]. The main advantage of wavelets is the ability to perform local analysis. Therefore, the WT may be used to analyse non-stationary signals, where frequency response varies in time. The time-domain signals are passed to various high-pass and low-pass filters to filter out either high frequency or low frequency portions of the signal. A filter is a linear time-invariant operator [94].

A filter bank is a structure that decomposes a signal into a collection of sub signals [94]. Depending on the application, these sub signals help to emphasis specific aspects of the original signal. It acts as a signal compression mechanism where the sub signals are used to represent the original signal. The key points in applying a filter bank to the input signal is that the sub signals (down-sampled) conveys important features (waveform, amplitude) of the original and are sufficient to reconstruct the original signal. The first stage of application involves two filter banks which necessitates the division of the signal into a low-pass and high-pass band, resulting in the scaling coefficients (approximate) and wavelet coefficients (detailed) respectively. The connection between filter banks and wavelets are that high-pass filters will lead to wavelet transform. The low-pass filter leads to a scaling function, with rescaling at each iteration [95].

A wavelet function can be viewed as a high-pass filter, which approximates a data set (a signal or time series). The result of the wavelet function is the difference between value calculated by the wavelet function and the actual data. The scaling function calculates a smoothed version of the data, which becomes the input for the next iteration of the wavelet function [95]. For example, if the sampled frequency range is 0 to 1024 Hz, the result of the wavelet function (high-pass filter) would be signals from 512 to 1024 Hz. The result of the scaling function (low-pass filter) would be signals from 0 to 511 Hz.

The Continuous Wavelet Transform (CWT) is used to decompose a signal into wavelets of small oscillations that are highly localised in time. CWT is defined by [96]:

$$C(s,p) = \int_{-\infty}^{\infty} y(t)\psi(s,p,t)dt \tag{2.5}$$

Where $\psi(s, p, t)$ is the mother wavelet with s as the scale and p the position in time t. The scale states how the signals are compressed. Therefore, it is possible to find any change in the signal by varying parameters such as scales and positions. In brief, this transformation just compares the function $y(t)$ with the mother wavelet ψ at specific magnitudes and intervals to identify any variation in the signal [96].

Serrano *et al.* [97] investigated the inspection of foundry pieces by applying wavelet transform analysis. The inspection of the pieces was carried out using ultrasonic sensing. They claimed that the application of the wavelet technique was appropriate for use in industrial environments. The treatment of the data was approached in two significant steps starting from the signal reflected from the foundry pieces. First, the Discrete Wavelet Transform (DWT) was applied to the ultrasonic signals to perform feature extraction. Second, a neural network was used on the extracted features to carry out the discrimination of the foundry pieces. The results of their analysis indicated that use of DWT analysis and neural networks in tandem was a successful approach for this type of application.

In a similar manner to Serrano *et al.* [97], Lázaro *et al.* [98] applied a DWT for thresholding the ultrasonic signals contaminated with grain noise. They successfully applied DWT in this de-noising process and suppressed the grain noise. The selection of appropriate DWT type is a critical step in the application of the wavelet transform as emphasised by Lázaro *et al.* [98]. However, the overall classification performance of the system will be influenced by other selected parameter such as number of filter used [95].

The wavelet transform is particularly effective at extracting features at multiple resolution levels in non-stationary ultrasonic signals [99]. Similarly, decomposing a signal into coefficient wavelets has also been used for signal pre-processing as it permits the determination of a particular time-scale where the signal has significant energy [100]. For example, the energy at small time-scales is mostly due to signal noise either from grain size variation or surface roughness. Therefore, by removing small-scale wavelet components from the original signal, it is possible to reduce signal noise and compress it to a certain extent. This process reduces the amount of input data to the neural network without losing the critical elements of the input signal [101].

Abbate *et al.* [102] stated in their work on signal processing that one of the advantages of WT was the flexibility of choosing the most suitable mother wavelet type. However, the quality of the output obtained from WT was not only related to the input signal and wavelet type but also to the types of filters used in the transformation process. In Abbate *et al.'s* [102] work, the application of different mother wavelets resulted in different classification percentages due to different levels of signal processing. In their application, different mother wavelets have been anlaysed to select a suitable mother wavelet type [102].

In some cases, applying a single signal pre-processing technique is not effective. In such situations, a combination of pre-processing methods is applied to achieve better understanding of the signal.

2.7.3.5 Combination of Signal Pre-Processing Techniques

In some applications, to achieve a better classification performance with neural networks, more effective feature extraction methods than single pre-processing methods might be required. The strategy adopted in those instances would be to apply well known signal processing tools such as Fast Fourier Transform (FFT), Wavelet Transform (WT) and Principal Component Analysis (PCA) in various combinations to determine the best approach [103-105].

A combination of wavelet transform and PCA has been applied for a face recognition application [103]. A more effective procedure is to use time-frequency analysis on the non-stationary received signal, and thereby transform it into a two-dimensional component. One dimension of the component is represented by frequency and other by time. This procedure should help the neural network to identify the salient features of the received images. Such an approach may also be inefficient due to the highly redundant nature of the time-frequency image, as often the case. The redundant components of the time-frequency image may be removed prior to processing, thereby enhancing the efficiency of computation. To do so principal component analysis is applied to the time-frequency signal. In this case, training sets were selected from the face database for signal pre-processing [103]. The training sets were used to extract key features from individual input data. Experiments were carried out to determine the best wavelet type to use, which was a critical factor in the effective combination of wavelet and PCA type signal processing tools. A recognition success rate of more than 95% was achieved with this signal pre-processing approach [103]. This application demonstrated the feasibility of applying two different signal pre-processing methods in combination to achieve a better pattern recognition and classification compared to using them separately.

Matalgah and Knopp [104] applied the combined Wavelet and Fourier transforms for efficient pre-processing of simulated and real data examples of non-stationary signals obtained from applications such as underwater acoustics and phonocardiograms. They used WT to display the time domain signal components and FFT to display the spectral components of the signal. The results of their work

demonstrated that improvements in signal processing can be achieved with a combination of WT and FFT techniques as opposed to using each technique separately. Similarly, Wang *et al.* [105] combined FFT and WT for a fingerprint image recognition application. The application of FFT on WT increased the efficiency of transient signal analysis due to the special wavelet function set that changes its size and position on the input image. The application of FFT on the high frequency component of the output from WT also produced improved results when applied on the images obtained from the fingerprints. The feasibility of this approach had been demonstrated by both experimentation and computer simulation [105]. This application demonstrates the benefits of using the Fourier transform on the high spectral component of the signal obtained from the Wavelet transform. All applications as described in this section have illustrated the capabilities of combined pre-processing techniques and their advantages over single pre-processing methods [103-105].

2.7.4 Different Signal Classifying Methods

Many approaches to processing ultrasonic signals for flaw detection have been reported in the literature. Lebowitz [88] described a Knowledge Based Inspection System (KBIS), comprised of neural classification of ultrasonic data and ultrasonic quantification methodologies. The intent of the KBIS program was to provide a tool with which an ultrasonic inspector could obtain enhanced information to improve the probability of correctly accepting products based on weld discontinuities. This system demonstrated the ability of KBIS to differentiate between crack, lack of fusion, slag and porosity discontinuities in welded structures. This system has also benefited the United States of America Navy by reducing the long-term cost associated with ownership of vessels [88]. A potential limitation of this, however, is that the knowledge base depends on the expert operators and their skills which would not be always available for all NDT related problems. However, this can be generated with understanding on the nature of the problem and material variations in the castings.

In ultrasonic NDT investigations carried out by Bilgutay *et al.* [106], it was found that one of the major limitations to effective signal processing results from time invariant additive noise. This noise was caused by small stationary targets such as grain boundaries in metals. Even targets, which were significantly larger than these random reflectors called clutter, were often difficult to detect due to the additional features of highly dense and interfering backscattering signals. The application of spatial compounding had not been very successful in reducing ultrasonic noise, especially when focused transducers were used. Spatial compounding is the process of combining ultrasonic images of the same region of interest (ROI), produced by transducers with different spatial locations [106]. However, a unique adaptation of the radar technique was applied to an A–Scan ultrasonic system for the inspection of large grained materials. This work also introduced a different method of signal processing of the ultrasonic signals obtained from focused transducers [106].

The use of Artificial Neural Networks (ANN) has become important for signal recognition and classification, particularly in ultrasonic inspection. Raj and Rajagopalan [89] investigated the benefits of AI, KBIS and ANN in different NDT&E problems. Their work on the use of Artificial Intelligence in NDT&E applications provided guidelines for selecting neural network parameters and determining the number of epochs that would lead to achieving the best possible outcomes in the processing of analog signals. They recommended the use of combined signal processing techniques such as Artificial Neural Networks (ANN), Knowledge Based Systems and Computer Aided Visualisation techniques to meet the requirements of NDT & E applications. Among the different AI methods there was a preference for use of ANN in signal classification applications. The major advantage of ANN was that classification and learning occurred simultaneously. They concluded that ANN better utilised NDT&E knowledge and data made available in relation to a specific problem [89].

2.7.5 History of ANN Application in NDT&E

A neural network architecture incorporating back propagation is often used due to its robustness. Networks used for classification have commonly as many input neurons as there are features, and as many output neurons as there are classes to be separated [48,107]. In the back propagation algorithm, which is based on a gradient descent method, each neuron of a layer is connected to each neuron in the previous and subsequent layers. A detailed description of the back propagation method is presented in Section 3.7.5.

Neural networks loosely model the human brain's multiple layers of connections, and possess the ability to approximate arbitrary mappings from sets of input to output patterns. Furthermore, neural networks are able to accommodate noise as well as deal with incomplete data [80]. A detailed description of ANN applications in ultrasonic NDT is presented in Section 2.7.6.

In the field of ultrasonic NDT, the application of ANN has a relatively long history. Pattern recognition and feature extraction have been applied to ultrasonic NDE signals for over three decades [107]. Several researchers have investigated the use of neural networks in solving NDE problems, particularly classification problems. Mucciardi and Dau [108] pioneered the use of neural network like models in the early 1980s. More recently, several researchers have investigated the use of neural networks in solving NDE problems. Neural networks are well suited for signal classification in instrumentation as they have the ability to generalise and produce a result on the basis of incomplete data, and when properly trained will produce a result nearly instantaneously. There are, however, different types of neural network architectures available and selection of the appropriate architecture is often difficult [109].

Untrained neural networks produce results with accuracy above 80%, but when trained, results are produced with nearly 100% accuracy as demonstrated in the classification of eddy current NDT data [110]. Probabilistic neural networks have also been used in classifying eddy current NDT data [110]. The evidence indicates that the neural network based approach provides a cost/time efficient solution to

classification problems when the available amount of data is limited and the time to classify is constrained by the manufacturing process [110].

In order to carry out meaningful testing, it is essential to eliminate or reduce unwanted signal noise when using any NDT signal processing method. Rao *et al.* [111] carried out eddy current based NDT experiments on austenitic stainless steel welds and applied ANN for signal processing to detect defect types despite the presence of disturbing signal noise. They applied a systematically optimised network method by comparing the maximum deviation in-depth evaluation and the correlation coefficient in Figure 2.6. The correlation coefficient is a parameter that gives the quality of a least square fitting to the original eddy current NDT data [111]. Rao *et al.* [111] described a systematic procedure for selecting suitable neural network parameters for the particular problem in their work. Even with a small number of data sets (i.e., 142) for two different defect types, they were able to train and test their network through appropriate selection of neural network parameters. They have demonstrated that it was essential to obtain appropriate network parameters to achieve successful classification of signals with small number of input data (less than 200).

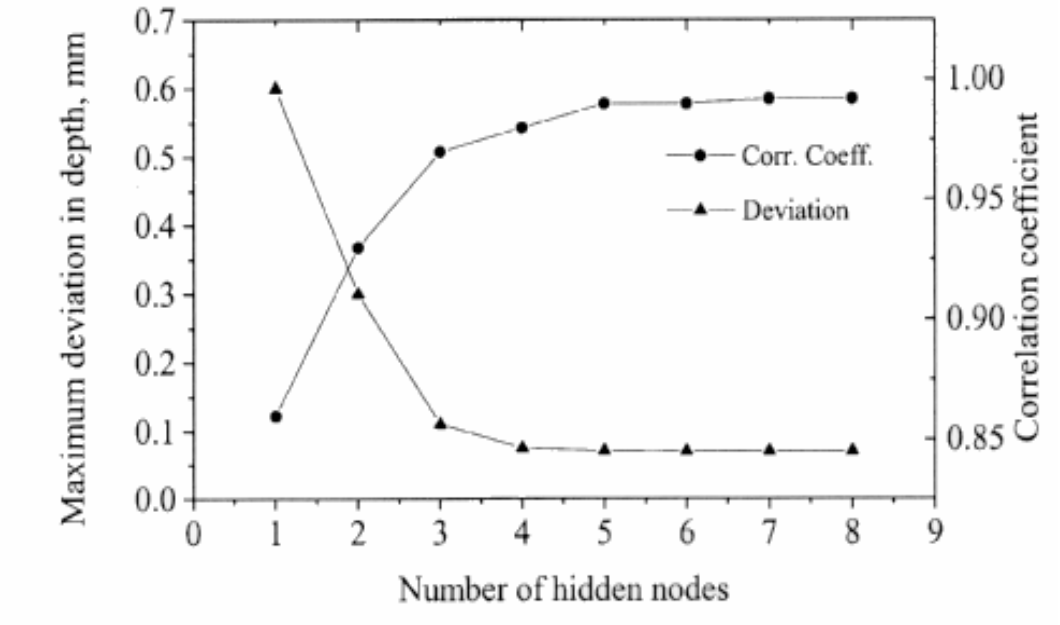

Figure 2.6 Optimisation of hidden nodes in the neural network and the maximum deviation in depth evaluation and the correlation coefficient [111]

In general, ultrasonic defect classification has been carried out using a variety of neural network topologies in different applications [52,78,79,80,107,111-114]. It has been determined from the literature that a feed-forward back propagation based neural network structure is appropriate for ultrasonic defect classification on plate, welded structures and shafts as presented in Section 2.7.6.

2.7.6 Applications of Neural Networks

2.7.6.1 Overview

A review of the literature has yielded several approaches used to implement neural networks in various inspection tasks. A few of the relevant case studies on the application of neural networks in the NDT field are presented in following sections.

2.7.6.2 Inspection of Shafts

Cotterill and Perceval [114] were successful in identifying the presence of fatigue cracks in shafts such as swing shafts, propel shafts applied in the coal industry using ultrasonic NDT. Manual ultrasonic inspection was used for locating the position of cracks along the axis of a shaft. A limitation of the technique was that the shape or extent of the crack was difficult to quantify with manual techniques. The accuracy and repeatability of test results was operator dependent. The ultrasonic testing operator must have a high level of skill in using the technique, and extensive experience on the particular shaft or pin geometry to recognise a crack indication and then attempt to determine the shape characteristics from the ultrasonic response. A further limitation with the technique lay in the storage and retrieval of ultrasonic data. The risk of erroneous analysis could be reduced if echoes obtained from cracks could be highlighted and secondary or mode converted echoes were suppressed. This was achieved by training artificial neural networks to discriminate between the different types of ultrasonic signals. Three different hidden neuron layers containing 16, 32, and 64 neurons were applied to the particular inspection task. It was found that the neural network with a small hidden layer of 16 units performed better due to

its improved generalisation ability, while the larger hidden layer networks over-fitted the training data. The prediction percentage varied from 80% to 100% for the classification of the cracks. However, the 600 neural network training sessions took a considerable amount of time (more than few hours) to complete due to computation limitations [114].

2.7.6.3 Predictions of Porosity in Al Alloy Castings

Another application of neural networks was for the prediction of location and volume fraction of porosity defects in cast A356Al alloy castings [115]. Huang *et al.* [115] evaluated the application of neural networks in predicting volume fraction of micro porosity in Aluminium alloys. The inputs to the neural network were the thermal parameters obtained from computer simulations and experimentally determined initial hydrogen content of the melt. The location and volume fraction of porosity predicted by the network were found to be in agreement with experimental measurements. The initial hydrogen content of the melt, thermal gradient, cooling rate and local solidification time were the variables used as inputs to the neural network to determine the pore volume fraction as the output. Data from eight castings was used as the training set to teach the neural network. The training set consisted of 64 patterns, obtained from the 8 castings. An optimum number of hidden units were used to establish the network architecture. Huang *et al.'s* [115] work described the steps involved in developing a successful neural network technique to predict porosity defects in aluminium alloy castings.

2.7.6.4 Classification of Weak Ultrasonic Signals

Thavasimuthu *et al.* [80] applied ultrasonic contact inspection to detect flat bottom holes of different diameter size from 1 mm to 7 mm in casting blocks. Their work focused on classifying weak ultrasonic signals using feed-forward neural networks trained using the back propagation method. Depending on the probe frequencies used (2.25, 5 and 8 MHz) different features of the signal (Table 2.2) were applied as input to the neural networks. Typical features of a signal, such as the rise-time position of different peaks, peak-to-peak distance and number of peaks in a

specified interval were used. The weak signals containing the background grass (noise) signal, which camouflaged the defect signal were obtained from the specimens. Prominent features such as 2nd greatest peak amplitude (2nd back wall echo for the part) and total area under 2nd peak were used as input to the neural network. The neural network classifier was able to achieve an overall 98% classification rate for the different frequencies used in the research [80].

Number	Features
1	Greatest Peak Position
2	Greatest Peak Amplitude
3	2nd Greatest Peak Amplitude
4	Total Area under 2nd Peak

Table 2.2 Some of the prominent features applied for ultrasonic defect signal classification [80]

2.7.7 Summary

In general, no practical non-destructive measurement technique allows for the selection of sufficient useful information to allow a general and unbiased reconstruction of a flaw [77]. Some of the methods described in this section allow assumptions to be introduced into the data-processing in a known and quantifiable manner. The various techniques as described were examined to identify the best possible defect classification method for the inspection of sub-surface defects in die cast parts.

Although neural networks have shown great potential in NDT flaw classification, the constraint to wider application of neural networks in NDT is the lack of sufficient training data from real defects [108]. As a consequence, neural networks can usually only be trained for very specific ultrasonic NDT applications, where there are sufficient real examples. It is also important to realise that neural networks generally require a significant amount of time for training. Over-training or

under-training will result in deviation from the required accuracy. However, the case studies presented in Section 2.7.6 have demonstrated that neural networks can be effective in defect classification tasks. From the literature, it can be concluded that the feed-forward back propagation neural network is suitable to carry out signal analysis for many ultrasonic signal processing applications. However for the current research problem, a suitable method of signal pre-processing which may be required prior to application of a neural network has not yet been thoroughly investigated.

2.8 CONCLUSIONS

The research findings presented by each of the authors cited in the literature review were critically examined to establish a sound foundation for this research project and to provide a basis for measuring its contribution to knowledge. Since this research relates to three different fields (die casting, ultrasonic NDT&E and artificial intelligence), it was important to provide a description of research activity in each of these disciplines.

The results of this review revealed that there have been rapid advances in many areas of NDT technology with regard to casting quality inspection. This was mainly brought on by the requirements to deliver defect-free castings to customers and increase the quality standards of casting products. An extensive search of the literature has also indicated that an ultrasonic inspection of aluminium die castings with surface roughness beyond 50 μm has not been explored to-date. This is the topic of research addressed in this thesis. The lack of previous research for this particular application may be due to the nature of castings and the sensitivity of ultrasound. This literature search was focused on obtaining information on ultrasonic inspection of castings with complex shape, varying grain structures and surface roughness, and containing irregular porosities. However, it was found that there was no published research addressing these issues within an integrated (a combination of earlier mentioned factors) framework. Hence, there is a need to find the limitation of NDT

to inspect aluminium die castings within this context. The literature review indicated that ultrasonic techniques had the potential to be used to detect sub-surface defects in castings. It was clear that factors such as surface roughness and grain structure are critical variables in the inspection of castings. Nevertheless, these factors have not been sufficiently addressed in current inspection systems.

From the different research contributions relating to the application of AI in the NDT&E field it was observed that ANN has been the approach of choice in ultrasonic signal classification. However, this approach has not been sufficiently explored for classification of weak signals obtained from rough surface die castings. Therefore, the development of an effective classification methodology for weak ultrasonic signals obtained from rough surface sections of castings through a neural network approach is investigated as part of this research program.

The possibility of applying signal pre-processing techniques in relation to noisy ultrasonic signals has been mentioned by researchers as described in the literature review. Nevertheless, the use of techniques such as FFT, PCA and WT in combination for the pre-processing of ultrasonic signals has yet to be explored. The research documented in this thesis addresses these issues in detail. A methodology and associated techniques have been developed to pre-process ultrasonic signals and provide a basis for the design of an ultrasonic inspection system for detecting porosity type defects in aluminium die castings with rough surfaces. Prior to designing an experimental procedure for this research program it is important to understand the background of ultrasonic inspection and signal processing. This background information is presented in Chapter 3.

CHAPTER 3.

ULTRASONIC INSPECTION AND NEURAL NETWORKS

3.1 OVERVIEW

The importance of understanding the ultrasonic NDT inspection method has been emphasised in Chapter 2. This chapter addresses the theoretical background to ultrasonic inspection (Section 3.2). Following on, the importance of selecting appropriate equipment for experimentation is highlighted. A brief description of different inspection methods and couplant types are provided. The basics of neural network systems are described in Section 3.7, which includes a description of neural network configurations specifically, the feed-forward and back propagation networks. Section 3.8 presents the application of MATLAB functions in carrying out training and testing of the neural network.

The background information on ultrasonics presented in this chapter is extracted from the work of Krautkrämer and Krautkrämer [5], Blitz and Simpson [22] and Hellier [25].

3.2 THEORETICAL BACKGROUND

The ultrasonic NDT method utilises sound waves at frequencies greater than 20,000 Hz, which is beyond the range of human hearing. Ultrasonic testing is based on time-varying deformations or vibrations in materials [22]. In solids, several types of wave propagation can occur and are based on the way the particles oscillate [116]. Longitudinal and shear waves are the two modes of propagation most widely used in ultrasonic testing and in this research work. The particle movement responsible for the propagation of longitudinal and shear waves is shown in Figure 3.1

In longitudinal waves, the oscillations occur in the direction of wave propagation. Since compressional and dilational forces are active in these waves, they are called pressure or compressional waves. They are also sometimes called density waves because their particle density fluctuates as they move. Compression waves can be generated in liquids as well as solids because the energy travels through the atomic structure by a series of compression and expansion movements [117].

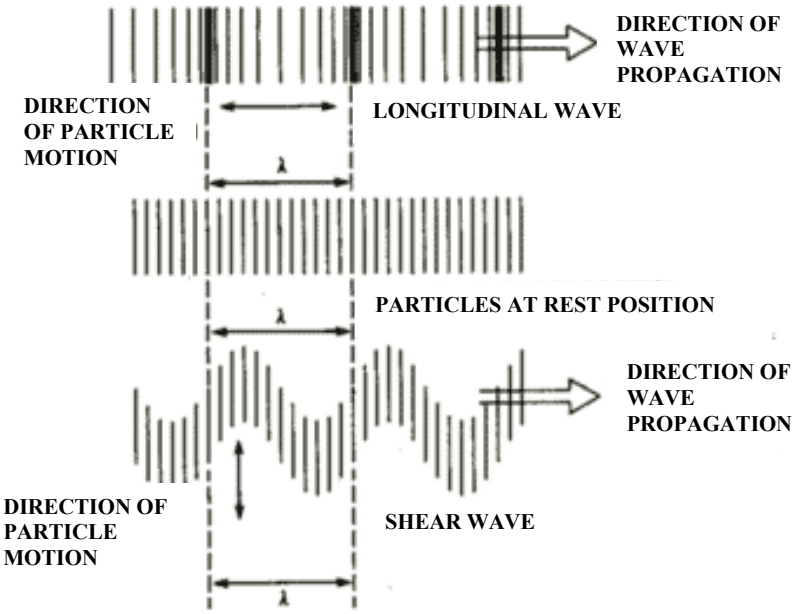

Figure 3.1 Longitudinal and shear wave propagation [116]

In the transverse or shear wave, the particles oscillate at right angles or transverse to the direction of propagation. Shear waves require an acoustically solid material for effective propagation and, therefore, are not effectively propagated in materials such as liquids or gasses. Shear waves are relatively weak when compared to longitudinal waves [118].

In ultrasonic testing, all discontinuity indications are compared to a reference standard. The reference standard may be one of many reference blocks or sets of blocks specified for an inspection method. Standardising does two things: it verifies that the instrument/transducer combinations perform as required, and it establishes sensitivity or gain setting at which all discontinuities of the size specified (or larger) will be detected [119]. However, in this research there were no specific standards available for calibrating the inspection of aluminium die castings except the general standards on the ultrasonic inspection of castings. Hence, a specific need arises to develop a standard for the aluminium die castings investigated in this research. This process is explained in detail in Chapter 4.

3.3 EQUIPMENT SELECTION

In an ultrasonic equipment, electrical energy is transformed into mechanical energy in the form of sound pressure waves through an ultrasonic transducer. All the information is presented in one of four presentation styles: A-scan, B-scan, C-scan and digital numeric. In an A-scan presentation (Figure 3.2), the initial sound pulse and the resulting rear wall echo or discontinuity reflections are displayed on a cathode ray tube (CRT). In a B-scan, the ultrasonic testing equipment displays the material being inspected as a cross-sectional view. In a C-scan, the ultrasonic testing equipment displays the casting in a topographical perspective. This presentation is useful when plotting thickness of material over a given area. With digital numeric presentation the ultrasonic testing equipment calculates the “flight time” of the ultrasonic pulse from the transmitter until it is received back at the receiver.

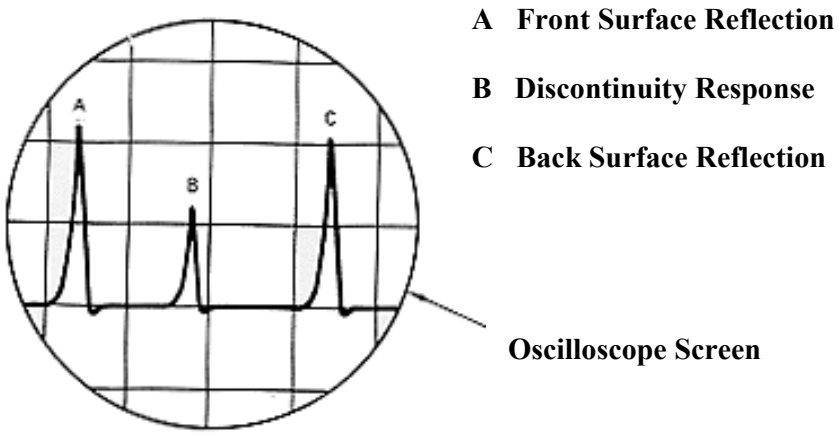

Figure 3.2 A-scan with a discontinuity response [120]

A thorough understanding of the sound beam, material and geometry of the part is required prior to development of an ultrasonic based inspection system. Once the appropriate equipment type is selected, the next step involves selecting the right ultrasonic transducer, which allows for the best penetration of the ultrasound. Additional information on the ultrasonic equipment used in this research is provided in Section 4.4.3.2.

3.4 ULTRASONIC TRANSDUCERS

The transducer is one of the most important components of any ultrasonic NDT system. The selection of the correct transducer is important in achieving the necessary sensitivity and resolution of the system [116]. Transducers are available in a variety of frequency ranges, sizes and application dependent housings. Ogilvy [73] emphasised that the selection of a transducer also depends on the type of material to be inspected. Another important criteria in the selection of a transducer is the type of inspection method used for testing castings. According to Silk [121], the frequency of a transducer is a major determining factor in its application. The work carried out by Silk [121], emphasised the importance of the study of penetration, depth resolution and sensitivity of an ultrasonic system, factors which are strongly

dependent upon the nature of the pulse emitted by the transducer. Given that the pulse emitted depends on the particular transducer characteristics such as crystal size and diameter, the selection of a suitable ultrasonic transducer for any given ultrasonic NDT problem is very important.

The resolution of a transducer can be defined as the minium size of a feature or discontinuity that can be determined by its use. The smallest defect size that can be detected or the resolution of the transducer is half the wavelength ($\lambda/2$). Therefore, smaller the defect, the higher is the frequency of ultrasound required for detecting it. Unfortunately, using a higher ultrasonic frequency results in a higher rate of signal damping in the material. The lower frequency probes are therefore preferred to reduce the damping of ultrasound within the test material. However, the testing capability of the probe is compromised if the frequency of the ultrasound is too low (1 - 2 MHz). Further, in order to obtain a satisfactory amplitude of the ultrasound signal, the probe diameter should not be less than 5 mm [5]. In summary, there is a need to correlate the sensitivity and other characteristics of the ultrasonic transducer and quality requirement of the castings to be inspected.

Transducer frequency and thickness of piezoelectric crystalline material that produces the ultrasound are related such that the thinner the crystal, the higher the ultrasonic frequency. Most ultrasonic NDT inspection tasks are carried out at frequencies from 0.2 to 25 MHz [44-46,122,123]. The higher the frequency of a transducer, the straighter the sound beams, and the greater the sensitivity, measurement resolution, and attenuation. Furthermore, for any given frequency, the larger the transducer, the more directional the sound beam and lower the sensitivity.

The ultrasonic waves generated by a transducer will emerge initially as a parallel beam that diverges later [124]. The ultrasonic beam can be divided into two fields: the near field and the far field (Figure 3.3). There are significant fluctuations in the sound intensity in the vicinity of the ultrasonic transducer due to constructive and destructive interference of the multiple waves which originate from the transducer face. As illustrated in Figure 3.3, the echo amplitude goes through a series of maximum and minimum regions and ends at the last maximum in the near field

[116]. If a flaw is positioned in the near field region it can be difficult to detect due to non-uniform sound intensity. The area where the ultrasonic beam is most uniform and spreads out in a pattern originating from the center of the transducer is called the far field [125]. The region at which the far field starts is important since this is where the sound wave is well behaved and at its maximum strength [125]. Therefore, this is the region in which optimal detection occurs.

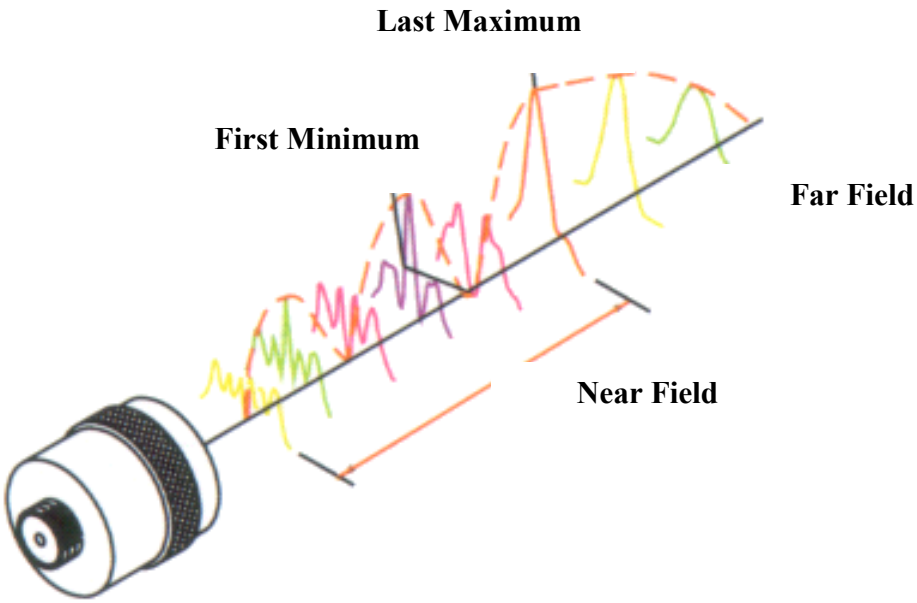

Figure 3.3 Sound fields of a transducer [116]

The area influenced by the ultrasonic vibrations transmitted by the probe is known as the sound field, and is important for the evaluation of defect size. A sound wave transmitted from a transducer radiates in one direction within a given angular range. The cross-section of the sound beam widens with increasing distance and the energy is distributed over a greater area. The intensity of sound energy per unit area thus becomes smaller. This phenomenon is known as beam divergence (Figure 3.4). The beam angle is the angle between the beam axis of a refracted wave and the angle to the refracting interface. The refraction when passing through the interface changes the direction of propagation of the sound wave according to Snell's reflection law [22] as presented in Section 2.5.5.

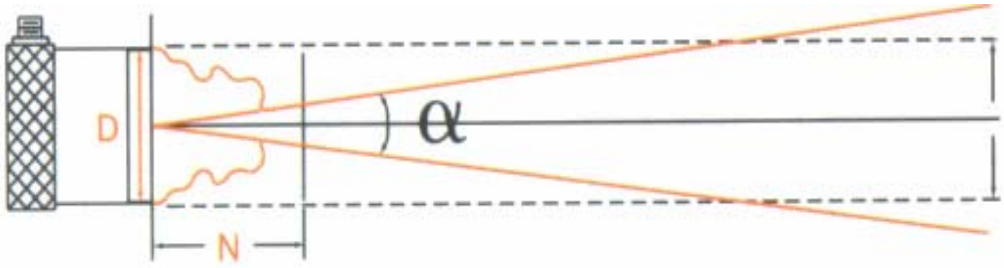

Figure 3.4 Beam divergence with beam angle spread (α) and near field area (N) for the diameter of the transducer (D) [114]

3.5 INSPECTION METHODS

An ultrasonic sound beam generated by the transducer travels perpendicular to the test piece in the normal pulse-echo method [5]. The pulse-echo method utilises the reflected part of the ultrasonic wave for the evaluation of defects. This is one of the most commonly used ultrasonic methods to inspect the quality of materials [126].

A normal beam through transmission is similar to the pulse echo, except a second transducer is placed on the opposite side of the test piece to detect the ultrasonic energy passing through the material [5]. This method is normally used when the test parts are easily accessible on both sides [127]. Prabhakar *et al.* [128] highlighted a similar kind of two-sided casting inspection method in their work. They also stated that an added advantage of the technique is that the received frequency can be varied for a chosen transmitter frequency. In most ultrasonic NDT applications the pulse-echo method is preferred ahead of the through-transmission method due to ease of use and no requirement to access both sides of the part being inspected.

3.6 COUPLANT METHODS

3.6.1 Overview

A couplant is a substance, usually a liquid or semi-liquid, used between the transducer unit and test surface to permit or improve transmission of ultrasonic energy [25]. Typically water, oil, or gel is used as couplants in ultrasonic testing. In this research, contact and immersion type couplant methods are investigated. This section provides a brief description of contact and immersion type ultrasonic inspection.

3.6.2 Contact Testing

In manual ultrasonic inspection, the transducer is typically placed in physical contact with the material being inspected. In contact testing, coupling is achieved with water–soluble or oil based liquid being placed between the transducer and material. This ensures that the maximum ultrasonic energy enters the material, when the transducer is placed in contact with the part, however, some pressure is manually applied to ensure good acoustic contact with the test piece. Hence, the result obtained from contact testing is dependent on the pressure applied by an operator on the transducer through the coupling medium.

According to Fallon [129], contact ultrasonic testing is difficult to employ on curved surface iron castings. The other critical issues are the grain size and surface roughness which affect the results in contact testing of castings. These critical factors are important to consider in the ultrasonic inspection of aluminium castings.

3.6.3 Immersion Testing

The principal method for achieving the necessary coupling is immersion, using water as a coupling medium. Although often oil, grease and glycerine are used

as couplants in ultrasonic inspection of castings, water is more likely to be used in an on-line production inspection system than oil or other liquid.

In automated ultrasonic inspection, the technique involving total immersion of the work piece under inspection has become universally accepted [130]. This requires the use of an immersion tank where the part and the transducer are placed under water as shown in Figure 3.5. Ultrasonic immersion inspection involves one of the following four procedures: normal beam pulse-echo, normal beam through-transmission, angle beam pulse-echo and angle beam through-transmission. The normal ultrasonic immersion inspection set-up is shown in Figure 3.5 along with the CRT screen of the flaw detector.

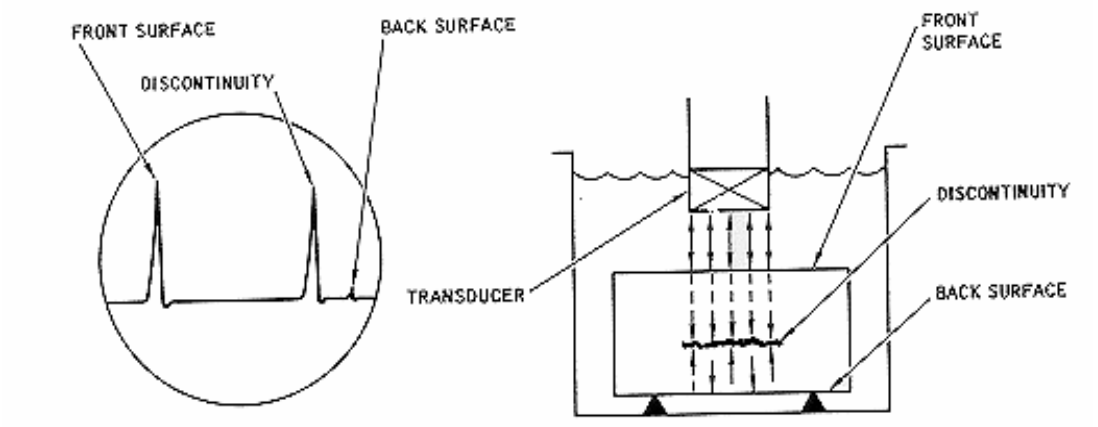

Figure 3.5 Immersion testing set-up and CRT screen with discontinuity [116]

3.7 BACKGROUND ON NEURAL NETWORKS

3.7.1 Overview

This section presents the background information on neurons and neural network configurations. A brief description of the feed-forward network and the back propagation training method is also presented in Sections 3.7.3 and 3.7.4

respectively. The neural network toolbox from MATLAB software is used for training and testing ultrasonic signals.

3.7.2 Neuron Model

An artificial neural network comprises a number of simple processing units called neurons, which are able to communicate by sending signals to each other through a large number of biased or weighted connections. Figure 3.6 shows an elementary neuron with inputs. Each input ($p_1, p_2, \ldots, p_R$) has a corresponding weight value ($w_1, w_2, \ldots, w_R$), where R = number of inputs to the neuron. The sum of the weighted inputs and the bias b, forms the input (n) to the transfer function f. Neurons may use any differentiable transfer function f to generate their output a from n, which is equal to the sum of w_p and b.

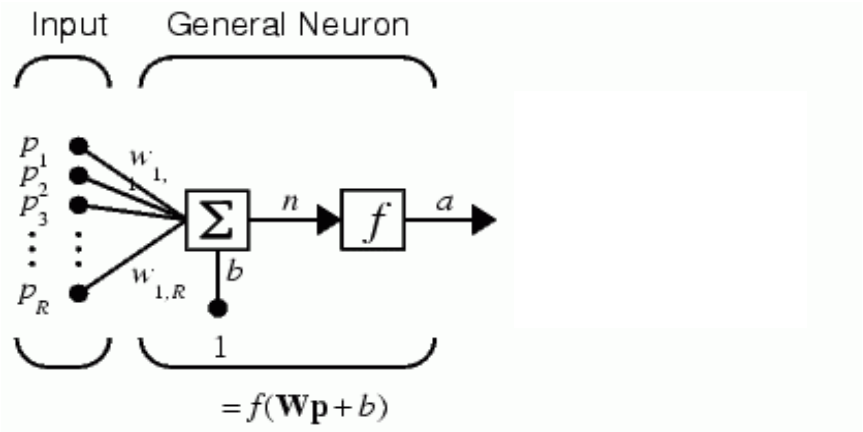

Figure 3.6 Neuron model [91]

Each neuron (including the neurons in the last layer) has an output that is limited according to the transfer function of the particular neuron. For instance, if the '*logsig*' transfer function is used, the output may vary between 0 and 1. However, if the '*tansig*' function is used, the output may vary between -1 and +1 [91]. The three transfer functions *logsig, tansig*, and *purelin* are the most commonly used transfer functions for the back propagation method [91].

The following guidelines are recommended in deciding the number of inputs to a network for an inspection application [87]:

- The inputs should contain sufficient data to distinguish between defect and non-defect signals.
- The inputs must be representative of that defect type and preserve the information required for successful classification.
- The number of representative training examples must be adequate.

3.7.3 Neural Network Configuration

Neural networks possess particular properties such as an ability to learn or adapt to changes, to generalise using incomplete data, and to cluster and organise data [131]. Generally, the neural network is trained by feeding it a set of teaching patterns and changing its weights according to a defined learning rule. The weights are changed at every epoch. During training and testing of a neural network, an *Epoch* is defined as processing of a single set of input signals of the network. According to Timothy [132], paradigms of learning may be categorised into two distinct types:

- Supervised/Associative: the network is trained by providing inputs and matched output patterns.
- Unsupervised/Self–organised: a network is trained in response to clusters of patterns. This method relies on a set of algorithms that discovers salient features of the input population statistically.

In this research, supervised learning was applied as there was no clear set of rules for the signal types generated from the rough surface sections of the castings.

3.7.4 Feed-forward Networks

Feed-forward networks allow signals to travel in one direction, from input to output. The feed-forward networks associate inputs with outputs. Amongst the numerous Artificial Neural Network (ANN) architectures described in the literature,

the feed-forward network is the most commonly used (refer Section 2.7.5). The neural network type used in this application is a feed-forward network. An example of a three layer network is shown in Figure 3.7 along with the input nodes, which are associated with the signal to be classified. The first group of units (neurons) comprise an input layer, which accepts the data values to be interpreted via the input nodes. The next group of units form a hidden layer, and the final layer of units is the output layer. Each neuron communicates through a defined function as shown in Figure 3.6.

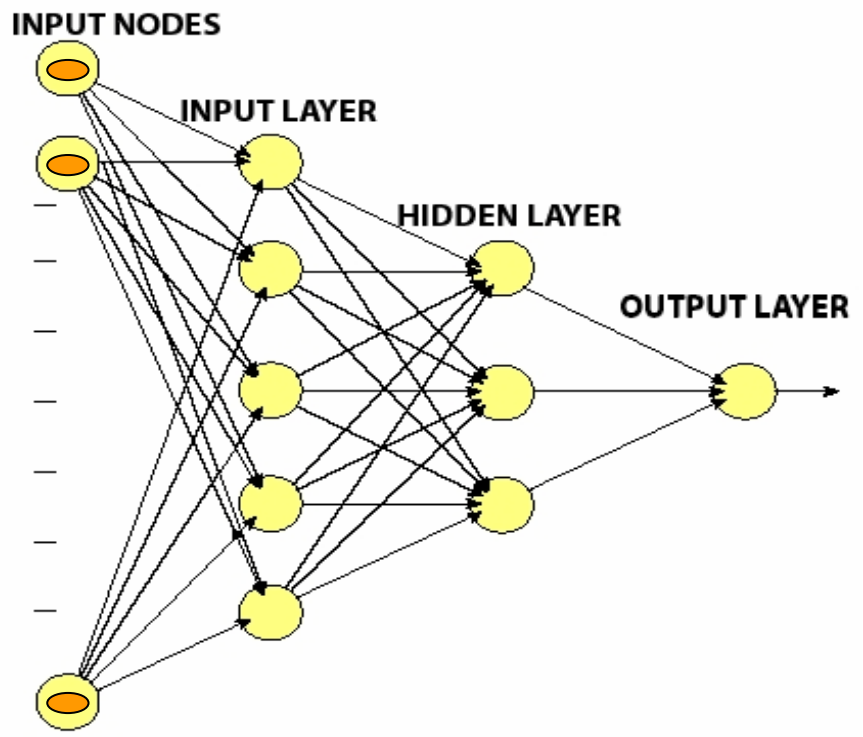

Figure 3.7 Three layer feed-forward neural network with input nodes

The feed-forward network with one or more hidden layers is mainly used in NDT defect classification [77,114]. Multiple layers of neurons with non-linear transfer functions allow the network to learn both non-linear and linear relationships between input and output vectors. In this investigation only two classifications *viz.,* "defect" and "no-defect" were used. Consequently, the output will be either "1" or "0".

The training process of the feed-forward network requires a set of examples consisting of network inputs and target outputs. During training, weights and biases

of the network are iteratively adjusted to minimise the network performance function which is the mean square error (*mse*). In MATLAB, this function is defined by *net.performFcn* [91]. The default performance function for a feed-forward network is mean square error (*mse*). The mean square error value is the average squared error between the network outputs and the target outputs [91]. There are several training algorithms for feed-forward networks such as variable learning rate, conjugate gradient and scaled conjugate gradient algorithms [91]. All of these algorithms use the gradient of the performance function to determine how to adjust the weights to maximise performance. The gradient is determined using a technique called backpropagation, which involves performing computations backwards through the network [91].

3.7.5 Back Propagation Network

The Back Propagation (BP) network training algorithm is an iterative gradient algorithm designed to minimise the mean square error between the actual output of a feed-forward network and the desired output [133]. BP was created by generalising the Widrow–Hoff learning rule to multiple–layer networks and non-linear differentiable transfer functions [91]. Input vectors and the corresponding target vectors are used to train a network until it can approximate a function, associate input vectors, or classify input vectors in an appropriate way defined by the target.

The gradient descent algorithm in BP can be implemented using two approaches *viz.*, incremental and batch mode. In the incremental mode, the gradient is computed and the weights are updated after each set of input is presented to the network (refer Figure 3.6). In the batch mode, the weights are updated after all the sets of inputs are presented to the network. The batch mode is generally used because of faster convergence to the mean square error (*mse*) when compared with the incremental mode [91]. Also given the fact that the inspection methodology is being developed for future automation, where the inspection cycle time factor is critical, the batch mode of processing is the preferred option.

3.7.6 Scaled Conjugate Gradient

One of the popular supervised learning algorithms is a Scaled Conjugate Gradient (SCG) mechanism. SCG is fully automated, includes non-critical user-dependent parameters, and avoids time consuming line search iteration to determine an appropriate step size. Based on experiments Moller [134] concluded that, SCG was (nearly 25 times) faster than other standard BP techniques and produced a high classification percentage. SCG was benchmarked against the standard back propagation algorithms [134]. The training parameters for *trainscg* (MATLAB function for SCG) are *epochs, show, goal, time, min_grad, max_fail, sigma* and *lambda*. The training status is displayed for every *show* iterations described in the network [91]. The other parameters determine when the training stops in the neural network. The training stops if the number of iterations exceeds a given number of *epochs*, if the performance function drops below a certain *goal* value, or the magnitude of the gradient value is less than *min_grad* function [91]. The function *max_fail* is associated with the early stopping technique during the network training process [91]. The parameters *sigma* determines the change in the weight for the second derivative approximation and the parameter *lambda* regulates the indefiniteness of the Hessian matrix [134]. All these parameters have been explained in detail by Moller [134].

3.8 ANN SYSTEM ARCHITECTURE

3.8.1 Overview

The first step in training a feed-forward network is to create the network object. The next step is to initialise the weights and biases of the network; then the network is ready for training. There are situations when the weights have to be reinitialised. Both theoretical analysis and simulations indicate that large networks tend to overfill the training data and thus have a poor generalisation, while networks that are too small have difficulty in learning through the training samples.

3.8.2 Transfer Function

The behaviour of a feed-forward ANN depends on weights and the input-output function (transfer function) that are specified for the units. They typically fall into one of the following three categories [91]:

- Linear - the output activity is proportional to the total weighted input
- Threshold - the output is set at one of two levels, depending on whether the total input is greater than or less than some threshold value, and
- Sigmoid - the output varies continuously but not linearly as the input changes. Sigmoid units bear a greater resemblance to real neurones than do linear or threshold units.

3.8.3 Initialising Weights

Before training a feed-forward network, the weights and biases have to be initialised. In general, the each separate weight value is set to a random value [91]. An automatic initialisation of the weights has to be carried out before each new training set is used. The initialisation function takes a network object as input and returns a new network object with all weights and biases initialised. The weights specify the strength, and influence the effects of each neuron on the applied transfer function [91].

The network weights and biases are initialised through a simulation process. The following procedure is followed in simulating the performance of a three-layer network:

- The network is presented with training examples with the desired pattern of the output units.
- The actual output of the network is compared with the desired output.
- The weight of each connection is changed so that the network produces an output closer to the desired output.

3.8.4 Simulation and Training of Network

Once the weights and biases are initialised, the network is ready for simulation and training. The simulation of the network takes the network input and the network object defined during the initialisation process and returns a network output. The training process requires a set of examples of proper network behaviour – network inputs *p* and target outputs *t*. The function shown in the single neuron model (Figure 3.6) would be applied to the three layer network, as shown in Figure 3.7. The weights are adjusted for each neuron in three layers depending on the mean square error (*mse*) and the desired target *t*.

The learning rate used in Feed-forward Neural Networks is a numeric value used during Back Propagation (BP) to adjust the weights or connections between neurons in adjacent layers. The learning rate is important because, if the amount of change is too small then it will take a long time to train the network and if it is too large, then the network may not find the set of weights that can provide an optimum solution [91]. During BP, the value predicted as the output of a Neural Network is compared against the actual output value and the difference used as an error estimate to adjust the weights used in the Neural Network. The rate of change of the weights during the BP phase where the weights and bias are being adjusted to reduce the prediction errors are controlled by the learning rate [91].

In the neural network training process, to avoid the network converging to a local minimum, the use of a momentum rate allows the network to potentially skip through local minima. Momentum can be applied to BP training by making weight changes equal to the sum of a fraction of the last weight change and the new change suggested by the BP algorithm [91]. A history of the change in momentum rate and direction are maintained and used, in part, to push the solution past the local minima. The momentum parameter controls the amount of error adjustment with each iteration during training the neural network for signal processing [91]. Learning rate and momentum parameter both affect the speed and quality of the training (learning) process, and error values provide information on which a decision is taken as when to stop training.

3.9 SUMMARY

This chapter has presented detailed background information on ultrasonic inspection. The most widely used reference on ultrasonic NDE was authored by Krautkrämer and Krautkrämer [5]. It discussed a wide range of test condition set-ups and described the underlying physics. An updated volume of the Non-destructive Testing Handbook [51] was also a reference source for basic ultrasonic inspection. Contributions by Silk [121], Halmshaw [50,127] Blitz and Simpson [22] and Hellier [25] were considered as references that discuss a variety of inspection principles. These references highlighted the importance of the selection of proper inspection equipment. This background information on ultrasonic inspection aided in the development of a suitable inspection procedure for the inspection of aluminium die castings with rough surfaces. This inspection procedure is presented in Chapter 4 along with the description of sample parts and equipment used in this research.

The background theory on neural networks (Section 3.7) provided an understanding of the network parameters and the steps involved in training and testing a neural network to process ultrasonic signals. The manual on neural network toolbox from MATLAB software [91] provides detailed information on the feed-forward back propagation neural network and its training algorithms. The literature review on neural networks emphasised the selection of appropriate neural network parameters such as number of neurons and number of epochs to achieve acceptable signal classification.

CHAPTER 4.

DESIGN OF EXPERIMENTAL SET-UP

4.1 OVERVIEW

This chapter discusses the selection processes that determine suitable experimental parameters required for the ultrasonic inspection of aluminium castings. A detailed description of sample castings used in this research is presented in Section 4.3. An extensive experimentation program is carried out on the selected sample castings to determine suitable experimental parameters. Thereafter, inspection of castings is carried out and the ultrasonic signals are analysed using signal processing techniques for the purpose of identifying gas porosity defects. This chapter also describes in detail the experimental set-up used for the research and the calibration process for the ultrasonic equipment (Section 4.6). Finally, a brief overview of the validation methodology for the ultrasonic signals obtained is also presented.

4.2 EXPERIMENTAL METHODOLOGY

In this section, the methodology used to obtain valid results is explained. This is illustrated in Figure 4.1.

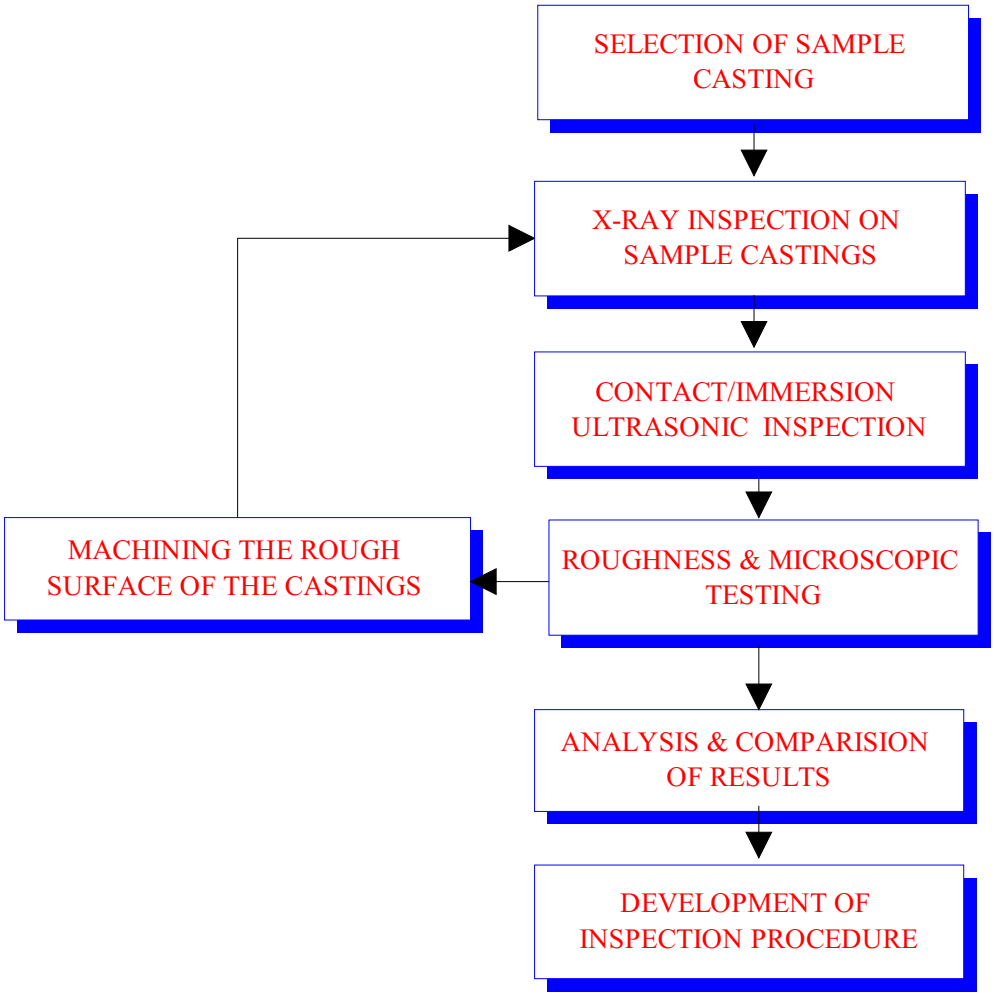

Figure 4.1 Flow chart of experimental methodology

The sample castings were obtained from two collaborating industry partners; Nissan and Ford, Australia. The critical sections where the defects were prominent were considered for ultrasonic testing. Initially, X-ray inspection was carried out on the sample parts to determine defective and non-defective castings' sections. X-ray results were stored in an image file format. Then, ultrasonic inspection experiments were carried out on the critical section of the castings to choose the appropriate

inspection technique from the available methods (contact and immersion techniques). Inspection parameters such as frequency, velocity and water path distance were determined to carry out inspection on the sample die castings. Finally, the results obtained from ultrasonic inspection were validated using visual analysis and X-ray NDT inspection on the defective sections of the castings.

4.3 SAMPLE PARTS

4.3.1 Overview

The sample castings used in this investigation were selected from the industry partners based on their requirement for detection of sub-surface discontinuities. The casting sections to be inspected were identified based on the predominant occurrence of sub-surface discontinuities. The sample parts used for ultrasonic inspection were the manual transmission case and structural oil sump pan from Nissan Casting Plant Australia Pty. Ltd., and Ford Motor Company Australia Limited respectively.

4.3.2 Selection of Castings

As manual transmission case (MTC) castings have little variation in surface roughness and grain size, they were selected for the purpose of calibration of the equipment. They were also used to obtain the initial experimental parameters. However, in order to investigate the effects of material variations on ultrasonic inspection performance, most of the subsequent experiments were carried out on structural oil sump pan (SOSP) castings. This component has significant variations in surface roughness and grain structure along critical areas of the casting. One other major difference between these two types of castings was the thickness. The thickness of MTC casting varied between 8 mm and 25 mm, however, the relevant sections of SOSP castings had a constant thickness of 8 mm.

Nissan casting plant Australia, uses X-rays to test parts off-line as a part of their quality control system. The X-ray inspection is reasonably effective and porosity is normally detected in castings from a sample lot. However, casting manufacturers need to detect defects in the early stages of the casting process and carry out inspection of the entire set of castings instead of inspecting a sample from each lot. Moreover, if a part is found defective at the customer's site the whole batch of castings is rejected, resulting in heavy financial penalties for the manufacturer. As such, there is a need for an advanced inspection system to detect sub-surface defects on-line at Nissan casting plant Australia and other organisations with similar practices of inspection.

4.3.3 Manual Transmission Case

The surface areas of the manual transmission case (MTC) near the sections to be machined were considered critical. They were inspected to determine the presence of porosity defects near the machining surface. Figure 4.2 shows the main areas of interest: the main bearing hole (A), shift rod holes (B), M8 x PL1.25 threaded holes (C) and counter bearing hole (D).

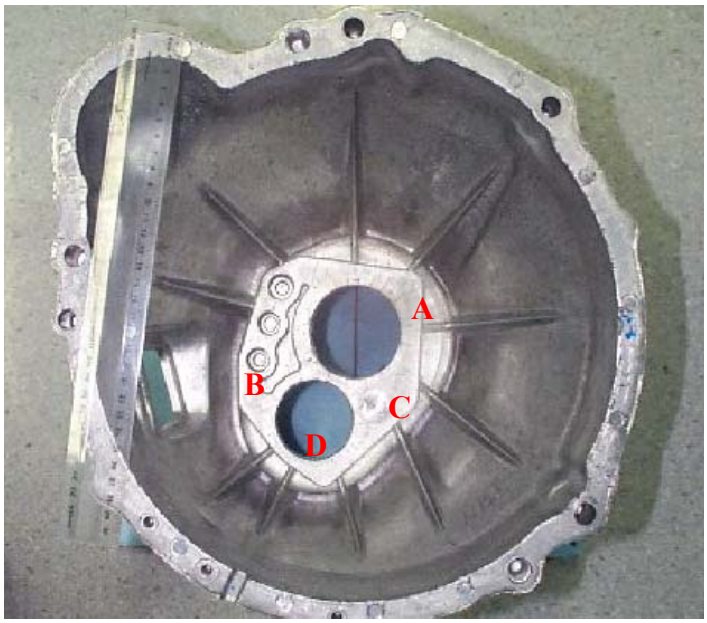

Figure 4.2 Top view of manual transmission case die casting

The critical areas in the castings were around bearing holes and seal bosses. Porosity defects were most noticed at these areas. Porosity type defects were identified as the most critical sub-surface defects in MTC castings, as they can lead to leakage in parts containing fluids.

4.3.4 Structural Oil Sump Pan

Structural oil sump pan (SOSP) castings suffer from leakage problems caused by vertical cracks and porosity at the in-gate region as shown in Figure 4.3. The in-gate area between the arrows in Figure 4.3 is the area where final solidification occurs, leading to shrinkage in this zone which, in turn, causes porosity. The porosity problem is further aggravated by the removal of the in-gate section from the sump through a trimming operation. This opens any porosity near the surface. A leak will result if porosity defects extend through the surface opening to the other side.

(a) **(b)**

Figure 4.3 Structural oil sump pan (a) outside view (b) inside view

The problem of leakage is critical in SOSP castings and occurs through an aluminium wall of the casting, or in a seal area after machining. The critical section is indicated between the arrows in Figure 4.3 (a), which was the focus of the inspection. Further, due to the trimming operation, the area of interest in this section is within a depth of approximately 3 mm from the surface of the casting. Failure due to leakage is usually the result of porosity defects in the casting wall, caused either by entrapped gas or shrinkage during solidification. This problem can result in leakage of compression oil and coolant in the engine assembly.

4.3.5 Aluminium Alloy

The chemical composition of Aluminium alloy CA313 and ADC12 from which castings are manufactured is presented in Table 4.1. The alloys have almost the same combination of elements. In addition to the elements listed in Table 4.1, a very small percentage of Titanium, Chromium, Calcium and Potassium are also present in the alloy.

Alloy	Composition in %								
	Base	**Silicon**	**Iron**	**Copper**	**Manganese**	**Magnesium**	**Nickel**	**Zinc**	**Tin**
ADC12 (MTC)	Al	9.5 – 11	0.8 - 0.9	2.5 – 3.5	0.4 (max)	0.5 (max)	0.5 (max)	1 (max)	0.1(max)
CA313 (SOSP)	Al	9.0 – 10	0.75 - 0.95	2.5 – 3.5	0.5 (max)	0.3 (max)	0.5 (max)	1 (max)	0.3 (max)

Table 4.1 Chemical composition of Aluminium alloy CA313 and ADC12

MTC and SOSP castings are made of ADC12 and CA313 industrial standard aluminium alloys. These alloys are the most widely used general-purpose alloy. They are used principally for high pressure die castings with thin walls, such as manual transmission cases, structural oil sump pans and crankcases. The tensile strength of this alloy is approximately 270 MPa (ultimate stress) and 160 MPa (yield stress). Since CA313 alloy is unsuitable for welding operations, rework is not usually possible on the rejected castings. As such, the rejected castings are scrapped.

4.4 EXPERIMENTAL METHODS AND EQUIPMENT

4.4.1 Overview

There are two types of coupling methods available in the ultrasonic NDT technique as described in Section 3.6. In some cases, air can also act as the couplant with the use of air-coupled transducer types. They mostly operate in the frequency range of 100 kHz up to approximately 2 MHz. In this research, the objective was to detect 0.5 mm diameter defects. However, to detect defects of this size, a higher frequency than is commonly used in air-coupled transducers (greater 2 MHz) is necessary. Therefore, air coupled transducers were not considered in the current research. The initial experiments were carried out using both methods (contact and immersion type) to determine the preferred process for inspecting rough surface aluminium die castings.

4.4.2 Contact Inspection

Contact inspection was carried out on the sample castings to confirm the viability of this method. Normal beam contact probes of 5 MHz and 10 MHz frequencies were used in ultrasonic contact testing (Table 4.2). The velocity of the ultrasonic beam in aluminium according to Australian Standard 2083 [119] is 6320 m/s and it is used in calculating the values in Table 4.2. The back wall echo (reflected ultrasound signal from the back surface of the casting) was not detected in certain sections of the castings due to surface roughness of the castings. In these experiments, a contact probe was moved by hand along the surface of both the manual transmission case and SOSP castings. Even with the use of a couplant, it was difficult to physically move the transducer along the surface. The ultrasonic instrument used in this application was an Epoch III from Panameterics, U.S.A.

Transducer	Frequency (MHz)	Diameter of transducer (mm)	Nearfield (mm)	6 dB Beam Spread	Wavelength (mm)
V109	5	12.7	6.4	0.05	1.264
V112	10	6.35	15.9	0.05	0.632
V535	5	6.35	7.975	0.1	1.264

Table 4.2 Contact transducers

In using the normal beam mode of inspection, it was not possible to detect a clear back wall echo signal due to the front surface roughness of the SOSP castings. To detect a clear back wall echo, it was necessary to have the probe placed with solid contact, at an angle close to perpendicular to the surface. However, due to the rough surface of the castings, it was not possible to reliably place the ultrasonic probe in such a manner. Without proper contact, it was not possible to ensure that a sufficient amount of ultrasonic energy was transmitted at an angle directly into the casting. Therefore, it was not possible to obtain a sufficiently strong signal reflected from the back surface to the probe.

Angle beam inspection was carried out with different angled wedges (30, 45, 60 and 90 degrees). The different combination of wedge shapes and frequency probes were investigated (Table 4.2). However, due to the rough surface of the casting, it was difficult to move the probe with a wedge along the surface of the casting. The outcomes of the ultrasound contact testing experiments carried out on the test cases supported the view of other researchers (refer to Sections 2.4.6.1 and 2.5.3.3) that it was difficult to obtain satisfactory results with contact inspection for complex shaped parts.

4.4.3 Immersion Testing Inspection Rig

4.4.3.1 Overview

The experimental set-up for ultrasonic immersion testing consisted of an ultrasonic flaw detector, immersion probes with different focal length in water, a water tank, calibration blocks, probe holding device and probe handling device. Figure 4.4 shows the experimental set-up where a rough surface casting or a cut section of the casting was inspected with an ultrasonic probe. The sample part was immersed in the water tank and a PUMA robot arm moved over the top of the casting and the ultrasonic signals stored in the flaw detector. Then, the ultrasonic data was transferred to a computer for analysis. The picture of the PUMA robot and water tank along with the ultrasonic equipment is shown in *Appendix B*.

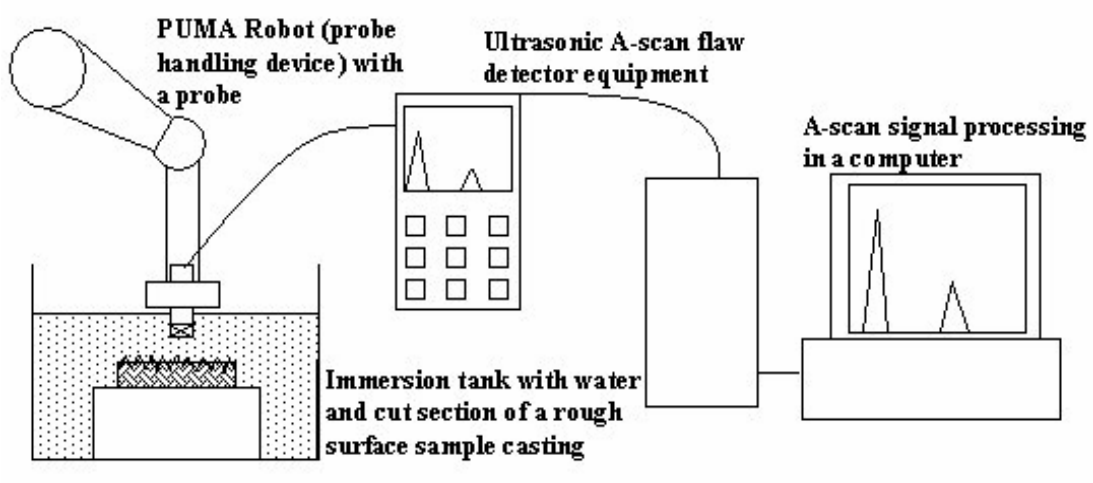

Figure 4.4 Schematic diagram of ultrasonic immersion testing experimental set-up

Water and Sintolin (a reducing agent or anti–oxidising substance) were used as the coupling medium to avoid formation of an oxide layer on the surface of the aluminium alloy casting. The reaction between aluminium (Al) and water (H_20) forms alumina or aluminium oxide as shown in Equation 4.1.

$$2Al + 3H_20 \longrightarrow Al_20_3 + 3H_2 \qquad (4.1)$$

The velocity of ultrasound in the coupling medium (water + 5% of Sintolin) was determined to be the same as that in water, 1480 m/s [119]. Commercial

lubricating oil of the lowest viscosity was also investigated for this application but found to be unsatisfactory on account of unpleasant fumes.

4.4.3.2 Epoch III

The Epoch III digital ultrasonic flaw detector, as shown in Figure 4.5, incorporates an internal alphanumeric data logger (a type of memory storage) that stores A-Scan waveforms with set-up information and flaw detection readings. A-scans stored in the Epoch III are transferred to the signal processing unit (Pentium III 750 MHz processing speed computer) via an RS232 cable.

Figure 4.5 Epoch III ultrasonic equipment with immersion transducers

4.4.3.3 Immersion Transducers

An immersion transducer is a single element longitudinal wave transducer. It is specially designed to transmit ultrasound in situations where the test part is partially or wholly immersed in water. The types of probes used in this research work are listed in Table 4.3. The 10 MHz and 20 MHz frequency probes selected for this research had a focal length of 25.4 mm (1").

Frequency (MHz)	Manufacturer	Diameter of Probe (mm)	Focal Length (mm)	Probe length (mm)
2.25	NDT Instruments Inc	9.525	Non-focal	36
5	Panametrics (V308)	19.05	101.6	6
7.5	Panametrics (V321)	19.05	101.6	6
10	Panametrics (V312)	6.35	25.4	30
15	Panametrics (V313)	6.35	25.4	30
20	Panametrics (V316-NSU)	3.5	25.4	64

Table 4.3 Immersion probes

4.4.3.4 Probe Handling Device

A PUMA robot was used to effect the X, Y and Z directional movement. It has six degrees of freedom and six joints. Table 4.4 provides detailed information on the general functional capabilities of the PUMA robot.

Feature	Specification
Position Repeatability	+/- 0.1 mm
Implement Velocity	470 mm/s straight line moves at VAL II (controller) speed 100
Payload	4 kg or 2.5 kg in the static mode and dynamic mode respectively

Table 4.4 General functional capabilities of PUMA robot

A special probe holding device (manipulator) was designed using Pro/Engineer, a CAD software package, and fabricated for this research. It was then attached to the end effector of the PUMA robot. The major factors considered in the design were the total payload of the end effector and ease of handling the probe. Based on the final design, the probe holding device had a mass of 1.25 kg.

Figure 4.6 illustrates the probe holding device with a 10 MHz ultrasonic probe attached. Two laser pointers were attached to the device for tracing the path of the ultrasonic transducer along the surface of the castings. They were also used to find the distance between the probe and castings (*Appendix C*). The set up was built such that the beam from the ultrasonic immersion probe was co-axial with the laser pointer assembly.

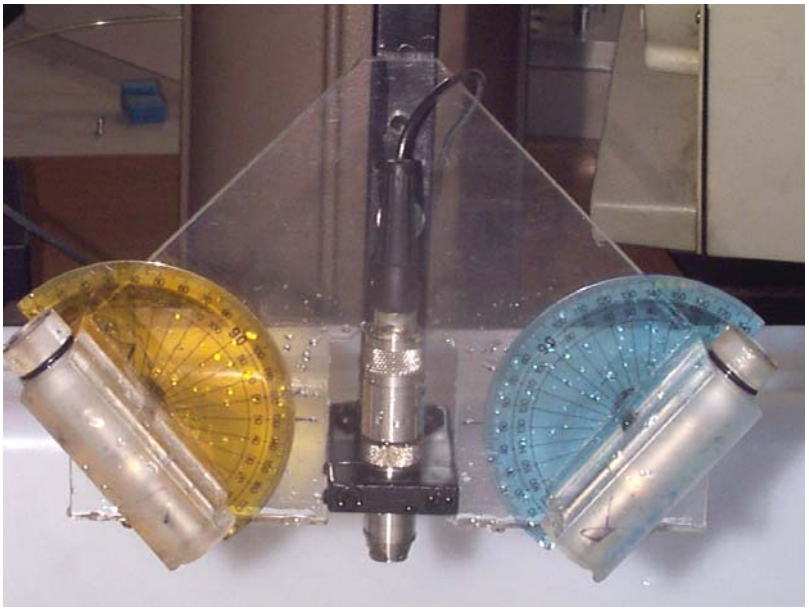

Figure 4.6 Probe handling device with 10 MHz immersion probe

4.5 TESTING PROCEDURE AND SAMPLE PREPARATION

4.5.1 Overview

In the process of developing a suitable ultrasonic immersion technique for the inspection of aluminium castings, many issues had to be considered. The defect parameters (size, location and orientation) had to be identified in the castings and variations in the values of parameters had to be determined. This section describes the preparation of sample castings to carry out ultrasonic immersion testing. The experimental procedure developed in this research minimised the effects of the factors which prevent the echo reflecting from the defect or back wall thereby enabling better defect identification. The following factors are important:

- In high pressure die casting, the variation of defects in terms of location and size is high [13]. To minimise this variation, sample castings were selected from a specific casting machine, and
- Unavailability of sufficient castings with porosity type defects necessitated the introduction of defects through side-drilled holes in good quality castings for the purpose of testing as shown in Figure 4.7.

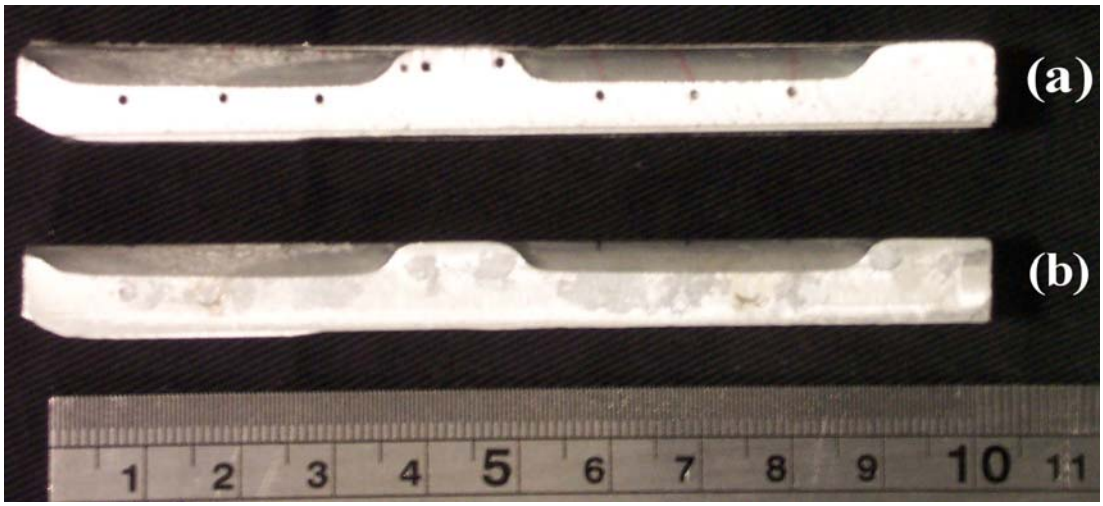

Figure 4.7 Side view of the in-gate casting section with the 1 mm side-drilled holes (a) unclosed holes (b) closed holes with a metallic cement paste

The sample preparation and inspection procedure used is listed in Table 4.5. The following steps were carried out on 30 casting sections.

Step No.	Inspection Procedure
1	Machining of in-gate section of the castings into small sections with dimension of 100 mm x 10 mm x 10 mm
2	X-ray inspection of small casting sections
3	Ultrasonic immersion testing at different frequencies (2.25 to 20 MHz)
4	Surface profile measurement
5	Side-drilled holes of size 0.5, 0.7 and 1 mm at different depth (2, 3 and 4 mm) along the thickness of the castings
6	X-ray inspection of casting sections with drilled holes
7	A metallic cement paste used to cover the openings in the casting produced from the side-drilled holes. It is covered in order to avoid water from entering the holes during ultrasonic immersion testing
8	Ultrasonic immersion testing at different frequencies
9	Machining of 0.3 mm thickness from top surface of the castings at the rough sections and surface profile measurement
10	Ultrasonic immersion testing of machined castings at different frequencies
11	Machining of another 0.3 mm thickness from top surface of the castings at the rough sections and surface profile measurement
12	X-ray inspection of casting sections
13	Ultrasonic immersion testing at different frequencies

Table 4.5 Inspection procedure

4.5.2 Simulated Defects

The literature has indicated that many researchers [58,60,125] have produced their own test blocks containing simulated defects (similar to the original defects). The main reason for the use of simulated defects is the inability to obtain a sufficient number of real defect samples in practice [60]. By using simulated defects, it is

possible to obtain an adequate number of defect signals for the training and validation of the neural network.

In this research, simulated defects were used to identify the capabilities and limitations of the ultrasonic inspection technique in detecting sub-surface defects in castings with significant surface roughness. Cut sections of the in-gate area of the structural oil sump pan casting (Figure 4.8) were used as test blocks. Simulated defects were then incorporated in these test blocks and used for training and validation of the neural network configuration used in the ultrasonic inspection system.

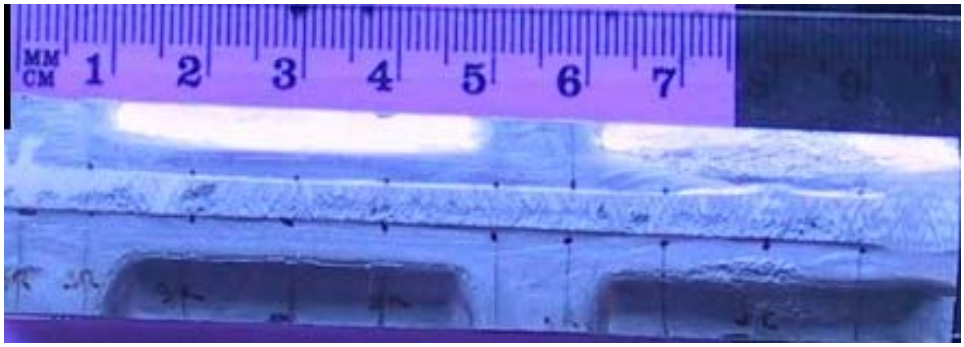

Figure 4.8 A cut section of the in-gate area of structural oil sump pan casting showing the rough surface area

Rajagopalan *et al.* [134] studied the effects of soft computing in a flexible framework for fault diagnosis in an eddy current based non-destructive application. In their case study they also compared the eddy current signals obtained from natural and simulated defects, and combined defects (natural and simulated) in stainless steel plates. One of the main conclusions of their study was the suitability of artificial defects to train a neural network, which can subsequently be used to correctly classify natural defects [134]. Their conclusion is important when there are not enough natural defects available to train and test the neural networks. Another issue with natural defects is that they have a number of parameters (location, size and orientation) that are difficult to control and verify without employing destructive testing. This also includes the morphological aspects like surface roughness of the flaw. Nevertheless, the implantation of artificial flaws introduces other parameters that are hard to control, such as the effect on surrounding material.

As stated previously, side-drilled holes were induced in the castings for purposes of this research. This was undertaken in a similar manner to Onozawa *et al.* [66], who applied side-drilled holes for near surface flaw detection in castings. Their work addressed only smooth surface parts, however, in this research rough surface castings were inspected using ultrasound. The side-drilled holes were placed at depths of 1, 2 and 3 mm (critical areas) below the inspection (front) surface of castings. The sizes of the holes were 0.5, 0.7 and 1 mm in diameter to satisfy the requirements of the research project. The depth and the size of the side-drilled holes were chosen to closely match the depth and size of the natural defects (gas porosity) of interest in this research (Section 4.3.4).

Each casting section contained between 5 and 10 side-drilled holes. Not all of the side-drilled holes were used for subsequent ultrasonic testing. This was due to the problems created either by the drill bits breaking off (as shown in Figure 4.9a) or holes being located in an area not suitable for ultrasonic inspection. Figure 4.9 shows the X-ray image of an in-gate section with simulated defects of 0.5, 0.7 and 1 mm diameter hole size. The actual casting sections, from which these X-ray images were taken is shown in Figure D.1 (*Appendix D*). It is evident from the visual comparison of the X-ray images in Figure 4.9 that 0.5 mm diameter holes are difficult to detect when compared to 0.7 mm and 1 mm diameter holes in the rough surface (Ra0) in-gate casting sections.

4.5.3 Surface Roughness Variation and Measurement

The surface roughness of castings is a critical issue in ultrasonic inspection. Hence, emphasis has been placed on the study of ultrasonic signal variation caused by surface roughness. The surface roughness was predominant in the critical sections of the SOSP castings where the in-gate section of the casting had to be removed. Once the in-gate sections of the casting were detached through a trimming operation (as mentioned in Section 4.3.4), the surface of the casting may open, and a leakage may result. Surface roughness cannot be reduced through machining because even light machining cuts are likely to penetrate the surface, exposing the unsatisfactory

structure with defects. Experiments were carried out on casting sections with different surface roughness ranging from the as-cast surface to the machined surface at the in-gate section of the SOSP castings with simulated and real defects.

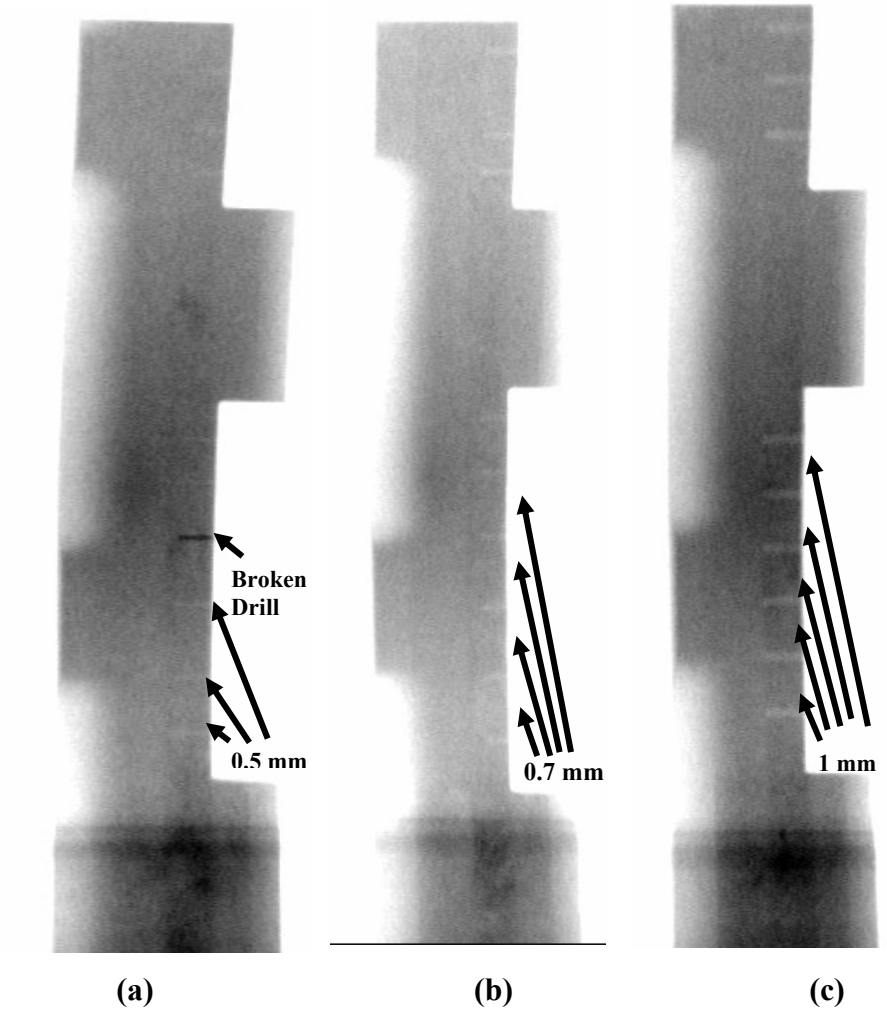

Figure 4.9 X-ray images of simulated defects in the in-gate section of rough surface (Ra0) castings with (a) 0.5 mm (b) 0.7 mm, and (c) 1 mm holes

The surface roughness of the casting was varied by machining the peaks[7] off the rough surface.

Figure **4.10** shows the surface roughness variation on the in-gate section of the same casting section (F56 – Ford casting part serial number) for three different surface types.

Figure **4.10**a shows an un-machined section (Ra0).

[7] Peak: According to Thomas [132] Peak is the highest point on the rough surface of the part which is above a selected reference level.

Figure **4.10**b shows the same section with a partially machined surface (Ra1). It can be seen in this example, that the peaks of the rough surface have been removed, leaving a smooth surface finish, however, there are still as-cast surface regions remaining.

Figure **4.10**c shows the same section with a machined surface (Ra2) in which all of the as-cast surface regions have been removed. The values of each surface roughness range Ra2, Ra1 and Ra0 are given in Table 5.2.

Figure 4.10 Surface roughness variation on F56 casting section (a) as-cast trim pressed, (b) partially machined and (c) machined surface

The surface roughness and topography were measured with the stylus instrument Perthometer S5P as shown in Figure 4.11. The experiments were carried out on castings with varying surface roughness using the ultrasonic inspection technique is described in Chapter 5.

Roughness is independent of the sampling interval but depends on the high-pass cut-off, while the slopes and curvatures are independent of the high-pass cut-off but depend on the sampling interval [135]. In the surface roughness measurement, correlation length is defined as the radial distance required for the area to be measured [136]. The amplitude parameters and those depending on the autocorrelation function are sensitive to long wavelengths, and texture and hybrid parameters are sensitive to sampling interval. Most machined surfaces tend to have a slight negative skew, because peaks are more easily removed than valleys [135]. The average roughness R_a is the arithmetic mean of all values of the roughness profile within the measured length. This parameter is the most effective surface roughness measure that is most commonly adopted in general engineering practice [137]. These surface roughness values provide a good general description of the height variations in the tested surface. A recent experimental study on the ultrasonic evaluation of surface roughness by Abdelhay and Mubark [137] used R_a values for assessment of surface roughness. All these surface measurements were carried out on 10 casting sections, each with between 5 and 10 side-drilled holes in them. Sample data obtained from the Perthometer instrument is presented in Table D.1 (*Appendix D*).

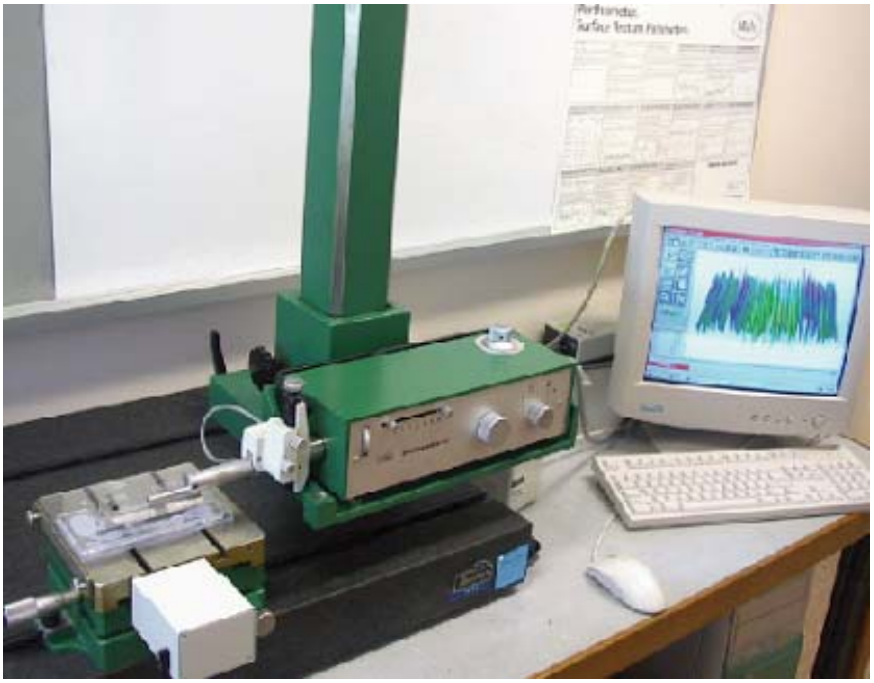

Figure 4.11 Perthometer –Surface profile measuring instrument

Prior to commencing the inspection process, the initial parameters (inspection method and frequency) were determined using the backscattering method. An indirect method of measuring attenuation involves the observation of pulse echoes reflected to the source by backscattered signals, received from scattered reflections due to material variation such as surface roughness [22]. Guo *et al*. [138] observed the effects of backscattered noise in ultrasonic signals due to periodic surface roughness. In their work they presented the effects of backscattering, which can obscure flaw signals and place a fundamental limitation on the ability to detect flaws. They also carried out a numerical and experimental study on the decay of Back Wall Echo (BWE) due to the increase in surface roughness. The result proved that the larger the surface roughness, the higher the roughness induced noise in the signals. Larger surface roughness also leads to reduction of the BWE amplitude.

4.5.4 Summary

The inspection procedure described was used in the ultrasonic inspection of castings. The gas porosity type defects were simulated with side-drilled holes in the

castings. Simulated holes in the castings sections were inspected within the framework of variations in surface roughness of the castings to determine a suitable frequency for inspection.

4.6 CALIBRATION & REPEATABILITY TESTS

4.6.1 Overview

The discussion so far has been in relation to effecting the ultrasonic inspection task itself, but in the overall preparation for an inspection, the calibration of instruments is also an important factor. The ultrasonic instrument set-up requires a range of calibration and sensitivity settings to be made according to given standards, using defined calibration blocks. Hence, calibration issues are addressed in this section. The calibration of equipment has to be carried out prior to commencing ultrasonic immersion testing and is essential for the PUMA robot and ultrasonic equipment used in the inspection of castings. These calibrations confirm the accuracy and repeatability of the test results.

4.6.2 PUMA robot

The calibration of the PUMA robot used in the immersion testing of components was carried out by moving the robot arm repeatedly to a particular point, to determine its repeatability. The variations in the co-ordinate values of the PUMA robot tool centre point were recorded using three dial-gauges for the three axes of movement (X, Y and Z) as shown in Figure 4.12.

Figure 4.12 Calibration set up of PUMA robot using dial indicators

Figure 4.13 illustrates the positional repeatability of the PUMA robot. It indicates a robot repeatability of ± 0.02 mm at a particular position in the three directions. The variation (standard deviation) of the positional placement of the robot end effector was 0.01, 0.02 and 0.01 mm in the X, Y and Z axes, respectively. The positional variation of the PUMA robot at a particular location was substantially smaller than the smallest defect size (0.5 mm) to be detected in this research. Hence, from these experiments it could be concluded that the repeatability of the PUMA robot was within the limits for carrying out ultrasonic immersion testing.

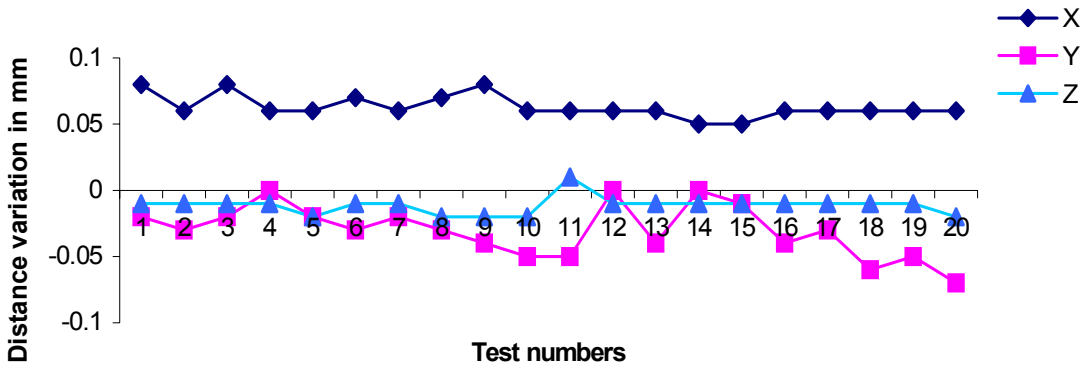

Figure 4.13 Positional repeatability of PUMA robot

4.6.3 A-scan Display Repeatability Tests

The A-scan signal amplitude of the back wall echo (vertical linearity) was obtained to evaluate the repeatability of the EPOCH III ultrasonic equipment. The amplitude of the back wall echo signal was measured with reference to the Full Screen Height (FSH) of the A-scan display. These tests were carried out on a sample casting section without defect (C2) and another section with a gas porosity type defect (C5). The actual casting sections are illustrated in *Appendix E*. In this experiment, the ultrasound signal amplitude was obtained for 20 cycles, where for each cycle the ultrasonic probe was moved from an arbitrary external location to the measurement location. The back wall echo amplitude was measured relative to the FSH of the A-scan display as shown in Figure 4.14. It can be observed from the figure that there was a reduction in ultrasonic signal amplitude during one measurement cycle. This was due to the movement of the transducer out of the couplant medium (i.e., static water column as shown in Figure B.2, *Appendix B*) at the end of the particular inspection cycle. This action resulted in the formation of air bubbles at the tip of the transducer, leading to a decrease in the back wall echo amplitude. This phenomenon necessitated checking for the formation of air bubbles at the tip of the transducer during each immersion testing cycle. Otherwise, there was only a variation of 1 dB in amplitude for the remaining signals observed from both the defect and non-defect sections of the castings, as shown in Figure 4.14.

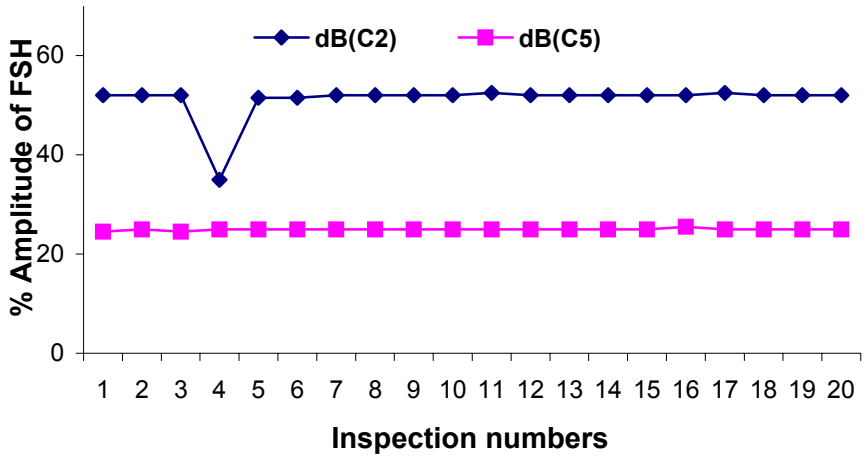

Figure 4.14 Repeatability test on the ultrasound equipment for the back-wall echo signals with C2 (without defect) and C5 (with defect) castings

The maximum error that can be tolerated is a 1% deviation in the normal value of the ultrasonic signal amplitude [5]. Since in this case only ± 1 dB variation occurred in the experiments, measurement of the vertical linearity of the signal was kept under control.

For this calibration procedure, it was necessary to set an appropriate signal gain for the amplification of the probe output signal. During the assessment of the vertical linearity, time-base readings were taken as the back wall echo was brought to a common amplitude (60 dB). This was done by increasing the electronic gain set up in the EPOCH III equipment to attain the same back wall echo amplitude. It is necessary to ensure that the gain value was not too high, such that the ultrasonic signals would saturate. Conversely, it is necessary to ensure that the gain value was not too low, such that low amplitude signals were undetected. A series of experiments were undertaken to evaluate an appropriate gain value on a selected range of sample casting sections, with varying surface roughness, both with and without defects. It was found that the gain of 60 dB for the EPOCH III equipment was suitable for majority of the castings. This gain value was used for all subsequent experimental work.

The same experimental conditions, in regard to the placement of casting sections, probe positional control and static water column, were used in all of the subsequent experiments carried out on casting sections.

4.7 VALIDATION OF ULTRASONIC RESULTS

Validation of results is important to ensure that NDT techniques produce reliable and repeatable results with an acceptable level of certainty. To qualify the procedures, extensive experimental work on test blocks is normally required. A large number of variables and possibilities have to be reduced to a limited group of statistically relevant NDT situations. In order to validate the ultrasonic inspection results, X-ray and Visual inspections have been used in this research.

The results obtained from immersion testing were validated against the X-ray results obtained from radiographic inspection. Figure 4.15 illustrates the ultrasonic defect signal obtained from a sample part. An arrow mark in the figure also shows that the defect signal from ultrasound testing corresponds to the gas porosity defect in the X-ray image obtained from the same part, at the same location. From the ultrasonic signal it was determined that the approximate depth of the defect was 7 mm from the front surface.

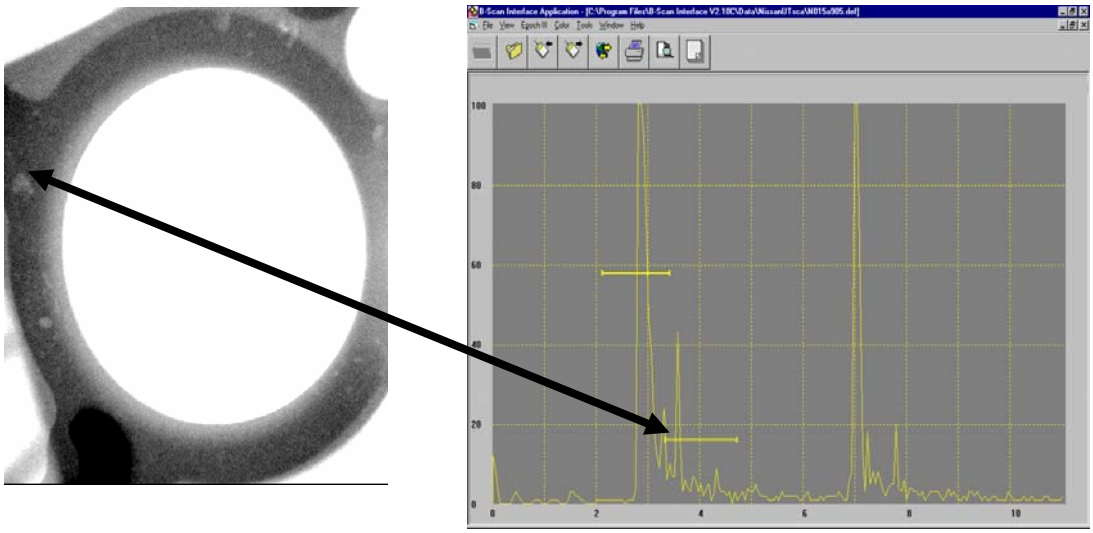

(a) **(b)**

Figure 4.15 Validation of results (a) X-ray image and (b) A-scan display of ultrasonic contact testing at the same location

Visual inspection of the defect was carried out on the cut section of the castings after the ultrasonic and X-ray inspections were completed. Given the estimated location of the defect, the castings were cut into small sections at that location. Figure 4.16 illustrates a casting section containing a single gas porosity defect, where the distance between vertical lines is 1 mm. It can be seen that the distance between the defect and the front surface is approximately 7 mm. The results of this visual inspection indicated that it was possible to identify defects using ultrasonic inspection.

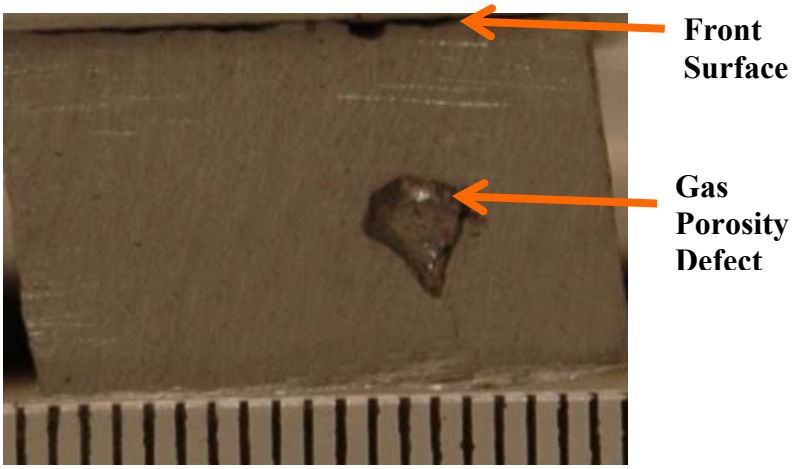

Figure 4.16 A cut-section of gas porosity defect in the sample casting

X-ray inspection was carried out to identify defective and non-defective sections of the castings. This information was required for the purpose of selecting appropriate ultrasonic parameters such as frequency (Section 5.5) and to train the neural networks (Section 6.3) to identify the defects.

4.8 SUMMARY

The methodology developed to carry out this research was based on the requirement to detect the gas porosity type defects in aluminium die castings. After suitable sample castings (structural oil sump pan and manual transmission case castings) were selected, the initial calibration of apparatus and equipment was carried out. The experimental set-up consisted of an ultrasonic flaw detector, immersion probes with different focal lengths in water, a water tank, calibration blocks, a probe holding device and a probe handling device. The X-ray and visual inspection methods were also described, and used for validating the results obtained from the ultrasonic immersion testing of castings. Suitable inspection parameters had to be identified to carry out successful experiments as described in the methodology. The following chapter presents the outcomes on the selection of suitable inspection parameters for ultrasonic inspection of aluminium die castings.

CHAPTER 5.
ULTRASONIC INSPECTION PARAMETERS

5.1 OVERVIEW

The experimental procedure adopted should ensure that the effects of ultrasound attenuation associated with the casting are minimised. This results in maximising signal amplitude from both the back surface and defect within the rough surface castings. In order to obtain the signals, experimental parameters had to be determined to carry out ultrasonic immersion testing on the selected sample die castings. These parameters were ultrasonic wave velocity in the casting material, water path distance and a suitable frequency for accommodating the structural variations in the castings. The major structural variations in the castings are grain size and surface roughness. As the signal-to-noise ratio is very important in quantifying sub-surface defects, the major factors relating to noise creation in the ultrasonic signal during ultrasonic immersion testing were identified and addressed as described in this chapter. The following sections describe the experiments performed to determine experimental parameters such as acoustic impedance, velocity of ultrasonic waves in aluminium alloy, frequency range and water path column distance.

5.2 ULTRASOUND VELOCITY IN MATERIAL

The velocity of ultrasound in aluminium is 6320 m/s, but varies in different aluminium alloys [120]. The castings being investigated in this research are made of Al-Si alloy (chemical combination is presented in Table 4.1) which is a series 4 alloy [139]. The simplest method of measuring the velocity of ultrasound in a part of known thickness, using the pulse-echo method, is to measure the time between receipt of the front wall echo and the first back-wall echo [22]. The velocity of ultrasound can be calculated from the calibration of the time base of the ultrasonic screen as shown in Figure 3.1. In general terms, it can be noted that the velocity is independent of frequency and it can be interpreted in terms of the ratio of a modulus of density of the material [29]. Ultrasonic testing was carried out on defect free sections of manual transmission case sample castings to determine the reference velocity of ultrasound in order to avoid the variation in the material density. X-ray inspection was used to find the defect-free sections of the castings. Thereafter, the actual thickness of the casting was measured using a vernier calliper. The thickness at the measurement location was 8.0 mm, measured to an accuracy of ±0.1 mm.

In order to ascertain the velocity of the ultrasound in the test material, the velocity as specified in the equipment was varied between 6200 – 6400 m/s and the thickness of the casting was determined using the EPOCH III flaw detector (Section 4.4.3.2). Thereafter, the actual thickness of the casting was measured using a vernier calliper and compared with the thickness measurement obtained from the flaw detector for the velocity of ultrasound in the test material. A similar process has been described by Papadakis [53] on the operation of flaw detectors in determining the velocity of ultrasound in a specific material.

After completion of the procedure described above two values of velocity of ultrasound in the material (6250 and 6270 m/s) were obtained. Thereafter, the velocity reading was varied in the equipment between 6250 m/s and 6270 m/s to determine the velocity reading which produced the maximum back wall echo signal amplitude. The maximum amplitude was found at a velocity of 6260 m/s, and this velocity reading was maintained throughout the inspection process.

5.3 ACOUSTIC IMPEDANCE

In the next stage of the experimental program, ultrasonic immersion inspection was carried out on the same set of castings used in ultrasonic velocity measurement to determine the effect of acoustic impedance. The ultrasound signal was focused at the surface of the casting using a focus beam probe. A velocity of ultrasound in water of 1480 m/s [120] was used in these experiments. To ensure that the highest possible amplitude echo was obtained from the casting surface, the probe location and orientation were adjusted so that it remained perpendicular to the casting surface. Similarly, the ultrasound signal was focused on the back surface of the aluminium alloy casting to obtain the maximum amplitude with the previously selected velocity of 6260 m/s. for normal pulse-echo ultrasonic testing [140]. If there was a slight change or loss in the back wall echo amplitude due to misalignment of the probe it could lead to misinterpretation of signals received from castings with defects. The probe handling device was adjusted using the above procedure to ensure that the probe was approximately perpendicular to the front and back surface of the casting to obtain an ultrasonic signal with the maximum possible amplitude.

In immersion ultrasound testing, the ultrasound travels from water (medium 1) to the Aluminium alloy sample part (medium 2). In general, part of the incident ultrasound in medium 1 is reflected back along incident path and the remainder is transmitted through medium 2. The transmission loss (α_t) of ultrasound [22] from medium 1 to medium 2 is calculated from the acoustic impedance as shown in Equation 5.1.

$$\alpha_t = 4 R_1 R_2 / (R1 + R_2)^2 \quad (5.1)$$

where R_1 = acoustic impedance of water = $1.5 * 10^6$ kg/m^{2}s

R_2 = acoustic impedance of aluminium = $1.7 * 10^7$ kg/m^{2}s

Substituting above values of R_1 and R_2 in Equation 5.1 resulted in α_t being equal to 0.2989, which means approximately 30% of the incident beam was transmitted into the smooth surface material and remaining 70% was reflected back

from the surface [120]. However, in this research the sample castings had rough surfaces which would result in further loss in the ultrasonic signal transmitted into the casting. A detailed discussion on the loss of ultrasonic signal due to the effect of a rough surface is presented in Section 5.6.5.

5.4 WATER PATH DISTANCE

As shown in Figure 5.1**,** the lens in the probe focuses the sound energy into a small and narrow beam**.** The velocity of sound in water is about a quarter of that in aluminium or steel parts. The distance between the probe and the part (sample casting) is called the water path (WP) distance. The WP distance [116] is obtained from Equation 5.2.

$$WP = F - \left[MD\left(\frac{V_m}{V_w}\right)\right] \tag{5.2}$$

where

F = Focal length in water (mm)

MD = Material Depth (mm)

V_m = Velocity of ultrasound in material = 6260 m/s, and

V_w = Velocity of ultrasound in water = 1480 m/s

Ultrasonic immersion testing was carried out on the castings using the experimental rig (as described in Chapter 4). Experiments were carried out with ultrasonic immersion probes with frequencies of 10 and 20 MHz and a focal point of 25.4 mm in water. These experiments were used for determining the optimum water path distance to focus the ultrasonic beam approximately 4.5 mm (material depth) from the front surface of the casting. It was important to inspect the castings to a depth of 4.5 mm in this research.

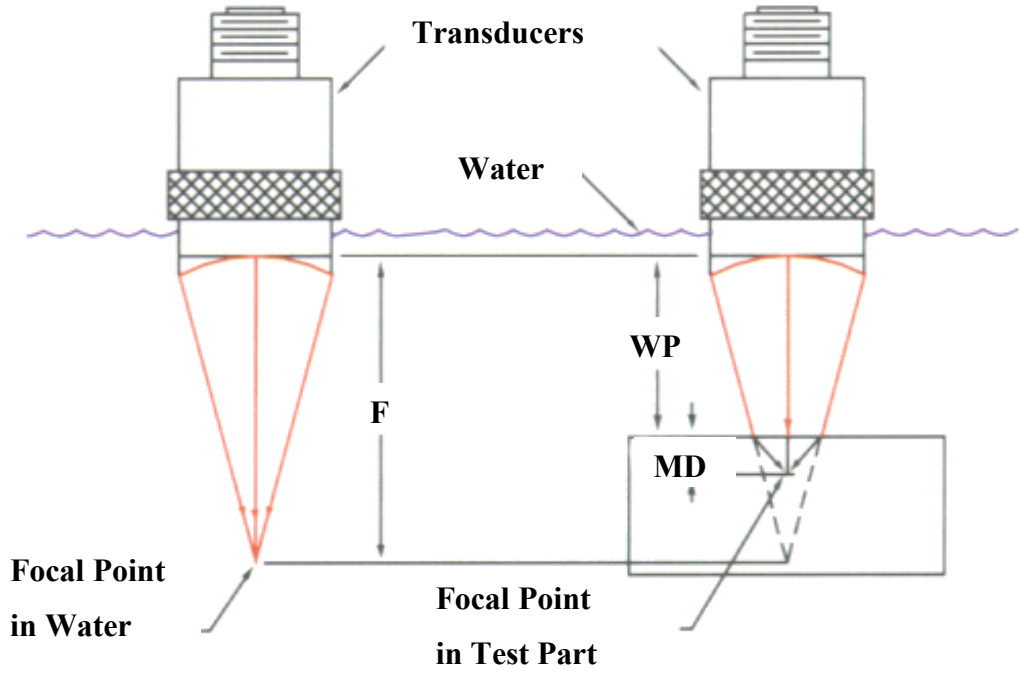

Figure 5.1 Immersion transducer sound path [116]

Ultrasonic testing was carried out at sixty different locations on selected castings without defects to obtain a suitable back wall echo. The castings were selected for these experiments as described in Section 5.2 (i.e. castings were selected according to the X-ray analysis). The mean percentage Back Wall Echo (BWE) of the Full Screen Height (FSH) amplitude signal obtained at different sections of the sample castings without defects is plotted in Figure 5.2. The maximum BWE amplitudes (85%) were obtained at a probe frequency of 10 MHz and 7.5 mm WP distance. In this instance the remaining 15% of BWE was lost due to the effects of grain size variation and surface roughness. These material variations are discussed in Section 5.5.

From the graph, it is evident that at 10 MHz and 7.5 mm water column distance the maximum BWE amplitude was achieved compared with BWE amplitude achieved with a 20 MHz frequency probe at different water path distances. The numerical water path distance value was calculated using Equation 5.2 to focus at the material depth (MD) of 4.5 mm inside the 8 mm casting section. As mentioned in Chapter 1, the first few millimetres below the front surface were considered to be the most critical for these casting sections. A distance of 4.5 mm was chosen such

that the majority of relevant defects would be identified. Then, substituting the MD value along with focal point of 25.4 mm in water for a 10 MHz probe gives the water path distance of 7.4 mm. The water path distance obtained from the experiment (7.5 mm) and from the Equation 5.2 (7.4 mm) was almost equal. After these initial experiments, a water path distance of 7.5 mm was selected to carry out further experiments in this research. Once the velocity of ultrasound in the material and water path distance were determined, the effects of material variation on the ultrasonic signal amplitude at different probe frequencies were measured.

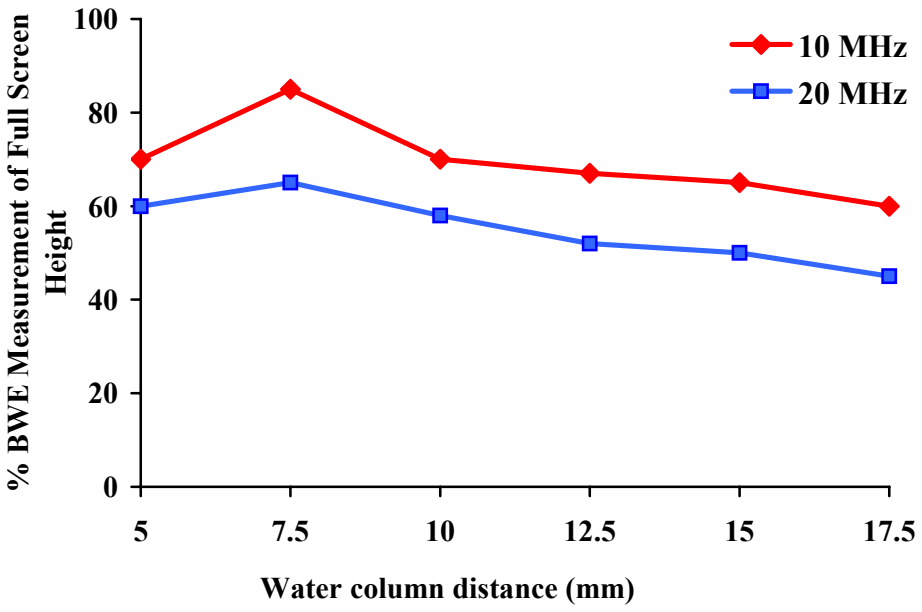

Figure 5.2 Optimisation of water path distance and probe frequency

5.5 PROBE FREQUENCY SELECTION

5.5.1 Overview

The aim of this section is to describe the development of a method to identify a suitable frequency for inspecting the castings. The selected frequency has to accommodate the varying material properties of aluminium die castings.

5.5.2 Total Attenuation Loss

According to Adler *et al.* [64] the total attenuation (L) in a casting consists of separate components as listed in Equation 5.3.

$$L = L_{Imp} + L_{Diff} + L_{Grain} + L_{Surf} + L_p \tag{5.3}$$

where L_{Imp} is the double transmission loss at the water and casting interface in ultrasonic immersion testing; L_{Diff} is the loss due to ultrasonic beam spread as it propagates back and forth within the castings; L_{Grain} is the loss due to grain size variation; L_{Surf} is the loss due to casting surface roughness and L_p is the loss due to porosity [64]. The research by Adler *et al.* [64] focused on calculating the porosity-induced attenuation and attenuation due to grain size variation and surface roughness [64]. These factors are important in evaluating casting quality using ultrasonic testing. In the current research, the focus was to evaluate the attenuation due to surface roughness and grain size variation. To achieve this, it was necessary to eliminate the factors of L_{Imp}, L_{Diff} and L_p.

After the initial parameters such as velocity and water column distance were obtained, experiments were carried out on the castings to determine the influence of L_{Imp} and L_{Diff} as a function of frequency.

Experiments were conducted to find the attenuation due to ultrasonic beam spread as it propagates back and forth within the castings (L_{Diff}). The application of the focused probe reduced the effect of beam spread in comparison to an un-focused probe [70]. The front surface echo was measured by focusing the transducer (10 MHz and 25.4 mm focus probe) on the smooth front surface of the casting (Figure 5.3a**)**. Similarly, the back wall echo was recorded with the transducer focused on the smooth back surface (Figure 5.3b). There was a loss of the ultrasonic signal amplitude due to multiple reflections in the material. The attenuation due to L_{Diff} was considered negligible in this research as the signal analysis was carried out up to the first back surface signal only. Hence, the effect of multiple reflections within the material was not relevant.

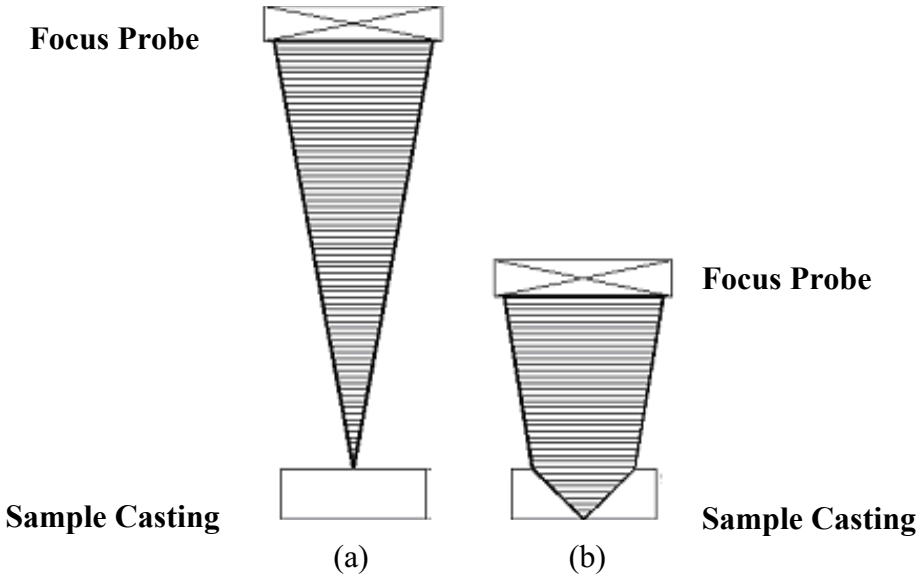

Figure 5.3 Beam profile as the transducer focused on (a) the front and (b) the back surface of the sample casting [141]

Another key factor was the difference in acoustic impedance at the water-aluminium interface that resulted in nearly 70% of the ultrasonic energy being reflected away from the material (refer Section 5.3). L_{Imp} is generally constant at any frequency due to the fact that there is no variation of the acoustic impedance in water and aluminium (as a function of frequency). This is due to the fact that the acoustic impedance is a function of velocity and density, which is a function of material properties and it is constant for any given probe frequency [22]. Velocity is generally constant for any applied frequency on a given material [5]. The total change of attenuation in the ultrasonic signal at different frequencies can be calculated by summing the changes in different parameters as shown in Equation 5.4a:

$$\Delta L = \Delta L_{\text{Imp}} + \Delta L_{\text{Diff}} + \Delta L_{\text{Grain}} + \Delta L_{\text{Surf}} + \Delta L_{\text{P}} \tag{5.4a}$$

$$\Delta L = \Delta(L_{\text{Grain}} + L_{\text{Surf}} + L_{\text{P}}), \text{ if } \Delta L_{\text{Imp}} \cong 0 \text{ and } \Delta L_{\text{Diff}} \cong 0 \tag{5.4b}$$

From the above findings it is determined that the ΔL_{Diff} and ΔL_{Imp} terms are negligible and eliminated from Equation 5.4a giving Equation 5.5.

$$\Delta L = \Delta L_{Grain} + \Delta L_{Surf} + \Delta L_{p} \tag{5.5}$$

Specifically, investigations were carried out to determine the difference in attenuation (ΔL) between the selected sample castings due to material variations. Further experiments were conducted with several smooth surface casting sections without defects. The X-ray inspection method was used to identify the defect-free sections of castings (Section 4.7). Hence for these defect free sections of castings, the total change in attenuation (ΔL) was only due to sum of the change in L_{Grain} and L_{Surf} without the contribution of porosity defect induced attenuation (ΔL_p). Thus Equation 5.5 reduces to Equation 5.6:

$$\Delta L = \Delta L_{Grain} + \Delta L_{Surf} \tag{5.6}$$

Finally, the sample castings for this investigation were selected with varying material features in relation to grain size and surface roughness. The grain structure of the material to be inspected posed a serious problem for ultrasonic inspection. The larger size of the grains in relation to the wavelength of ultrasound led to an increase in the noise level. This fact necessitated separate in-depth studies of the effects of grain size and surface roughness variations on total attenuation of the ultrasonic signal.

5.5.3 Geometry

The geometry of the part determines the ability of the ultrasonic beam to access the defects. It also determines the choice of modes for inspection. At the critical sections of the selected sample castings, the thickness of the part did not have any major variations. However, both sides of the casting are not normally accessible for castings considered in this research for through transmission ultrasonic inspection. Hence, the pulse-echo method of ultrasonic inspection was used due to geometrical constraints.

5.5.4 Grain Size

The intensity of ultrasonic waves passing through the aluminium material is reduced due to scattering at the grain boundaries within the material [29]. Grain size measurements were taken on the sample parts and correlated with the ultrasonic signal amplitude at different frequencies in the range of 2.25 to 20 MHz. Castings were sectioned by the standard cutting method as described in the Metals Handbook [142]. Roland [143] discussed at length the grain size and porosity measurement techniques for cast light metal alloys, and a similar procedure for the grain size measurement has been applied in this research.

In this research, the grain size type (fine, medium or coarse grain) was determined using the following process:

1. The samples were polished by mechanical means to a high polish grade
2. The samples were anodised in a solution made of 6 ml Hydrofluoroboric acid (HBF_4), 6 ml of Hydrofluoric acid (HF), 144 ml Ethanol and 444 ml H_20 at potential of 30 volts for 2 minutes.
3. The anodised samples were examined under polarised light. The separate grains were clearly distinguished by colour variations (purples, blue, yellow, red, brown, etc) indicating different crystallographic orientations as seen in Figure 5.4.

The average grain size was then measured using the linear intercept method [71], in which the distance between the centres of two adjacent grains were measured to give an indication of the grain size present in the casting.

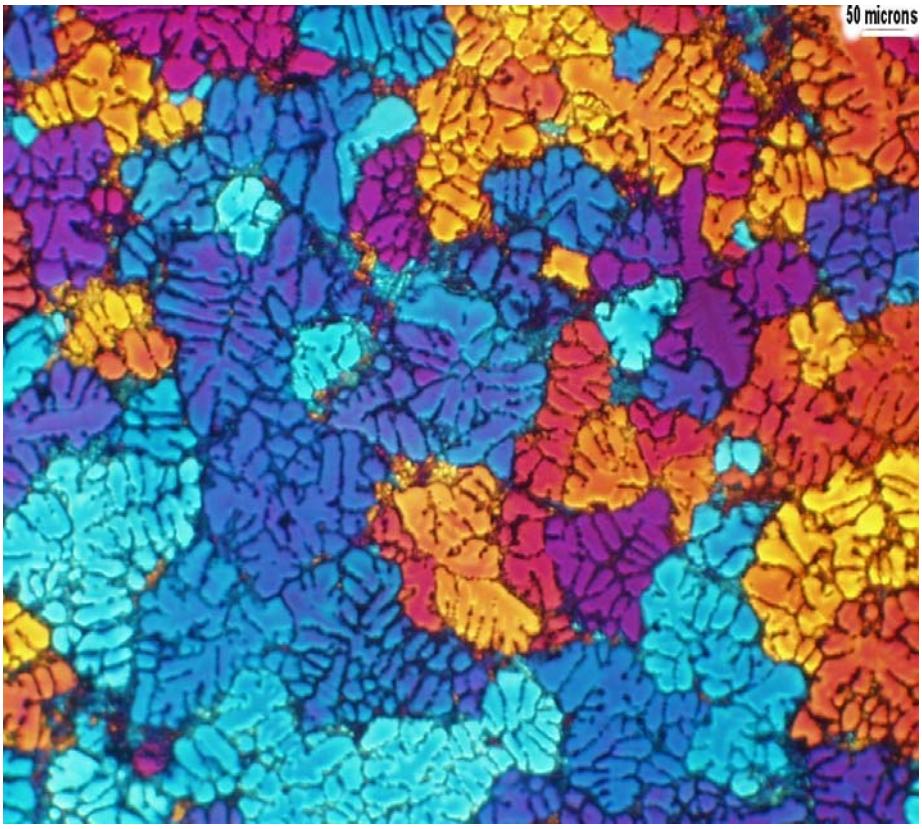

Figure 5.4 Microstructure of CA313 aluminium alloy showing different grain orientation at the in-gate section of the casting

After ultrasonic inspection was carried out on the in-gate casting sections, a number of polished samples were obtained from those sections. Then, the grain size values were obtained by analysing a total of 60 randomly selected areas in the polished samples. The grain size measurement values ranged between 0.1 to 1.2 mm. They were grouped into three grain structures as shown in Table 5.1 depending on their grain size and dendrite arm spacing range. The values were determined as mentioned above from the metallographically prepared specimens. The grouping of grains by size enabled the investigation of the effects of the different grain size on ultrasonic signal amplitude [71]. For each of the measurement areas, the line intercept method was used to measure the distance between two adjacent dendrite arm spacing and width. This is illustrated by the double headed arrow marks shown in Figure 5.5.

Sample Casting Grain Structure	Grain Size (mm)	Dendrite arm spacing range (μm)
Fine	0.1- 0.25	10-30
Medium	0.26 – 0.50	31-50
Coarse	> 0.50	51-100

Table 5.1 Three grain structures of sample castings

Most of the castings under investigation consisted of fine to medium sized grains, typical of the high-pressure die casting process in which molten metal solidifies in seconds. It was found that coarse grains were rarely present, and always at the sections with varying thickness (baffle area of the in-gate section) due to slower solidification rates at those sections. The medium grain size was located near the area adjacent to the baffle area of the in-gate casting section. The reason for this was due to the uniform solidification rate and constant in-gate thickness apart from the baffle area.

Further, it was found that the grain size values were relatively consistent for each sample. For instance, those samples selected from regions away from the baffle area only had grain size values within the fine grain structure range (0 to 0.25 mm), and those samples selected from the baffle area regions only had grain size values within the coarse grain structure range (> 0.5 mm).

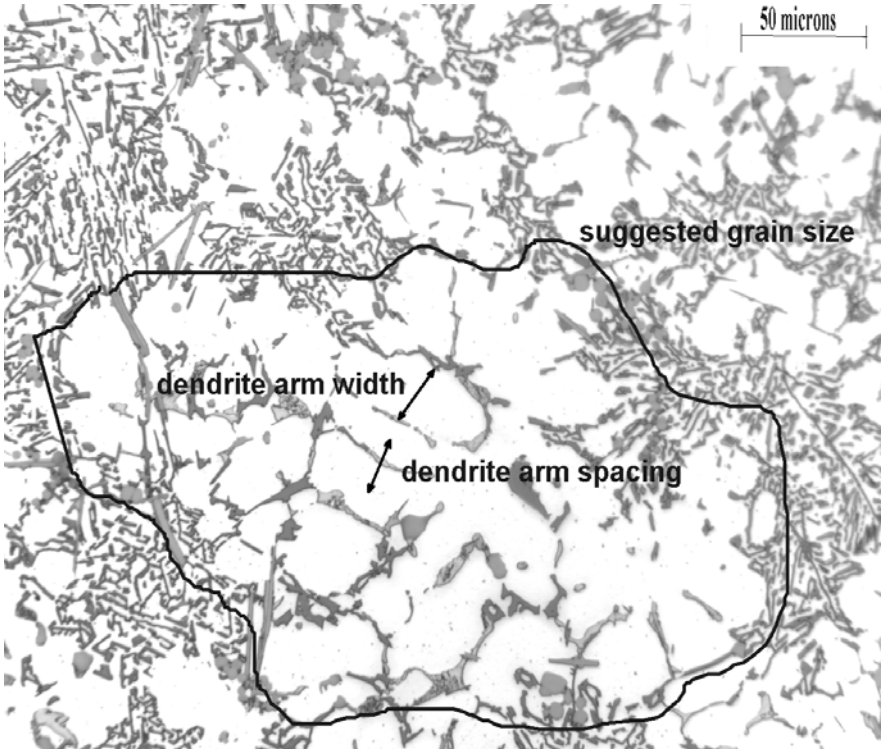

Figure 5.5 A typical microstructure of CA313 aluminium alloy casting

Experiments were carried out on surfaces with a roughness value (R_a) less than 5 μm for 8 mm thickness casting sections at the defect-free areas. In these experiments only smooth machined surfaces ($R_a < 5$ μm) were used for studying the effect of grain size variation, using the selected frequency range of 2.25 MHz to 20 MHz. Regardless of the frequency within this range, the wavelength of the ultrasonic signal was significantly larger than the surface roughness. For instance, the smallest wavelength ($\lambda = 0.3$ mm), corresponding to the frequency of 20 MHz, was significantly larger than the surface roughness ($R_a = 5$ μm). Therefore, for all frequencies within this range, the attenuation due to surface roughness was considered to be negligible ($L_{Surf} \approx 0$). From this, the change in attenuation due to surface roughness as a function of frequency was also considered to be negligible ($\Delta L_{Surf} \approx 0$). Therefore, Equation 5.6 can be further simplified to Equation 5.7, and it can be seen that the change in attenuation (ΔL) is only caused by grain size variation (for the smooth surface castings in this section).

$$\Delta L = \Delta L_{Grain} \tag{5.7}$$

The relationship between back wall echo amplitude and probe frequency for different grain structures is described in Figure 5.6. As can be seen in Figure 5.6, as the frequency increased, the BWE for a given grain size generally decreased. However, it can also be seen that for all grain size types that there was a decrease in BWE amplitude for the 2.25 MHz probe compared to the 5 MHz probe. A possible reason for this is the particular probe types used. The 2.25 MHz probe was the only unfocused probe used in this experiment, and the un-focused nature of the beam may have lead to more scattering and higher beam spread within the material when compared to the focused probe [67].

A further finding of this analysis was that an increase in grain size resulted in a decrease in BWE amplitude. For instance, a 10% loss in BWE amplitude was observed between fine and medium grain size as compared to a nearly 50% (i.e., equal to 6 dB drop) loss between the fine and coarse grain structure. This was due to multiple scatter happening at coarse grain structure. Similarly, the standard deviation of ultrasonic signal amplitude was larger for coarse grain structure compared to medium and fine grain structure. The standard deviation was obtained when 5 measurements were obtained for different grain structures at a particular frequency. The high standard deviation values were obtained for high frequencies (15 MHz and 20 MHz) compared to frequencies up to 10 MHz. The 5 MHz focused probe attained the maximum BWE amplitude in relation to all other frequencies for all the grain sizes. As a result of these experiments, it could be concluded that frequencies up to 10 MHz would provide higher amplitude BWE compared to high frequencies. Hence, the frequency range of 5 MHz to 10 MHz was selected as the most suitable for inspecting the die castings considered in this research.

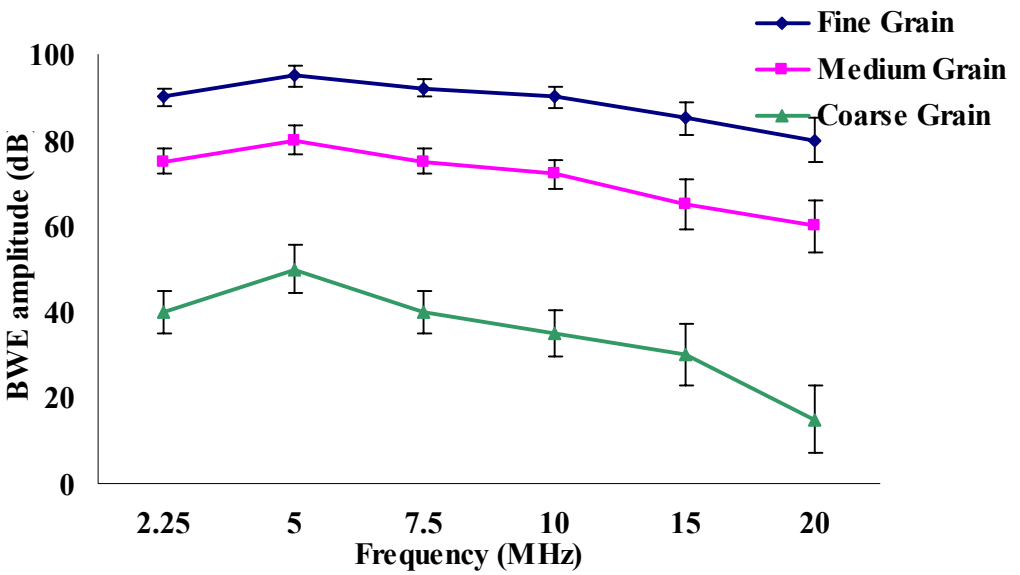

Figure 5.6 Variation of BWE and probe frequencies for different grain sizes

The described experiments enabled the identification of the effect of grain size variation on ultrasonic back wall echo signals. Further experiments were carried out on casting sections with fine grain structure to investigate the effects of surface roughness on the ultrasonic signals.

5.5.5 Surface Roughness

Surface roughness affects the resolution and sensitivity of ultrasonic signals in the same manner as the grain structure does [5]. A spreading out of the front surface echo due to the rough surface causes the loss of resolving power in the ultrasonic signal. This is seen as a wide front surface echo on the oscilloscope and is caused by reflection of the transducer side lobe energy. Side lobe energy is normally not reflected back into the transducer from smooth surfaces. This condition masks the discontinuity below the surface. Widening of the beam due to scatter from the rough surface leads to the requirement for a lower frequency to reduce scatter. Ultrasonic signals obtained from both smooth and rough surfaces are illustrated in Figures 7.3 and 7.4 (Section 7.2).

In this work, ultrasonic immersion testing experiments were conducted with castings having different surface roughness values. The literature review (Section 2.5.3) indicated that past investigations have been confined to castings with roughness values (R_a) less than 50 μm [54, 64, and 65]. However, most of the castings analysed in this work had surface roughness values varying between 50 μm and 150 μm. The back wall echo (BWE) was evaluated as a function of surface roughness and incident frequency. The measurement of BWE amplitude provides the in-direct measurement of attenuation due to surface roughness when the BWEs of the rough and smooth surface castings are compared i.e., with and without attenuation respectively [5]. The roughness on the rear side (back surface) of the casting was ignored because surface roughness R_a in this region was less than 5 μm. It was not considered as a factor in the loss of BWE amplitude.

The major reason for studying the effect of BWE compared to the effect of Front Wall Echo (FWE) was due to the fact that there is a significant loss of amplitude and presence of multiple FWEs for castings with increased surface roughness (above 50 μm). In the earlier studies, Adler *et al.* [64] and Ambardar *et al.* [65] measured both FWE and BWE amplitudes to investigate the effects of surface roughness on ultrasonic echo amplitude in aluminium alloy castings. Their measurements involved castings with surface roughness less than 50 μm. However, in this research surface roughness above 50 μm was investigated and it had a significant effect on the FWE amplitude. Hence only the BWE amplitude was measured to study the effect of varying surface roughness on ultrasonic signal amplitude.

Further experiments were confined to sections of the castings with a thickness of 8 mm and with fine grain structure. The surfaces of the castings were machined such that roughness values (R_a) varied from 150 μm (rough) to less than 10 μm (smooth). As mentioned in Section 5.5.4, it was found that the grain size was relatively consistent throughout each section (i.e., for the fine grain structure, all grain size values were within the range of 0 to 0.25 mm). Since there was only a small variation in grain size within the sections inspected, the change in attenuation

due to grain size variation was considered to be negligible. Therefore, $\Delta L_{Grain} \approx 0$, and then Equation 5.6 is reduced to Equation 5.8.

$$\Delta L = \Delta L_{Surf} \tag{5.8}$$

The results of the effects of surface roughness on the ultrasonic signals are presented in Figure 5.7. A series of back wall echo amplitude measurements was carried out to assess the effects of surface roughness and frequency on attenuation. Figure 5.7 shows that detection of the BWE for castings with surface roughness (R_a) values in the region of 150 μm, with any of the selected frequencies, would be difficult. This was due to the ultrasonic signal scattering at the rough front surface. The unfocused probe of 2.25 MHz frequency was not considered for further experiments. The reason for this was due to a general increase in loss from scattering of ultrasonic waves from the front surface. In particular, it can be seen in Figure 5.7 that for the surface roughness range between 50 and 125 μm, the loss of signal amplitude when using the 2.25 MHz probe was significantly greater than with the 5, 7.5 and 10 MHz probes. As stated earlier, a possible reason for the decrease in BWE amplitude with the increase in surface roughness for the 2.25 MHz probe may be due to the un-focused nature of the probe. For instance, it was shown in a previous study on unfocused probes, that the measurement of the BWE amplitude was generally reduced compared to focused probes, on parts with large surface roughness [70].

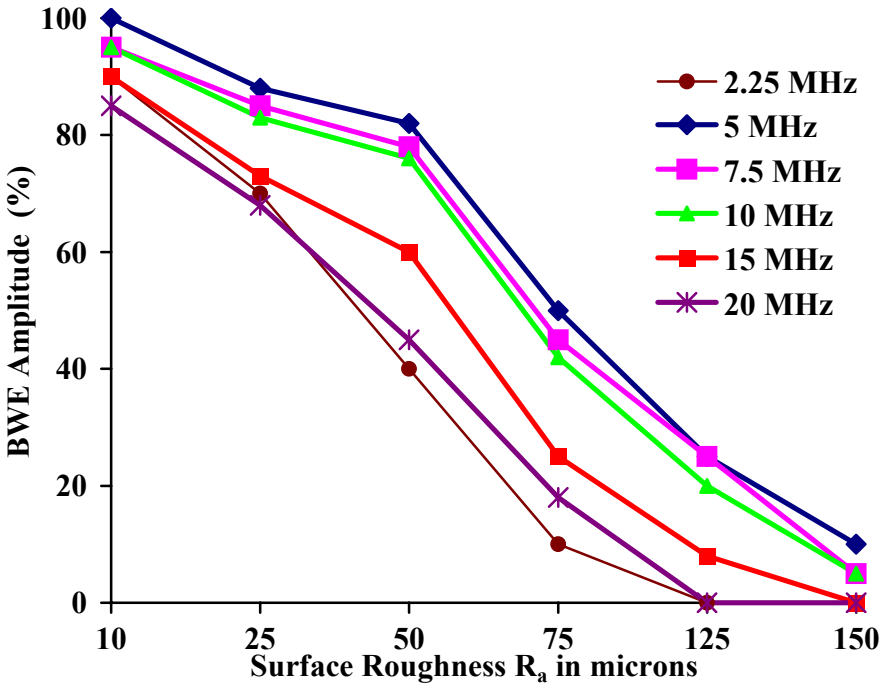

Figure 5.7 BWE amplitude variation with surface roughness for different frequencies

Nearly 95% of the signal was scattered from the surface of the castings with 150 μm roughness value for the selected frequency range. The lower frequencies up to 10 MHz provided a larger BWE than higher frequencies (15 MHz and 20 MHz) for surface roughness values up to 100 μm. There was no BWE signal obtained from the castings with surface roughness values beyond 125 μm for the 20 MHz frequency probe. This was due to significant scattering of ultrasonic waves at the front surface of the castings.

The frequency range from 5 to 10 MHz was most suitable for inspection of castings with surface roughness (R_a) values varying between 50 μm and 100 μm. To study in detail the effect of surface roughness on the ultrasonic signals obtained from the castings with defects, the surface roughness was varied from an original rough surface (around 150 μm) to a machined smooth surface (around 5 μm). The results of this study are presented in Section 7.2.

Sample surface roughness data obtained from a Perthometer –Surface profile measuring instrument (Figure 4.11) is presented in *Appendix D* (Table D.1) for smooth surface (Ra2) type. Due to the large variation in the mean surface roughness values, the surface roughness of castings was grouped into three categories as shown in Table 5.2.

Range	**Surface Roughness Values (R_a)**
Ra0	101 to 150 μm
Ra1	51 to 100 μm
Ra2	5 to 50 μm

Table 5.2 Surface roughness range

Finally, the decision on the selection of a suitable ultrasonic frequency to inspect aluminium die castings depends on the discontinuities to be detected. Since the detectable minimum size of the defect depends on the wavelength of the ultrasonic signal, the frequency of the probe required to inspect these castings should be selected based on the critical defect size to be inspected. The frequency selected is also constrained to be in the range previously determined by the experiments described in this section and illustrated in Figure 5.7.

5.6 SUMMARY

The effects of material variation on ultrasound signals in inspecting selected die castings of type alloy CA313 were identified and quantified with the experiments described previously. The major conclusions that can be drawn from the experiments are:

- The ultrasonic velocity in the castings investigated was found to be 6260 m/s
- A 10% loss in back wall echo was observed between casting sections with fine to medium grain size, as compared to nearly 50% (6 dB drop) loss

between castings with fine and coarse grain structure due to grain boundary scattering (Figure 5.6)

- The frequency range from 5 to 10 MHz was most suitable for inspection of aluminium die castings with surface roughness (R_a) values varying between 50 μm and 100 μm (Figure 5.7), and
- The grain size in high pressure automotive die castings is mostly uniform and in the range of fine to medium grain size. Hence, the loss of back wall echo due to grain size variation is small, and less than that caused by changes in the surface roughness.

The in-gate section of the structural oil sump pan was the critical part of the casting in relation to the ultrasonic inspection task addressed in this research. So the frequency range for further investigation was selected primarily to accommodate signal variation caused by surface roughness at the in-gate section. The experimental results were used as a framework in developing an inspection procedure for aluminium alloy die castings. This procedure also provided guidelines for selecting suitable transducer frequencies that accommodate variations in material properties while taking into account the critical defect size to be detected. In order to do this, weak and noisy ultrasonic signals have to be subjected to further signal processing. Suitable signal processing procedures have to be developed to achieve the highest possible defect identification rates. These procedures are described in Chapter 6.

CHAPTER 6.

ULTRASONIC DATA PROCESSING

6.1 OVERVIEW

The previous chapter described the selection of parameters for ultrasonic immersion testing of aluminium castings. However, the processing of ultrasonic signals obtained from immersion testing of the castings was not straight-forward. There are many material parameters that affect ultrasonic signals. Even though a suitable frequency was selected, due to the noise generated within the ultrasonic signals particularly with rough surface castings it was difficult to identify defects. Therefore, there was a requirement for signal processing to aid the process of classifying the ultrasonic signals. The detection of discontinuities in aluminium alloy die castings using an ultrasonic non-destructive testing method in the final analysis is a classical problem of signal processing.

The aim of this chapter is to report and discuss the processing of ultrasonic signals. The flowchart on the data processing methodology is presented in Section 6.2 along with the data collection procedure. Processing of signals using Artificial Neural Networks, and signal pre-processing is investigated in order to develop a novel approach to ultrasonic data processing. This investigation is described in this chapter. Selection of neural network parameters and signal pre-processing methodologies are described in Section 6.3. Finally, the application of combined pre-processing methods is described in Section 6.6.

6.2 DATA COLLECTION AND PROCESSING METHODOLOGY

In this work, ultrasonic immersion testing experiments were conducted with castings having different surface roughness values, which were in the range of Ra0, Ra1 and Ra2 types (Section 5.5.5). The ultrasonic inspection parameters such as ultrasonic velocity in CA313 alloy (6260 m/sec), suitable water path distance (7.5 mm), and probe frequency (10 MHz) were applied in these experiments as presented in Chapter 5. The ultrasonic immersion testing procedure used in this research is described in Chapter 4 (Section 4.4.3).

The overall steps involved in converting the output ultrasonic A-scan file type into an input signal processing file type is presented in *Appendix F*. Signal processing was subsequently carried out using MATLAB software version 6.1. Finally, the classification of ultrasonic signals was done using Artificial Neural Networks (ANN). The training of ANN plays a crucial role in signal processing. It involves the following steps [91]:

- Assemble the training data
- Create the network object
- Train the network and
- Test the network.

In Table 6.1, the number of signals obtained from simulated defects (side-drilled holes), natural defects (gas porosity) and mixed defects, i.e. the combination of both side-drilled holes and gas porosity signal types is presented. In addition to those signals, 80 non-defect signals were also obtained from Ra0, Ra1 and Ra2 surface types for defect and no-defect type classification with ANN. X-ray inspection was used to find the defect-free sections of the castings (Section 4.7). Out of 80 non-defect signals obtained, 50 were used for training and 30 for testing. In total, 130 defective signals were obtained from each surface type (Ra0, Ra1 and Ra2). A detailed description on the simulated defects was provided in Section 4.5.2, the size and location of the simulated defects within the casting section was such that they were as closely matched to the natural defects as possible. As described in this chapter only ultrasonic signals obtained from the simulated defects were used to

select the suitable signal processing parameters. However, the ultrasonic signal classification results presented in the Section 7.5 (Chapter 7) onwards were obtained from natural defects. The training and testing signals for the neural network implementation were kept separately in different folders in the signal database.

Neural Network Process	**Number of Simulated Defect Signals**	**Number of Natural Defect Signals**	**Number of Mixed Defect Signals**
Training	50	30	80
Testing	30	20	50

Table 6.1 Number of training and testing data for different signal types

The size of natural defects (gas porosity defects) varied between 0.5 mm to 2 mm. X-ray inspection of the castings with defects provided information on the approximate location and size of the natural defects. Those defects were un-evenly distributed along the in-gate section of the structural oil sump pan castings, which were manufactured in three high-pressure die casting machines in the casting plant. However, the casting sections with defects which were similar to the simulated defects (in location) as identified by X-ray inspection (Section 4.7) were used in this research.

The real-time ultrasonic signal provides very valuable information for signal processing. Figure 6.1 illustrates the major steps involved in signal processing. The signals were collected through an ultrasonic probe suitable for the die castings investigated in this research. Then, the measured values were sent to the digital measurement device, Epoch III. The data was converted in to M-file for MATLAB neural network application (*Appendix F*). The data collected from all transducers were divided into two parts; training data and testing data. In other words, data used to train the neural networks were not used for testing.

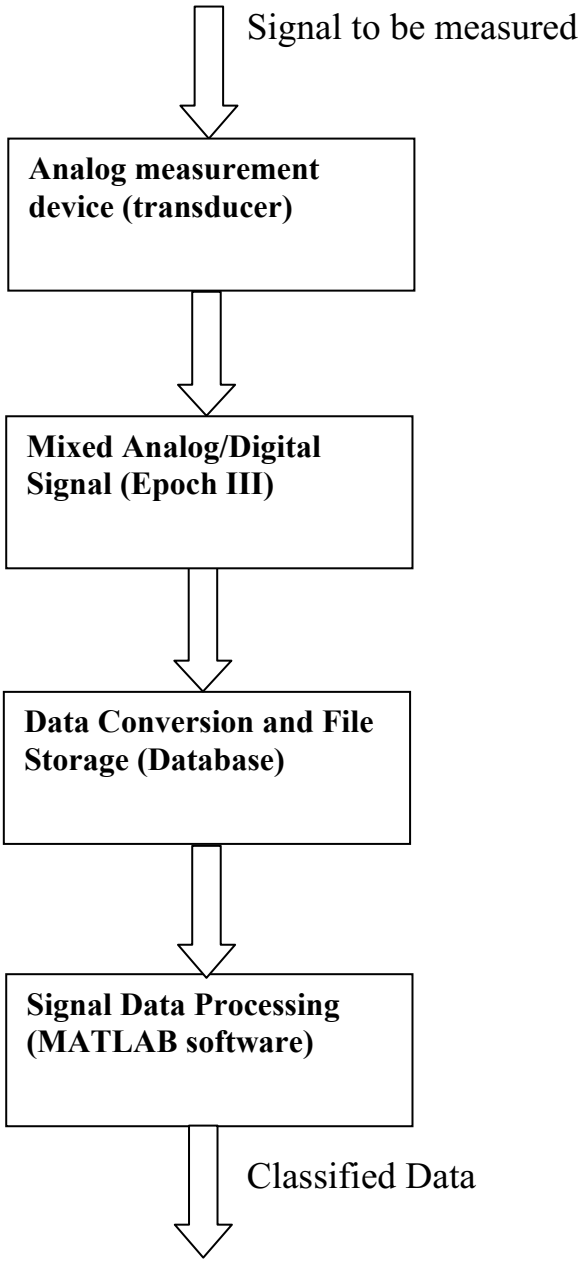

Figure 6.1 Block diagram of ultrasonic measurement system

Figure 6.2 illustrates the surface plot of Ra0 training data input to the neural network, where the *x-axis* is the number of samples, *y-axis* is the number of signals (50 for the training set), and *z-axis* is the amplitude of each sample signal (in dB). It can be observed from Figure 6.2 that the signals were scattered and the location of Front Wall Echo (Orange colour rectangle) was randomly present in the plot and the Back Wall Echo (Grey colour rectangle) was also scattered at the end of the plot. These values were obtained by transferring all data signals into a single matrix 'M' as explained in *Appendix F* (Figure F.2). The plot of matrix 'M' has illustrated the

variation in the signal echo amplitude due to the surface roughness of the casting. It has also shown the need for a suitable signal processing method to detect the defect echo in the weak ultrasonic signals. The dimensions of the matrix containing the training and testing data used in the experiments were of 220 x 80 and 220 x 50 size matrices respectively, since one input signal consists of a 220 x 1 array.

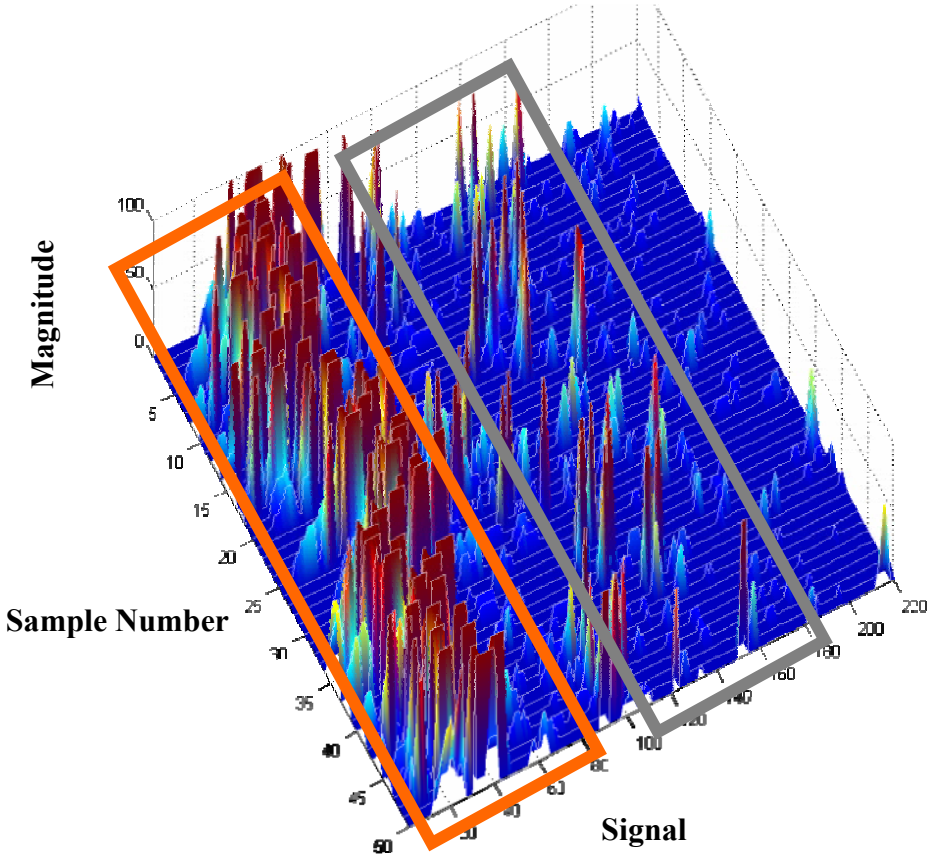

Figure 6.2 Surface plot of Ra0 training data

The value of the data processing steps in this ultrasonic NDT&E exercise was mainly two-fold, namely, identification and classification. An important factor in the data processing was the enhancement of the signal-to-noise ratio. To achieve this, unwanted components of the signal, relating to scattering from the rough surface and grain boundaries of the casting were to be separated from the signal. The different signal pre-processing techniques (i.e. FFT, PCA and WT) described in Section 2.7.3 were used in pre-processing the ultrasonic signal data. The procedures involved in using these pre-processing techniques are explained in Section 6.5. The MATLAB program written to carry the ultrasonic signal pre-processing and classification is presented in *Appendix G.*

6.3 SELECTION OF NEURAL NETWORK PARAMETERS

6.3.1 Overview

Different ANNs have different computation and storage requirements, and no one algorithm is best suited to one type of problem. Normally, the number of inputs to the network is constrained by the problem, and the number of neurons in the output layer is constrained by the number of outputs required from the network. In this research, the outputs '0' and '1' represented the 'no-defect' and 'defect' categories respectively.

Care has to be taken in the selection of parameters such as number of epochs and number of hidden layer neurons, as there could be the risk of over-fitting to the training data set. Incorrect selection of parameters would lead to the network performing poorly on a new data set. To avoid the problem of over-fitting, trial runs (iterations) were conducted to determine a suitable number of epochs and number of neurons in the hidden layer as presented in Section 6.3.4 and Section 6.3.5 respectively. These selection processes were carried out on the signals obtained from rough surface sections of the castings (as-cast surface) with and without simulated defects. To determine the effect of each parameter, the characterisation rate of the neural network was evaluated by varying one parameter at a time, and the remaining parameters were kept constant, as presented in this section. For each of these experiments, the MATLAB '*init*' function was applied to initialise the network weights (as described in Section 3.8.3).

6.3.2 Transfer Function

Sigmoid units (*logsig* and *tansig* transfer functions) were selected based on the connections that determine the influencing neuron. An experiment was undertaken to evaluate the most appropriate combination of the non-linear transfer functions of *logsig (L)* and *tansig (T)* for the three layers of the feed-forward network used in this research. The classification percentage and standard deviation (SD) were

calculated for the different types of transfer function combinations as presented in Table 6.2. For instance, *TTT* (in Table 6.2) represents the application of transfer function *tansig (T)* in each layer of the neural network respectively. The different types of transfer function combinations were applied in a loop 50 times to obtain the mean classification percentage and standard deviation. The transfer function combination of *TLT* was selected, as it performed best with raw input signals obtained from rough surface castings (Table 6.2). Further, signal processing required for this research was carried out with the transfer function combination of *TLT*.

Transfer Function Types	**Mean Classification (%)**	**SD (%)**
TTT	61.3	7.3
TTL	56.6	7.1
TLL	56.0	8.3
LLL	61.0	6.6
LLT	60.7	5.6
LTT	62.0	8.7
TLT	62.7	3.3
LTL	59.3	9.3

Table 6.2 Classification % and SD of different transfer function combinations

6.3.3 Training Algorithm

The scaled conjugate gradient (SCG) method was selected as the training algorithm in this neural network application due to its advantage over other methods as presented in Section 3.7.6. The training parameters for *trainscg* (MATLAB function for SCG) are *epochs, show, goal, time, min_grad, max_fail, sigma* and *lambda*. The number of *epochs* required for training is presented in Section 6.3.4. The *show* was set to 20, so after each 20 epochs training status was displayed to see the progress made by the training algorithm. If *show* is set to 0, then the training status never displays the output. The maximum time taken to train the network is set by the *time* function. However, the time factor is not considered to be too critical in

this defect classification application. The performance *goal* is a critical factor in determining when the training stops. The training is stopped when the performance function goes below *goal*. Normally, a value equal to zero or close to zero is selected as the *goal*. A very small *goal* value such as $1e^{-5}$ and $1e^{-6}$ will mean that the network takes a longer time to converge. In this case, *goal* was selected such that it was close to zero but not a very small value, 0.001 was used as the *goal*. The SCG algorithm does not have any affect on the learning rate and momentum parameter values.

6.3.4 Number of Epochs

The selection process in terms of number of epochs used in training the network is critical for generalisation of the network. During training for each epoch, an input data set is submitted to the network, then target and actual output values are compared and error value is calculated. The calculated error is the difference between the target output and the network output. The network will tend to minimize the average of the sum of these errors (mean square error). This error value is used in a transfer function (Section 3.7.2) to calculate the new weights for the next training epoch. Random weights are used in the initial network configuration and weights are adjusted continuously during the training process. Training stops when a given number of epochs elapse, when the error reaches an acceptable level, or when the error value is minimised [91]. Basically, if the number of epochs is not correctly selected it can result in a neural network that is not optimised or one that does not produce generalised results.

The signals obtained from the rough surface section of castings with and without simulated defects were selected for the experiments to choose the number of epochs. When the number of epochs was increased in neural network training, the ultrasonic signal classification percentage increased (Figure 6.3). This can be attributed to the increase in the overall training inputs to the network. However, it was important that the network should not be over-trained. At approximately 500 epochs the mean square error value reached a minimum value. After 500 epochs, the mean square value increased and classification percentage decreased. Hence, 500

epochs were selected based on the maximum classification level and minimum mean square error value (as shown by double-headed arrow in Figure 6.3).

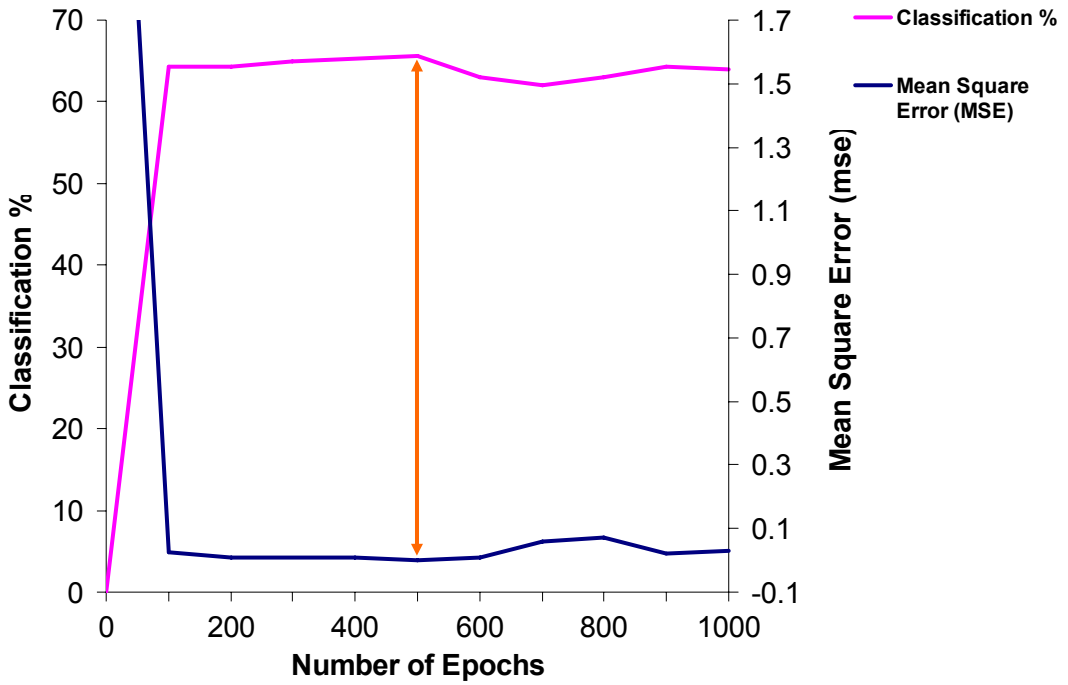

Figure 6.3 Effect of number of epochs on the percentage classification and Mean Square Error

6.3.5 Number of Hidden Layer Neurons

The number of neurons in the output layer is determined by the nature of the problem. Determination of the number of neurons for the hidden layer is often accomplished through experimentation [144]. A small number of neurons in the hidden layer may prevent correct mapping of inputs to outputs, while too many may allow the network to over-classify the training patterns reducing generalisation capability [145]. It would also increase the training time, which is unacceptable for an on-line inspection process. Several differently sized neural networks were designed and tested in order to determine the smallest usable structure. Figure 6.4 illustrates the classification performance of neural network configurations based on various combinations of input and hidden layer neurons. It also indicates a general

random variation in classification performance for network configurations with an increasing number of hidden layer neurons.

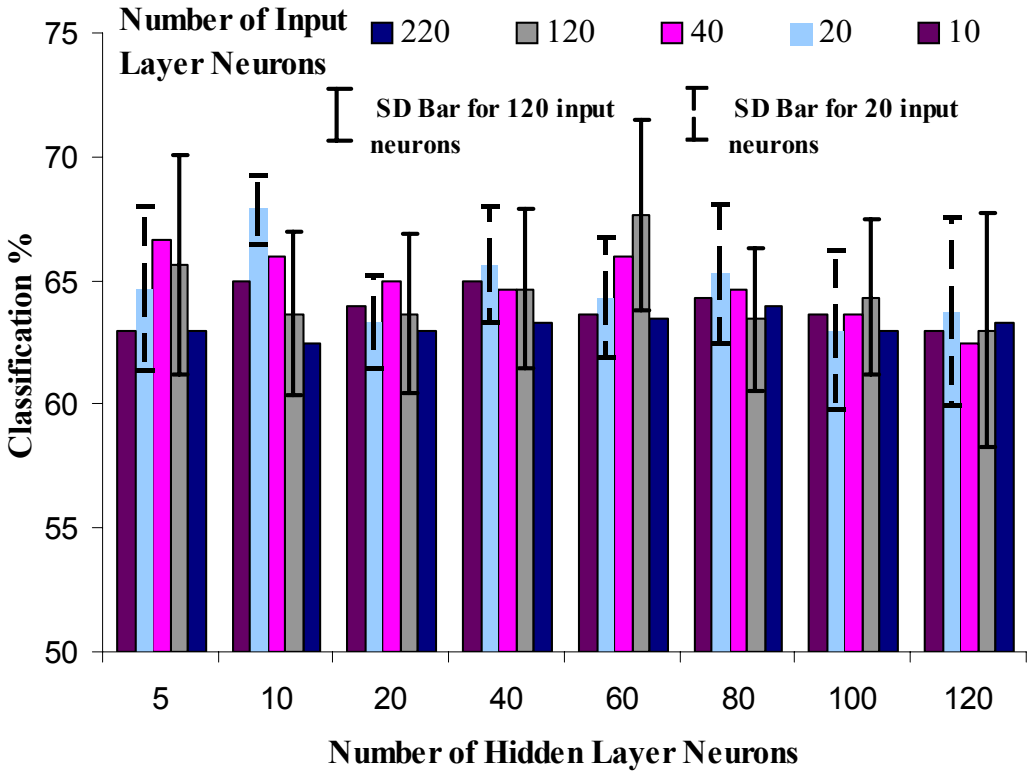

Figure 6.4 Effect of hidden and input layer neurons on classification percentage

Figure 6.4 illustrates that the highest classification was obtained for neural network configurations containing the combination of 20-10 and 120-60 neurons in the input - hidden layers, respectively. The 20-10 network configuration was selected due to its smaller size and low standard deviation (SD) of classification percentage. It was observed that the inclusion of an additional layer did not improve the network performance. In conclusion, the network selected for ultrasonic signal classification contained 20, 10 and 1 neurons in the first, hidden and output layers respectively.

In summary, the selected neural network topology had 220 inputs representing the ultrasonic A-scan signal, and one output to determine whether the signal represented a defect or not. The outputs ‘0’ and ‘1’ represented the ‘no-defect’ and ‘defect’ categories respectively. The selected parameters are listed in Table 6.3. The learning rate (Section 6.4.2), momentum term rate and error goal were fixed

throughout the training and testing phase since they did not have any effect on the final outcome of the neural network with SCG training function (Section 6.3.3).

Parameters	**Value**
Number of input nodes	220
Number of layers	3
Number of neurons in input layer	20
Number of neurons in hidden layer	10
Number of neurons in output layer	1
Show	20
Epochs	500
Goal	0.001
Activation Function	*TLT*

Table 6.3 Feed-forward back propagation neural network parameters

6.4 DEFECT CLASSIFICATION

Once the ultrasonic signal data was obtained from the sample aluminium die castings, signal analysis was carried out. The waveform of an ultrasonic signal obtained from a defective casting has significant information. The application of signal pre-processing techniques will reduce the dimensionality of the input signal. The first defect classification step involved the conversion of the raw signal data into input signals for the neural network. This conversion included normalisation, which scaled the raw data to continuous values between 0 and 100, and ensured that signal classification using the neural network was undertaken based on the signal wave shape. The MATLAB neural network toolbox was used for the defect classification application. It provided the in-built functions such as *logsig,* and *tansig* which were used as a transfer function between each layer of neural network [91].

6.5 SIGNAL PRE-PROCESSING

6.5.1 Overview

A received signal can be directly applied to a neural network, thereby forcing the neural network to discover the inherent features characterising the signals and then performing the desired detection. A practical drawback of this approach is that it can be very slow, particularly in the context of a large-scale problem such as the one addressed in this research project. Hence, pre-processing is essential to remove redundant information, thereby enabling more effective classification of data. A number of pre-processing steps are required before a successful classification is possible. In order to achieve an improved result, different signal pre-processing techniques, namely, Fast Fourier Transform (FFT), Wavelet Transform (WT) and Principal Component Analysis (PCA) were investigated. The categories are as follows:

- FFT – ultrasonic signal data pre-processed by passing through FFT and fed into the input nodes of the neural network
- WT – ultrasonic signal data pre-processed by passing through WT and fed into the input nodes of the neural network, and
- PCA – ultrasonic signal data pre-processed by passing through PCA and fed into the input nodes of the neural network

The following sections explain, in detail, each of the above pre-processing methods applied in this research.

6.5.2 FFT Procedure

The first type of pre-processing used in this research was the Fast Fourier Transform (FFT) which was applied to the raw ultrasonic signals. Fourier analysis breaks down a signal into constituent sinusoids of different frequencies, and is a mathematical technique used for transforming the view of the signal from the time domain to the frequency domain. This pre-processing approach enabled the exploitation of the power spectrum, a measurement of power at various frequencies [91]. The usefulness of this approach is based on the fact that echoes due to flaws

differ in spectral content from the echoes caused by background scattering noise [90].

The FFT function, '*fft*' available in the MATLAB signal processing toolbox was applied on the matrix of input signals. However, applying the *fft* function to a matrix produces another matrix with real and complex values as presented in Equation 2.4 (Section 2.7.3.2). In this analysis, the power spectrum of the frequency components was then obtained by multiplying the FFT output with its conjugate in a process to obtain the magnitude of the real and complex values of the FFT. The power spectrum of the raw signal was then applied as input to the neural network to carry out defect identification. A sample MATLAB m-file program with the FFT function is presented in *Appendix G*.

FFT was applied to the ultrasonic signal to obtain the frequency spectrum [91]. To compare the signals using their spectral content, often the use of the FFT alone is not sufficient. If additional techniques could be used to obtain a more complete representation of the behavior of spectral components within the signal, it would be advantageous to do so.

6.5.3 PCA Procedure

Another approach used to improve the neural network performance was to construct a basis on which given data sets yield the best compression. The idea behind compression is to represent data using only a limited number of its components for which the variance is sufficiently large. This procedure is known as Principal Component Analysis (PCA) and it can be summarised as follows [87]:

- A sample covariance matrix of the raw training signal is calculated.
- The eigenvalues and eigenvectors of the covariance matrix are then evaluated.
- The eigenvectors are sorted according to the magnitude of their respective eigenvalues, and

- The eigenvectors with the largest eigenvalues (variances) corresponding to the dimensions that have the strongest correlation to the raw training data are selected.

The original measurements are then projected onto the reduced dimension vector space defined by the set of selected eigenvectors (defined according to the largest eigenvalues).

MATLAB m-file code was written to carry out the above procedure as presented in *Appendix G*. For example, the training data in this analysis consisted of 220, 50-dimensional signals. A covariance matrix was obtained from the training data using the function '*Cov*' from the MATLAB signal processing toolbox. From this a set of eigenvectors and their corresponding eigenvalues were obtained, using the function '*EIGS*' from the MATLAB signal processing toolbox. The vectors were sorted according to their respective eigenvalues to obtain a number of principal components. The set of principal components forms a transformation matrix, which was used to provide a linear transformation such that the input data (220 nodes) could be projected onto a lower dimension sub-space.

The optimum number of principal components to be used in this investigation was determined by carrying out experiments with varying number of principal components and determining the configuration that provided the best classification with neural networks. Between 10 and 120 principal components were investigated. The signal classification was undertaken with the Feed-forward back propagation neural network using the selected parameters as presented in Section 6.3. These tests were carried out on the signals obtained from both rough (Ra0) and smooth (Ra2) surface sections of castings with and without simulated and real defects. X-ray inspection was carried out to identify the defect free areas of the casting (Section 4.7). Figure 6.5 shows that the highest classification percentage was obtained with 40 principal components for the given ultrasonic signal inputs with both smooth surface (Ra2) and rough surface (Ra0) casting sections. When the number of principal components used as input to the neural network was either smaller or larger than 40 principal components, it resulted in a lower classification performance. This was a consequence of loosing important signal data when a number smaller than 40

principal components were used. Conversely, a larger number of principal components led to redundant data being presented to the neural network. This lead to an increased number of input nodes in the network, and a subsequent increase in the number of network weight values. This in turn resulted in a reduction in the overall training performance of the network. Hence, 40 principal components were selected to carry out further analysis on the ultrasonic signal as this configuration provided the best classification percentage.

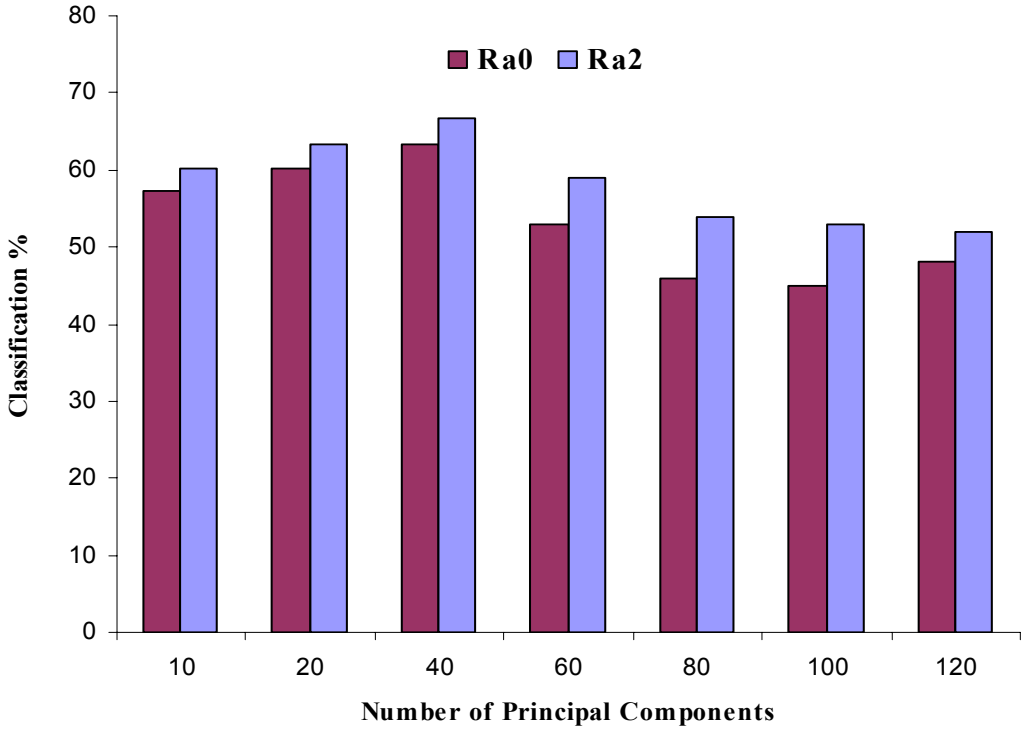

Figure 6.5 Selection of number of principal components with the plot of classification percentage for Ra0 and Ra2 surface types

6.5.4 Wavelet Procedure

In this section, the transformation of time-based signals using the wavelet transform is described. The objective of this transformation was to compress the ultrasonic signal prior to input into the ANN for classification. Detailed information on the wavelet transform pre-processing technique as applied to non-stationary waveform was presented in Section 2.7.3.4. In this research, due to surface roughness

of the casting, ultrasonic signal waves were observed to vary significantly. Furthermore, the defect information was also embedded in the front wall echo when the defect was close to the front surface of the casting.

Wavelet analysis involves the breaking up of a signal which is a shifted and scaled version of the original wavelet or "mother wavelet". The central frequency of the mother wavelet is chosen close to that of the ultrasonic pulse. There are a variety of wavelet types to choose from for a mother wavelet. There are a variety of wavelet types to choose from for a mother wavelet. In this case, wavelets belonging to the Haar and Daubechies, were applied on the input signal to determine which configuration was best suited to represent the defect signal (gas porosity defects). Symlets are nearly symmetrical wavelets proposed by Daubechies [146] as modifications to the Daubechies family that has found widespread application in feature extraction.

The implementation of the wavelet transform with MATLAB was undertaken using the continuous wavelet transform (CWT*)* function [96] in wavelet toolbox. It returns the coefficients of the CWT of a single signal. This function has three input parameters. The first parameter is the signal, the second is the scale and the last parameter is the type of mother wavelet. This function produces a matrix of N values (number of samples) defined by the scale of the signal tested. Figure 6.6 illustrates the surface plot of the CWT of a signal, which belongs to Ra0 surface type. As shown, the discontinuities or abrupt changes in the signal are represented by peaks depending on their frequency.

The drawback of the use of the continuos wavelet transform for signal analysis is that it increases the complexity and memory required to calculate large number of coefficients. For example, for one batch of training signals, which is a matrix of N (data points) by 50 signals, the CWT has to create a 3D matrix of S x N x 50, where S is the magnitude of scale values. Not all of these wavelet coefficients provide a significant contribution, with respect to the evaluation of defect signals. In other words, it is not necessary to use all the coefficients with a (ANN) signal classification process. Another drawback of the CWT is that the representation of the

signal often contains redundant components. Therefore, another function called Discrete Wavelet Transform (DWT) was applied which enables the specification of the scale and position of the signal [96]. This transformation is more efficient since it enables the conversion of the important coefficients obtained from the signal.

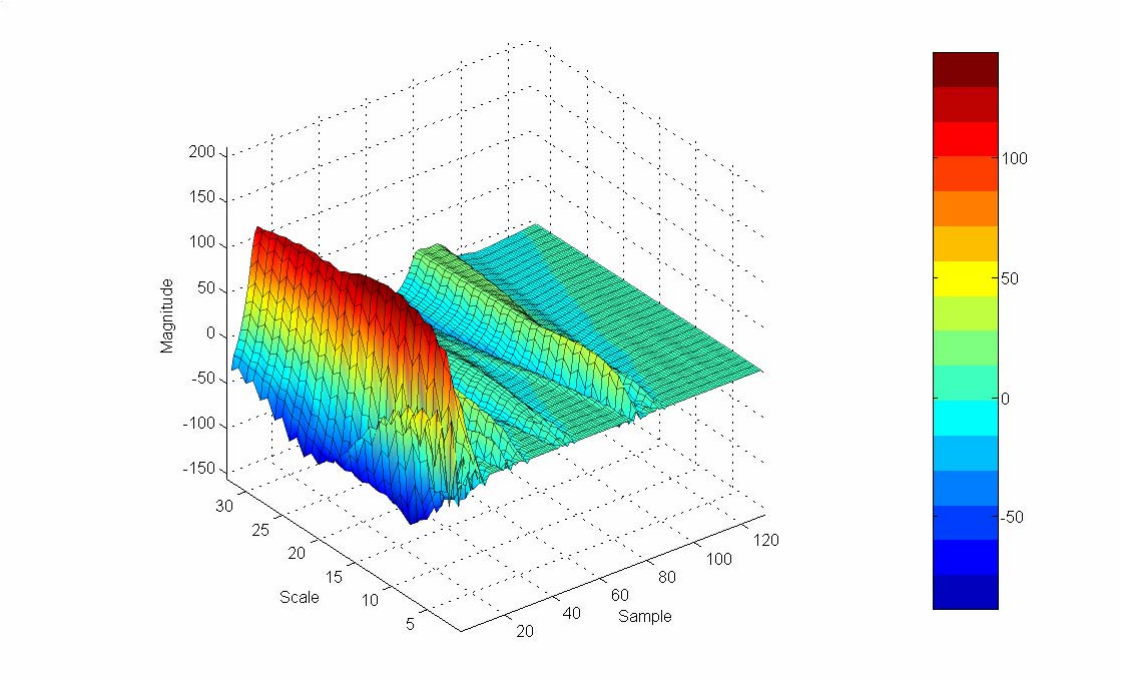

Figure 6.6 Surface plot of CWT coefficients of the ultrasonic signal obtained from Ra0 surface type

The idea of DWT starts from decomposing discrete time signals into their approximate (scaling) and detail (wavelet) coefficients after passing them through a high-pass and a low-pass filter [99]. The procedure is repeated for further decomposition of the low-pass filtered signals and the high-pass filtered signals which constitute the DWT as presented in Section 2.7.3.4.

When choosing the mother wavelet, there are generally no straight forward methods to determine the most appropriate wavelet type for a given application. Hence, various mother wavelets were tested on the input ultrasonic signals in order to identify the wavelet type that best suited the flaw signals. Figure 6.7 is an example of a WT using Haar as the mother wavelet on the smooth surface (Ra2) casting signal. A single-level discrete wavelet transform of Haar wavelet type was used on the input signal. The values of both approximate (scaling) and detailed (wavelet)

coefficients were obtained for this wavelet type using the wavelet filters directly on the input signal (Section 2.7.3.4). These detailed coefficients were only used to ensure exact global reconstruction of the input signal. The approximate coefficient produced a smoothed version of the signal which was used at the next scaling stage. The red line in Figure 6.7, represents the original signal while the blue line represents the signal compressed using the Haar type of WT. The Haar wavelet was explored for this purpose because of its simplicity. The other reason for exploring the use of the Haar wavelet was its sharp had some similarity with the defect signal.

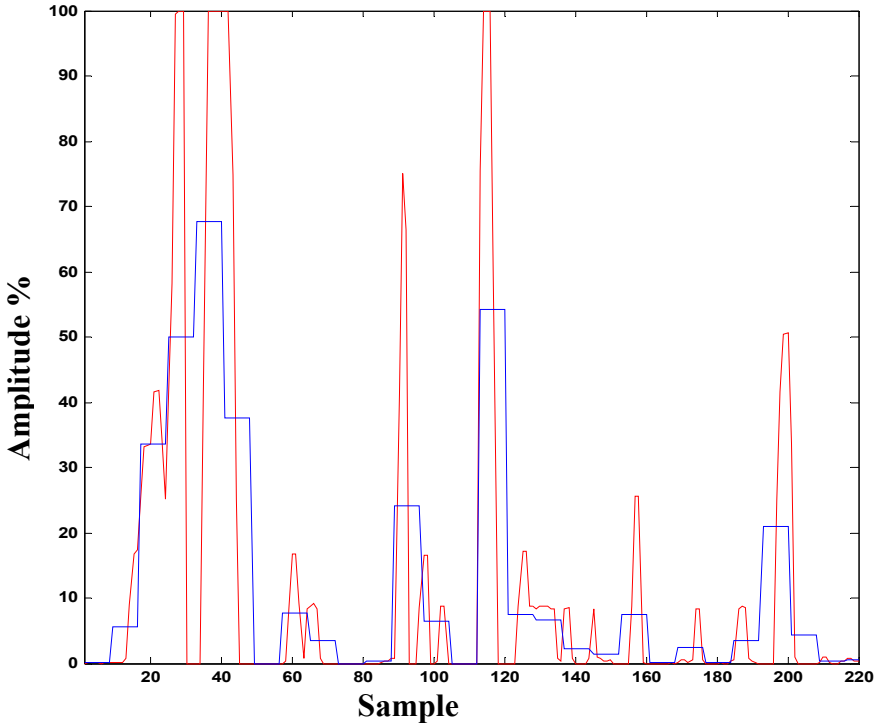

Figure 6.7 Haar mother wavelet type applied on original defect signal from Ra2 surface casting

The performance in relation to minimisation of error in terms of classification percentage depends on the choice of wavelet and its order. After experimenting with a number of different wavelets on the input ultrasonic signal data, the Dauchebies type wavelets (db) was found to outperform other wavelets based on classification performance. To select the optimum order of the wavelet, the pre-processing of the signal was carried out from the 2nd Dauchebies (db2) wavelet up to a maximum of 13th order Dauchebies wavelet (db13). Even though the Dauchebies wavelet does not provide good data compression, it demonstrated a good match with the flaw signals. Figure 6.8 illustrates the wavelet transform ‘db5’ for a flaw signal from the smooth

surface (Ra2) casting. The red line represents the original signal while the dotted blue line represents the signal compressed using the WT 'db5'. As the approximation level increases, the variation within the signal is progressively reduced, and longer variation features (signals) become more obvious. Approximation level 5 (db5 – Figure 6.8) enables the exhibition of the necessary features of the signal whereas Haar wavelet has removed too much information and only broad signal information is displayed (Figure 6.7).

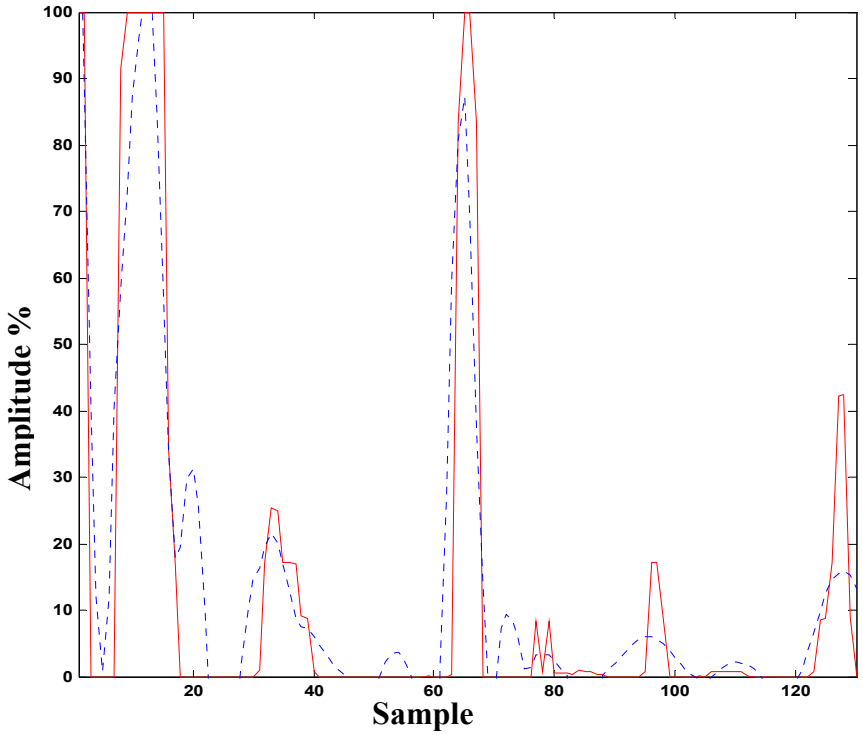

Figure 6.8 Daubechies wavelet level 5 applied on original defect signal from smooth surface casting

The classification performance of different wavelet transforms was evaluated on the signals obtained from both rough (Ra0) and smooth (Ra2) surface sections of castings with and without simulated defects. The plot of the classification percentages obtained using different wavelets is shown in Figure 6.9. The different db values lead to different final classification percentage of ultrasonic signals as different filter levels are applied to match the input signal type (rough and smooth surface signals). As the db level increases from db1 to db13, there is increasing levels of filtering of the signal (i.e., fluctuations caused by noise and surface roughness were removed). As the db level increases beyond db5, there is a

fluctuation in the classification percentage. As such it can be deduced at this point the useful information relating to defect is being filtered out. Figure 6.9 indicates that the highest classification percentage for both rough (Ra0) and smooth (Ra2) surface types is obtained with the db5 wavelet type.

The above analysis demonstrated that the selection of the proper wavelet type is critical to effective signal pre-processing. As the results have indicated, the information contained in the DWT provides a more accurate representation of flaw signals than the CWT in this particular application. Hence, further application of WT was carried out with its discrete form and Dauchebies mother wavelet type of db5.

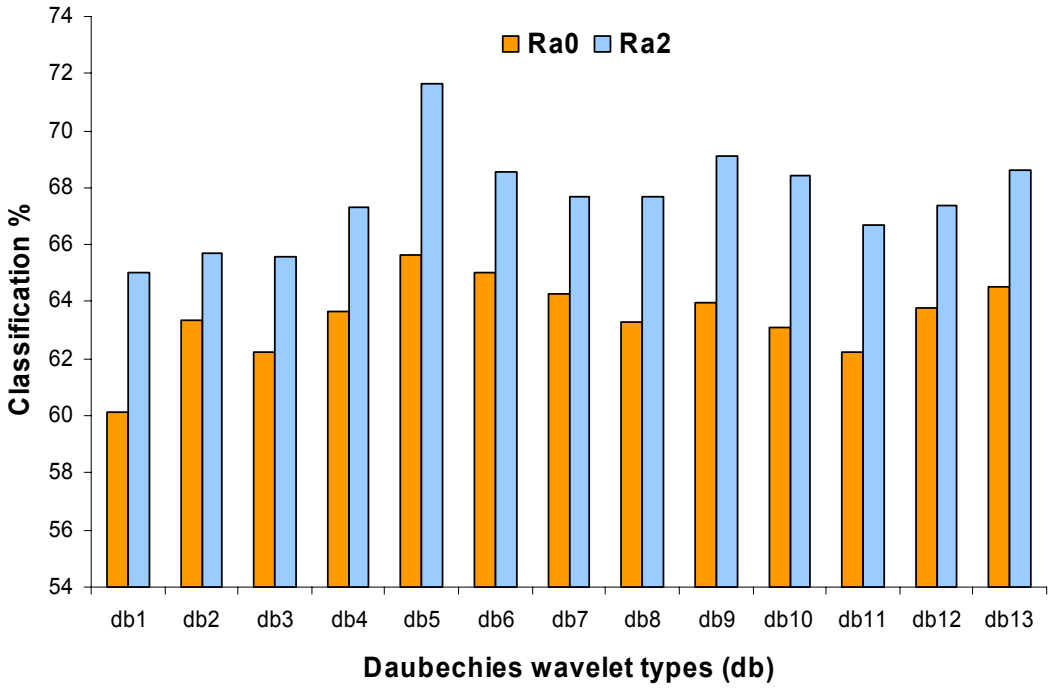

Figure 6.9 Selection of Daubechies family wavelet type with the plot of classification percentage for Ra0 and Ra2 surface types

6.6 COMBINED PRE-PROCESSING TECHNIQUES

An investigation was carried out in this research to evaluate whether it was preferable to use a combination of pre-processing techniques rather than a single pre-processing technique to obtain acceptable levels of signal classification. To achieve a better classification performance with neural networks, other feature extraction methods were explored. The strategy adopted in this research was to apply well known signal processing tools such as Fourier Transforms (FT), Wavelet Transforms (WT) and Principal Component Analysis (PCA) in various combinations to determine the best approach. It was decided to use time-frequency analysis on the non-stationary signals, so that they could be transformed into a two-dimensional waveform. Normally, frequency represents one dimension and time represents another dimension of the waveform. This procedure assists the neural network in identifying the salient features of the received signals. Such an approach may be inefficient due to the highly redundant nature of the time-frequency ultrasonic input signals from the castings. The redundant components of the time-frequency signal can be removed prior to processing by the neural network, thereby enhancing the efficiency of computation. PCA was applied to the time-frequency data to eliminate the redundant components that might be present in the signal.

Figure 6.10 shows the block diagram of the use of WT or FFT type and PCA analysis as a combined pre-processing method for the input ultrasonic signals. In this method the raw signals were passed through the WT or FFT and then, through PCA. The final signal obtained after pre-processing was fed into the neural network classifier for signal classification. PCA was used to reduce the dimensionality of the input data to the neural networks while retaining useful information for signal classification. The key to dimensionality reduction is the selection of suitable principal components.

An approach to signal pre-processing not attempted previously is described in Section 7.6. The FFT and WT pre-processing methods were applied in sequence to investigate the possibility of achieving an improved classification percentage.

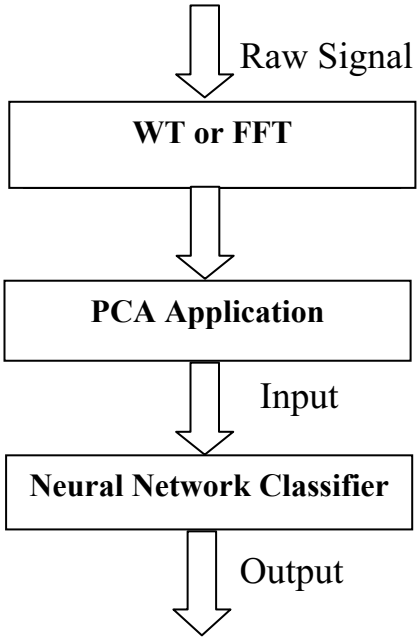

Figure 6.10 Block diagram of combined signal processing method

6.7 SUMMARY

It is impossible to know in advance which combinations of neural network parameters are most suitable to address a given problem. It depends on many factors, and usually a trial-and-error method has to be used to determine the optimum neural network configuration and training regime. Listed below are the critical findings of this research in relation to neural network characteristics that are best suited to address the issue of ultrasonic inspection of rough surface castings:

- Sigmoid units such as *tansig* and *logsig* transfer functions were selected based on the initial trial runs with the neural network, and using random initialisation of weights for the neural network (Section 6.2)
- 500 epochs were selected after investigating the variation in the mean square error and classification percentage with changes in the number of epochs (Figure 6.3), and similarly, the optimum number of nodes for the input and

hidden layers were found to be 20 and 10 respectively as illustrated in Figure 6.6, and

- A neural network topology with 220 input nodes was used to represent the ultrasonic input signal and one output neuron to determine the nature of the output signal (i.e., defect and non-defect).

The final parameters as selected of the feed-forward back propagation neural network for this research were presented in Table 6.3. The procedures for the application of FFT, PCA and WT type signal pre-processing techniques were presented in Section 6.5. The artificial neural networks were used to classify signals from smooth and rough surface castings and their performance was compared. The next chapter presents the results obtained from the feed-forward back propagation neural network classifier after subjecting the input signals to different pre-processing techniques as described in this chapter.

CHAPTER 7.

RESULTS

7.1 OVERVIEW

This chapter presents the results obtained from ultrasonic immersion testing on rough and smooth surface castings in order to evaluate the performance of this defect detection system. After the experimental parameters were optimised, ultrasonic immersion testing was carried out on selected castings. The signals obtained from both the defect and non-defect regions of the castings were stored for further signal processing. The defect signals were collected from castings with different sized porosity defects, which were either real or simulated (side drilled holes). In this chapter, it has been specified whether the defect signals used for analyses were obtained from real or simulated defects.

Some sample ultrasonic signals obtained from castings with varying surface roughness are presented in Section 7.2. A learning approach based on neural networks and different signal processing techniques was applied to classify the signals (Section 7.3). The percentage classification performance using different combinations of signal processing techniques is presented in Section 7.5. The ultrasonic signals were validated against X-ray and visual inspection results to ensure reliability of the experimental results.

7.2 INFLUENCE OF SURFACE ROUGHNESS ON DEFECT SIGNAL

In order to determine the influence of surface roughness on the defect signal amplitude, the surface roughness of the castings was measured and grouped as shown in Table 5.2. Experiments were carried out on castings of 8 mm thickness and fine grain size range (as shown in Section 5.6.4). Then, the amplitude of the defect signal was evaluated as a function of surface roughness and incident frequency. In order to evaluate the effect of surface roughness on ultrasonic signals obtained from castings with defects, simulated defects (side drilled holes) with hole size of 0.5, 0.7 and 1 mm were used in these experiments. The roughness of the rear side of the casting was ignored because it was less than 5 μm (i.e., similar to a smooth surface) and did not exceed 10 μm. Similarly, as smooth surfaced side drilled holes were used in these experiments, the surface roughness associated with the holes was considered to have a negligible effect on the ultrasonic signal. The inspection parameters selected in Chapter 5 were used in the experiments presented in this section.

Experiments were carried out on 5 casting sections each with 10 simulated defects of 0.7 mm diameter. The results of this analysis are presented in Figure 7.1. It can be seen that the defect signal decreases with increases in surface roughness (R_a). Negligible defect signal amplitude was observed in the region where surface roughness was 150 μm with all of the selected frequencies. This was due to the high scattering effect of the ultrasonic signal at the rough surface. The low frequencies (up to 10 MHz) showed larger defect signal amplitude than the high frequencies (15 MHz and 20 MHz) for any surface roughness up to 100 μm. No defect signal amplitude was observed for surface roughness values above 125 μm when 15 MHz and 20 MHz frequency probes were used. These results indicate that both the surface roughness and frequency have a significant influence on the ability to detect the defects in castings. The larger the relative surface roughness when compared to the wavelength of the ultrasonic signal, the greater the energy scattered at the surface interface. This then reduces the amount of ultrasonic energy entering the casting. Further, the reflected echo from defect and back surface has to be transmitted via the

rough surface interface back to the ultrasonic transducer (probe). Once again, more energy was scattered at the interface, and less ultrasonic energy was detected at the probe.

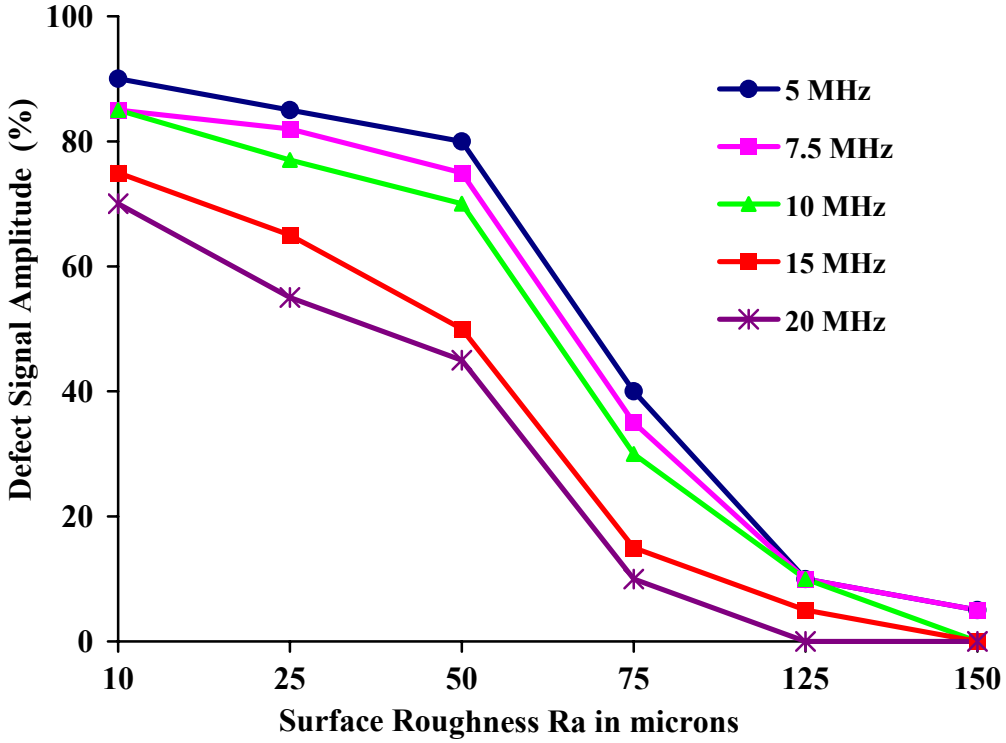

Figure 7.1 Variation of defect signal amplitude with surface roughness for different frequencies

Ultrasonic C-scan inspection was also carried out on the same sample casting sections to obtain a detailed understanding of the A-scan results from castings with different surface roughness values. A probe with frequency of 10 MHz and with a 25.4 mm point focus in the water column was used for these inspections. C-scan analysis was carried out with the aid of a robotic arm manipulator moving in the raster scan format on top of the sample casting immersed in the water column. The raster scan step was set up at 0.5 mm. Figure 7.2 illustrates C-scan analysis of castings with surface roughness Ra0, Ra1 and Ra2 types containing 0.7 mm diameter side drilled holes. The colour variation in Figure 7.2 represents the signal amplitude variation in the time window set by the electronic gate in the equipment. The electronic gate was applied between the front wall and back wall echo signal to enable the measurement of the simulated defect signal amplitude. The threshold value was set at 20 dB in the

equipment during the C-scan measurements. C-scan inspections were carried out on castings with different surface roughness. It was difficult to detect the defect signals from the rough surface (Ra0) C-scan image (Figure 7.2a). However, in the case of machined smooth surface sections (Ra2), the defect signals were clearly observed (Figure 7.2c).

Figure 7.2 C-scan amplitude image of the SOSP part gate section with varying surface (a) Ra0, (b) Ra1 and (c) Ra2

A frequency of 10 MHz had been selected as an outcome from these experiments to carry out further inspection on the rough surface castings to detect gas porosity defects that are smaller than 1 mm diameter in size. Figure 7.3 shows the signals obtained from a non-defect area of a casting. The original rough casting section was inspected to obtain the signal shown in Figure 7.3 (a). Following this, the casting section was machined to obtain the signal shown in Figure 7.3 (b). The *Y-axis* of the figure is in decibels (dB) and in *X-axis* each division represents 1.6 mm. The defect sections of the casting were also inspected. However, as indicated in Figure 7.4a, it was difficult to identify the defect (0.7 mm diameter side-drilled hole

at a depth of around 3.5 mm) from the rough surface by observing the ultrasonic A-scan display. The location of the defect was identified with the aid of X-ray inspection. The horizontal bars in Figures 7.3 and 7.4 represent the electronic gates set in the EPOCH III equipment. These electronic gates are used to select the appropriate time base (*X-axis* in Figure 7.3 and 7.4). This section of the time base is displayed across the full width of the A-scan screen. These electronic gates are used to eliminate the part of the ultrasonic signals that are not relevant to the investigation (signal from the transducer face up to the front surface of the casting). At the front rough surface, the defect signal merges with the clustered FWE due to the signal scattering effect at the rough surface. Some of the side lobe energy returns to the transducer in multiple reflections from the front wall. This is referred to as clustering. This causes loss of resolving power in the transducer and increases the length of the dead zone.

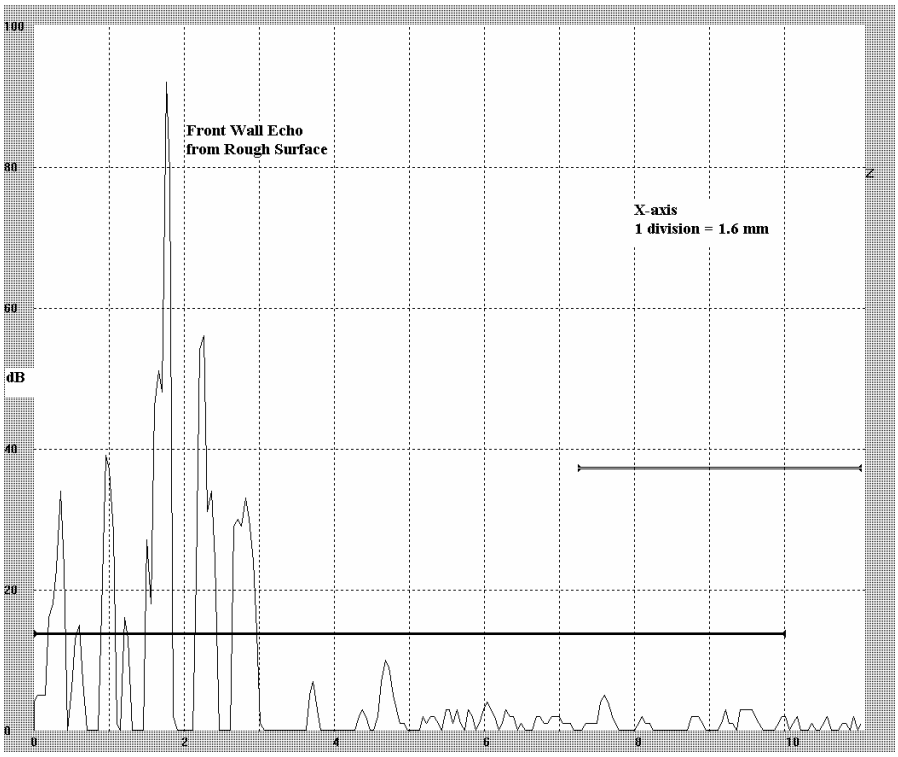

(a)

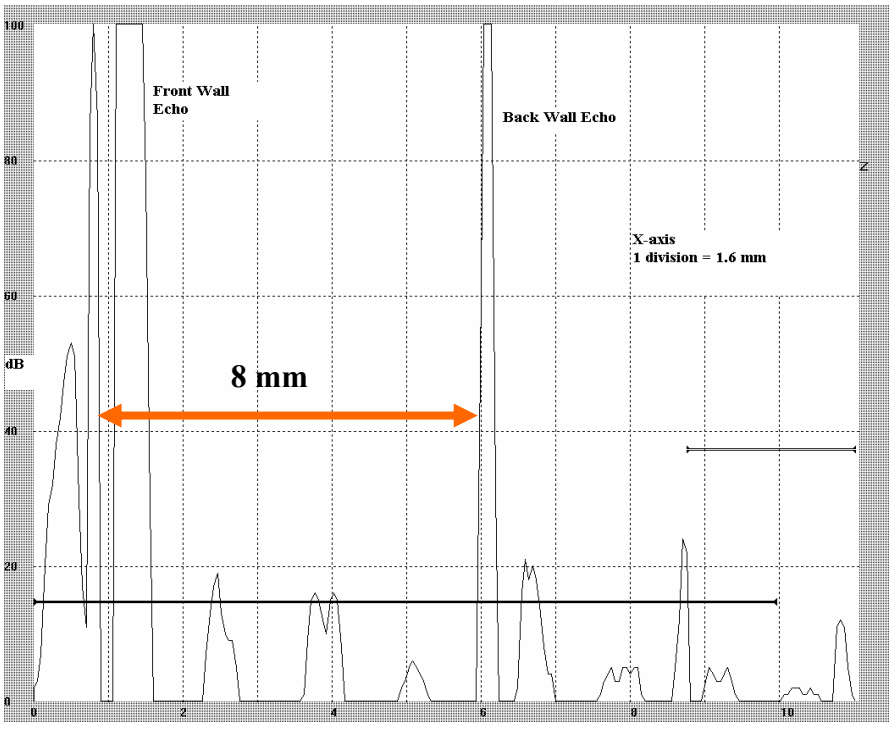

(b)

Figure 7.3 Ultrasonic A-scan signal display from a non-defective casting having (a) Rough surface (b) Machined smooth surface using 10 MHz frequency probe

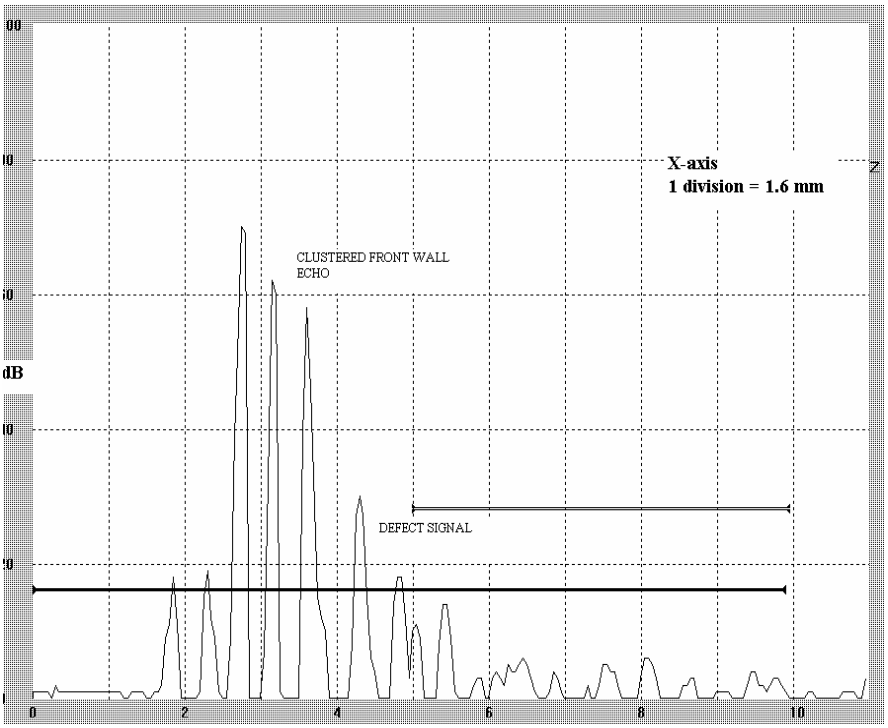

(a)

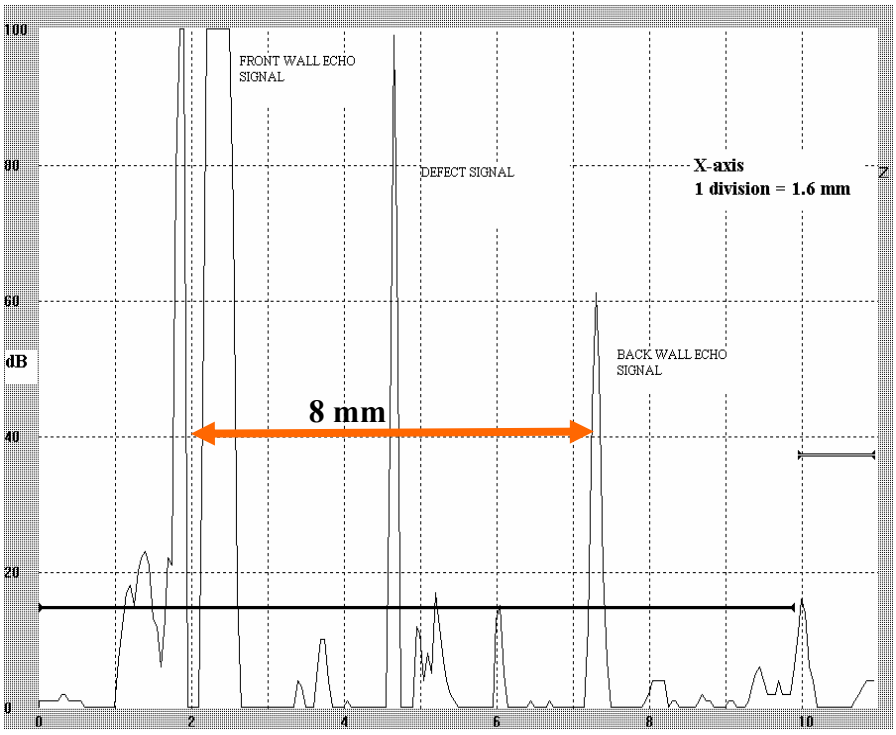

(b)

Figure 7.4 Ultrasonic A-scan signal display from a defective casting having (a) Rough surface (b) Machined smooth surface using 10 MHz frequency probe

In the case of machined surfaces, the defect signal and back wall echo were clearly identified (Figure 7.4b). This was not the case for rough surface castings. Therefore, to identify the defect signal echoes from the rough surface castings, a suitable signal processing technique was required to be applied to the signals. The next section presents the results obtained from using different signal pre-processing techniques to classify the defect and non-defect ultrasonic signals.

7.3 ULTRASONIC SIGNAL CLASSIFICATION

7.3.1 Overview

The choice of the input features is critical for the success of any signal processing technique. The total signal from the front to the back wall echo was applied as an input to the neural network. The part of the signal representing the defect cannot be passed into the neural network on its own as the neural network based inspection system has to classify the castings with and without defects. As such the entire signal (Figure 7.3 and 7.4) has to be used as input to the neural network for classification purposes. The use of the complete signal enables the design of a robust neural network for defect identification that accommodates noise produced by surface roughness.

The neural network parameters were optimised as described in Chapter 6. Following on from the previous chapter, in this section the results obtained from the artificial neural network based classification process using different signal pre-processing techniques, namely Fast Fourier Transform (FFT), Principal Component Analysis (PCA) and Wavelet Transform (WT) are presented. The performance of each signal pre-processing type for different surface roughness values of castings was evaluated only after the neural network based classification process was completed. The defect classification percentages obtained from the output of the ANN provide the performance level indicator for each pre-processing method along with the standard deviation of the classification percentage after 10 numbers of

loops. In each loop both training and testing was carried out for the given set of input signals and the MATLAB programming codes were used to carry out this exercise (*Appendix G*).

7.3.2 FFT Classifier

The purpose and procedure of the FFT application on the ultrasonic signal has been presented in Section 6.5.2. The application of FFT as a pre-processor of the ultrasonic signal data resulted in a better signal classification than with the raw signal (without pre-processing) classification alone. The noisy signal obtained from the rough surface casting is converted to the frequency domain with the FFT. Figure 7.5 illustrates the classification percentage results obtained from the ANN after FFT pre-processing the input ultrasonic signal obtained from the smooth surface (Ra2) casting. The different colour lines in Figure 7.5 shows the number of loops (10 loops). In each loop both training and testing was carried out for the given set of input signals and the MATLAB programming codes were used to carry out this exercise (*Appendix G*). In each loop, 500 epochs were carried out to obtain the mean and standard deviation of the classification percentage. It was found that there was a high fluctuation in the classification percentage at the start of each loop and as the number of epochs increase gradually a steady classification state was reached after 300 epochs. A steady classification was achieved at 300 epochs in most of the loops instead of 500 epochs, which was selected earlier (as presented in Section 6.3.4). It is apparent that the FFT pre-processing technique enables faster convergence compared to raw signal classification (Section 6.3.4). In most of the epochs only 80% classification was achieved with the input signals, even though 93% classification has been achieved for simulated defect signals at one particular epoch as shown in Figure 7.5.

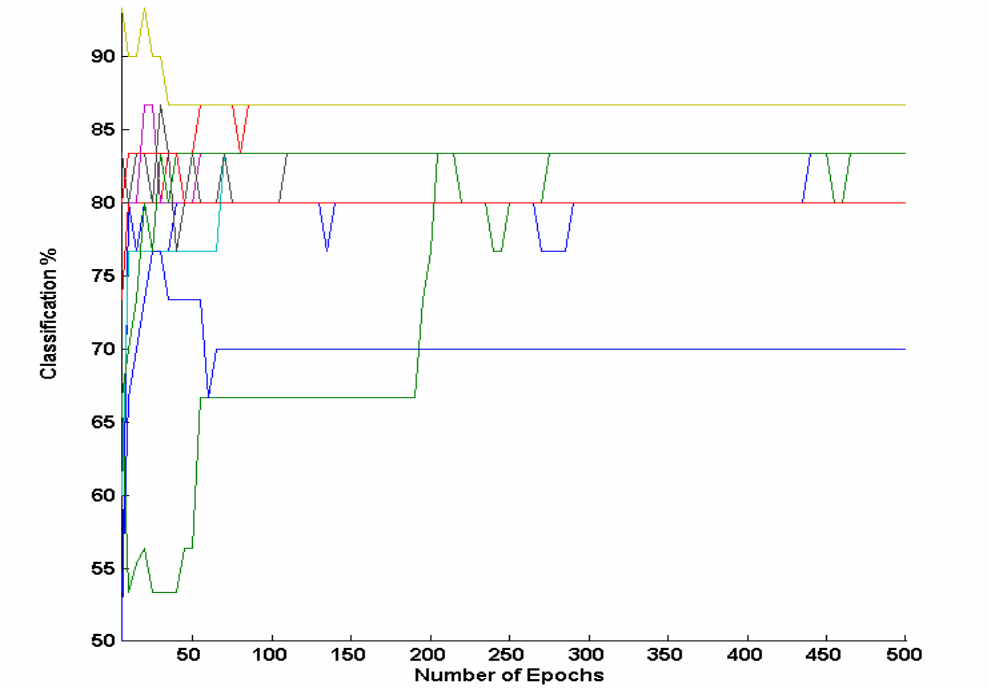

Figure 7.5 FFT type pre-processing classification % for signals obtained from the smooth surface section of the castings (Ra2)

The ultrasonic defect signals were difficult to classify when the neural network was presented with the FFT of signals obtained from rough surface (Ra0) castings. The defect signal echoes were affected due to the random multiple reflections occurring at the rough interface surface of the casting and water column in ultrasonic immersion testing. The FFT classification was carried out as explained in Section 6.5 using the neural parameters as described in Section 6.3. The purpose of the ANN is to identify those frequency spectrums that are uniquely associated with physical defects within the castings. Figure 7.6 illustrates the classification percentage results obtained from ANN after pre-processing the input signal obtained from rough surface (Ra0) casting with FFT pre-processing type. The different colour lines in Figure 7.6 show the different number of loops (10 loops) applied on the given set of input signals for testing in 500 epochs to determine the mean classification percentage and their standard deviation. At the start of each testing loop, there is a high fluctuation in the classification percentage, and as the number of epochs increase gradually a steady classification state is reached after 200 epochs. The mean classification percentage of signals obtained from the real defects with

rough surface section was 72.3% when compared to 81.3% obtained with the smooth surface castings.

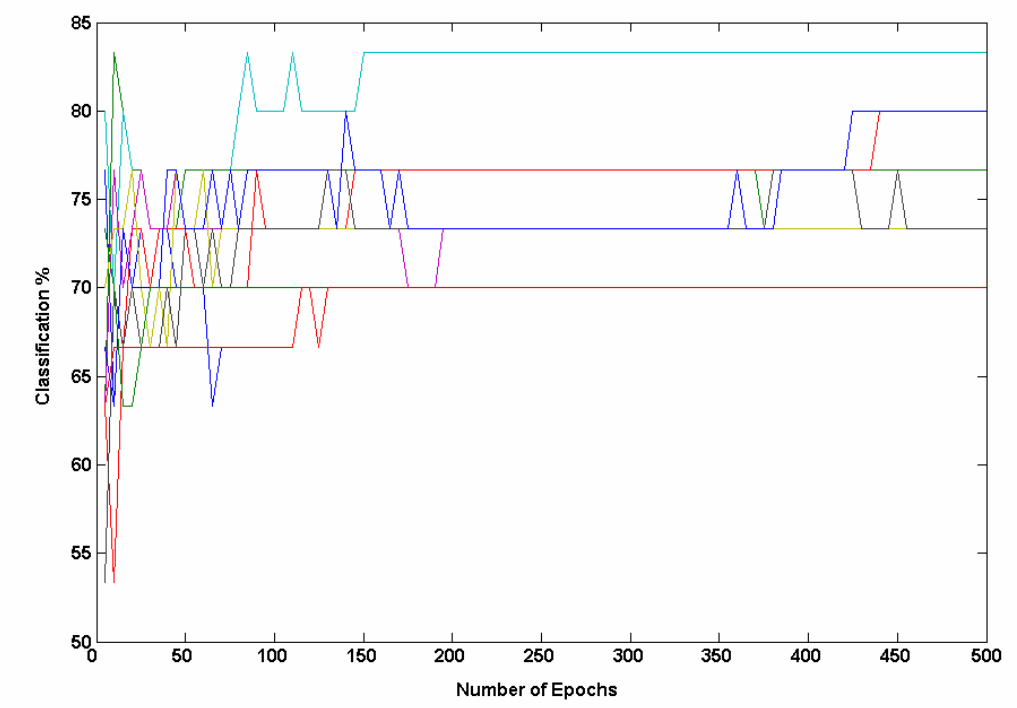

Figure 7.6 FFT type pre-processing classification % for signals obtained from the rough surface section of the castings (Ra0)

7.3.3 PCA Classifier

The next pre-processing method investigated was Principal Component Analysis (PCA). The application of PCA eliminates those components of the signal that contribute less variation in the ultrasonic input signals. It was applied to the input signals obtained from castings with different surface roughness according to the procedure described in Section 6.5.3. A MATLAB program was written to create eigenvectors and to apply principal components as presented in *Appendix G*. From the initial observation, forty principal components were selected for this investigation. This number of principal components was used based on the maximum classification percentage achieved for the given set of input signals (refer to Figure 6.5).

The covariance matrix obtained from the raw signal contains the transformed input vectors after removing the less significant ultrasonic signal components. Then, the covariance matrix was processed through a pre-selected ANN structure for defect classification. However, this approach to signal pre-processing of the input data proved insufficient for achieving improved signal classification with the chosen number of principal components compared with the FFT classifier.

Figure 7.7 illustrates the variation in the classification percentage for number of epochs in the neural network during the testing process. The classification percentage is calculated after each epoch. The ANN classification of ultrasonic signals was carried out as described in Section 6.5.3 by applying the optimised neural network parameters as presented in Section 6.3. The different colour lines in Figure 7.7 shows the number of loops (10 loops). In each loop both training and testing was carried out for the given set of input signals and the MATLAB programming codes were used to carry out this exercise (*Appendix G*). In each loop, 500 epochs were carried out to obtain the mean and standard deviation of the classification percentage.

The mean classification percentage obtained for the ultrasonic signals using PCA was only 63.6% for signals obtained from rough surface castings. The classification of rough surface signals had a standard deviation of 7.3% for 50 loops. Figure 7.7 illustrates that the classification percentage of the ultrasonic signals fluctuates approximately from 44% to 76%. The relative performance in terms of signal classification for ultrasonic signals obtained from rough surface castings in comparison with those from smooth surfaces did not improve with the application of the PCA pre-processing technique (Figure 7.9). Signal pre-processing of ultrasonic signals from different types of surfaces with PCA did not improve the classification percentage as presented in Figure 7.9. Hence, there was a need to investigate other signal pre-processing techniques to classify the weak ultrasonic signals that are associated with rough surface castings.

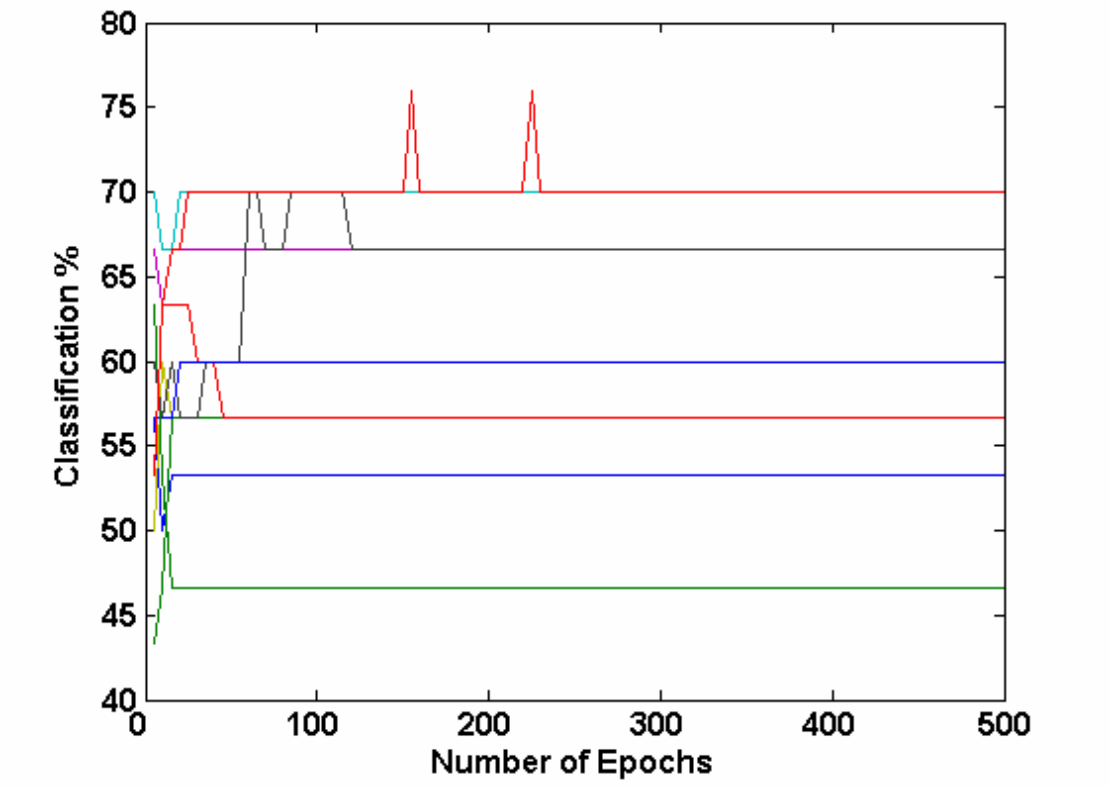

Figure 7.7 PCA signal pre-processing classification percentage for number of epochs with rough surface castings

7.3.4 WT Classifier

Wavelet Transform (WT) was the next signal pre-processing technique investigated. The appropriate wavelet type was selected after comparing the performance of various wavelet types (as described in Section 6.5.4) in relation to signal classification using an Artificial Neural Network (ANN). Daubechies' wavelet db5 type was selected as explained in Section 6.5.4, and illustrated in Figure 6.9.

Figure 7.8 represents a graph of the corresponding approximation coefficients of the training signals in the Ra0 surface roughness group. The best results were obtained from db5 (Section 6.5.4), and the data was composed of 66 DWT coefficients for each of 50 training signals with amplified magnitude. The testing data consisted of 66 DWT coefficients for each of 30 testing signals.

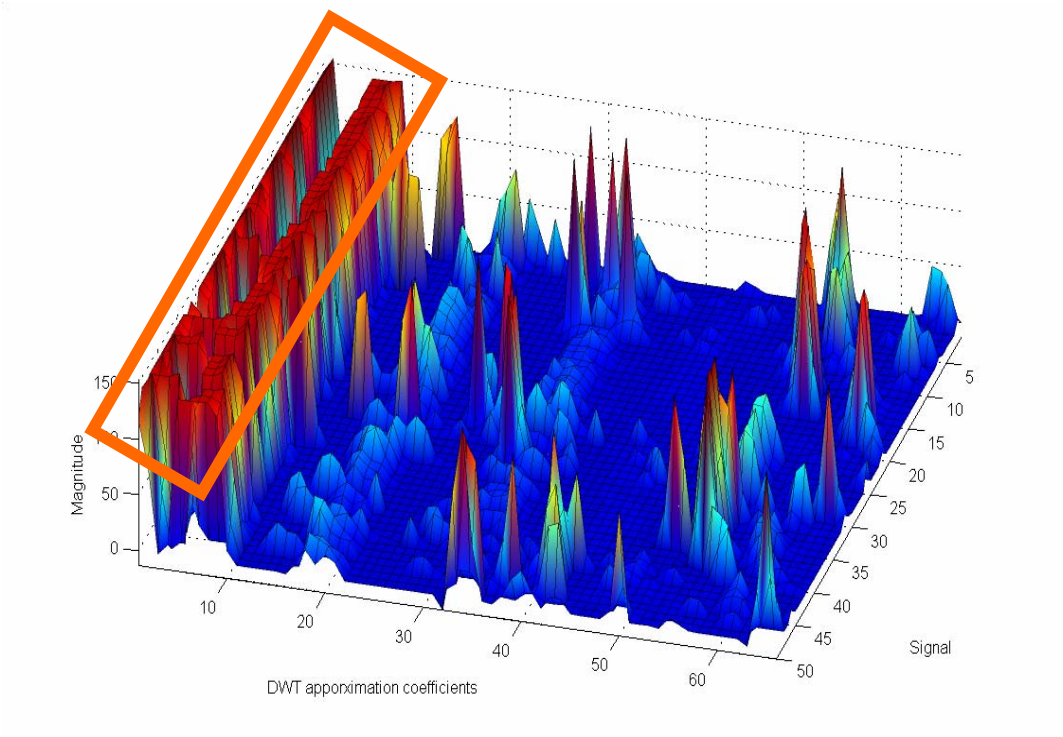

Figure 7.8 DWT approximation coefficient plot for 50 Ra0 signals

The application of WT pre-processing technique enabled the re-alignment of the ultrasonic signal as shown in Figure 7.8. An improved classification percentage was obtained with this pre-processing type compared to that obtained without WT pre-processing (Figure 6.2). Different scaling levels were investigated for WT analysis to determine the DWT coefficients that provided the highest classification percentage of defects. The applications of DWT coefficients along with the filter banks (Section 2.7.3.4) have significantly modified the input to the ANN for signal classification. The detail coefficients at low scale corresponded to the high frequency components of the signal, and also showed the spikes (i.e., noise) produced by the surface roughness. The results obtained from the feed-forward neural network classification of signals from three different surface types are shown in Figure 7.9. The results were compared after pre-processing ultrasonic signals using FFT, WT and PCA. Figure 7.9 indicates that feeding the raw signal to the neural network had the least successful classification percentage when compared to signals classified with FFT and WT pre-processing types. However, the FFT produced a better classification percentage compared to PCA and WT.

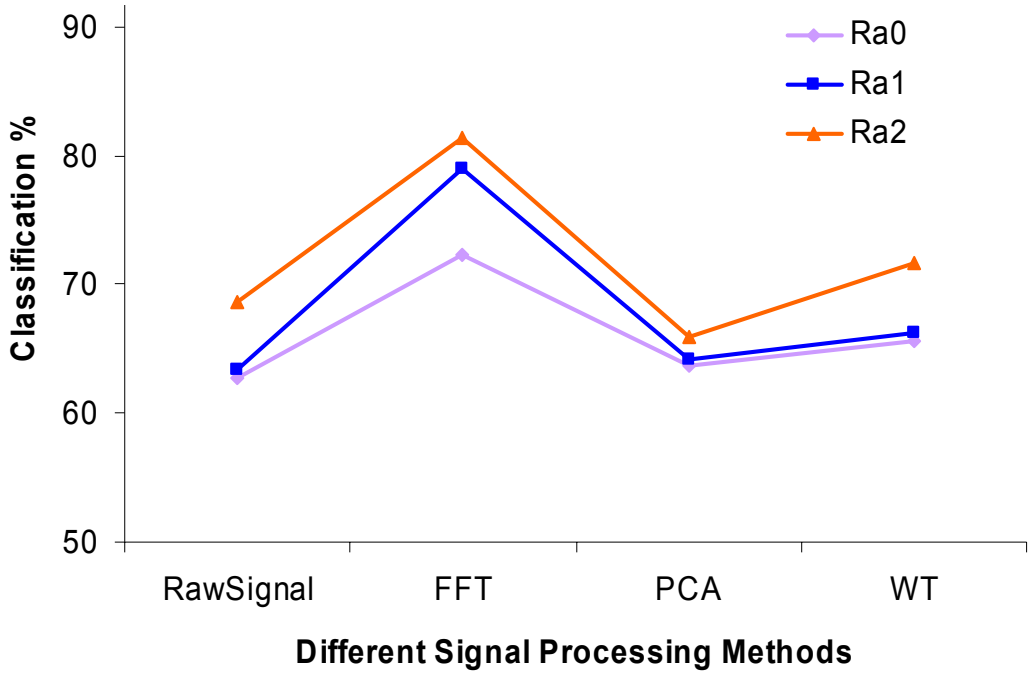

Figure 7.9 Successful classification percentage using different signal processing techniques with both rough and smooth surface castings

The variation in classification percentage for different surface types with WT technique was not significantly higher than for the FFT pre-processing technique (Figure 7.9). In spite of data compression the performance of the WT classifier was in the same order as that for raw signal classification. The wavelet method required the largest number of coefficients to achieve the desired performance. Hence, it can be concluded that the pre-processing of ultrasonic signals using FFT provided a better classification percentage than WT or PCA within the context of a neural network based classification system.

7.4 SIMULATED AND NATURAL DEFECT CLASSIFICATION

Figure 7.10 presents the classification percentage for simulated defects (side-drilled holes), natural defects (gas porosity) and mixed defects, i.e. the combination of both side-drilled holes and defects caused by gas porosity. The number of signals

obtained for each defect type was given in Table 6.1 (Section 6.2). Figure 7.10 provides details on the classification percentages for different signal processing techniques with Ra0 and Ra2 surface types. Figure 7.10 also illustrates the plot of the signal classification achieved with simulated, natural and mixed defect signal (combination of simulated and natural defects) types. Figure 7.10 indicates that the classification performance with simulated defects was almost equal to that obtained with natural defects. Further, as documented in Section 4.5.2, the sizing and location of the simulated defects within the casting section was done such that they closely matched the natural defects. Therefore, it was concluded that the use of simulated defects for the initial testing and validation (as documented in Chapter 6) was justified.

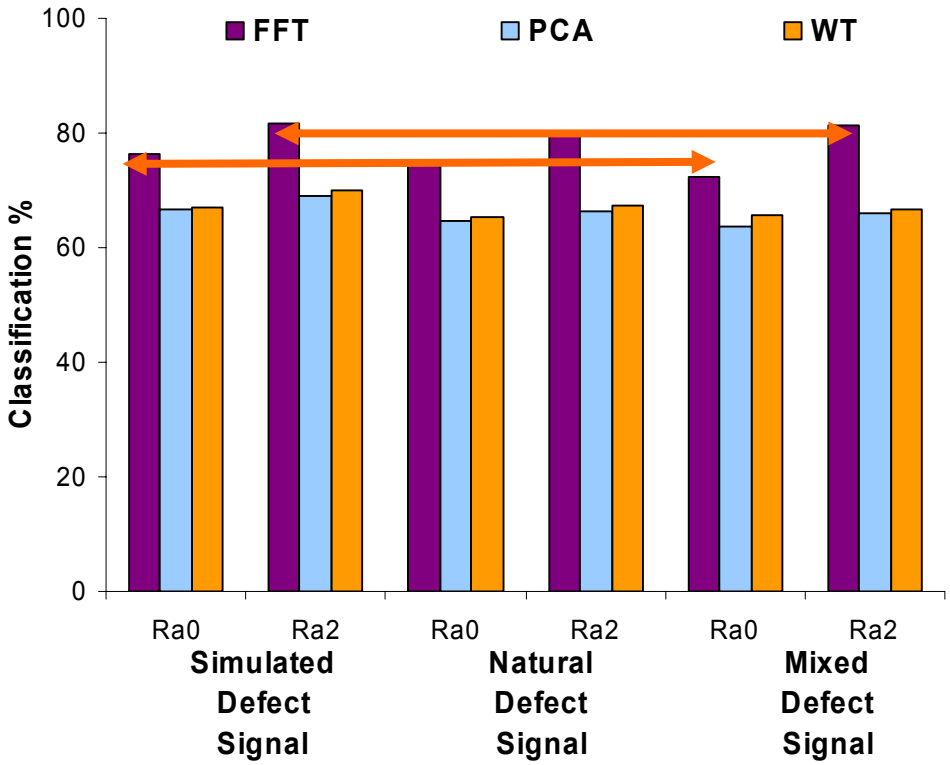

Figure 7.10 Classification percentage for simulated, natural and mixed signal with Ra0 and Ra2 surface roughness using different signal pre-processing techniques

However, since this research focused on identifying real defects within the rough surface castings, further signal processing was carried out only on the ultrasonic signals obtained from castings with natural defects. The classification percentage presented in Figure 7.10 is the mean classification percentage (out of 50

iterations) of the ultrasonic signals pre-processed with FFT, WT and PCA prior to inputting to the ANN.

7.5 CLASSIFICATION WITH COMBINED PRE-PROCESSING METHODS

7.5.1 Overview

The specific objective of this section is to describe the approach used to improve the classification performance of ultrasonic signals (defect and non-defect). The results obtained without pre-processing and with using only a single pre-processing method on the input signals indicated that it was not possible to achieve classification level of over 73% for signals from rough casting sections. The strategy used in the research described in this section was to apply well known signal processing tools such as Fast Fourier Transforms, Wavelet Transforms and Principal Component Analysis in various combinations to ascertain whether this lead to an increase in classification percentage. A similar approach has been adopted by other researchers for different pattern recognition problems, as presented in Section 2.7.3.5. It was envisaged that the combination of signal processing tools would enable both time variant and frequency variant features of the signal to be analysed together.

Hybrid pre-processing represents a combination of two or more pre-processing techniques presented earlier in this chapter (Section 7.3). In this section, the results obtained from the hybrid pre-processing of ultrasonic signals are presented. The defect signals obtained from castings with real defects and varying surface roughness were pre-processed using various combinations of techniques listed above prior to input of the signals to an ANN for classification. The classification results and their associated mean and standard deviation values were obtained after executing the neural network in a loop fifty times. This was carried out for each combination of pre-processing methods. This process provided an

understanding of the stability and consistency of each approach to signal pre-processing applied in this research.

7.5.2 FFT/PCA

In this combined pre-processing method, at first the FFT of the input signal was obtained. Normally, the highly attenuated signal is partially embedded in the incoherent backscattered noise. The incoherent spatial noise due to surface roughness cannot be eliminated with FFT alone. Hence, PCA was then applied to remove the redundant noisy signal, if any, present from the frequency component. PCA was applied to the output of FFT. Figure 7.11 shows the variation in the classification percentage with the number of epochs for ultrasonic signals from the rough surface. The mean classification percentage achieved with this signal pre-processing approach was around 73.3%. Even though the highest classification achieved was approximately 90%, with this type of pre-processing, the standard deviation (SD) was 6.1%, which is still a large value. When compared with the PCA single mode pre-processing method classification (Figure 7.7) there was an improvement in the classification percentage with this approach (Figure 7.11). However, as stated above there was still a large variation (high SD value) in the classification percentage.

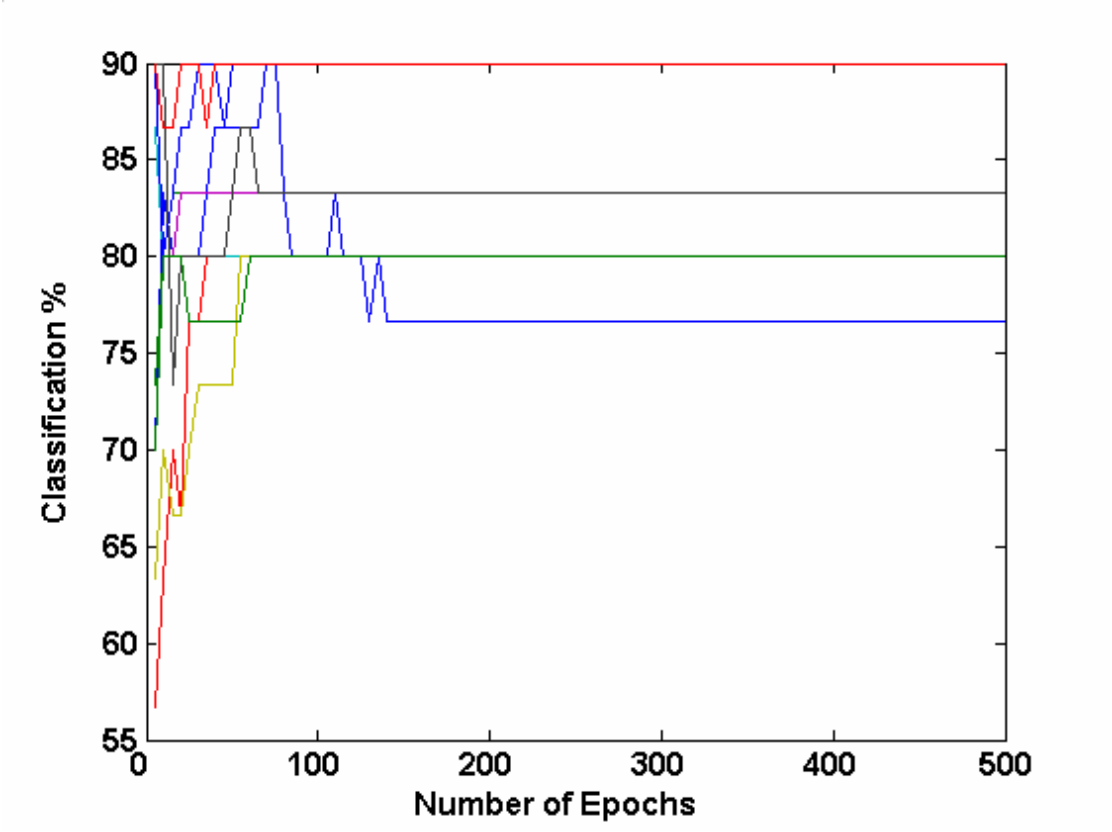

Figure 7.11 FFT/PCA combination signal pre-processing classification percentage for number of epochs with rough surface ultrasonic signals

The application of the FFT/PCA combination resulted in 76.6% classification for the smooth surface castings compared with 73.3% classification for rough surface castings, with a standard deviation (SD) of 8.3% (Table 7.1). The classification percentage does not vary significantly for the different surface types (Ra0, Ra1 and Ra2) with the application of the FFT/PCA pre-processing approach.

Classification %	**Ra0**	**Ra1**	**Ra2**
Mean	73.3	74.6	76.7
SD	8.3	6.4	5.3

Table 7.1 Signal classification percentage for FFT/PCA

7.5.3 WT/PCA

In this combination of classifiers the output of the WT was passed on to PCA to eliminate the redundant WT coefficients. PCA was applied to the approximation component of the wavelet coefficients. The number of principal components used in this combination pre-processing was 40 principal components. It was selected based on the signal pre-processing procedure as described in Section 6.5.3. The application of the wavelet transform, combined with principal component analysis, lead only to a marginal increase in the classification percentage compared to the raw signal classification. The performance of this configuration was not satisfactory. The important factor to consider with this classification method was the large SD values for the all the three surface types was observed as shown in Table 7.2.

Classification %	**Ra0**	**Ra1**	**Ra2**
Mean	64.6	68.4	73.3
SD	7.3	6.3	8.5

Table 7.2 Signal classification percentage for WT/PCA

7.5.4 WT/FFT

In this signal pre-processing approach, WT was applied to the original ultrasonic signal as a first step of pre-processing. It was carried out by applying DWT filters (as described in Section 6.5.4), which divide the signal into frequency bands. Since DWT divides the original signal into low and high-pass frequency bands, it was possible to analyse each frequency band independently. A typical characteristic of DWT was that in each decomposition stage, due to the down-sampling operation, the wavelet coefficients of each layer still contain information of the original signal. The analysis of wavelet was carried out with Daubechies' mother wavelet type. The suitable db5 wavelet type was selected for signal classification as presented in Section 6.5.4.

The application of db5 wavelet type on the input signals resulted in the determination of both detailed and approximate coefficients. FFT was then applied on the approximate coefficients which retained the time-frequency information of the original signal in down-sampled form. The power spectrum of FFT output was used as an input to the neural network classifier. The results presented in Table 7.3 show the mean and standard deviation of classification percentages of the ultrasonic signals obtained from three rough surface types after pre-processing through the WT/FFT combination. However, in the case of signals without higher frequency components (low values of WT down-sampling method) the condition was different and it resulted in a low classification percentage (See results of various combined pre-processing techniques in Figure 7.12).

Classification %	**Ra0**	**Ra1**	**Ra2**
Mean	79.3	83.3	90.6
SD	1.9	3.6	3.4

Table 7.3 Signal classification percentage for WT/FFT

A graph showing the performance of the different signal processing methods and associated classification percentages for castings with varying surface roughness is presented in Figure 7.12. The WT/PCA combination signal pre-processing method resulted in the lowest classification percentage among the different methods described in this section (Figure 7.12).

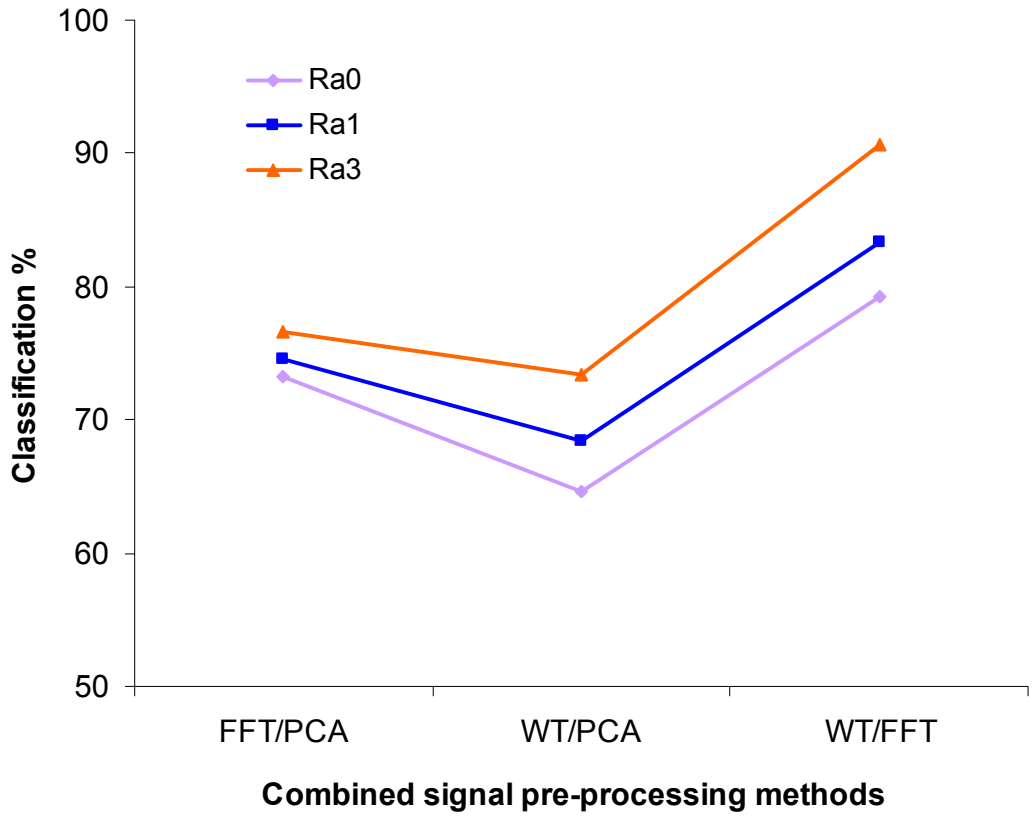

Figure 7.12 Successful classification percentage using combined signal pre-processing techniques

7.6 A NEW COMBINED PRE-PROCESSING APPROACH

7.6.1 Overview

An approach to signal pre-processing not attempted previously is described in this section. The FFT and WT pre-processing methods were applied in sequence to investigate the possibility of achieving an improved classification percentage than that achieved previously (Section 7.5).

7.6.2 FFT/WT

In this method a wavelet transform was applied on the FFT output (power spectrum) of the raw signal. Ultrasonic signals from the rough surface castings contain reflections from defects which manifest in the A-scans as abrupt time localised changes resulting in time varying characteristics. Consequently, the simple FFT technique alone might not be an appropriate method for signal pre-processing. The application of the wavelet transform (time-frequency representation) technique on the power spectrum of the raw signal obtained from different surface classification is presented in Table 7.4. The results from signal pre-processing using a combination of FFT/WT suggest that performing a WT prior to ANN classification enables the exploitation of useful information contained in the FFT output. One of the major reasons to apply WT on the power spectrum of the FFT output (which contains both real and complex parts) is to reduce the fluctuation in the signal due to noise. This also enables reduction in the number of inputs to the neural network. As stated previously, as determined by other researchers reduction of the number of inputs to neural network while retaining all important information with regard to defects leads to improvement in performance (defect classification percentage in this instance). This approach enabled the achievement of an improved signal classification in association with the neural network. As observed from the Table 7.4, the highest signal classification was achieved for smooth surfaces (Ra2) with small variations in the standard deviation (SD). A successful classification of 83.3% was achieved from the signals with rough surfaces (Ra0).

Classification %	**Ra0**	**Ra1**	**Ra2**
Mean	83.3	91.6	96.3
SD	2.9	2.3	2.2

Table 7.4 Signal classification percentage for FFT/WT

Figure 7.13 illustrates the combination of FFT/WT type function application on the ultrasonic signal input to an ANN. The application of WT followed by FFT acts as a filter on the power spectrum of the FFT output on the ultrasonic signal. It

could be also stated that the FFT/WT combination pre-processing approach produces a smooth spectrum of the un-filtered ultrasonic signal.

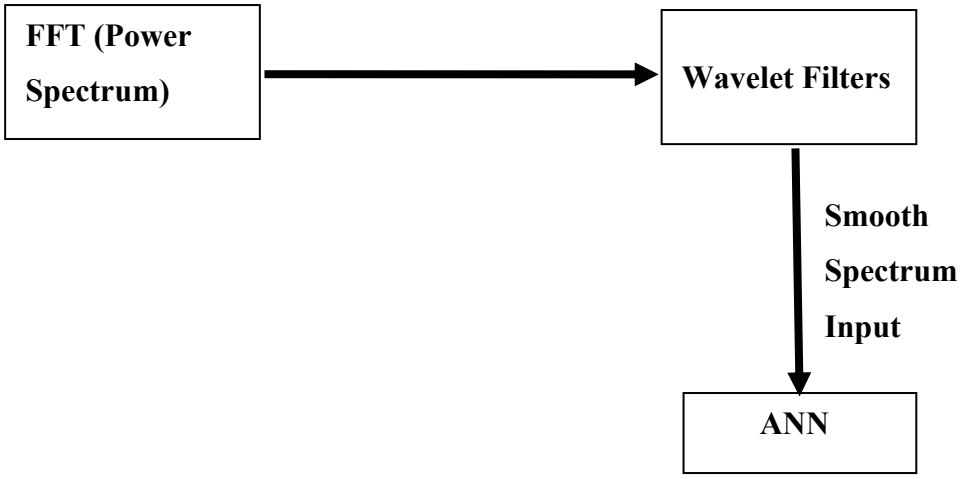

Figure 7.13 FFT/WT combination type pre-processing

Even though a high classification percentage (more than 95%) was achieved for smooth surface castings with this combination of signal pre-processing techniques, it should be noted that 100% classification was not usually achieved except in a couple of iterations.

7.6.3 FFT/WT/PCA

The next step was to apply the combination of FFT/WT/PCA signal pre-processing techniques to the input signals in order to explore the possibility of achieving 100% classification of ultrasonic signals with artificial neural networks. The same approach as with the FFT and WT combination has been followed in this instance. In order to eliminate any redundant values from the FFT/WT output combination, the PCA was applied to the pre-processing step. The eigenvectors and eigenvalues were calculated on the output of FFT/WT combination. In this method also 40 principal components were used as described in Section 6.5.3. Table 7.5 shows the classification performance using the combination FFT/WT/PCA pre-processing method. The maximum classification percentage of 99.8% was obtained with the mean of 96.6% for the smooth surface Ra2 type. Similarly there was an

improvement in the classification percentage of rough surface signals (82.3%) compared to other pre-processing methods presented in Section 7.3 and 7.4.

Classification %	Ra0	Ra1	Ra2
Mean	82.3	89.6	96.7
SD	4.6	2.3	3.2

Table 7.5 Signal classification percentage for FFT/WT/PCA

7.7 DEFECT CLASSIFICATION PERFORMANCE

Given the importance of developing an inspection technique for rough surface castings, various pre-processing combination methods were compared for Ra0 and Ra2 type surfaces. Figure 7.14 shows the classification percentage achieved with different signal pre-processing techniques applied on the ultrasonic signals. More than 90% classification for smooth surface casting signals was achieved only with three signal pre-processing approaches and they were WT/FFT, FFT/WT and FFT/WT/PCA types. Figure 7.14 indicates that the highest classification percentages are obtained from combined pre-processing types of FFT/WT and FFT/WT/PCA. However, the standard deviation (error bars in Figure 7.14) for the FFT/WT/PCA type was greater than for the FFT/WT method. Hence, it can be concluded that, based on consistency of signal classification percentage and the low standard deviation (SD) variation, the FFT/WT method out performs the FFT/WT/PCA combination approach.

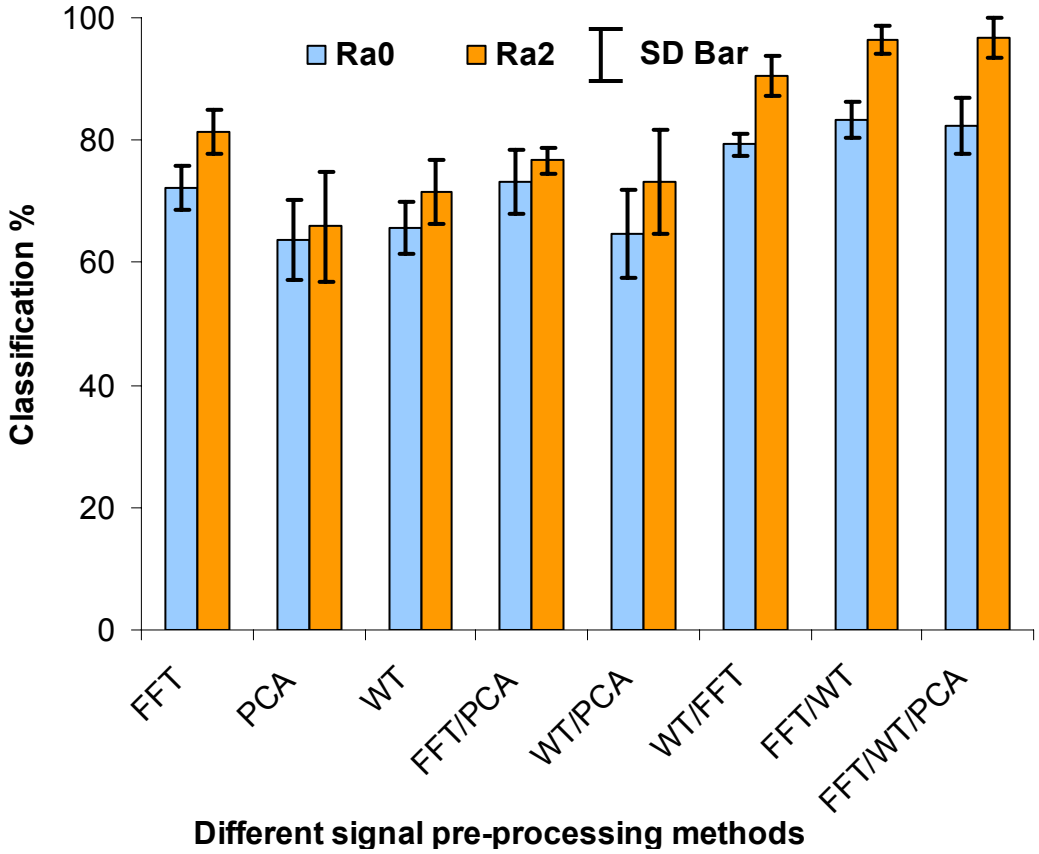

Figure 7.14 Defect classification percentage and standard deviation of different signal pre-processing techniques on Ra0 and Ra2 type surfaces

These signal pre-processing approaches investigated in this research did not require a large amount of computational effort or time (not more than couple of hours) for classification. The algorithm (as described in Figure F.2, *Appendix F*) presented in this research to carry out ultrasonic signal classification required low computational memory and executed at acceptable speed to identify defects in the rough surface castings.

7.8 ULTRASONIC SIGNAL VALIDATION

In the analysis described previously (Sections 7.4 to 7.6), the ultrasonic signals used for the classification included both defect and non-defect signals.

Validation was necessary to ensure that those signals identified as defect signals actually corresponded to physical defects in the casting sections. Similarly, it was necessary to ensure that those signals identified as non-defect signals actually corresponded to regions in which defects were not present.

As explained in Chapter 1 (Section 1.3), one objective of this research was identifying the smallest possible gas porosity defects, within castings containing varying surface roughness. Although X-ray images were previously used to determine where the real defects were located within the castings, it was not possible to obtain an accurate estimate of the defect size. Therefore, based on the X-ray images the casting sections were cut into small sections such that it was possible to examine and measure the defects.

As mentioned in Section 4.7, ultrasonic inspection was validated against radiography (X-ray) inspection results obtained from the sample castings. X-ray and visual inspections were carried out on the castings inspected with ultrasound and successfully classified with an appropriate signal pre-processing technique.

Similarly, X-ray inspection was carried out on the defect sections of the castings to detect the defects after ultrasonic inspection. Figure 7.16 shows a casting section with cracks and porosity defects at the in-gate section of the casting. In this research, emphasis was given to gas porosity defects when compared to crack-like defects in the sub-surface region of the in-gate sections of the castings. This was mainly due to the predominant presence of gas porosity defects in aluminium castings.

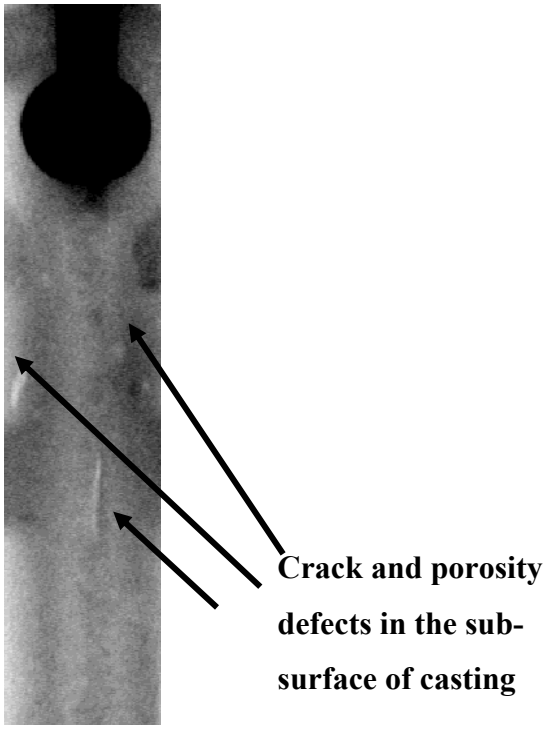

Figure 7.15 X-ray result of a part of the structural sump oil pan casting with sub-surface defects in the in-gate section

To visualise the gas porosity defects, the castings were cut into small sections as shown in Figure 7.17. These casting sections in the in-gate area were selected based on the locations associated with a positive defect classification output from ultrasonic signal processing. Figure 7.17a illustrates a cut section of a casting with 0.5 and 0.7 mm gas porosity defects from a smooth surface type (Ra2). Figure 7.17b illustrates a cut section of a casting with 0.7 mm size defect from a Ra1 surface type (50-100 μm). The defects with 0.5mm and 0.7 mm diameter were detected by ultrasonic inspection of a casting section with surface roughness (Ra2 type up to 50 μm). However, defects of less than 0.7 mm diameter within castings with surface roughness Ra0 and Ra1 (above 50 μm) were not detected using ultrasonic inspection. Defects of diameter 0.7 mm in size and higher were detected using ultrasonic inspection for castings with surface roughness values ranging from 50 to 100 μm. The defect information contained in the signal was indistinguishable from noise when the surface roughness was in the range of 100 to 150 μm. Hence, the small defects of size less than 1 mm diameter was not detected in this surface roughness range using ultrasonic inspection technique.

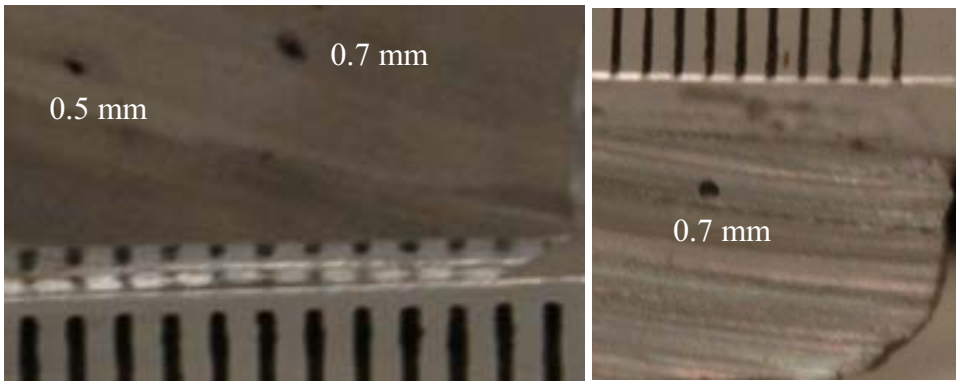

(a) **(b)**

Figure 7.16 Cut-section of the sample castings with gas porosity defects of (a) 0.5 mm and 0.7 mm gas porosity defect in Ra2 section and (b) 0.7 mm diameter defect in Ra1 section

7.9 SUMMARY

The raw signal analysis of the results obtained from ultrasonic immersion testing of rough surface castings showed that with the selected frequency range it was difficult to detect gas porosity defects. Therefore, artificial neural networks were applied on the raw ultrasonic signal data. However, the results were not satisfactory as indicated by the low classification percentages for the different surface types. This has created a need to pre-process the signals before classifying with artificial neural networks. It was demonstrated that by applying suitable signal pre-processing techniques, it was possible to identify defects of minimum 0.5 mm size in castings with surface roughness up to 50 μm (Ra2).

FFT, PCA and WT signal pre-processing techniques were applied separately on the raw ultrasonic signals which were passed into the ANN to achieve a better classification percentage. Still, the classification percentage of ultrasonic signals obtained from rough surface castings after the application of different signal pre-processing techniques did not result in more than 80% classification. This was due to

the presence of the clustered front wall echo. To avoid overlapping class boundaries and achieve a better classification performance, a different approach was required. Hence, a combination of signal pre-processing techniques was applied on the raw ultrasonic signal. The results showed that poor classification was achieved with the combination of FFT/PCA and WT/PCA. However, the classification of the signals pre-processed with the combination of WT/FFT, FFT/WT and FFT/WT/PCA classifiers provided improved classification of more than 90% for castings with smooth surfaces and in the range of 75% to 83% for castings with rough surfaces. The results obtained from castings with different surface roughness, and the classification performances achieved with different pre-processing methods are discussed in the next chapter.

CHAPTER 8.

DISCUSSION

8.1 OVERVIEW

The aim of this chapter is to describe the validation of a methodology, and the establishment of a procedure for ultrasonic inspection of castings in the as-cast state. However, this research did not attempt to address all types of defects present in aluminium die castings. The discussion presented in this chapter focuses on the main research findings such as experimental methodology (Section 8.2) and results (Sections 8.3, 8.4 and 8.5). Also discussed are backscatter effects due to the rough surface of castings in the as-cast state, and the comparison of the different signal pre-processing techniques. The results obtained from using different signal pre-processing methods alone, and in combination, are discussed. The discussion also focuses on benefits and limitations of the achievement of the project objectives as stated in Chapter 1.

8.2 DISCUSSION ON EXPERIMENTAL PROCEDURE

The experimental method described in Chapter 4 focused on obtaining best possible ultrasonic signals from rough surface sections of aluminium die castings. This was achieved through the selection and implementation of a suitable inspection method and inspection parameters to carry out investigations on aluminium castings.

Ermolov's [56] work on the optimisation of conditions in the implementation of the ultrasonic pulse echo method clearly emphasised the importance of selecting suitable inspection parameters and also recommended procedures to obtain them. The selection of proper inspection parameters was aided by the literature on relevant past research as presented in Chapters 2, 4, and 5.

Burningham [126] used the knowledge of expert operators to identify a suitable frequency for ultrasonic inspection of iron castings in his doctoral research work. The expert operators conducted a series of tests and calibrated the equipment with simulated defects, and finally, selected the 5 MHz frequency based on the maximum signal amplitude obtained from the simulated defects. However, Burningham [126] did not provide detailed information on the selection of the frequency, and did not consider the effects of material parameters such as surface roughness and grain size variations. This research work addressed these issues in Chapter 5. The developed selection process not only enabled the study of characteristics of the material (casting) being inspected, but also provided information on the effect of material properties on ultrasonic inspection.

Experiments were carried out to determine the effect of grain size variation on ultrasonic signals in aluminium die castings as presented in Section 5.5.4. The results presented in Figure 5.6 support the earlier findings of Ambardar *et al.* [65] in relation to the effect of grain size on the ultrasonic signal. However, their results were obtained from sand castings that had a coarser grain structure in contrast to the fine and medium grain structures in high-pressure die castings investigated in this research. The attenuation loss experienced in Ambardar *et al.'s* [65] research was higher than the attenuation loss in the castings investigated in this work. It can be observed from Figure 5.6 that the attenuation loss (L) due to variation in grain structure is comparatively low for castings with fine to medium grain structure at higher frequencies (10 to 20 MHz).

The next step in the evaluation of the effects of materials properties on ultrasonic signals involved examination of the effects of surface roughness variation. The results were presented in Section 5.5.5. These results were comparable to those

obtained by Adler *et al.* [64] and Ambardar *et al.* [65] (Section 2.5.3). Nevertheless, their work was carried out on castings with surface roughness below 50 μm. While the research described in this thesis relates to castings with surface roughness between 50 and 150 μm.

Adler *et al.* [64] used both the front wall echo (FWE) and back wall echo (BWE) for evaluation of porosity type defects in aluminium cast materials with varying surface roughness. Ambardar *et al.* [65] also used the FWE and BWE in their study on the effects of surface roughness on ultrasonic echo amplitude in aluminium alloy castings. In this research only the BWE has been used to investigate the effects of grain size and surface roughness variations on ultrasonic signals. This was due to the fact that there was a substantial loss of amplitude and increased noise associated with the front wall echo due to the larger surface roughness of the castings. The results on the effect of surface variation were presented in Figure 5.7.

In the ultrasonic inspection of castings, rough surface sections affect the ultrasonic beam as it propagates through them. In turn, these effects determine the characteristic behaviour of the backscatter signals as observed in Chapter 7 (Section 7.2). The application of focused probes on the rough surface of castings is described frequently in the literature [70,73], and researchers have also clearly demonstrated the benefit of using focused probes compared to unfocused probes on rough surface materials. In this research, the detection of sub-surface defects within rough surface casting sections was difficult with unfocused ultrasonic probes due to the large scattering effect. The application of focused probes assisted in achieving better results compared to the unfocused probes. These results enabled the elimination of the use of unfocused probes at an early stage in this research.

This research work has demonstrated the effect of surface roughness on the back wall echo (BWE). The amplitude of the BWE was degraded with an increase in the surface roughness. As mentioned earlier in Section 4.5.3, Abdelhay and Mubark [137] studied the effects of surface roughness variation on the ultrasonic signal with the normal pulse-echo technique. Their results have shown that as surface roughness increases the attenuation increases. Their work involved surface roughness values

(R_a) over 100 μm. However, this work was carried out on machined steel and with contact type ultrasonic testing. Furthermore, they did not investigate the effect of variation in frequency used in ultrasonic testing. The effective frequency for the measurement of ultrasonic signal amplitude in a situation of varying surface roughness was investigated and determined in this research as presented in Section 5.5.5.

The use of simulated defects within the castings was another important issue in the development of the inspection procedure. The unavailability of standard calibration blocks from the same material as the castings being inspected led to development of the calibration technique used in this research. The use of simulated defects in the castings for investigative purposes is not a new approach and has been validated by other researchers [46,56,146]. Side-drilled holes were produced in the casting to simulate gas porosity defects. The investigation of the effects of surface roughness on ultrasonic signals was investigated based on these simulated defects.

8.3 DEFECT DETECTION ON ROUGH SECTIONS

The rough surfaces greatly altered the signal-to-noise ratio of the ultrasonic signals. As described in Chapters 2 and 5, there has been much published research dealing with the analysis of ultrasonic signals from rough surface parts in different applications. However, there is no published evidence of investigation on the variation of ultrasonic signal amplitude with castings having surfaces with roughness values over 50 μm, which is normal un-machined surface roughness in the majority of aluminium castings.

From Figure 5.8 (Section 5.5.5) and Figure 7.1 (Section 7.2) it was evident that there was an increased loss of BWE and defect signal amplitude as the surface roughness increased. Also it could be seen that there was an increased loss of defect signal amplitude as the ultrasonic frequency increased (within the range of 2.25 MHz

to 20 MHz). Blessing *et al.* [54] achieved similar results with steel samples at a frequency range of 1 to 20 MHz, where BWE decreased with increased surface roughness. It can be seen from Figure 2.4 (Section 2.5.3) that their investigations were confined to surfaces with roughness values up to 23 μm. The main difference between the research undertaken by Blessing *et al.* [54] and the current research is that the current research is concerned with castings containing rough surfaces (with R_a values mostly varying between 50 μm and 150 μm). It should be emphasised that in the current research, even a single BWE could not be obtained when surface roughness values exceeded 100 μm at a frequency of 20 MHz. This was different from the research undertaken by Blessing *et al.* [54], who observed multiple BWEs (a total of four) due to multiple reflection within the steel samples at frequencies identical to those used in this research. The current research has indicated that for surface roughness values up to 50 μm, the effect of surface roughness is minimal when frequencies are kept equivalent to or below 10 MHz.

The inability to detect an ultrasonic defect signal may be caused by the following factors. For instance, the defect signal amplitude may be reduced due to the general scattering losses of the ultrasonic signal at the rough front surface of the casting. This was illustrated in Figure 7.1, in which it could be seen that the defect signal amplitude was reduced for large surface roughness (in particular for the R_a value of 150 μm). Next, the defect signal might be difficult to detect due to the noisy backscattered signal in the region of the rough front surface. For example, Figure 7.4a shows the ultrasonic signal obtained from a rough surface (Ra0) casting section with a 1 mm diameter side-drilled hole at a depth of approximately 3.5 mm. It could be observed that there was a significant clustered front wall echo signal which affected the signal up to a depth of approximately 4.5 mm (Figure 7.4a). Therefore, for this example, it was difficult to identify the defects located close to the front surface of the particular casting section. Further, the defect signal amplitude, was also dependent upon the defect surface (i.e. simulated holes or real defects) within the castings – when the surface of the defect was rough, more scattering occurs, resulting in a low signal amplitude than for a similar sized defect within a smooth surface. A similar trend in relation to the first back wall echo amplitude was

observed at different frequencies used in this research as presented in Figure 5.8 (Section 5.6.5) for castings with surface variation from 100 μm to 150 μm.

Adler *et al.* [64] studied the effect of backscatter in their work on the ultrasonic inspection of aluminium cast materials. They also found that the transmitted wave was attenuated in a similar way to the reflected wave at the water-aluminium interface during ultrasonic immersion testing. However, the backscatter effect observed in the current research showed that the ultrasonic signal depended on both the selected frequency range and surface roughness if it was over 10 μm R_a value (as shown in Figure 5.8 and Figure 7.1). There was a significant loss in the back wall echo after 50 μm R_a value for the selected frequency range in this research (as shown in Figure 7.1). At a surface roughness below 10 μm, the loss of signal amplitude from the back wall and defect was minimal for any selected frequency. The unsatisfactory effect of the lower frequency range up to 2.25 MHz on the signal amplitude was due to less ultrasound energy being sent into the region of interest in the casting. Hence, the lower frequency range with unfocused probe was eliminated from further experiments in this research as discussed in Sections 5.6.5 and 8.2. The selection of a frequency range suitable to inspect castings with surface roughness of more than 50 μm has been successfully achieved in this research. The suitable frequency range was identified as being between 5 and 10 MHz. With this frequency range the signal patterns obtained from the castings with surface roughness between 50 μm to 150 μm were suitable for further analysis in relation to defect detection.

The smallest defect that can be detected with this inspection approach was identified as approximately 0.5 mm in diameter with a 10 MHz frequency probe for castings with surface roughness up to 50 μm (Section 7.2). The identification of a defect of size 0.5 mm diameter is consistent with the research objectives discussed in Section 1.3. The inspection carried out on castings with simulated defects of less than 0.5 mm diameter did not yield a signal of sufficient amplitude for further analysis. Defects of diameter between higher than 0.7 mm were detected within castings with surface roughness values ranging from 50 to 100 μm using an inspection frequency of 10 MHz.

It was difficult to detect any back surface or defect echo in the ultrasonic signals obtained from the castings with the naked eye as observed from Figure 7.4a. This was due to clustering of the front wall echo and difficulty in identifying the defect signals close to the front surface of the casting. Even an increase in the electrical gain (dB) in the equipment to offset the effect of attenuation did not assist in identifying the defect echoes. This emphasised the need for ultrasonic signal processing to obtain meaningful information from castings with rough surface as considered in this research.

8.4 SIGNAL PROCESSING PARAMETERS

In this research, results were obtained in a one-dimensional signal output format named A-scan from the ultrasonic testing unit. The ultrasonic A-scan offers amplitude as the parameter to be monitored. Back-scattered noise in A-scan is important since it contains information that can be used to characterise the microstructure as well as placing a limit on flaw detectability. The signal obtained from within the thickness of the casting was subjected to signal processing. With the rough surface range (Ra0) the scattering was the most prominent feature and variation in signal amplitude due to defects was hard to detect. It was difficult to uncover the prominent features as listed in Table 2.2. It was also hard to detect the multiple defect echo amplitude due to the large reduction in the amplitude of the ultrasonic signal caused by the rough sections of the casting. Therefore, features to be input to the neural network classifier were confined to the signal waveform.

In terms of the neural network configuration, in order to determine the smallest applicable number of neurons in the hidden layer, training and testing were carried out on several different sized neural networks. This is a well known general procedure which has been followed by a number of researchers [77,80,97,102-114].

As mentioned in Section 2.7.5, Rao *et al.* [111] applied a systematically optimised method to select neural network parameters for signal processing. Even though their work was carried out using a different NDT method (eddy current testing), it is relevant to this research in terms of selecting suitable neural network parameters. The results of their work as presented in Figure 2.5 are comparable with the results of this research presented in Figures 6.3 and 6.4 (in Section 6.3). The relevance of Rao *et al.* [111]'s work lies in the fact that they also successfully extracted useful information from a noisy analog signal. It is pertinent to state that Roberts and Penny [145] have successfully implemented the method used by Rao *et al.* [111] in an ANN application, while studying the advantages and disadvantages of neural networks.

As presented in Section 2.7.4, Raj and Rajagopalan [89] in their work recommended the use of combined signal processing techniques such as Artificial Neural Networks (ANN), Knowledge Based Systems and Computer Aided Visualisation techniques to meet the requirements of NDT & E applications. A similar approach (combination of different signal processing techniques) has been followed in this research with regard to the pre-processing of ultrasonic signals prior to input to an optimised neural network. The application of different types of pre-processing techniques to ultrasonic signals prior to input to a neural network for defect identification was discussed in Section 6.5.

Rajagopalan *et al.* [134] compared outcomes associated with using natural and artificial defects, and a mixture of them in their work on an eddy current based inspection application. This is identical to the approach followed in this research and presented in Section 7.4. The important conclusion drawn from their work was that use of simulated defects to train artificial neural networks for identifying real defects (gas porosity defects) was effective. This supports the approach adopted in this thesis where simulated and actual defects were used for training and testing of the neural networks respectively as described in Chapter 7 (Section 7.4).

8.5 DEFECT CLASSIFICATION

8.5.1 Overview

In this section, the process of selecting signal processing parameters has been described with reference to the work carried out by other researchers on similar NDT applications. It is apparent that the choice of the signal processing technique is application dependent (Section 2.7.4). The next step was the analysis of the performance of the different signal pre-processing techniques. The results of this exercise were presented in Chapter 7. Other researchers' contributions to this field are presented in the following sections, with reference to the research described in this thesis.

8.5.2 Single Mode Pre-processing

In all these methods broadband ultrasonic signals were used, which were analysed either in the time or frequency domains. These signals were usually time-limited or band-limited. The important point observed while using frequency analysis in the first place was the breakup of the time domain ultrasonic signal into frequency components. In the case of smooth surface castings this procedure allowed differentiation between frequency components caused by background signal noise and those caused by a defect. However, this was not the case for rough surface castings, as the frequency components associated with defects could not be separated from those associated with signal noise from the rough surface. The frequency-domain processing techniques are not appropriate when the defects are close to the surfaces or when the echoes overlap due to a rough surface. This fact was demonstrated by the significant difference in classification percentages between smooth and rough surface castings as mentioned in Section 7.3.2.

As described in Section 2.7.3.3, PCA is a classical multivariate data analysis method that is useful in linear feature extraction and data compression. The application of PCA to the noisy signal changed the covariance matrix of the

investigated signal by adding a diagonal matrix, with corresponding variances of individual noise components on the diagonal. In the case of a defect free signal with noise, this led to the same increase of all eigenvalues as computed for the clear signal. When the signal-to-noise ratio was sufficiently high, the noise would mainly affect the directions of the principal components (Section 2.7.3.3) corresponding to smaller eigenvalues. This allowed the neural network to discard the finite variance due to the noise by projection of the data onto the principal components corresponding to higher eigenvalues (Section 6.5.3). This in turn also led to a higher loss of the signal information; i.e. one has to deal with the balance between noise reduction and information loss. In this case, the loss of information along with the clustered front wall echo resulted in a lower classification percentage with the neural network classifier.

The selection of a suitable mother wavelet is a critical step in the application of the wavelet transform in any signal processing application [102]. The selection of an appropriate WT type to pre-process the ultrasonic signals was described in Chapter 6. This approach enabled the achievement of a slightly better classification percentage than with the raw signal for both rough and smooth surface casting sections as presented in Figure 7.9. Through experimentation Daubechies wavelet type (db5) was identified as the most suitable in achieving the highest classification percentage for both the rough and smooth surface castings (Section 6.5.4). However, the selection of a suitable mother wavelet for pre-processing did not generate a classification performance of more than 95% for the ultrasonic signals from smooth surface castings. The performance of the wavelet transform (WT) in relation to the rough and smooth surface signals varied significantly with the standard deviation of 4.1% and 5.3% respectively.

The results illustrated in Figure 7.9 demonstrate that a low classification percentage was obtained with both WT and PCA signal pre-processing techniques. This could be compared with the results obtained by Lázaro *et al.* [98], who applied the discrete wavelet transform for de-noising ultrasonic signals contaminated with grain noise. In their case, the increase in the grain noise reduced the performance of the wavelet transform. In the research described in this thesis, it has been observed

that the increasing surface roughness leads to a reduction in defect classification percentage when the wavelet pre-processing techniques was used.

The difference in classification percentage for rough and smooth surfaces was illustrated in Figure 7.9. The overlapping feature regions encountered with rough surface castings resulted in deteriorating of signal classification performance. This was mainly due to the clustered front wall signal echo obtained at the rough casting surfaces. To minimise the negative effects of multiple front wall echoes and to achieve a better classification performance more effective feature extraction approaches have to be identified. Therefore, the use of a combination of signal pre-processing techniques was investigated to achieve improved signal classification using a neural network.

8.5.3 Hybrid Mode Pre-processing

As stated in Section 8.5.2, there was a need to apply different signal pre-processing approaches to achieve an improved classification percentage (> 75%) for the signals obtained from rough surface castings. A different approach was investigated, in which time-frequency analysis on the non-stationary received signal was carried out, and thereby transformed it into a two-dimensional component. One dimension of component is represented by frequency and other by time. This procedure should assist the neural network to identify the salient features of the received signals. Such an approach might also be inefficient due to the highly redundant nature of the time-frequency signal. The redundant components of the time-frequency signal might be removed prior to processing, thereby enhancing the efficiency of computation. To do so, principal component analysis was applied to the time-frequency signal. This process of applying the two or more pre-processing approaches is known as hybrid mode pre-processing and is used to achieve improved signal classification outcomes.

In this research, FFT, PCA and WT type signal pre-processing techniques were combined in different modes as presented in Chapter 7. The classification

performance obtained by combining PCA and WT pre-processors was not improved when compared to a situation where a FFT type pre-processor was used on its own (Figure 7.12). Combining the WT and FFT pre-processing techniques provided an improved classification percentage in comparison with those involving PCA with either FFT or WT.

The application of FFT on a signal processed using WT (WT/FFT type) has been carried out by Matalgah and Knopp [104] and Wang *et al.* [105] and this has been presented previously in this thesis (Section 2.7.3.5). There was a difference in their approaches of combining WT and FFT type pre-processing techniques. Matalgah and Knopp [104] initially applied WT then inverse WT, and finally, the FFT on the original signal in their work. However, Wang *et al.* [105] applied FT directly on the output signal processed using WT. The wavelet coefficients were obtained after down-sampling in their method and were used for further signal analysis. The research described in this thesis adopted a similar approach to that of Wang *et al.* [105], where FFT was applied on the output obtained by applying WT to the original signal (Section 2.7.3.5). In this case, the WT acts as a low pass filter on the raw input signal. Then, the FFT provides the power spectrum of the filtered signal. Hence, the combination could be stated as the spectrum of the smooth signal (filtered), which was used as an input to the neural network classifier. It should be also noted that WT provides a time resolution of the signal while, FFT provides frequency resolution. These two transforms combine to produce a better resolution in both time and frequency domains as confirmed by the results presented in Section 7.5.4.

A different approach, the application of WT on the output signal produced after the FFT operation (FFT/WT type) produced a significant improvement in the ultrasonic signal classification percentage from 62.6% (raw signal classification) to 83.3% for Ra0 surface type (Section 7.6.2). Though the WT exploits both time and frequency information of a signal, an output processed using a FFT will contain only the frequency information. The application of FFT on the raw signal resulted in a power spectrum. Then, the application of Wavelet filters on the power spectrum of the signal removed the fine spectral details i.e., small spectral details which contain

very little significant information in relation to the raw signal. It is important to make the correct choice of filters (i.e. suitable coefficients for WT) to ensure the best possible classification of weak ultrasonic signals using the neural network approach. This approach smoothens the spectrum of the signal (acts as a low pass filter), which improves the performance of the neural network classifier significantly. Another important factor that assists in this classification approach is the reduction in the number input nodes from 220 (raw signal type) to 128 (out of FFT/WT combination pre-processing type). This decreasing number of input nodes in the network, lead to a decrease in the number of network weight values to be calculated.

The advantage of combining FFT and WT in that order lies in the fact that the WT exploits the frequency information contained in the signal after processing through FFT. Subjecting the signal output of FFT to successive approximations through the application of WT, renders the signal less noisy and lowers its amplitude. However, successive approximation results in loss of frequency information particularly in the high frequency bands (due to low pass filter). This research has demonstrated that the use of both stationary (FFT) and non-stationary (WT) signal processing techniques have the ability to improve performance in terms of analysis of weak and noisy ultrasonic signals in order to detect defects in castings.

The combination of FFT/WT resulted in the removal of unwanted signal noise contained in the data. As stated earlier the input nodes were reduced from 220 to 128 in this combination type. Further signal pre-processing with PCA resulted in further reduction in the number of input nodes in the neural network classifier. There was no significant improvement in the classification percentage with FFT/WT/PCA combination type as presented in Figure 7.14. There was a large variation in the standard deviation of the classification percentage when the FFT/WT/PCA type pre-processing method was used in comparison with the FFT/WT type pre-processing method. This might due to the fact that the application of PCA to FFT/WT combination type resulted in the loss of useful information in the process of noise removal. It could be concluded that the hybrid FFT/WT type pre-processing method results in the best classification performance and minimum variation in standard

deviation of classification when compared with all other pre-processing methods investigated in this research.

Finally, it could be concluded from the results presented in Chapter 7 (Sections 7.3, 7.5 and 7.6) that:

- The information relating to the frequency domain works better than that relating to the time domain with the neural network, because it is less sensitive to the shift in the signal and possibly relative shift of the defect component in the signal caused by surface roughness (i.e., movement of front wall echo, defect echo and back wall echo signals) with respect to time.
- The application of PCA as a pre-processing tool in this research did not improve the classification percentage of the ultrasonic signals obtained from both smooth and rough surface castings due to loss of useful signal information.

8.6 LIMITATIONS

According to Krautkrämer and Krautkrämer [5], the major limitations in the application of ultrasonic NDT to castings are associated with their material properties, surface roughness and shape. This problem can be reduced with the selection of appropriate ultrasonic inspection parameters and the application of appropriate signal processing techniques, as presented in Chapters 5, 6 and 7. However, there is no common system that is able to accommodate and solve all the problems related to ultrasonic inspection of castings.

In this thesis, a neural network classifier used the waveform of the signal for classification purpose. However, other prominent features (Table 2.2), as mentioned by Thavasimuthu *et al.* [80] could not be applied in this research problem due to high ultrasonic signal scattering from the front rough surface of castings. The surface roughness could not be reduced through machining because even light machining

cuts would penetrate the relatively sound surface, exposing the unsatisfactory structure with defects. Furthermore, this research focused on castings in the as-cast state. Application of the features used by Thavasimuthu *et al.* [80] in this research could have contributed to the achievement of a higher classification percentage. However, the application of signal pre-processing techniques in combination with neural networks assisted in improving the accuracy of detecting gas porosity defects. This is in comparison with a scenario where signal pre-processing was not carried out on the ultrasonic signals prior to submitting them to a neural network for classification. Nevertheless, 100% classification was not achieved with the signals from rough surface sections of castings. Until a satisfied level of classification is achieved, the ultrasonic inspection methodology investigated in this research cannot be successfully implemented in industrial environments to detect defects in aluminium die castings. What is termed a satisfactory level of classification can vary from industry to industry as presented earlier in the thesis (Section 1.2).

Another limitation to the methodology presented here is associated with the signal processing speed of the MATLAB toolbox. Further improvements in processing speed may be made through the compilation of MATLAB code into a stand-alone application such as MATLAB complier. However, the application of MATLAB for signal processing can affect the classification time and it might not be a long term solution for an on-line inspection system. Hence, there is a need to develop dedicated software for this specific application to achieve high speed classification.

8.7 SUMMARY

This research program was based on the use of rough surface castings containing a mix of actual and simulated defects. The effect of material properties of the casting on ultrasonic inspection was investigated. It aided in the selection of a suitable frequency range to detect gas porosity defects in the rough surface sections

of the castings. Even though calibration assisted in developing a suitable experimental methodology, the near surface defect detection was still difficult due to the clustered front wall echo obtained from the rough surface castings. The scattering from the rough surface of the castings masked the defect signal when the defect was close to the front surface.

In contrast to the work of other researchers, this research attempted to classify defect signals from aluminium castings with surface roughness over 50 μm. The research led to the successful neural network classification of defects from surfaces with roughness values up to 100 μm. A success rate of 84% was achieved with pre-processing of ultrasonic signals using combinations of (a) Fast Fourier Transform (FFT) and Wavelet Transform (WT) type and (b) FFT, WT and principal component analysis. FFT/WT was selected as the most suitable pre-processing method for this research problem due to its low variation in classification performance. The inclusion of PCA as a pre-processing tool in the FFT/WT pre-processing combinational approach did not improve the classification percentage of the ultrasonic signals obtained from both smooth and rough surface castings.

The analysis of the performance of the different signal pre-processing methods when used on their own emphasised the need for a hybrid type pre-processing approach. However, it is evident from previous research that what is termed the most suitable pre-processing approach varies with the characteristics of the signal received from the sensing system used.

The methodology described in this thesis has application in the development of ultrasonic inspection techniques for as-cast products. However, the limitation of the research outcomes is that the current research was only undertaken in a narrow domain namely, detecting defects of size 0.5 mm or higher in aluminium casting with surface roughness up to 100 μm and small grain size.

CHAPTER 9.
CONCLUSIONS AND FUTURE WORK

9.1 OVERVIEW

Limits of defect detectability are of serious concern to both manufacturers and users of castings. Due to the complex nature of castings and the casting process, it is difficult to set definite rules for inspection systems to detect sub-surface defects. Hence, the thrust of this research was to investigate, within the specified domain, the possibility of detecting sub-surface gas porosity defects in aluminium die castings with rough surfaces. This final chapter of the thesis outlines the specific contributions of this research work and future directions arising from the research findings.

9.2 CONTRIBUTIONS OF THE RESEARCH

Because of the scope of the industry and the widespread use of castings, engineers often find themselves in a position where knowledge of the casting process and its problems becomes a vital part of their work. Specifically the quality of the casting process is the important concern of engineers in this field, and quality control is dependent on Non Destructive Testing & Evaluation (NDT&E). Ultrasonic NDT

inspection techniques are at times used to inspect castings, however, their use is restricted by the metallurgical and physical characteristics of the castings. Hence, this research program was undertaken in accordance with the following problem statement:

To investigate the possibility of using an ultrasonic inspection technique to detect small sub-surface defects (gas porosity) near the front rough surface of castings with varying grain size by classifying weak and noisy ultrasonic signals using suitable signal processing techniques.

The following were the major outcomes from each chapter presented in this thesis:

1. The literature search (Chapter 2) focused on obtaining information on ultrasonic inspection of castings with complex shape, varying grain structures and surface roughness and containing irregular porosities. The literature review revealed that there has been a great deal of research work relating to the above factors, which have been separately examined in the context of ultrasonic inspection of castings. The literature identified a need to determine the limitations of NDT in the inspection of aluminium die castings. Additionally, the literature indicated that the application of an artificial intelligence approach had not been explored to its full potential for classification of weak ultrasonic signals obtained from rough surface aluminium die castings.
2. The background information on ultrasonic inspection and neural networks (Chapter 3) aided in the development of a suitable procedure for the inspection of aluminium die castings with rough surfaces.
3. The development of a reliable calibration methodology (Chapter 4) greatly reduced the uncertainty and significantly increased the accuracy and reliability of the experimental results. It also provided a foundation for developing a generalised procedure to ensure the reliability of results of any set of experiments involving ultrasonic immersion testing.

4. Research as described in this thesis demonstrated that the loss of the ultrasonic signal echo due to grain size variation was comparatively small when compared with the variation caused by changes in the surface roughness of the casting. Subsequently, a methodology (Chapter 5) was developed to identify a suitable frequency for inspecting aluminium die castings with appreciable surface roughness and small to medium grain structure. The results provided guidelines for the selection of a suitable ultrasonic transducer frequency range (5 to 10 MHz) that accommodates variations in material properties as well as the critical defect size to be detected.
5. Use of a neural network approach to defect identification in combination with suitable signal pre-processing techniques successfully eliminated the effect of noise in ultrasonic signals from castings with surface roughness ranging from 50 μm to 100 μm. The raw signals were difficult to classify using only the neural network approach. Hence, the use of Fast Fourier transform (FFT), Principal Component Analysis (PCA) and Wavelet Transform (WT) in pre-processing of signals prior to input to the neural network for signal classification was investigated (Chapter 6).
6. The results presented in Chapter 7 were obtained from ultrasonic immersion testing of castings with varying surface roughness. The results showed that with the selected frequency range it was difficult to detect sub-surface defects close to the front rough surface of the castings by analysing only the raw ultrasonic signal (Section 7.2). However, there was a possibility of applying signal processing techniques to achieve the defect identification for castings with surface roughness up to 100 μm. Hence, a combination of signal pre-processing techniques was applied on the raw ultrasonic signal. The results showed similar poor classification was achieved with the combination of FFT/PCA, WT/FFT and WT/PCA type signal pre-processing techniques. The classification of the signals pre-processed with the combination of FFT/WT and FFT/WT/PCA classifiers provided much better classification of more than 95% and 84% for signals from castings with smooth and rough surfaces respectively. The overall best signal pre-processing technique was FFT/WT combination type. X-ray and visual inspections were carried out on the

castings inspected with ultrasound and successfully classified with an appropriate signal pre-processing technique to independently confirm the results (Section 7.8). It was found that defects as small 0.5 mm could be detected with the ultrasonic technique for castings with surface roughness up to 50 μm. Further, when the surface roughness was in the range of 50 to 100 μm, it was not possible to detect defects of a size less than 0.7 mm in diameter. As expected it was found that there was a lower classification percentage for the castings with rough surface (Ra0) compared to smooth surface (Ra2) as presented in Figure 7.14. This was due to the fact that the defect amplitude was much lower than the amplitude of the noise caused by the surface roughness, as such it was not possible to distinguish the defect.

7. The discussion of the results (Chapter 8) compared the outcomes of this research work with the work of other researchers. The inspection technique developed in this research lead to identification of the both real and simulated defects from ultrasonic signals obtained from the casting sections with surface roughness over 50 μm, which has not been achieved previously. In this research the investigation of different signal pre-processing methods has been carried out. This work has also demonstrated the advantages of using a hybrid signal pre-processing approach to address a classical signal processing problem.

There were a number of important contributions made throughout the research program in relation to the ultrasonic inspection of gas porosity defects in aluminium die castings. These contributions relate to the literature survey, ultrasonic inspection of castings, ultrasonic data processing, and use of artificial intelligence in ultrasonic inspection applications. Finally, significant contributions of this research can be summarised as follows:

- Real sample castings were used in this research. This is important as in the past there has been poor correlation between tests conducted in the research laboratory and in practice on the shopfloor.
- An investigation was carried out to select an appropriate inspection technique for aluminium die castings. Ultrasonic immersion testing experiments were carried out on castings with real and simulated defects.

- An ultrasonic inspection methodology was developed for detecting gas porosity type defects in aluminium die castings with varying surface roughness from 50 μm to 100 μm.
- The effectiveness of classification of ultrasonic signals using neural networks was demonstrated and it was shown that it was possible to detect porosity type defects as small as 0.5 mm in castings with surface roughness up to 50 μm. Defects with 0.7 mm diameter can be detected in the castings with surface roughness up to 100 μm with the signal pre-processing combination of WT/FFT, FFT/WT and FFT/WT/PCA techniques. The best classification performance was achieved with FFT/WT type signal pre-processing technique.

9.3 PROPOSED FUTURE WORK

The influence of surface roughness on the ultrasonic inspection of castings was investigated in this research. Furthermore, the experimental approach developed in this research can be extended for investigation of the ultrasonic wave propagation in castings with surface roughness levels above 150 μm. This will be of immense assistance in carrying out research on casting with rough surfaces such as sand castings and gravity die castings in the future.

The algorithms developed in this research program were executed on a computer system on which the signal processing tests were undertaken. Given the continuous increase in computation speed, the algorithms could be executed in under a few minutes compared to hours of processing time in the work to date. It is anticipated that this execution time would decline as computing technology improves. Another factor, with respect to the current system, is the application of MATLAB for signal processing. This is not the preferred solution in an industrial inspection system. There is a need for incorporating the signal processing unit within

the ultrasonic inspection system to provide solutions for both on-line and off-line inspection. This is worthy of investigation.

A future investigation with regard to signal processing could incorporate signal pre-processing and artificial neural network software codes in a single toolbox (similar to toolboxes available in MATLAB). This toolbox could also incorporate expert systems and data interpretation techniques with the ability to accommodate different materials, defects and component shapes for ultrasonic inspection of castings. Such a toolbox could be effectively integrated into the casting production system.

A recommendation from this research is to develop a mother wavelet with a shape similar to that of the ultrasonic signal section relating to a defect instead of selecting a pre-defined mother wavelet type such as Daubechies and Haar wavelets which were investigated in this research. If a new mother wavelet can be developed to match the defect signal, the ANN will more easily identify sharp flaw echoes during defect classification. Similarly, further research work has to be carried out on hybrid signal pre-processing methods, which have been explored in this research. Even though the highest signal classification has been achieved with the FFT/WT type of pre-processing in this research, in-depth theoretical and mathematical analysis is required to determine more detailed reasons for the effectiveness of this approach. The combination of FFT, WT and PCA in combination with other signal pre-processing methods should be investigated in order to achieve improved defect classification from weak and noisy ultrasonic signals.

The sizing of defects has not been investigated in this research work. Hence, the follow up of this research could involve the application of fuzzy neural networks in determining the type of defects such as cracks, gas porosity, inclusions shrinkage porosity and their size, location and orientation.

9.4 FINAL SUMMARY

The main thrust of this research on ultrasonic inspection of aluminium die castings was to detect gas porosity defects in rough surface castings. A methodology was developed to address the project objective. The in-gate section of the structural oil sump pan was the critical part of the casting in relation to the ultrasonic inspection task addressed in this research. The developed experimental procedure provided guidelines for selecting suitable transducer frequencies that accommodate variations in material properties while taking into account the critical defect size to be detected. Then, the final parameters of the feed-forward back propagation neural network were selected for processing the ultrasonic signals. The results showed that the classification of the signals pre-processed with the combination of WT/FFT, FFT/WT and FFT/WT/PCA classifiers provided improved classification compared to other combinational and single technique approaches investigated in this research. Not withstanding the fact that 100% classification has not been achieved for the signals obtained from rough surface castings with this technique, it can be stated that a significant step has been taken in developing an approach to classify gas porosity defects. The analysis of the performance of the different signal pre-processing methods emphasised the requirement for a hybrid type pre-processing approach.

The research documented in this thesis provides an insight into the operation and performance of the ultrasonic NDT method in detecting gas porosity defects in aluminium die castings. The work has led to a number of contributions to the field as mentioned previously, and demonstrated the effectiveness of the hybrid signal pre-processing approach in classifying weak and noisy ultrasonic signals using artificial neural networks.

REFERENCES

[1] RICHARD, W. H., Carl, R. L. Jr., and Philip, C. R. *Principles of Metal Casting*, New York: McGraw-Hill, 1967.

[2] DUCKETT, G. Quality-whose definition? *Foundry Trade Journal*, vol.163, 1988 pp. 660-661.

[3] RICKARDS, P. J. and Wickens, M. Testing of iron castings, *Foundry International*, vol. 17, no. 4, 1994 pp. 162-166.

[4] LONG, J. Nondestructive testing: 5 ways to ensure defect-free deliveries, *Modern Casting*, vol. 88, no. 4, 1998 pp. 49-52.

[5] KRAUTKRÄMER, J. and Krautkrämer, H. *Ultrasonic testing of materials*, ed. 4 New York: Springer-Verlag, 1990.

[6] TAYLOR, H. F., Wulff, J., and Flemings, M. C. *Foundry engineering*, New York: John Wiley, 1959.

[7] MIKELONIS, P. L. Foundry technology. In: *Quality Management Handbook*, eds. Walsh, L., Wurster, R., and Kimber, R. J. Marcel Dekker. New York, 1986 pp. 753-790.

[8] ANON. *Aluminium technology book 6: Casting aluminium*, Canberra: Aluminium Development Council of Australia Ltd, 1978.

[9] DAHLE, A. K. and StJohn, D. H. Processing via liquid state. In: *Encyclopaedia of Life Support Systems (EOLSS)*, Eolss Publishers. Oxford, 2002

[10] BARRESI, J., Chen, Z., Davidson, C., Murray, M., Nguyen, T., StJohn, D., and Thorpe, W. Casting of aluminium alloy components, *Materials Forum*, vol. 20, 1996 pp. 53-70.

[11] BEVER, M. B. *Encyclopaedia of materials science and engineering*, Oxford Oxfordshire, Cambridge: Pergamon. MIT Press, 1986.

[12] CHEN, Z. W. and Jahedi, M. Z. Metallurgy of soldering in high pressure die

casting of Al-Si-Cu alloy. In: *Materials '98 Proceedings of the Biennial Materials Conference of The Institute of Materials Engineering*, ed. Ferry, M. Institute of Materials Engineering. Sydney, vol. 1, 1998 pp. 101-106.

[13] CAMPBELL, J. *Castings*, Oxford: Butterworth-Heinemann, 2000.

[14] SINHA, V. K. Manufacturing defects and their effects on type of failure in castings and forgings - some case studies. In: *Proceedings of 14th World Conference on Non Destructive Testing*, New Delhi, vol. 2, 1996 pp. 993-996.

[15] DAVIES, G. J. *Solidification and Casting*, London: Applied Science, 1973.

[16] BEELEY, P. *Foundry Technology*, Oxford: Butterworth Heinemann, 2001.

[17] ROWLEY, M. T. *International atlas of casting defects*, Des Plaines, IL: American Foundrymen's Society, 1974.

[18] DOEHLER, H. H. *Die casting*, New York: McGraw-Hill, 1951.

[19] ANON. *The OEM design sourcebook- Product design for die casting in recyclable Aluminium, Magnesium, Zinc and ZA alloys*, LaGrange, IL, USA: Diecasting Development Council, 1996.

[20] SENIW, M. E., Fine, M. E., Chen, E. Y., Meshii, M., and Gray, J. Relation of defect size and location to fatigue failure in Al alloy A356 cast specimens. In: *Proceedings of the TMS Fall Meeting*, Minerals, Metals & Materials Soc (TMS). Warrendale, PA, USA, 1997 pp. 371-379.

[21] GUPTA, A. K., Sena, B. K., Tiwari, S. N., and Malhotra, S. L. Pore formation in cast metals and alloys, *Journal of Materials Science*, vol. 27, 1992 pp. 853-862.

[22] BLITZ, J. and Simpson, G. *Ultrasonic methods of non-destructive testing*, London: Chapman & Hall, 1996.

[23] RAJ, B. NDT for realising better quality of life in emerging economies like India. In: *Proceedings of 15th World Conference on NDT, Roma, Italy*, NDT.net. http://www.ndt.net/article/wcndt00/papers/idn905/idn905.htm 2000 viewed 20-01-2001.

[24] SATTLER, F. J. Improving Quality Through Nondestructive Testing, *Chemical Engineering*, vol. 96, no. 4, 1989 pp. 116-119.

[25] HELLIER, C. J. *Handbook of Nondestructive Evaluation*, New York: McGraw-Hill, 2001.

[26] ANON. Testing/Inspection/Measurement, *Foundry Management and Technology*, vol. 121, no. 1, 1993 pp. H2-H7.

[27] BAILEY, W. H. Magnetic particle inspection evaluations. In: *Through the Eyes of an Eagle: 11th World Conference on Nondestructive Testing*, International Committee on Nondestructive Testing. Columbus, OH, USA, 1985 pp. 348-351.

[28] GLATZ, J. Krypton gas penetrant imaging, *Advanced Materials & Processes*, vol. 152, no. 5, 1997 pp. 21-23.

[29] THOMPSON, R. B. Ultrasonic measurement of mechanical properties *IEEE Ultrasonic Symposium*, vol. 1, 1996 pp. 735-744.

[30] CHEN, J., Shi, Y., and Xia, Z. Focal Line Calculation in a Cylinder Interrogated by a Line Focused Transducer in Ultrasonic Immersion Testing, *Materials Evaluation*, vol. 57, no. 1, 1999 pp. 61-64.

[31] ENSMINGER, D. *Ultrasonics the low and high-intensity applications*, New York: Marcel Dekker, Inc., 1973.

[32] ANON. Radiography update, *Foundry Management and Technology*, vol. 125, no. 3, 1997 pp. 42-45.

[33] BARBERIS, N. Non-destructive testing in foundries, *Fonderia*, vol. 44, no. 3, 1995 pp. 64-66.

[34] BOWLAND, G. Inspection of castings. In: *Proceedings of Non-destructive Testing Conference*, ed. Steel Castings Research and Trade Association. The Institute of Metals. London, 1989 pp. 112-153.

[35] UCHIDA, K. Development of ultrasonic data recording system for three dimensionally curved components. In: *Proceedings of the 13th International Conference on NDE in the Nuclear and Pressure Vessel Industries*, Japan. Kyoto, 1995 pp. 231-236.

[36] HOFFMANN, J. Leak detectors provide data for better quality control, *Die Casting Engineer*, vol. 41, no. 5, 1999 pp. 94-97.

[37] HEINE, H. J. Leak testing reliably, *Foundry Management and Technology*, vol. 126, no. 6, 1998 pp. 32, 34-37.

[38] HANKE, R. Radioscopic system for post cast perfection, *Foundry Trade Journal*, vol. 176, no. 3594, 2002 pp. 6-9.

[39] LAVENDER, J. D. How clean is clean? The implication of NDT methods, *Foundry Trade Journal*, vol. 165, no. 3438, 1991 pp. 593-596.

[40] LAVENDER, J. D. and Wright, J. C. A new philosophy in the application of ultrasonic techniques in the foundry industry, *Proceedings of the Annual Meeting,*

80th, vol. 84, 1977 pp. 155-168.

[41] KLEVEN, S. and Blair, M. Limitations on the Detection of Casting Discontinuities Using Ultrasonic and Radiography, *Materials Evaluation*, vol. 61, no. 4, 2003 pp. 478-485.

[42] LAVENDER, J. D. Historical Note on Ultrasonic Examination of Steel Castings, *Insight*, vol. 38, no. 8, 1996 pp. 589-593.

[43] BOSTROM, A. Theoretical modelling of ultrasonic non-destructive testing, *Materials & Design*, vol. 15, 1994 pp. 164-168.

[44] KUPPERMAN, D. S., Reimann, K. J., and Abrego-Lopez, J. Application of ultrasonic waves to assess grain structure in cast stainless steel. In: *Through the Eyes of an Eagle: 11thWorld Conference on Nondestructive Testing*, International Committee on Nondestructive Testing. Columbus, OH, USA, 1985 pp. 1685-1691.

[45] KUPPERMAN, D. S., Reimann, K. J., and Abrego-Lopez, J. Ultrasonic NDE of Cast Stainless Steel *NDT International*, vol. 20, 1987 pp. 145-152.

[46] BOVEYRON, C., Villard, D., and Boudot, R. Ultrasonic testing of Cast Stainless Steel Components. In: *Proceedings of 11th International Conference on NDE in the Nuclear and Pressure Vessel Industries*, New Mexico, USA, 1992 pp. 403-408.

[47] KAPRANOS, P. and Rheinlander, J. Quantitative NDE by X-ray radiography for optimization of the thixocasting process, *Insight: Non-Destructive Testing and Condition Monitoring*, vol. 41, no. 1, 1999 pp. 25-30.

[48] YAO, X. and Liu, Y. A new evolutionary system for evolving artificial neural network, *IEEE transactions Neural Networks*, vol. 8, no. 3, 1997 pp. 694-713.

[49] NELLIGAN, T. Ultrasonic testing of nonferrous castings, *Die Casting Engineer*, vol. 36, no. 2, 1992 pp. 14-16.

[50] McINTIRE, P. *Nondestructive testing handbook*, Columbus: American Society for Nondestructive Testing, 1991.

[51] HALMSHAW, R. *Introduction to the Non-Destructive Testing of welding joints*, Cambridge: EdiAbington, 1988.

[52] GINZEL, E. Ultrasonic inspection 2: training for nondestructive testing-variables affecting test results. In: *NDT.net*, ed. Diederichs, R. http://www.ndt.net/article/v04n06/gin_ut2/gin_ut2.htm#top vol. 4, no. 6, 1999 viewed 14-05-2001.

[53] PAPADAKIS, E. P. Ultrasonic attenuation and velocity in three transformation products of steel, *Journal of Applied Physics* , vol. 35, no. 5, 1964 pp. 1474-1482.

[54] BLESSING, G. V., Bagley, P. P., and James, J. E. The effect of surface roughness on ultrasonic echo amplitude in steel, *Materials Evaluation*, vol. 42, no. 11, 1984 pp. 1389-1392.

[55] NAGY, P. B. and Adler, L. Surface Roughness induced attenuation of reflected and transmitted ultrasonic waves, *Journal of Acoustical Society of America*, vol. 82, no. 2, 1987 pp. 193-197.

[56] ERMOLOV, I. N. Optimization of the conditions of inspection by the ultrasound echo method III. Main service characteristics of the echo method and optimization of these characteristics, *Russian Journal of Nondestructive Testing*, vol. 32, no. 3, 1996 pp. 247-260.

[57] BRUNK, J. A. Influence of ambient temperature changes on angle-beam ultrasonic testing of steel, *Materials Evaluation*, vol. 46, no. 9, 1988 pp. 1148-1152.

[58] AMBARDAR, R., Jayakumar, T., Pathak, S. D., and Prabhakar, O. Ultrasonic velocity measurement to access casting quality, *Insight*, vol. 38, no. 7, 1996 pp. 502-508.

[59] ROSE, J. H., Bilgen, M., Nagy, P. B., and Adler, L. Effect of surface roughness on ultrasonic backscatter. In: *Review of Progress in Quantitative Nondestructive Evaluation*, eds. Thompson, D. O. and Chimenti, D. E. Plenum Press. New York, NY, USA, vol. 12B, 1992 pp. 1693-1700.

[60] THAVASIMUTHU, M., Rajagopalan, C., Jayakumar, T., and Raj, B. Effect of front surface roughness on ultrasonic contact testing: A few practical observations, *Materials Evaluation*, vol. 56, no. 11, 1998 pp. 1302-1308 .

[61] BRIDGE, B. and Tahir, Z. Study of omnidirectional scattering of 4-30 MHz ultrasound from periodically rough machined surfaces. Part 2, *British Journal of Non-Destructive Testing*, vol. 31, no. 4, 1989 pp. 189-195.

[62] BRIDGE, B. and Tahir, Z. Omnidirectional scattering of 4-20 MHz ultrasound from randomly rough-machined aluminium surfaces, *British Journal of Non-Destructive Testing*, vol. 31, no. 6, 1989 pp. 322-326.

[63] ROSE, J. H., Adler, L., and Mobley, C. Ultrasonic method to determine gas porosity in aluminium alloy casting theory and experimentation, *Journal of Applied Physics*, vol. 59, no. 2, 1986 pp. 336-347.

[64] ADLER, L., Nagy, P. B., Rypien, D. V., and Rose, J. H. "Ultrasonic Evaluation of Porosity in Aluminium Cast Materials," Ohio State University, Columbus, OHIO, USA, May 1989.

[65] AMBARDAR, R., Jayakumar, T., Pathak, S. D., and Prabhakar, O. Effect of surface roughness on ultrasonic echo amplitude in aluminium-coper alloy castings. In: *14th World Conference on Non Destructive Testing, New Delhi, India*, vol. 2, 1996 pp. 981-984.

[66] ONOZAWA, M., Katemine, A., Ishii, Y., and Ohira, G. Ultrasonic testing for near surface flaws in castings, *British Journal of Non-Destructive Testing*, vol. 31, no. 11, 1989 pp. 611-616.

[67] BILGEN, M. Effects of randomly rough surfaces on ultrasonic inspection, Iowa State University, IOWA, USA, 1993.

[68] TSAI, D. M. and Tseng, C. F. Surface Roughness classification for castings, *The Journal of Pattern Recognition*, vol. 32, 1999 pp. 389-405.

[69] KLINMAN, R., Webster, G. R., Marsh, F. J., and Stephenson, E. T. Ultrasonic prediction of grain size, strength and toughness in plain carbon steel, *Materials Evaluation*, vol. 38, no. 10, 1980 pp. 26-32.

[70] BILGEN, M. and Rose, J. H. Focused ultrasonic probes and the effects of surface roughness on material noise. In: *Review of Progress in QNDE*, eds. Thompson, D. O. and Chimenti, D. E. Plenum Press. New York, vol. 13B, 1996 pp. 1769-1776.

[71] AMBARDAR, R., Jayakumar, T., Muthu, M. T., and Prabhakar, O. Effect of porosity, pore diameter and grain size on ultrasonic attenuation in aluminium alloy castings, *Insight*, vol. 37, no. 7, 1995 pp. 536-542.

[72] HOWARD, Q. and Enzukewich, S. The effects of microstructure on the ultrasonic testing of alloy steels, *Materials Evaluation*, vol. 55, no. 12, 1997 pp. 1323-1327.

[73] OGILVY, J. A. Use of focused beams in austenitic welds, *British Journal of Non-Destructive Testing*, vol. 29, no. 4, 1987 pp. 238-246.

[74] STEPINSKI, T. and Wu, T. Evaluation of ultrasonic attenuation and estimation of ultrasonic grain noise in copper. In: *Nondestructive Characterization of Materials IX*, ed. Green, Jr. R. E. American Institute of Physics. New York, 1999.

[75] THAVASIMUTHU, M., Hemamalini, R., Subramanian, C. V., Jayakumar, T.,

Kalyanasundaram, P., and Raj, B. Detectability of mis-oriented defects by ultrasonic examinations - a few observations, *Insight: Non-Destructive Testing and Condition Monitoring*, vol. 40, no. 11, 1998 pp. 766-768.

[76] ENGL, G., Schmitz, V., and Barbian, O. A. Requirements for the data acquisition during ultrasonic testing search techniques and defect analysis. In: *New Procedures in Nondestructive Testing (Proceedings)*, ed. Holler, P. Springer-Verlag. Berlin, 1983 pp. 3-12.

[77] MARGRAVE, F. W., Rigas, K., Bradley, D. A., and Barrowcliffe, P. Use of neural networks in ultrasonic flaw detection, *Measurement: Journal of the International Measurement Confederation*, vol. 25, no. 2, Mar, 1999 pp. 143-154.

[78] ROSE, J. L., Ganglbauer, O., Ausserwoger, J., Wallner, F., Niklas, L., Frielinghaus, R., and Nestleroth, J. B. Computer Aided Ultrasonic Flaw Characterization system for welds. In: *Through the Eyes of an Eagle: 11th World Conference on Nondestructive Testing*, International Committee on Nondestructive Testing. Columbus, OH, USA, 1985 pp. 1260-1267.

[79] RAJAGOPALAN, C., Raj, B., and Kalyanasundaram, P. Role of artificial intelligence in non-destructive testing and evaluation, *Insight: Non-Destructive Testing and Condition Monitoring*, vol. 38, 1996 pp. 118-123.

[80] THAVASIMUTHU, M., Rajagopalan, C., Kalyanasundaram, P., and Raj, B. Improving the evaluation sensitivity of an ultrasonic pulse echo technique using a neural network classifier, *NDT & E International*, vol. 29, no. 3, 1996 pp. 175-179.

[81] EMERSON, P. J. Advantages in automating ultrasonic testing of iron castings in the foundry, *Foundry Trade Journal*, vol. 158, no. 3305, 1985 pp. 357-360, 363-364, 383.

[82] GAYER, A., Saya, A. and Shiloh, A. Automatic recognition of welding defects in real-time radiography, *NDT International*, vol. 23, no. 3, 1990 pp. 131-136.

[83] CARTER, P. Future computer aids for manual ultrasonic operators, *NDT International*, vol. 33, no. 8, 1991 pp. 389-394.

[84] SYKES, M. Automated Inspection in Modern Manufacturing, *Aircraft Engineering*, vol. 62, no. 7, 1990 pp. 11-13 .

[85] ATKINSON, I., Charlesworth, J. P., Hawker, B. M., and Rogerson, A. Automated ultrasonic inspection of austenitic castings and welds. In: *Proceedings of 12th world conference on Non-Destructive Testing*, eds. Boogaard, J. and van Dijk,

G. M. Elsevier Sciences. Amsterdam, 1989 pp. 1019-1024.

[86] MCNAB, A. and Dunlop, I. A review of Artificial Intelligence applied to ultrasonic defect evaluation, *Insight*, vol. 37, no. 1, 1991 pp. 11-16.

[87] LINGVALL, F. and Stepinski, T. Automatic detecting and classifying defects during eddy current inspection of riveted lap-joints, *NDT & E International*, vol. 33, no. 1, 2000 pp. 47-55.

[88] LEBOWITZ, C., Spencer, R., Brown, L., Kok, R., and Udpa, L. Overview of the Knowledge Based Inspection System, *Proceedings of SPIE - The International Society for Optical Engineering*, vol. 3585, Mar 3, 1999-Mar 5, 1999 pp. 154-162.

[89] RAJ, B. and Rajagopalan, C. Artificial intelligence to maximise contributions of nondestructive evaluation to materials science and technology. In: *Trends in NDE Science & Technology: 14th World Conference on Non Destructive Testing*, Ashgate Publishing Company. New Delhi, vol. 1, 1996 pp. 47-56.

[90] BRIGHAM, O. E. *The Fast Fourier Transform*, New Jersey: Prentice-Hall, 1979.

[91] DEMUTH, H. and Beale, M. *Neural Network Toolbox for use with MATLAB*, Natick: The Math Works, Inc., 1998.

[92] BAE, S., Udpa, L., Udpa, S. S., and Taylor, T. Classification of ultrasonic weld inspection data using principal component analysis. In: *Review of Progress in Quantitative Nondestructive Evaluation*, eds. Thompson, D. O. and Chimenti, D. E. Plenum Press. New York, NY, vol. 16, 1997 pp. 741-748.

[93] MALLAT, S. G. *A wavelet tour of signal processing*, New York: Academic Press, 1998.

[94] STRANG, G. and Nguyen, T., Wavelets and Filter Banks, Wellesley-Cambridge Press, Wellesley, USA, 1997.

[95] BURRUS, C.S., Gopinath, R.A. and Guo, H. *Introduction to wavelets and wavelet transforms A Primer*, New Jersey, Prentice-Hall, 1998.

[96] MICHEL, M., Georges, O., and Jean-Micheal, P. *Wavelet Toolbox for use with Matlab, Version 1*, USA: The Mathworks, Inc., 1997.

[97] SERRANO, I., Lazaro, A., and Oria, J. P. Ultrasonic inspection of foundry pieces applying wavelet transform analysis, *IEEE International Symposium on Intelligent Control - Proceedings*, 1999 pp. 375-380.

[98] LÁZARO, J. C., Emeterio, J. L. S., Ramos, A., and Fernandez-Marron, J. L.

Influence of thresholding procedure in ultrasonic grain noise reduction using wavelets, *Ultrasonics*, vol. 40, 2002 pp. 263-267.

[99] POLIKAR, R., Udpa, L., Udpa, S. S., and Taylor, T. Frequency invariant classification of ultrasonic weld inspection signals, *IEEE Transactions on Ultrasonics, Ferroelectrics, and Frequency Control*, vol. 45, no. 3, May, 1998 pp. 614-624.

[100] POLIKAR, R., Udpa, L., Udpa, S. S., and Spanner, J. Time scaling and frequency invariant multiresolution analysis of ultrasonic NDE Signals. In: *Review of Progress in Quantitative Nondestructive Evaluation*, eds. Thompson, D. O. and Chimenti, D. E. Plenum Press. New York, NY, vol. 17, 1998 pp. 743-749.

[101] VAPNIK, V. N. Principles of risk minimization for learning theory. In: *Advances in Neural Information Processing Systems*, eds. Moody, J. E. , Hanson, S. J., and Lippmann, R. P. Morgan Kaufmann. San Mateo, CA, vol. 4, 1992 pp. 831-838.

[102] ABBATE, A., Koay, J., Frankel, J., Schroeder, S. C., and Das, P. Signal detection and noise suppression using a wavelet transform signal processor: application to ultrasonic flaw detection, *Transactions on Ultrasonics, Ferroelectronics and Frequency Control*, vol. 44, no. 1, 1997 pp. 14-26.

[103] CHEN, C. F., Teng, Y. S., and Chen, C. Y. Combination of PCA and wavelet transforms for face recognition on 2.5D images. In: *Proceedings of Image & Vision Computing*, Palmerston North, New Zealand, 2003 pp. 343-347.

[104] MATALGAH, M., and Knopp, J. Time-varying spectral analysis of non-stationary signals based on wavelet and Fourier transforms, *Electronics*, vol. 78, no. 3, 1995, pp.463-476.

[105] WANG, R.L., Hua, T.J., Wang, J. and Fan, Y.J. Combination of FT and WT for fingerprint recognition, *SPIE – Wavelet Applications*, vol. 2242, 1994, pp 260-270.

[106] BILGUTAY, N. M., Newhouse, V. L., and Amir, I. Theoretical analysis and performance of the minimisation algorithm in NDT applications. In: *Through the Eyes of an Eagle: 11th World Conference on Nondestructive Testing*, International Committee on Nondestructive Testing. Columbus, OH, USA, vol. 3, 1985 pp. 1048-1055.

[107] ROSE, J. L. Neural nets for flaw classification potential with guided waves. In:

Proceedings of 14th World Conference on Non Destructive Testing, New Delhi, vol. 1, 1996 pp. 41-46.

[108] MUCCIARDI, A. N. and Dau, G. J. Role of signal processing in NDE. In: *Vortraege - 4th Internationale Konferenz ueber Zerstoerungsfreie Pruefung in der Kerntechnik.*, Dtsch Ges fuer Zerstoerungsfreie Pruef (Berichtsband 8). Berlin, Germany, 1981 pp. 63-78.

[109] CHIOU, C. P. and Schmerr, L. W. J., Neural network model for ultrasonic flaw sizing, *Non-destructive Testing and Evaluation*, vol. 10, no. 3, 1993 pp. 167-182.

[110] ANGELI, M., Burrascano, P., Cardelli, E., Fiori, S., and Resteghini, S. Classification of eddy current NDT data by Probabilistic Neural Networks, In: *Proceedings of the International Joint Conference on Neural Networks*, IEEE. USA, vol. 6, 1999 pp. 4012-4014.

[111] RAO, B. P. C., Raj, B., Jayakumar, T., and Kalyanasundaram, P., An artificial neural network for eddy current testing of austenitic stainless steel welds, *NDT&E International*, vol. 35, 2002 pp. 393-398.

[112] SETHI, I. K., Neural implementation of tree classifiers, *IEEE Transactions on Systems, Man and Cybernetics*, vol. 25, 1995 pp. 1243-1249.

[113] CAVACCINI, G., Agresti, M., Borzacchiello, G., Bozzi, E., Chimenti, M., and Salvetti, O. An evaluation approach to NDT ultrasound processes by wavelet transform. In: *15th World Conference on NDT*, NDT.net. http://www.ndt.net/article/wcndt00/papers/idn775/idn775.htm 2000 viewed 20-01-2001.

[114] COTTERILL, G. and Perceval, J. A new approach to ultrasonic inspection of shafts. In: *10th Asia Pacific Conference on Non Destructive Testing,* NDT.net. http://www.ndt.net/article/apcndt01/papers/1213/1213.htm 2001 pp. viewed 10-04-2002.

[115] HUANG, J., Conley, J. G., and Callau, P. Alternative methods for porosity prediction in aluminum alloys. In: *SAE Special Publications*, SAE. Warrendale, PA, USA, vol. 1336, 1998 pp. 93-103.

[116] ANON, Ultrasonic transducers for non-destructive testing, Panametrics, Inc. Waltham, 1999.

[117] ROSE, J. L. *Ultrasonic waves in solid media*, Cambridge: Cambridge University Press, 1999.

[118] ARTURO, G., Andrea, O., and Marco, T. *Nondestructive testing NDT: Physics-Techniques-Applications*, Lecco, Italy: Tipolitografia A.C., 1981.

[119] AUSTRALIAN STANDARD 2083. *Calibration blocks and their methods of use in ultrasonic testing*, ed. 2, Sydney: The Standards Association of Australia, 1981.

[120] ANON. *Classroom training handbook Nondestructive Testing - Ultrasonic testing*, San Diego: General Dynamics Convair Division, 1967.

[121] SILK, M. G. *Ultrasonic transducers for Nondestructive testing*, Bristol: Adam Hilger, 1984.

[122] SERRE, M., Viard, A., de Mathan, N., and Villard, D. Ultrasonic NDE Techniques Enhancement for Cast Stainless Steel Components. In: *6th European Conference on NDT*, Nice, France, 1994 pp. 831-835.

[123] BOOLER, R. V., Pearce, J. E., and Lucas, M., An ultrasonic inspection procedure for the sizewell B CAST austenitic pump blows, *British Journal of Non-Destructive Testing*, vol. 32, no. 7, 1990 pp. 351-354.

[124] HULL, J. B. and John, V. B. *Non-destructive testing*, London: MacMillan Education, 1988.

[125] PRICE, D. C., Martin, B. J., and Scott, D. A., Ultrasonic guided waves for inspection of bonded panels, *Acoustics Australia*, vol. 27, no. 3, 1999 pp. 95-101.

[126] BURNINGHAM, J. S., Development of an automated ultrasonic inspection cell for detecting subsurface discontinuities in cast iron, University of Northern Iowa, IOWA, USA, 1992.

[127] HALMSHAW, R. *Nondestructive testing*, London: Edward Arnold, 1991.

[128] PRABHAKAR, O., Ambardar, R., and Wah, H. K., Percentage porosity measurement by a through-transmission ultrasonic technique, *Insight: Non-Destructive Testing and Condition Monitoring*, vol. 39, no. 2, 1997 pp. 100-103.

[129] FALLON, M. J., Practice and problems during ultrasonic examination for defects in iron castings, *Foundryman*, vol. 84, no. 4, 1991 pp. 140-144.

[130] BANKS, B., Oldfield, G. E., and Rawding, H. *Ultrasonic flaw detection in metals*, New Jersey: Prentice-Hall, 1962.

[131] HAYKIN, S. *Neural networks: a comprehensive foundation*, New York: Maxwell Macmillan International, 1994.

[132] TIMOTHY, M. *Signal and image processing with neural networks: a C++*

sourcebook, New York: John Wiley & Sons, Inc., 1994.

[133] LIPPMANN, R. P. An introduction to computing with neural nets, In: *Fuzzy Models for Pattern Recognition - method that search for structures in data*, eds. Bezdek, J. C. and Pal, S. K. The Institute of Electrical and Electronics Engineers Inc., New York, 1992 pp. 417-435.

[134] RAJAGOPALAN, C., Raj, B., and Kalyanasundaram, P. A soft-computing framework for fault diagnosis, *Information Sciences*, vol. 127, 2000 pp. 87-100.

[135] THOMAS, T. R. *Rough surfaces*, London: Imperial College Press, 1999.

[136] ANON, Surface texture measuring and recording instruments – Perthometer, Frinprugf GmbH. Gottingen, Germany, 1988.

[137] ABDELHAY, A. M. and Mubark, M. I. Ultrasonic evaluation of surface roughness using normal incidence pulse-echo technique, In: NDT.net. http://www.ndt.net/article/v09n04/abdelh1/abdelh1.htm vol. 9, no. 4, 2004 viewed 26-5-2004.

[138] GUO. Y, Margetan, F. J., and Thomson, R. B. Effect of periodic surface roughness on ultrasonic backscattered noise. In: *Review of Progress in Quantitative Nondestructive Evaluation*, eds. Thompson, D. O. and Chimenti, D. E. vol. 20, 2001 pp. 1306-1312.

[139] KAUFMAN, J. G. *Properties of aluminium alloys - tensile, creep and fatigue data at high and low temperatures*, Ohio, US: The Materials Information Society, The Aluminium Association, 1999.

[140] ANON. Standard guide for evaluating characteristics of ultrasonic search units - E1065-98. In: *Annual book of ASTM standards - Metals test methods and analytical procedures*, American Society for Testing and Materials. Philadelphia, vol. 03.03, 1999 pp. 455-473.

[141] GHAFFARI, B., Potter, T. J., and Mozurkewich, G. Ultrasonic maps of porosity in aluminium castings. In: *Review of Progress in Quantitative Nondestructive Evaluation*, eds. Thompson, D. O. and Chimenti, D. E. Plenum Press vol. 21, New York, 2002 pp. 1526-1534.

[142] ANON. *Metallography and microstructure - Metals Handbook*, Ohio, US: American Society for Metals, 1999.

[143] ROLLAND, T., Macrosegregation in squeeze cast light metal alloys, University of Trondheim, 1995.

[144] LÁZARO, A. and Serrano, I., Ultrasonic recognition technique for quality control in foundry pieces, *Measurement Science and Technology*, vol. 10, no. 9, 1999 pp. N113-N118.

[145] ROBERTS, S. J. and Penny, W., Neural networks: friends or foes? *Sensor Review*, vol. 17, no. 1, 1997 pp. 64-70.

[146] DAUBECHIES, I., The wavelet transform, time-frequency localization and signal analysis, *IEEE Transactions on Information Theory*, vol. 36, 1990 pp. 961-1005.

[147] SILK, M. G., Sizing crack like defects by ultrasonic means, *Research Techniques in Nondestructive Testing*, vol. 3, 1977 pp. 51-99.

APPENDIX A
LIST OF PUBLICATIONS & PRESENTATIONS

A.1 JOURNAL ARTICLE AND CONFERENCE PROCEEDING

1. Palanisamy, S., Nagarajah, C.R., Iovenitti, P., *Effects of grain size and surface roughness on ultrasonic testing of aluminium alloy die castings*, Materials Evaluation, 2005 Vol. 63, No. 8, p. 832-836

2. Palanisamy, S., Nagarajah, C.R., and Iovenitti, P., *A study on ultrasonic flaw detection of aluminium die castings*, 8th International Conference on Manufacturing & Management (PCMM), Brisbane 8th -10th December, 2004 Vol. 1, p. 61-68

3. Palanisamy, S., Nagarajah, C.R. and Iovenitti, P., *Automated ultrasonic classification of defects in aluminium die castings*, Transactions of 22nd International Die Casting Congress, Indianapolis, Indiana, USA, 2003 p. 93-100

4. Palanisamy, S., Nagarajah, C.R., Iovenitti, P., *Ultrasonic inspection of sub-surface defects in aluminium die castings*, Non-Destructive Testing, Australia, 2002 39(5), p. 130-132

A.2 RESEARCH PRESENTATIONS

1. Palanisamy, S., Nagarajah, C.R., Iovenitti, P., *Ultrasonic Inspection of Aluminium Die Castings*, Technical Talk - Indian Society for Non-Destructive Testing Kalpakkam Chapter, Indira Gandhi Atomic Research Centre, Tamil Nadu, India October 9th, 2003.

2. Palanisamy, S., Nagarajah, C.R., Iovenitti, P., *Ultrasonic Inspection of Defects in Aluminium Die Castings*, Ford Research Lab, Detroit, Michigan, USA September 19th, 2003.

3. Palanisamy, S., Nagarajah, C.R., Iovenitti, P., *Ultrasonic Inspection of Sub-surface defects in Aluminium Die-castings,* 10th Asia Pacific Conference on Non-destructive testing, Brisbane, Australia September 17th - 19th, 2001.

APPENDIX B
ULTRASONIC IMMERSION TESTING SET UP

Figure B.1 shows the ultrasonic immersion testing experimental set-up. This figure expands on the ultrasonic immersion testing experimental rig presented in Section 4.4.3.

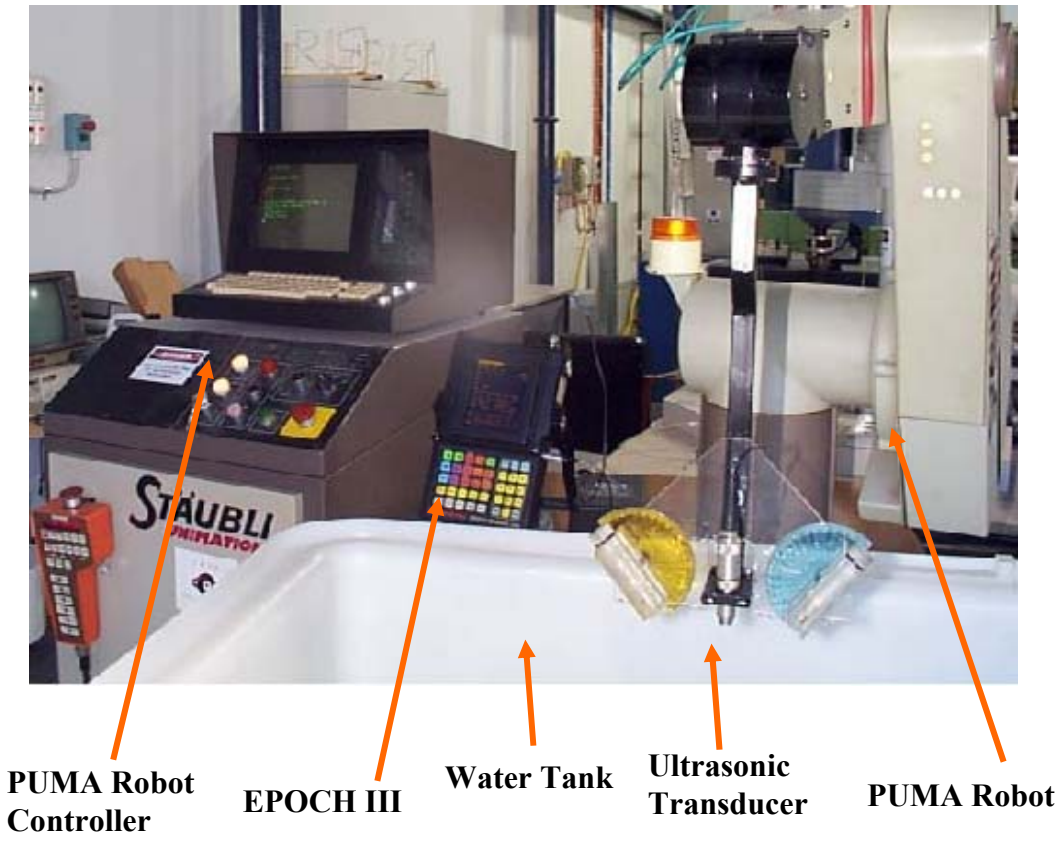

Figure B.1 Ultrasonic immersion testing experimental set up

In Figure B.2 the structural oil sump pan part (A) was immersed in water and Sintolin solution, which makes the water pale green in colour. The casting was mounted on the Perspex sheet (B) with the help of the alignment pins (C) to keep the casting in the same position every inspection cycle. The probe handling section (D)

holds the 10 MHz 25.4 mm focus probe (E). The inspection was carried out along the in-gate section of the casting.

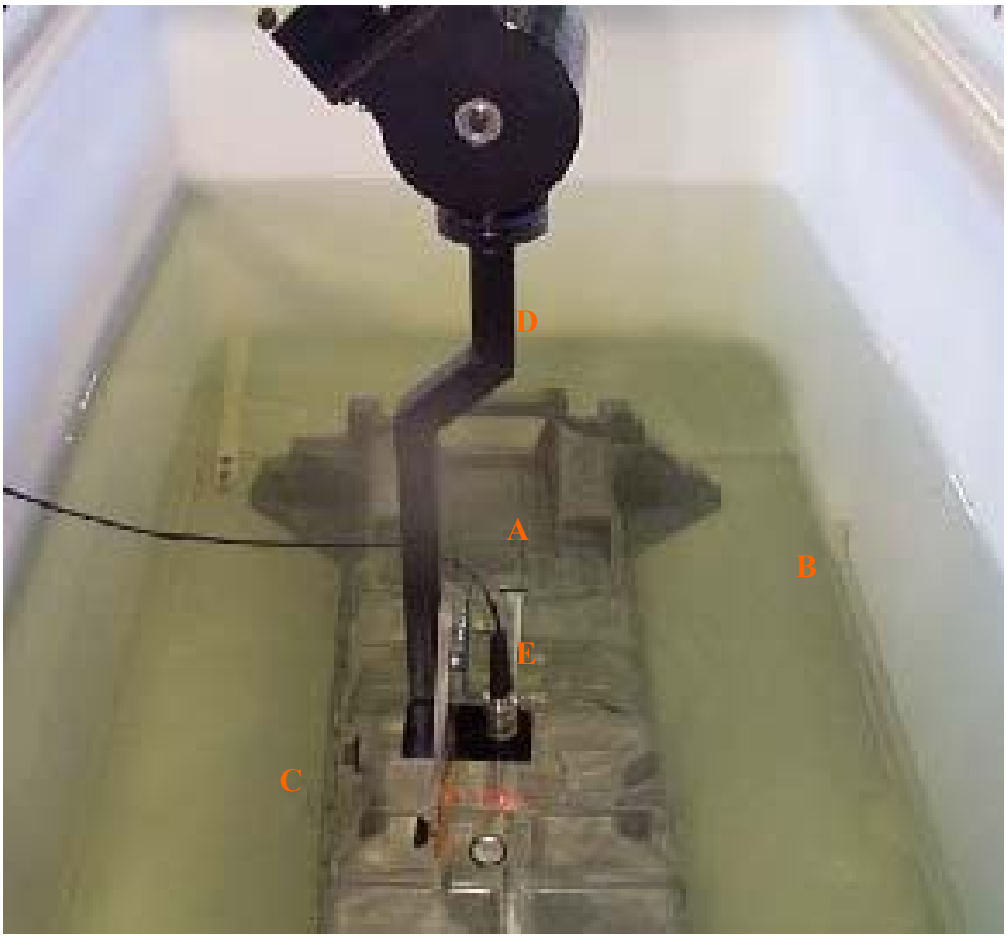

Figure B.2 Ultrasonic inspection of structural oil sump pan part with 10 MHz 25.4 mm focus probe

A cut section of the structural oil sump pan (SOSP) casting is shown in Figure B.3. The arrow mark at 'A' shows the starting point of the PUMA robot with ultrasonic transducer scanning path up to point 'B' in Figure B.3. The probe handling device (PUMA robot) was programmed to move along the in-gate section with a constant water path distance. Ultrasonic A-scan signal type was stored while the part was scanned with the ultrasonic transducer. Each A-scan signal stored in the EPOCH III equipment provided information of the part at a particular location long the in-gate section of the casting.

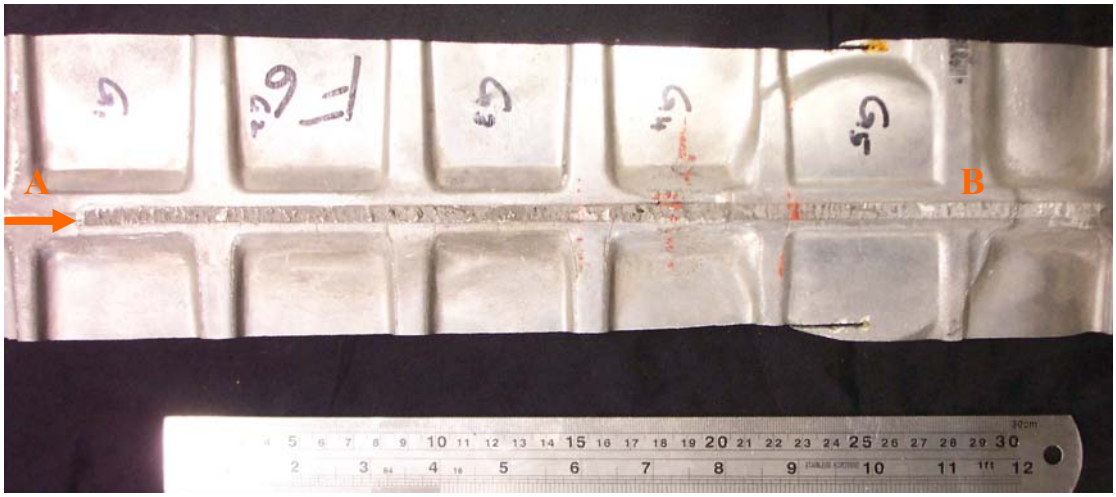

Figure B.3 PUMA robot scanning path on the critical section of SOSP part

APPENDIX C
PROBE AND PART DISTANCE CALCULATION

This appendix presents how the distance between probe and part were calculated for Chapter 4, Section 4.4.3.4. The laser pointer angle (α) can be used to find the distance between the probe and the part (*x*). The distance between the probe and the laser pointer was fixed at 50 mm during the design of the device as shown in Figure C.1.

x can be calculated from the Figure 3.8. Tan α is equal to the ratio of distance between probe/part distance and probe/laser pointer i.e.:

Tan α = opposite side/ adjacent side and it implies that Tan α = x / 50
Therefore, x = Tan α * 50

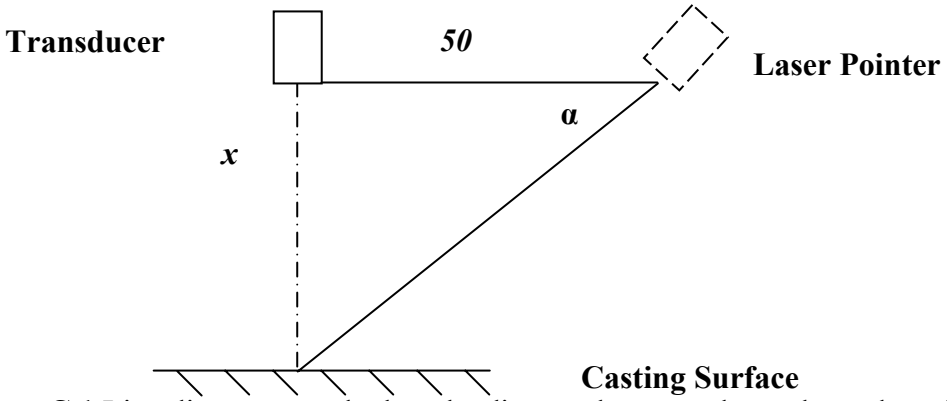

Figure C.1 Line diagram to calculate the distance between the probe and casting surface

Hence, from the laser pointer angle, the distance between the probe and part can be calculated. It provides the water path distance in the immersion testing. According to ASTM E 1001-99a[1] standards, the maximum variation in the water path distance that can be allowed for the ultrasonic immersion testing is +/- 1.6 mm. Hence, the tolerance of the laser pointer angle allowed in this inspection process is +/- 1˚.

[1] E 1001-99a – Standard practice for detection and evaluation of discontinuities by the immersed pulse-echo ultrasonic method using longitudinal waves, Annual Book of ASTM Standards, PA, USA, 1999 p 1-9.

APPENDIX D
SURFACE PROFILE MEASUREMENTS

This appendix gives details of the surface roughness measurements carried out on small casting sections. This follows on from Section 4.5.3 in relation to surface roughness analysis of the in-gate casting sections. The surface roughness measurements were carried out using a surface profile measuring instrument (Perthometer S5P). Figure D.1 shows the sample casting sections with part numbers F48, F50 and F55. These were the cut sections of structural oil sump pan castings.

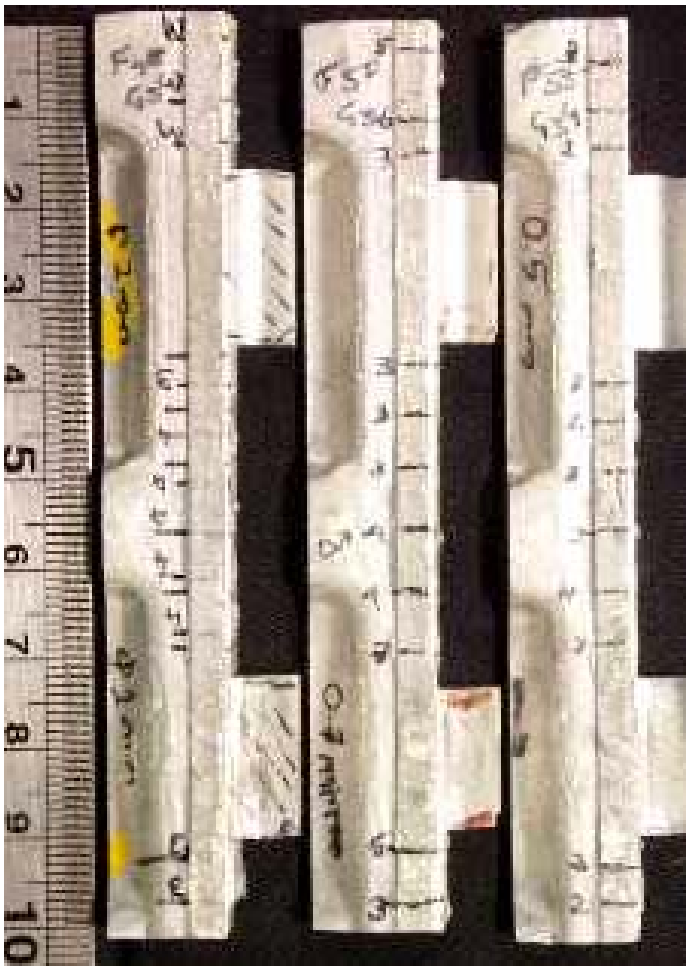

Figure D.1 Sample casting sections F48, F50 and F55 with simulated defects 1 mm, 0.7 mm and 0.5 mm diameter holes respectively

Table D.1 presents the measurement carried out on three in-gate casting sections with part numbers F48, F50 and F55 (as shown Figure D.3) after machining the rough front surface. Three surface roughness values were obtained at each point of measurement and average values of three measurements are obtained at the end. These average surface roughness values have been used for classifying the castings into three different groups Ra0 (101-150 μm), Ra1 (51-100 μm) and Ra2 (0-50 μm) Different surface roughness parameters such as R_a, R_z and R_q were also obtained during each measurement. However, only R_a values were used in final analysis in this research. Similarly, the measurements were obtained for Ra1 (50 to 99 μm) and Ra0 (100 to 150 μm) surface groups on the same casting sections before machining the front rough surface.

Particular areas of the castings were referred to P1 to p10 for the ten side-drilled holes as shown in Figure D.1. However, as mentioned in Section 4.5.2 not all of the 10 locations were suitable for subsequent analysis. Therefore, it can be seen that only profile measurements for selected regions were documented in this appendix. For example, for part number F48G3, only P1, P2, P5, P6, P7 and P8 were recorded.

Part No	Section No	Ra0(1)	Ra0(2)	Ra0(3)	Ra0 (average)	Ra1(1)	Ra1(2)	Ra1(2)	Ra1 (average)	Ra2(1)	Ra2(2)	Ra2(3)	Ra2 (average)
F48G3	P1	121.5	126.2	112	119.90	80.9	98.6	51.7	77.07	17.9	21	10	16.30
	P2	102.6	120.4	112.6	111.87	75.9	84.2	52.1	70.73	17.6	15.8	10.1	14.50
	P5	120	125.7	134	126.57	65.1	122.1	59.7	82.30	16.6	20.5	8.4	15.17
	P6	122.7	117	129.9	123.20	86	60.7	53.6	66.77	16.4	12.8	7.1	12.10
	P7	127.5	144.4	117.1	129.67	99.6	94.4	80.5	91.50	22	27.1	11.8	20.30
	P8	118.8	122.2	116.7	119.23	69.9	80.5	65	71.80	16.1	16.8	13.1	15.33
F50G3	P1	102.7	118.8	113.3	111.60	89.4	69.4	51.3	70.03	16.2	15.4	10.9	14.17
	P2	117.4	119.4	113.6	116.80	68.1	79	57.5	68.20	14.2	14.9	11.1	13.40
	P3	129	139.8	124.9	131.23	88.9	99.4	53.3	80.53	22.2	42.1	12.5	25.60
	P5	119.2	123.4	134	125.53	74.7	82.8	55.2	70.90	16.1	19.3	10.7	15.37
	P7	125.6	122.9	139.9	129.47	98.7	86.1	60.3	81.70	19.9	18.7	7.4	15.33
	P9	149.7	124	121.1	131.60	73.8	88.3	81.8	81.30	16.1	19.3	17.1	17.50
F55G3	P1	137.1	119.9	122.5	126.50	65.6	79.4	50.7	65.23	14.6	15.9	9.6	13.37
	P5	115.2	120.6	148.4	128.07	55.1	74.5	50.1	59.90	11.8	16.7	6.6	11.70
	P8	138	125.3	120.6	127.97	79.5	88.7	83.8	84.00	20.5	20.8	16	19.10
	P9	111.3	140.9	101.5	117.90	84.7	92.3	75.1	84.03	19.9	17.4	15.9	17.73
	P10	105.5	119.5	104.8	109.93	98.6	74.6	55.2	76.13	20.3	15.6	12	15.97

Table D.1 Surface roughness measurement values (μm) from Perthometer instrument for F48G3, F50G3 and F55G3 parts

APPENDIX E
RELIABILITY TESTING SECTIONS

This appendix presents the part used in the reliability testing of the equipment in Chapter 4, Section 4.6.4. Figure E.1 shows the bearing plate section of the manual transmission case with C2 and C5 sections. In Figure E.1, C2 is shown as A, the defect free section, and C5 is shown as B, the section with defect. The X-ray inspection was carried to detect the defect and defect free sections in the casting.

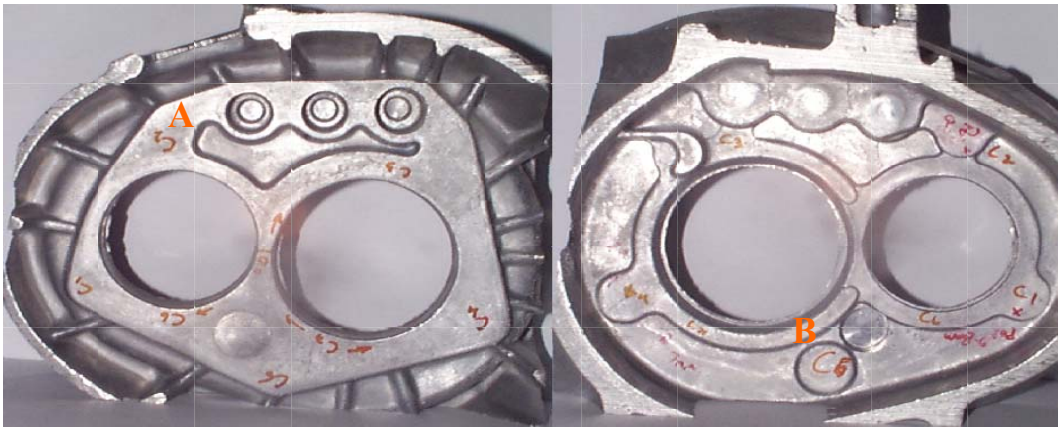

(a) **(b)**

Figure E.1 Bearing plate cut section of manual transmission case with sections (a) C2 – A and (b) C5 - B

APPENDIX F
A-SCAN FILE CONVERSION TO M-FILE TYPE

This appendix expands on the data processing methodology explained in Chapter 6, Section 6.2. It focuses on the third stage in Figure 6.1. i.e., the conversion of A-scan file data format to M-file type (MATLAB format). The steps involved in this conversion process are shown in Figure F.1.

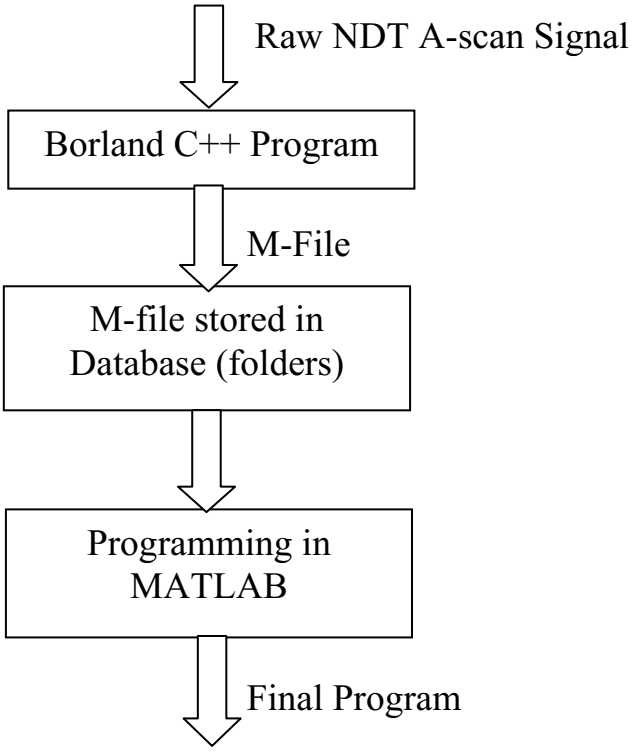

Figure F.1 Conversion of M-file to MATLAB input file format

The A-scan file obtained from the EPOCH III has a particular format of storing data, and only critical values such as amplitude values of the waveform were needed for the signal processing. A-scan files were stored in text file format with txt extension. Then, a program was written in Borland C++ software to obtain the critical elements (position and amplitude of the waveform) for the signal processing. Once the A-scan files were read the output of the program was an M-file, which had

only a matrix of [220 x 1]. Hence, the signal had 220 input nodes to be sent into the artificial neural networks for classification. Figure F.2 is a flowchart of the algorithm developed to read the signals from the hard disk of the computer and to store them in a single structure called 'M'. The files are read from data input folders which contains the data files and all these 'sig' values are read into 'M' matrix and all the target T values are read into't' matrix.

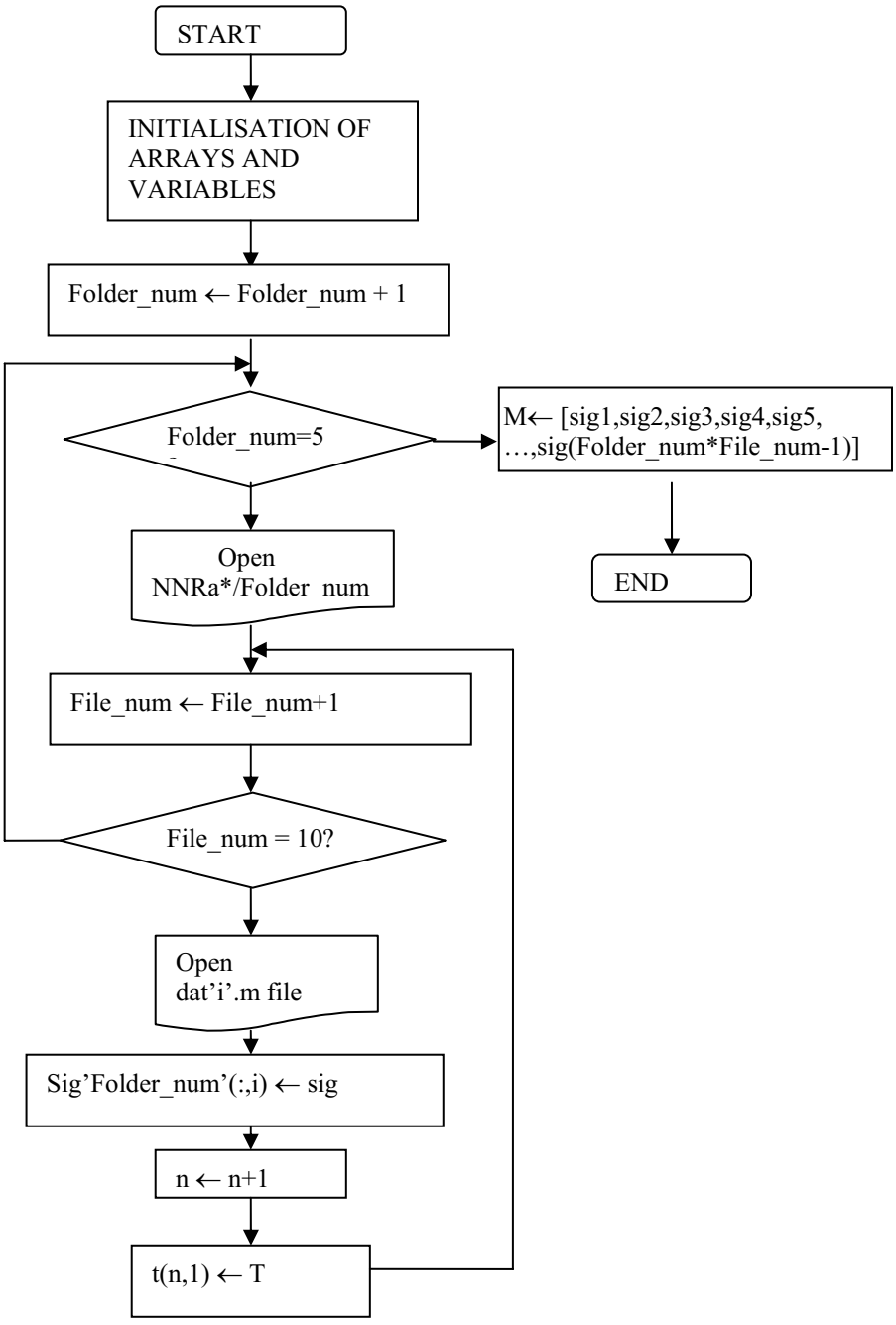

Figure F.2 Algorithm to store training signals and target values

APPENDIX G
MATLAB NEURAL NETWORK PROGRAM

This appendix shows a sample program for the FFT and PCA in Chapter 6, Sections 6.5.2 and 6.5.3. The following program is written using MATLAB in an m-file format. The purpose of the program is to read an array of signals from the folders stored in the system (database of signals). Then the FFT and PCA were applied on the input signals to artificial neural networks. The neural network parameters were defined and training, simulating and testing were carried out on the input signals. The complete process was carried out in a loop. Finally, the output was sent to separate the m-file with the mean classification percentage and standard deviation.

```
% clear all the contents in the memory
clear all;
%defining variables
int folder_num; % number of folders with training signals
int testfolder_num; % number of folders with test signals
int file_num; % number of file within the folders
int file_num_max; % maximum number of files within the folders
int testfile_num; % number of file within the folders
int x;
int y;
int z;
int b;
int folder_num_max; % maximum number of folders for training
int testfolder_max; % maximum number of folders for testing
int test_file_max; % maximum number of files within the test folders
test_file_max = 10;
folder_num_max = 5;
file_num_max = 10;
testfolder_max = 3;
LOOP_MAX=1; % number of training and testing loops
EPOCH_MAX = 10; % number of maximum epochs

% creating and opening result file
fid = fopen('E:\NNInputFiles\Results\FFT_Plot_Ra0.m','wb');
fprintf(fid, 'OUTPUT_PERCENTAGE= [');
% for to read the input data
```

```
for file_num = 1:file_num_max
   for folder_num = 1:folder_num_max;
      x = folder_num + ((file_num -1) * folder_num_max);
      eval(['cd E:\NNInputFiles\NNRa0\',num2str(folder_num)])
      eval(['dat' num2str(file_num)])
      X = fft(sig,256); % applying fft
      Xyy = X.*conj(X)/256; % calculating power spectrum of FFT output
      M(:,x) = Xyy; % input to the M array
   end
end

% for loop to get the target values
for file_num = 1:file_num_max
   for folder_num = 1:folder_num_max;
      x = folder_num + ((file_num -1) * folder_num_max);
      eval(['cd E:\NNInputFiles\NNRa0\',num2str(folder_num)])
      eval(['dat' num2str(file_num)])
      t(:,x) = T;
   end
end

f = 100*(0:256)/256;
% PCA functions for training data
[length, width]=size(M); % finding out the length and width of the matrix M
A= Cov(M'); % takes covariance of transpose of matrix M
B=eye(size(A)); % Dim is loaded from file as the dimension of eigenspace

%No of eigenvector/value combinations found
SIGMA='LM';%Largest Magnitude
[V,D, FLAG]=EIGS(A,B,40,SIGMA); % 40 principal components
C = V'*M;
% for loop to get testing data
for testfile_num = 1:test_file_max
   for testfolder_num = 1:testfolder_max;
      y = testfolder_num + ((testfile_num -1) * testfolder_max);
      eval(['cd E:\NNInputFiles\NNRa0\Test\',num2str(testfolder_num)])
      eval(['dat' num2str(testfile_num)])
      Y =fft(sig,256);
      Yyy = Y.*conj(Y)/256;
      %plot (Yyy,128)
      %pause(0.5)
      S(:,y) = Yyy;
   end
end

% PCA functions for testing data
[length, width]=size(S); % finding out the length and width of the matrix M
A= Cov(S'); % takes covariance of transpose of matrix M
B=eye(size(A)); % Dim is loaded from file as the dimension of eigenspace
```

```
%No of eigenvector/value combinations found
SIGMA='LM';%Largest Magnitude
[V,D, FLAG]=EIGS(A,B,40,SIGMA); % 40 principal components
U = V'*M;

        % for loop to get testing data target values
        for testfile_num = 1:test_file_max
           for testfolder_num = 1:testfolder_max;
              z = testfolder_num + ((testfile_num -1) * testfolder_max);
              eval(['cd E:\NNInputFiles\NNRa0\Test\',num2str(testfolder_num)])
              eval(['dat' num2str(file_num)])
              P(:,z) = T;

           end
        end

        errormat=zeros(EPOCH_MAX,LOOP_MAX);
        charmat=zeros(EPOCH_MAX,LOOP_MAX);

        % for loop to carry out network training and testing
        for loop = 1:LOOP_MAX

        net = newff(minmax(C),[20,10,1], {'tansig','logsig','tansig'}, 'trainscg');
                 net =init(net);
                 net.performFcn = 'mse';
                 net.trainParam.show = 20;
                 net.trainParam.epochs= 500;
                 net.trainParam.goal = 0.001;
                 net.trainParam.lr = 0.05;
                 net.trainParam.mc = 0.9;

                 %Output Percentage Correctness
                 int THERSOLD;
                 int PERCENT1;
                 int PERCENT2;
                 int PERCENT;
                 int OUTPUT_PERCENTAGE
                 int a;
                 int output_max;
                 output_max = testfolder_max * test_file_max;
        for epoch_no=1:EPOCH_MAX
              %load train sigs
              [net, tr] = train(net, C, t);
              trainoutput = sim(net,C)
              %load test sigs

              %testing
              output = sim(net,U)
              PERCENT1 = 0;
```

```
THERSOLD = 0.5;
PERCENT2 = 0;
OUTPUT_PERCENTAGE = 1

%simuate &test
for a = 1 : output_max % Number of output signals is equal to 20

% for output <0.5 ie., no defect signals
   if ((P(a)== 0) & (output(a)< THERSOLD))

      PERCENT1 = PERCENT1 + 1;
   else
      PERCENT1;
   end
   if ((P(a)== 1) & (output(a) > THERSOLD))
      PERCENT2 = PERCENT2 + 1;
   % for output > 0.5 i.e, defect signals
   else
      PERCENT2;
   end
end
PERCENT1
PERCENT2

PERCENT = PERCENT1 + PERCENT2;

% Final output correct percentage
   OUTPUT_PERCENTAGE = (PERCENT/output_max)*100

   errormat(epoch_no)=0.5;

   charmat(epoch_no,loop)=OUTPUT_PERCENTAGE;
   figure(1)
   plot(charmat);
   pause(0.1)
      end
      fprintf(fid, '%f\n',OUTPUT_PERCENTAGE);
      Output_Matrix(:,loop) = OUTPUT_PERCENTAGE;

end % End of loop

fprintf(fid, '];\n');
fprintf(fid,'\nMean =');
fprintf(fid,'%f\n', mean(Output_Matrix'));
fprintf(fid,'\nStandard Deviation = ');
fprintf(fid,'%f\n', std(Output_Matrix'));
fclose(fid);
```